RM cores

Core type	Standards	Mounting dimensions (mm) of assembly set Base area × H [1]	Individual parts of assembly set	Part number	Page
RM 4	IEC 60431		Core	B65803	184
		$10{,}16^2 \times 10{,}8$	Coil former	B65804	186
			Insulating washers	B65804	187
			Clamp	B65806	187
			Adjusting screws	B65539	188
RM 4 LP	IEC 61860		Core	B65803	189
		$10{,}5^2 \times 8{,}1$	Coil former	B65804	190
			Clamp	B65804	191
			Insulating washers	B65804	191
		$14 \times 17{,}5 \times 8{,}1$	Coil former/Clamp SMD	B65804	192
RM 5	IEC 60431		Core	B65805	194
		$12{,}7^2 \times 10{,}8$	Coil former	B65806	196
			Clamp	B65806	197
			Insulating washers	B65806	197
		$16{,}5 \times 19 \times 10{,}6$	Coil former SMD	B65822	198, 199
			Clamp SMD	B65806	198, 199
			Adjusting screws	B65539/ B65806	200
RM 5 LP	IEC 61860	$20 \times 16 \times 8$	Core	B65805	201
RM 6	IEC 60431		Core	B65807	203
		$15{,}24^2 \times 12{,}8$	Coil former	B65808	205, 206
			Coil former for SMPS transf.	B65808	207
		$19{,}5 \times 25 \times 12{,}8$	Coil former for power appl.	B65808	208, 209
			Clamp/Insulating washers	B65808	210
		$19{,}6 \times 22{,}2 \times 13$	Coil former SMD	B65821	211, 212
			Clamp SMD	B65808	211, 212
			Adjusting screws	B65659	213
RM 6 LP	IEC 61860		Core	B65807	214

1) Height above mounting plane

RM cores (continued)

Core type	Standards	Mounting dimensions (mm) of assembly set Base area × H [1]	Individual parts of assembly set	Part number	Page
RM 7	IEC 60431		Core	B65819	216
		17,78² × 13,8	Coil former	B65820	218
			Clamp/Insulating washers	B65820	219
			Adjusting screws	B65659	220
RM 7 LP	IEC 61860		Core	B65819	221
			Coil former	B65820	222
RM 8	IEC 60431		Core	B65811	224
		20,32² × 16,8	Coil former	B65812	226, 227
			Coil former for SMPS transf.	B65812	228
		26 × 30 × 16,8	Coil former for power appl.	B65812	229
			Clamp/Insulating washers	B65812	230
			Adjusting screws	B65812	231
RM 8 LP	IEC 61860		Core	B65811	232
			Coil former	B65812	233
			Clamp/Insulating washers	B65812	234
RM 10	IEC 60431		Core	B65813	236
		25,4² × 19	Coil former	B65814	238
		31 × 40 × 19	Coil former for power appl.	B65814	239
			Clamp/Insulating washers	B65814	240
			Adjusting screws	B65679	241
RM 10 LP	IEC 61860		Core	B65813	242
RM 12	IEC 60431		Core	B65815	244
		30,48² × 24,9	Coil former	B65816	246
		32 × 45,7 × 24,9	Coil former for power appl.	B65816	247
			Clamp/Insulating washers	B65816	248
RM 12 LP	IEC 60431		Core	B65815	249
RM 14	IEC 60431		Core	B65887	251
		35,56² × 30,5	Coil former	B65888	253
		44 × 29 × 30,5	Coil former for power appl.	B65888	254
			Clamp/Insulating washers	B65888	255
RM 14 LP	IEC 61860		Core	B65887	256
Adjusting tools (see individual data sheets)				B63399	

1) Height above mounting plane

PM cores

Core type	Standards	Mounting dimensions (mm) of assembly set Base area × H [1)]	Individual parts of assembly set	Part number	Page
PM 50/39	IEC 61247	65 × 52 × 45	Core	B65646	259
			Coil former	B65647	260
			Mounting assembly	B65647	261
PM 62/49	IEC 61247	76 × 64 × 55	Core	B65684	262
			Coil former	B65685	263
			Mounting assembly	B65685	264
PM 74/59	IEC 61247	85,5 × 75 × 65	Core	B65686	265
			Coil former	B65687	266
			Mounting assembly	B65687	267
PM 87/70	IEC 61247	101 × 87 × 72	Core	B65713	268
			Coil former	B65714	269
			Mounting assembly	B65714	270
PM 114/93	IEC 61247	114 × 92 × 93	Core	B65733	271
			Coil former	B65734	272

1) Height above mounting plane

EP cores

Core type	Standards	Mounting dimensions (mm) of assembly set Base area × H [1]	Individual parts of assembly set	Part number	Page
EP 5	—		Core	B65855	275
		8 × 6,2 × 5,7	Coil former SMD	B65856	276
EP 7	IEC 61596		Core	B65839	277
		7,5 × 10 × 10	Coil former/Cap yoke	B65840	279
		14 × 9,4 × 8,9	Coil former SMD	B65840	280
EPX 7/9	—		Core	B65857	281
		12,6 × 9,4 × 12,4	Coil former SMD	B65858	282
EP 10	IEC 61596		Core	B65841	283
		12 × 14,2 × 12,5	Coil former	B65842	285
			Mounting assembly	B65842	286
			Cap yoke	B65842	286
EPX 10	—		Core	B65859	287
		15,5 × 13,2 × 12,2	Coil former SMD	B65860	288
EP 13	IEC 61596		Core	B65843-A	289
		15 × 16 × 13,7	Coil former	B65844	291
		15 × 16 × 13,7	Coil former for high-voltage applications	B65844	292
			Mounting assembly	B65844	293
			Cap yoke	B65844	293
		19,5 × 13 × 12,5	Coil former SMD	B65844	294
EPO 13	—		Core	B65843-P	295
		15 × 16 × 13,7	Coil former	B65844	296
		15 × 16 × 13,7	Coil former for high-voltage applications	B65844	297
		19,5 × 13 × 12,5	Coil former SMD	B65844-F	298
EP 17	IEC 61596		Core	B65845	299
		20 × 21,6 × 16,2	Coil former	B65846	300
			Mounting assembly	B65846	301
			Cap yoke	B65846	301
EP 20	IEC 61596		Core	B65847	302
		23 × 27,5 × 20,5	Coil former	B65848	303
			Mounting assembly	B65848	304

1) Height above mounting plane

P cores (pot cores)

Core type	Standards	Mounting dimensions (mm) of assembly set Base area × H [1)]	Individual parts of assembly set	Part number	Page
P 3,3 × 2,6			Core	B65491	306
P 4,6 × 4,1			Core	B65495	308
		5,5 × 5 × 5,1	Coil former	B65496	309
		6,8 × 5 × 5,1	Terminal carrier	B65496	310
			Adjusting screws	B65496	311
P 5,8 × 3,3			Core	B65501	312
P 7 × 4			Core	B65511	314
		7,5 × 7,5 × 7,1	Coil former	B65512	315
			Mounting assembly	B65512	316
P 9 × 5	IEC 60133		Core	B65517	318
		9,9 × 9,9 × 8,3	Coil former/Insulating washer	B65522	319
		(4 solder terminals)			
		9,9 × 12,3 × 8,3			
		(6 solder terminals)			
		12,2 × 17 × 6,0	Coil former SMD	B65524	320
			Mounting assembly	B65518	321
			Adjusting screws	B65518	322
P 11 × 7	IEC 60133		Core	B65531	324
			Coil former/Insulating washer	B65532	325
		12,3 × 12,3 × 9,5	Mounting assembly	B65535	326
		(4 solder terminals)			
		12,3 × 14,6 × 9,5			
		(8 solder terminals)	Adjusting screws	B65539	327
P 14 × 8	IEC 60133		Core	B65541	329
		16,8 × 15 × 11,3	Coil former/Insulating washers	B65542	330
		(4 solder terminals)			
		16,8 × 19,6 × 11,3	Mounting assembly	B65545	331
		(6 solder terminals)	Adjusting screws	B65549	332
P 18 × 11	IEC 60133		Core	B65651	334
		19,9 × 20,7 × 13,5	Coil former/Insulating washers	B65652	335
			Mounting assembly	B65655	336
			Adjusting screws	B65659	337

1) Height above mounting plane

P cores (pot cores) (continued)

Core type	Standards	Mounting dimensions (mm) of assembly set Base area × H [1)]	Individual parts of assembly set	Part number	Page
P 22 × 13	IEC 60133	24,5 × 26 × 16,6	Core	B65661	339
			Coil former/Insulating washers	B65662	340
			Mounting assembly	B65665	341
P 26 × 16	IEC 60133	27,8 × 28,5 × 19	Core	B65671	343
			Coil former/Insulating washers	B65672	344
			Mounting assembly	B65675	345
			Adjusting screws	B65679	346
P 30 × 19	IEC 60133	32,5 × 33,5 × 22,8	Core	B65701	348
			Coil former/Insulating washers	B65702	349
			Mounting assembly	B65705	350
			Adjusting screws	B65679	351
P 36 × 22	IEC 60133	40 × 41,8 × 27,5	Core	B65611	353
			Coil former/Insulating washer	B65612	354
			Mounting assembly	B65615	355
			Adjusting screws	B65679	356
P 41 × 25		39 × 55 × 28,1	Core	B65621	358
			Coil former	B65622	359
			Mounting assembly	B65623	360
Adjusting tools (see individual data sheets)				B63399	

1) Height above mounting plane

P core halves and PS cores

Core type (∅ × height)	Material	Individual parts of assembly set	Part number	Page
PS 7,35 × 3,6	N22, M33	Core	B65933	362
		Coil former	B65512	362
PS 9 × 3,5	N22, M33	Core	B65935	363
		Coil former	B65936	363
14,4 × 7,5	N22	Core	B65937	364
		Coil former	B65542	364
PS 25 × 8,9	N22	Core	B65939	365
		Coil former	B65940	365
PS 30,5 × 10,2	N22	Core	B65941	366
		Coil former	B65942	366
PS 35 × 10,8	N22	Core	B65947	367
PS 47 × 14,9	N22	Core	B65943	368
		Coil former	B65944	368
PS 68 × 14,5	N22	Core	B65928	369
		Coil former	B65946	369
70 × 14,5	N22	Core	B65945	370
		Coil former	B65946	370
150 × 30	N27	Core	B65949	371

TT/PR cores

Core type	Individual parts of assembly set	Part number	Page
TT 14 × 8	Core	B65754	373
PR 14 × 8	Core	B65755	373
TT 18 × 11	Core	B65756	374
PR 18 × 11	Core	B65757	374
TT 23 × 11	Core	B65716-L	375
PR 23 × 11	Core	B65738-L	375
TT 23 × 18	Core	B65716-J	376
PR 23 × 18	Core	B65738-J	376
TT 30 × 19	Core	B65730	377
PR 30 × 19	Core	B65735	377

1) Height above mounting plane

E cores

Core type [1])	Standards	Mounting dimensions (mm) of assembly set L × W × H [2])	Individual parts of assembly set	Part number	Page
E 5			Core	B66303	384
E 6,3			Core	B66300	385
		9 × 8 × 5,7	Coil former/Cover cap SMD	B66301	386
E 8,8	IEC 61246		Core	B66302	387
		10 × 12,5 × 5,5	Coil former/Cover cap SMD	B66302	388
E 10/5,5/5			Core	B66322	389
E 13/7/4	IEC 61246		Core	B66305	390
(EF 12,6)		15 × 17 × 12	Coil former (horizontal)	B66202	392
		10 × 15 × 17	Coil former (vertical)	B66202	393
		13,5 × 19,5 × 9,3	Coil former SMD	B66306	394
			Cover plate	B66414	395
			Yoke	B66202	393, 395
E 14/8/4			Core	B66219	396
E 16/8/5	IEC 61246		Core	B66307	397
(EF 16)		18 × 20 × 14	Coil former (horizontal)	B66308	399
		11 × 18 × 20	Coil former (vertical)	B66308	400
			Yoke	B66308	400
E 16/6/5			Core	B66393	401
E 19/8/5 E 187 [3])			Core	B66379	402
E 20/10/6	IEC 61246		Core	B66311	403
(EF 20)		22 × 22 × 17	Coil former (horizontal)	B66206	405
		15 × 22 × 24	Coil former (vertical)	B66206	405
		24 × 21,5 × 14	Coil former (right-angle pins)	B66206	406
		15 × 22 × 24	Coil former for luminaires	B66206	408
			Yoke	B66206	408
E 21/9/5			Core	B66314	409
E 25/13/7	IEC 61246		Core	B66317	410
(EF 25)		28 × 28 × 21	Coil former (horizontal)	B66208	412
		18 × 28 × 29	Coil former (vertical)	B66208	413
		19 × 26 × 30	Coil former for SMPS	B66208	414
			Yoke	B66208	414

1) The E core designations have been brought into line with IEC; the previous designations are given in parentheses.
2) Height above mounting plane
3) US designation (size based on U.S. lam. size E cores)

E cores (continued)

Core type [1]	Standards	Mounting dimensions (mm) of assembly set L × W × H [2]	Individual parts of assembly set	Part number	Page
E 25,4/10/7 E2425 [3]			Core	B66315	415
E 30/15/17			Core	B66319	416
		36 × 36 × 12	Coil former (horizontal)	B66232	417
		19 × 36 × 36	Coil former (vertical)	B66232	418
			Yoke	B66232	418
E 32/16/9	IEC 61246		Core	B66229	419
(EF 32)		35 × 37 × 24	Coil former	B66230	420
			Yoke	B66230	420
E 32/16/11			Core	B66233	421
E 34/14/9 E 375 [3]			Core	B66370	422
E 36/18/11			Core	B66389	423
		39 × 38 × 31	Coil former	B66390	424
E 40/16/12 E 21 [3]			Core	B66381	425
E 42/21/15	IEC 61246		Core	B66325	426
E 42/21/20	IEC 61246		Core	B66329	427
		38 × 46 × 52	Coil former	B66243	428
E 47/20/16 E 625 [3]			Core	B66383	429
E 55/28/21	IEC 61246		Core	B66335	430
E 55/28/25			Core	B66344	431
E 56/24/19 E 75 [3]			Core	B66385	432
E 65/32/27			Core	B66387	433
E 70/33/32			Core	B66371	434
E 80/38/20			Core	B66375	435

1) The E core designations have been brought into line with IEC; the previous designations are given in parentheses.
2) Height above mounting plane
3) US designation (size based on U.S. lam. size E cores)

ELP cores

Core set	Standards	Core types	Individual parts of assembly set	Part number w/o clamp recess	Part number with clamp recess	Page
EELP 14	IEC 61860	ELP 14/3,5/5	Core	B66281-G		437
EILP 14	IEC 61860	I 14/1,5/5 (+ ELP 14/3,5/5)	Core	B66281-P		438
EELP 18	IEC 61860	ELP 18/4/10	Core	B66453-G	B66283-G	439, 441
			Clamp		B65804	439
EILP 18	IEC 61860	I 18/2/10 (+ ELP 18/4/10)	Core	B66453-P	B66283-P	440, 442
EELP 22	IEC 61860	ELP 22/6/16	Core	B66455-G	B66285-G	443, 445
EILP 22	IEC 61860	I 22/2,5/16	Core	B66455-P	B66285-P	444, 446
		(+ ELP 22/6/16)	Clamp		B65804	444
EELP 32	IEC 61860	ELP 32/6/20	Core	B66457-G	B66287-G	447, 449
			Clamp		B65808	447
EILP 32	IEC 61860	I 32/3/20	Core	B66457-P	B66287-P	448, 450
		(+ ELP 32/6/20)	Clamp		B66288	448
EELP 38	IEC 61860	ELP 38/8/25	Core	B66459-G	B66289-G	451, 453
EILP 38	IEC 61860	I 38/4/25 (+ ELP 38/8/25)	Core	B66459-P	B66289-P	452, 454
EELP 43	IEC 61860	ELP 43/10/28	Core	B66461-G	B66291-G	455, 457
EILP 43	IEC 61860	I 43/4/28 (+ ELP 43/10/28)	Core	B66461-P	B66291-P	456, 458
EELP 58	IEC 61860	ELP 58/11/38	Core	B66293-G		459
EILP 58	IEC 61860	I 58/4/38 (+ ELP 58/11/38)	Core	B66293-P		460
EELP 64	IEC 61860	ELP 64/10/50	Core	B66295-G		461
EILP 64	IEC 61860	I 64/5/50 (+ ELP 64/10/50)	Core	B66295-P		462

ER cores

Core type	Standards	Mounting dimensions (mm) of assembly set L × W × H [1)]	Individual parts of assembly set	Part number	Page
ER 9,5/5	IEC 61860		Core	B65523	464
		12 × 10 × 5,7	Coil former SMD	B65527	465
			Yoke	B65527	465
ER 11/5	IEC 61860		Core	B65525	466
		12,8 × 11,7 × 6	Coil former SMD	B65526	467
			Yoke	B65526	467
ER 14,5/6	IEC 61860		Core	B65513	468
ER 28/17/11			Core	B66433	469
ER 35/20/11			Core	B66350	470
ER 42/22/15			Core	B66347	471
		33 × 46 × 55	Coil former	B66348	472
ER 46/17/18			Core	B66377	473
ER 49/27/17			Core	B66391	474
ER 54/18/18			Core	B66357	475

1) Height above mounting plane

ETD, EC cores

Core type	Standards	Mounting dimensions (mm) of assembly set L × W × H [1]	Individual parts of assembly set	Part number	Page
ETD cores					
ETD 29/16/10	IEC 61185		Core	B66358	477
		35,5 × 35,5 × 25,5	Coil former (horizontal)	B66359	479
		24 × 35,5 × 41,2	Coil former (vertical)	B66359	480
			Yoke	B66359	479, 480
ETD 34/17/11	IEC 61185		Core	B66361	481
	CECC 25301-001	43 × 40 × 35	Coil former (horizontal)	B66362	483
		27,5 × 40 × 46	Coil former (vertical)	B66362	484
			Yoke	B66362	483, 484
ETD 39/20/13	IEC 61185		Core	B66363	485
	CECC 25301-002	48 × 45 × 38	Coil former/Yoke	B66364	487
ETD 44/22/15	IEC 1185		Core	B66365	488
	CECC 25301-003	53 × 50 × 41	Coil former/Yoke	B66366	490
ETD 49/25/16	IEC 61185		Core	B66367	491
	CECC 25301-004	58 × 55 × 43,5	Coil former/Yoke	B66368	493
ETD 54/28/19	IEC 61185		Core	B66395	494
		62 × 62 × 47	Coil former/Yoke	B66396	496
ETD 59/31/22	IEC 61185		Core	B66397	497
		67 × 71 × 50	Coil former/Yoke	B66398	499
EC cores					
EC 35/17/10	IEC 60647		Core	B66337	500
EC 41/20/12	IEC 60647		Core	B66339	501
EC 52/24/14	IEC 60647		Core	B66341	502
EC 70/35/16	IEC 60647		Core	B66343	503

1) Height above mounting plane

EFD, EV, DE cores

Core type	Mounting dimensions (mm) of assembly set L × W × H [1]	Individual parts of assembly set	Part number	Page
EFD cores				
EFD 10/5/3		Core	B66411	506
EFD 15/8/5		Core	B66413	507
	19,3 × 17 × 8	Coil former/Yoke	B66414	508
	21 × 16 × 8	Coil former/Yoke SMD	B66414	509
		Cover plate	B66414	509
EFD 20/10/7		Core	B66417	510
	24,3 × 22 × 10	Coil former/Yoke	B66418	511
EFD 25/13/9		Core	B66421	512
	29,3 × 27,3 × 12,5	Coil former/Yoke	B66422	513
EFD 30/15/9		Core	B66423	514
	34,4 × 32,5 × 12,5	Coil former/Yoke	B66424	515
EV cores				
EV 15/9/7		Core	B66434	516
EV 25/13/13		Core	B66408	517
EV 30/16/3		Core	B66432	518
DE cores				
DE 24		Core	B66426	519
DE 28		Core	B66399	520
DE 35		Core	B66409	521

1) Height above mounting plane

U, UI cores

Core set	Core types	Individual parts of assembly set	Part number	Page
UU 93/152/16 UI 93/104/16	U 93/76/16 I 93/28/16 (+ U 93/76/16)	Core Core	B67345-B3 B67345-B4	524
UU 93/152/20 UI 93/104/20	U 93/76/20 I 93/28/20 (+ U 93/76/20)	Core Core	B67345-B10 B67345-B11	525
UU 93/152/30 UI 93/104/30	U 93/76/30 I 93/28/30 (+ U 93/76/30)	Core Core	B67345-B1 B67345-B2	526
	U 101/76/30	Core	B67370	527
	U 141/78/30	Core	B67374	528

Toroids (ring cores)

Toroids R 2,5 … R 200	Technical report IEC 61604	Core	B64290	534

Double-aperture cores

Core height 2,0 … 14,5 mm	6,2; 8,3 and 14,5: DIN 41279, shape G	Core	B62152	558

FPC film

Material	Part number	Page
C 350, C 351	B68450, B68451, B68452	559

Index of Part Numbers

(In numerical order)

Index of Part Numbers

Part number	Page	Type
B65651	334	P 18 × 11 core
B65652	335	P 18 × 11 coil former, insulating washer
B65655	336	P 18 × 11 mounting assembly
B65659	213, 220, 337	Adjusting screw for RM 6, RM 7, P 18 × 11
B65661	339	P 22 × 13 core
B65662	340	P 22 × 13 coil former, insulating washer
B65665	341	P 22 × 13 mounting assembly
B65671	343	P 26 × 16 core
B65672	344	P 26 × 16 coil former, insulating washer
B65675	345	P 26 × 16 mounting assembly
B65679	241, 346, 351, 356	Adjusting screw for RM 10, P 26 × 16, P 30 × 19, P 36 × 22
B65684	262	PM 62/49 core
B65685	263, 264	PM 62/49 coil former, mounting assembly
B65686	265	PM 74/59 core
B65687	266, 267	PM 74/59 coil former, mounting assembly
B65701	348	P 30 × 19 core
B65702	349	P 30 × 19 coil former, insulating washer
B65705	350	P 30 × 19 mounting assembly
B65713	268	PM 87/70 core
B65714	269, 270	PM 87/70 coil former, mounting assembly
B65716-J	376	TT 23 × 18
B65716-L	375	TT 23 × 11
B65730	377	TT 30 × 19
B65733	271	PM 114/93 core
B65734	272	PM 114/93 coil former
B65735	377	PR 30 × 19
B65738-J	376	PR 23 × 18
B65738-L	375	PR 23 × 11
B65754	373	TT 14 × 8
B65755	373	PR 14 × 8
B65756	374	TT 18 × 11
B65757	374	PR 18 × 11
B65803	184, 189	RM 4 core, RM 4 low-profile core
B65804	186, 187, 190 ...192, 439, 444	RM 4 coil former, clamp, insulating washer, ELP18 clamp, ELP 22 clamp
B65805	194, 201	RM 5 core, RM 5 low-profile core
B65806	187	RM 4 clamp
	196, 197	RM 5 coil former, clamp, insulating washer

Part number	Page	Type
B65807	203, 214	RM 6 core, RM 6 low-profile core
B65808	205…210, 447	RM 6 coil former, clamp, insulating washer, ELP 32 clamp
B65811	224, 232	RM 8 core, RM 8 low-profile core
B65812	226…231, 233, 234	RM 8 coil former, clamp, insulating washer, adjusting screw
B65813	236, 242	RM 10 core, RM 10 low-profile core
B65814	238, 239, 240	RM 10 coil former, clamp, insulating washer
B65815	244, 249	RM 12 core, RM 12 low-profile core
B65816	246, 247, 248	RM 12 coil former, clamp, insulating washer
B65819	216, 221	RM 7 core, RM 7 low-profile core
B65820	218, 219, 222	RM 7 coil former, clamp, insulating washer
B65821	211, 212	RM 6 coil former (SMD)
B65822	198, 199	RM 5 coil former (SMD)
B65839	277	EP 7 core
B65840	279, 280	EP 7 coil former, cap yoke
B65841	283	EP 10 core
B65842	285, 286	EP 10 coil former, mounting assembly, cap yoke
B65843	289, 295	EP 13 core, EPO 13 core
B65844	291…294, 296, 297, 298	EP 13 coil former, mounting ass., cap yoke, EPO 13 coil former
B65845	299	EP 17 core
B65846	300, 301	EP 17 coil former, mounting assembly, cap yoke
B65847	302	EP 20 core
B65848	303, 304	EP 20 coil former, mounting assembly
B65855	275	EP 5 core
B65856	276	EP 5 coil former, cap yoke
B65857	281	EPX 7/9 core
B65858	282	EPX 7/9 coil former
B65859	287	EPX 10 core
B65860	288	EPX 10 coil former, cap yoke
B65887	251, 256	RM 14 core, RM 14 low-profile core
B65888	253, 254, 255	RM 14 coil former, clamp, insulating washer
B65928	369	PS core 68 × 14,5
B65933	362	PS core 7,35 × 3,6
B65935	363	PS core 9 × 3,5
B65936	363	PS core 9 × 3,5 coil former
B65937	364	P core half 14,4 × 7,5
B65939	365	PS core 25 × 8,9

Index of Part Numbers

Part number	Page	Type
B65940	365	PS core 25 × 8,9 coil former
B65941	366	PS core 30,5 × 10,2
B65942	366	PS core 30,5 × 10,2 coil former
B65943	368	PS core 47 × 14,9
B65944	368	PS core 47 × 14,9 coil former
B65945	370	P core half 70 × 14,5
B65946	369, 370	P core half 68 × 14,5 clf., P core half 70 × 14,5 clf.
B65947	367	PS core 35 × 10,8
B65949	371	P core half 150 × 30
B66202	392, 395	E 13/7/4 coil former, yoke
B66206	405, 406, 408	E 20/10/6 coil former, yoke
B66208	412, 414	E 25/13/7 coil former, yoke
B66219	396	E 14/8/4 core
B66229	419	E 32/16/9 core
B66230	420	E 32/16/9 coil former, yoke
B66232	417	E 30/15/7 coil former, yoke
B66233	421	E 32/16/11 core
B66243	428	E 42/21/20 coil former
B66281	437, 438	ELP14/3,5/5 core, I 14/1,5/5 core
B66283	439, 440	ELP18/4/10 core, I 18/2/10 core
B66285	443, 444	ELP 22/6/16 core, I 22/2,5/16 core
B66287	447, 448	ELP 32/6/20 core, I 32/3/20 core
B66288	447	ELP 32/6/20 clamp
B66289	451, 452	ELP 38/8/25 core, I 38/4/25 core
B66291	455, 456	ELP 43/10/28 core, I 43/4/28 core
B66293	459, 460	ELP 58/11/38 core, I 58/11/38 core
B66295	461, 462	ELP 64/10/50 core, I 64/5/50 core
B66300	385	E 6,3 core
B66301	386	E 6,3 coil former (SMD), cover cap
B66302	387, 388	E 8,8 core, coil former (SMD), cover cap
B66303	384	E 5 core
B66305	390	E 13/7/4 core
B66306	394	E 13/7/4 coil former (SMD)
B66307	397	E 16/8/5 core
B66308	399	E 16/8/5 coil former, yoke

Index of Part Numbers

Part number	Page	Type
B66311	403	E 20/10/6 core
B66314	409	E 21/9/5 core
B66315	415	E 25,4/10/7 core
B66317	410	E 25/13/7 core
B66319	416	E 30/15/7 core
B66322	389	E 10/5,5/5 core
B66325	426	E 42/21/15 core
B66329	427	E 42/21/20 core
B66335	430	E 55/28/21 core
B66337	500	EC 35/17/10 core
B66339	501	EC 41/20/12 core
B66341	502	EC 52/24/14 core
B66343	503	EC 70/35/16 core
B66344	431	E 55/28/25 core
B66347	471	ER 42/22/15 core
B66348	472	ER 42/22/15 coil former
B66350	470	ER 35/20/11 core
B66357	475	ER 54/18/18 core
B66358	477	ETD 29/16/10 core
B66359	479, 480	ETD 29/16/10 coil former, yoke
B66361	481	ETD 34/17/11 core
B66362	483, 484	ETD 34/17/11 coil former, yoke
B66363	485	ETD 39/20/13 core
B66364	487	ETD 39/20/13 coil former, yoke
B66365	488	ETD 44/22/15 core
B66366	490	ETD 44/22/15 coil former, yoke
B66367	491	ETD 49/25/16 core
B66368	493	ETD 49/25/16 coil former, yoke
B66370	422	E 34/14/9 core
B66371	434	E 70/33/32 core
B66375	435	E 80/38/20 core
B66377	473	ER 46/17/18 core
B66379	402	E 19/8/5 core
B66381	425	E 40/16/12 core
B66383	429	E 47/20/16 core
B66385	432	E 56/24/19 core
B66387	433	E 65/32/27 core
B66389	423	E 36/18/11 core

Part number	Page	Type
B66390	424	E 36/18/11 coil former
B66391	474	ER 49/27/17 core
B66393	401	E 16/6/5 core
B66395	494	ETD 54/28/19 core
B66396	496	ETD 54/28/19 coil former, yoke
B66397	497	ETD 59/31/22 core
B66398	499	ETD 59/31/22 coil former, yoke
B66399	520	DE 28 core
B66408	517	EV 25/13/13 core
B66409	521	DE 35 core
B66411	506	EFD 10/5/3 core
B66413	507	EFD 15/8/5 core
B66414	508, 509, 395	EFD 15/8/5 coil former, yoke, cover plate, E 13/7/4 cover plate
B66417	510	EFD 20/10/7 core
B66418	511	EFD 20/10/7 coil former, yoke
B66421	512	EFD 25/13/9 core
B66422	513	EFD 25/13/9 coil former, yoke
B66423	514	EFD 30/15/9 core
B66424	515	EFD 30/15/9 coil former, yoke
B66426	519	DE 24 core
B66432	518	EV 30/16/3 core
B66433	469	ER 28/17/11 core
B66434	516	EV 15/9/7 core
B66453	441, 442	ELP 18/4/10 core, I 18/2/10 core
B66455	445, 446	ELP 22/6/16 core, I 22/2,5/16 core
B66457	449, 450	ELP 32/6/20 core, I 32/3/20 core
B66459	453, 454	ELP 38/8/25 core, I 43/4/25 core
B66461	457, 458	ELP 43/10/28 core, I 43/4/28 core
B67345	524	U 93/76/16, UI 93/104/16 cores
	525	U 93/76/20, UI 93/104/20 cores
	526	U 93/76/30, UI 93/104/30 cores
B67370	527	U 101/76/30 core
B67374	528	U 141/78/30 core
B68450	562	FPC film
B68451	562	FPC film
B68452	562	FPC film

Based on IEC 60401, the data specified here are typical data for the material in question, which have been determined principally on the basis of toroids (ring cores).

The purpose of such characteristic material data is to provide the user with improved means for comparing different materials.

There is no direct relationship between characteristic material data and the data measured using other core shapes and/or core sizes made of the same material. In the absence of further agreements with the manufacturer, only those specifications given for the core shape and/or core size in question are binding.

1 Material application survey

Usage	Frequency range	Material	Specific application	Core type
High Q inductors in resonant circuits and filters	up to 0,1 MHz	N 48	Filters in telephony, MW IF filters	Gapped P and RM cores, adjusting cores
	0,2 – 1,6 MHz	M 33		
	1,5 – 12 MHz	K 1		
Broadband transformers (e.g. antenna transformers, ISDN transformers, digital data transformers (xDSL, LAN)	up to 3 MHz	T 56	Impedance and matching transformers (ISDN, xDSL using paired core shapes with air gap)	Toroids
		T 46		
		T 42		EP, RM, TT/PR, toroids
		T 38		
	up to 5 MHz	N 26	Radio-frequency transformers	Double aperture, toroids
	up to 10 MHz	M 33		
	up to 100 MHz	T 57	LAN (also suitable for xDSL in paired core shapes)	Toroids
	up to 100 MHz	M 33	Balun transformers	Double aperture, toroids
		K 1		
Electromagnetic Interference (EMI)	up to 3 MHz	T 38	Current-compensated chokes	DE, toroids
		T 37		
		T 35		
		T 65		
	up to 5 MHz	N 30		
	up to 100 MHz	M 13	Line attenuation, current-compensated chokes	Toroids
		K 6		
		K 7		
		K 8		
		K 10		
Sensors, ID systems	up to 1 MHz	N 22	Inductive proximity switches	P core halves
	up to 2 MHz	M 33		
	up to 100 MHz	FPC		

Usage	Frequency range	Material	Specific application	Core type
Medium and high frequency switch-mode power supplies	up to 100 kHz	N 27	Power transformers and chokes	E, ETD, ER, EFD, EV, ELP, RM, RM LP, PM
	up to 500 kHz	N 87		
		N 97		
	300 kHz to 1 MHz	N 49		
	up to 100 kHz	N 41	Chokes	E, ETD, ER, EFD, EV, ELP, RM, RM LP, PM
	up to 500 kHz	N 92	High voltage transformers and power chokes	
	up to 200 kHz	N 72	Electronic lamp ballast devices	E, ETD

LP = Low Profile

2 Material properties

Preferred application			Resonant Circuit inductors			Inductors for line attenuation	
Material			K 1	M 33[1)]	N 48	K 10	K 8
Base material			NiZn	MnZn	MnZn	NiZn	NiZn
Color code (adjuster)			violet	white	—	—	—
	Symbol	Unit					
Initial permeability (T = 25 °C)	μ_i		80 ± 25 %	750 ± 25 %	2300 ± 25 %	800 ± 25 %	860 ± 25 %
Meas. field strength Flux density (near saturation) (f = 10 kHz)	H B_S (25 °C) B_S (100 °C)	A/m mT mT	5000 310 280	2000 400 310	1200 420 310	5000 320 240	1200 340 240
Coercive field strength (f = 10 kHz)	H_c (25 °C) H_c (100 °C)	A/m A/m	380 350	80 65	26 19	40 25	40 25
Optimum frequency range	f_{min} f_{max}	MHz	1,5 … 12	0,2 … 1,0	0,001 … 0,1	0,1 … 1	0,1 … 0,5
Relative loss factor at f_{min} at f_{max}	tan δ/μ_i	10^{-6} 10^{-6}	< 40 < 120	< 12 < 20	< 2,7 < 4,2	< 15 < 60	< 20 < 30
Hysteresis material constant	η_B	10^{-6}/mT	< 36	< 1,8	< 0,4	< 5	< 4,5
Curie temperature	T_C	°C	> 400	> 200	> 170	> 150	> 150
Relative temperature coefficient at 25 ... 55 °C at 5 ... 25 °C	α_F	10^{-6}/K	 2 ... 8 7 ... 1	 0,5 ... 2,6 —	 0,3 ... 1,3 0,3 ... 1,3	 — —	 — —
Mean value of α_F at 25 ... 55 °C		10^{-6}/K	4	1,6	0,70	10,0	9,2
Density (typical values)		kg/m^3	4650	4500	4700	5000	5100
Disaccommodation factor at 25 °C	DF	10^{-6}	20	8	2	—	—
Resistivity	ρ	Ωm	10^5	5	3	10^5	10^5
Core shapes			RM, P, Toroid, P core half	RM, P, Toroid, Double-aperture, P core-half	RM, P	Toroid, Double-aperture	Toroid
Other material properties (graphs) see page			50	57	70	55	54

1) For threaded cores μi = 600 ± 20%

Material properties (continued)

Preferred application			Inductors for line attenuation			Proximity switch
Material			K 6	K 7	M 13	N 22
Base material			NiZn	NiZn	NiZn	MnZn
Color code (adjuster)			—	—	—	red
	Symbol	Unit				
Initial permeability (T = 25 °C)	μ_i		1000 ± 25 %	1500 ± 25 %	2300 ± 25 %	2300 ± 25 %
Meas. field strength Flux density (near saturation) (f = 10 kHz)	H B_S (25 °C) B_S (100 °C)	A/m mT mT	1200 270 180	1200 280 150	1200 280 135	1200 370 260
Coercive field strength (f = 10 kHz)	H_c (25 °C) H_c (100 °C)	A/m A/m	43 32	24 17	12 8	18 14
Optimum frequency range	f_{min} f_{max}	MHz	0,1 … 0,5	0,1 … 0,5	0,001 … 0,1	0,001 … 0,2
Relative loss factor at f_{min} at f_{max}	tan δ/μ_i	10^{-6} 10^{-6}	< 20 < 40	< 15 < 60	< 5 < 20	< 2 < 20
Hysteresis material constant	η_B	10^{-6}/mT	< 4,0	< 4,0	< 4,0	< 1,4
Curie temperature	T_C	°C	> 130	> 110	> 105	> 145
Relative temperature coefficient at 25 ... 55 °C at 5 ... 25 °C	α_F	10^{-6}/K	 — —	 — —	 — —	 — —
Mean value of α_F at 25 ... 55 °C		10^{-6}/K	3,7	3,5	3,7	0,9
Density (typical values)		kg/m^3	5100	5150	5200	4700
Disaccommodation factor at 25 °C	DF	10^{-6}	—	—	—	4
Resistivity	ρ	Ωm	10^7	$5 \cdot 10^6$	10^5	1
Core shapes			Toroid	Toroid	Toroid, Double-aperture	P core half
Other material properties (graphs) see page			52	53	56	59

Material properties (continued)

Preferred application			Broadband transformers			
Material			N 26	T 57	N 30	T 65
Base material			MnZn	MnZn	MnZn	MnZn
	Symbol	Unit				
Initial permeability (T = 25 °C)	μ_i		2300 ± 25 %	4000 ± 25 %	4300 ± 25 %	5200 ± 30 %
Meas. field strength Flux density (near saturation) (f = 10 kHz)	H B_S (25 °C) B_S (100 °C)	A/m mT mT	1200 380 260	1200 430 270	1200 380 240	1200 460 320
Coercive field strength (f = 10 kHz)	H_c (25 °C) H_c (100 °C)	A/m A/m	23 17	14 12	12 8	12 11
Optimum frequency range	f_{min} f_{max}	MHz	0,001 … 0,1	0,01 … 0,5	0,01 … 0,40	0,01 … 0,20
Relative loss factor at f_{min} at f_{max}	tan δ/μ_i	10^{-6} 10^{-6}	< 2,8 < 3,8	< 5 < 70	< 2 < 60	< 1,5 < 25
Hysteresis material constant	η_B	10^{-6}/mT	< 0,3	< 0,3	< 1,1	< 1,1
Curie temperature	T_C	°C	> 130	> 140	> 130	> 160
Relative temperature coefficient at 25 ... 55 °C at 5 ... 25 °C	α_F	10^{-6}/K	 0 … 1,5 0 … 1,8	 — —	 — —	 — —
Mean value of α_F at 25 ... 55 °C		10^{-6}/K	1,0	0,5	0,6	– 0,5
Density (typical values)		kg/m^3	4700	4930	4800	4930
Disaccommodation factor at 25 °C	DF	10^{-6}	—	—	—	—
Resistivity	ρ	Ωm	2	3	0,5	0,30
Core shapes			RM, P, EP	RM, P, EP, Toroid	RM, P, EP, E, Toroid, Double-aperture	RM, P, Toroid, EP
Other material properties (graphs) see page			60	102	65	104

Material properties (continued)

Preferred application			Broadband transformers		
Material			T 35	T 37	T 38[1)]
Base material			MnZn	MnZn	MnZn
	Symbol	Unit			
Initial permeability (T = 25 °C)	μ_i		6000 ± 25 %	6500 ± 25 %	10000 ± 30 %
Meas. field strength Flux density (near saturation) (f = 10 kHz)	H B_S (25 °C) B_S (100 °C)	A/m mT mT	1200 390 270	1200 380 240	1200 430 260
Coercive field strength (f = 10 kHz)	H_c (25 °C) H_c (100 °C)	A/m A/m	12 9	9 8	8 7
Optimum frequency range	f_{min} f_{max}	MHz	0,01 … 0,20	0,01 … 0,30	0,01 … 0,10
Relative loss factor at f_{min} at f_{max}	tan δ/μ_i	10^{-6} 10^{-6}	< 4 < 60	< 2 < 60	< 2,0 < 20
Hysteresis material constant	η_B	10^{-6}/mT	< 1,1	< 1,1	< 0,3
Curie temperature	T_C	°C	> 130	> 130	> 130
Relative temperature coefficient at 25 ... 55 °C at 5 ... 25 °C	α_F	10^{-6}/K	 — —	 — —	 — —
Mean value of α_F at 25 ... 55 °C		10^{-6}/K	0,8	– 0,3	– 0,2
Density (typical values)		kg/m^3	4900	4900	4950
Disaccommodation factor at 25 °C	DF	10^{-6}	—	—	—
Resistivity	ρ	Ωm	0,2	0,2	0,1
Core shapes			RM, P, EP, Toroid	Toroid, DE	RM, P, EP, ER, Toroid, TT/PR, E
Other material properties (graphs) see page			90	92	94

1) Improved, new data

Material properties (continued)

Preferred application			Broadband transformers		
Material			T 42[1)]	T 46[1)]	T 56[1)]
Base material			MnZn	MnZn	MnZn
	Symbol	Unit			
Initial permeability (T = 25 °C)	μ_i		12000 ± 30 %	15000 ± 30 %	20000 ± 30 %
Meas. field strength Flux density (near saturation) (f = 10 kHz) (f = 10 kHz)	H B_S (25 °C) B_S (100 °C)	A/m mT mT	1200 400 250	1200 400 240	400 350 250
Coercive field strength (f = 10 kHz)	H_c (25 °C) H_c (100 °C)	A/m A/m	7 6	7 6	6 5
Optimum frequency range	f_{min} f_{max}	MHz	0,01 … 0,10	0,01 … 0,10	0,01 … 0,10
Relative loss factor at f_{min} at f_{max}	tan δ/μ_i	10^{-6} 10^{-6}	< 2 < 20	< 8 < 100	< 10 < 60
Hysteresis material constant	η_B	10^{-6}/mT	< 1,4	< 2,0	< 1,5
Curie temperature	T_C	°C	> 130	> 130	> 90
Relative temperature coefficient at 25 ... 55 °C at 5 ... 25 °C	α_F	10^{-6}/K	 — —	 — —	 — —
Mean value of α_F at 25 ... 55 °C		10^{-6}/K	– 0,3	– 0,6	0,22
Density (typical values)		kg/m^3	4950	5000	5040
Disaccommodation factor at 25 °C	DF	10^{-6}	—	—	—
Resistivity	ρ	Ωm	0,1	0,01	0,1
Core shapes			RM, EP	Toroid	Toroid
Other material properties (graphs) see page			96	98	100

1) Material values defined on the basis of small toroids (≤ R10)

Material properties (continued)

Preferred application			Power transformers			
Material			N 49[1]	N 92	N 27	N 67[2]
Base material			MnZn	MnZn	MnZn	MnZn
	Symbol	Unit				
Initial permeability (T = 25 °C)	μ_i		1500 ± 25 %	1500 ± 25 %	2000 ± 25 %	2100 ± 25 %
Flux density (H = 1200 A/m, f = 10 kHz)	B_S (25 °C) B_S (100 °C)	mT mT	490 400	500 440	500 410	480 380
Coercive field strength (f = 10 kHz)	H_c (25 °C) H_c (100 °C)	A/m A/m	38 33	24 13	23 19	20 14
Typical frequency range		kHz	300 … 1000	25 … 500	25 … 150	25 … 300
Hysteresis material constant	η_B	10^{-6}/mT	< 0,4	< 1,4	< 1,5	< 1,4
Curie temperature	T_C	°C	> 240	> 280	> 220	> 220
Mean value of α_F at 25 … 55 °C		10^{-6}/K	—	—	3	4
Density (typical values)		kg/m³	4800	4850	4750	4800
Relative core losses (typical values)	P_V					
25 kHz, 200 mT, 100 °C		kW/m³	—	70	155	80
100 kHz, 200 mT, 100 °C		kW/m³	—	410	920	525
300 kHz, 100 mT, 100 °C		kW/m³	330	410	—	560
500 kHz, 50 mT, 100 °C		kW/m³	80	230	—	—
1 MHz, 50 mT, 100 °C		kW/m³	475	—	—	—
Resistivity	ρ	Ωm	17	8	3	6
Core shapes			RM, EFD, ELP, Toroid	RM, ETD, EFD, ER, E, ELP, Toroid	P, PM, ETD, EC, ER, E, U, Toroid	ETD, EFD, E
Other material properties (graphs) see page			72	84	62	75

1) Improved, new data
2) Not for new design

Material properties (continued)

Preferred application			Power transformers			
Material			N 87[1)]	N 97	N 72	N 41
Base material			MnZn	MnZn	MnZn	MnZn
	Symbol	Unit				
Initial permeability (T = 25 °C)	μ_i		2200 ± 25 %	2300 ± 25 %	2500 ± 25 %	2800 ± 25 %
Flux density (H = 1200 A/m, f = 10 kHz)	B_S (25 °C) B_S (100 °C)	mT mT	490 390	510 410	480 370	490 390
Coercive field strength (f = 10 kHz)	H_c (25 °C) H_c (100 °C)	A/m	21 13	21 12	15 11	22 20
Typical frequency range		kHz	25 … 500	25 … 500	25 … 300	25 … 150
Hysteresis material constant	η_B	10^{-6}/mT	< 1,0	< 1,0	< 1,4	< 1,4
Curie temperature	T_C	°C	> 210	> 230	> 210	> 220
Mean value of α_F at 25 … 55 °C		10^{-6}/K	4	4	3	4
Density (typical values)		kg/m³	4850	4920	4800	4800
Relative core losses (typical values)	P_V					
25 kHz, 200 mT, 100 °C		kW/m³	57	45	80	180
100 kHz, 200 mT, 100 °C		kW/m³	375	300	540	1400
300 kHz, 100 mT, 100 °C		kW/m³	390	340	500	—
500 kHz, 50 mT, 100 °C		kW/m³	215	205	—	—
1 MHz, 50 mT, 100 °C		kW/m³	—	—	—	—
Resistivity	ρ	Ωm	10	8	12	2
Core shapes			RM, TT, P, PM, ETD, EFD, E, ER, ELP, U Toroid	RM, PM, ETD, EFD, ER, E, ELP, Toroid	E, EFD	RM, P
Other material properties (graphs) see page			81	87	78	67

1) Improved, new data

Material properties (continued)

Preferred application			Injection-molded parts	Film	
Material			Ferrite Polymer Composite (FPC)		
Base material			C302	C350	C351
	Symbol	Unit			
Initial permeability f = 1 MHz	μ_i		17 ± 20 %	9 ± 20 %	9 ± 20 %
Flux density (near saturation) H = 25 kA/m f = 10 kHz	B_S (25 °C)	mT	330	255	255
Remanent induction H = 25 kA/m f = 10 kHz	B_r (25 °C)	mT	15	9	9
Coercive field strength H = 25 kA/m f = 10 kHz	H_C (25 °C)	A/m	770	600	600
Relative loss factor f = 1 MHz f = 100 MHz f = 1 GHz	$\tan\delta/\mu_i$		 < 0,0004 < 0,03	 < 0,005 < 0,400	 < 0,005 < 0,400
Hysteresis material constant	η_B	10^{-3}/mT	< 0,25	< 2	< 2
Temperature coefficient	$\alpha=\Delta\mu/\mu\Delta T$	1/K	< 0,0002	$< 5 \cdot 10^{-5}$	$< 5 \cdot 10^{-5}$
Density		kg/m^3	3500	2930	2930
Resistivity f = 1 kHz f = 10 kHz f = 10 MHz	ρ	Ωm	 21 13	 500 100	 500 100
Relative permittivity f = 1 kHz f = 10 kHz f = 10 MHz	ε_r		 280 100	 700 21	 700 21
Maximum operating temperature	T_{max}	°C	180	120	200
Dielectric strength		kV/mm	—	1	0,8
Tensile strength[1)]	σ_Z	N/mm^2	—	1,5	2,5
Tearing resistance[1)]		%	—	25	25
Compressibility[1)]	κ	N/mm^2	—	70	70
Other material properties (graphs) see page			49	—	—

1) T = 23 °C and 50 % relative humidity

3 Measuring conditions

The following measuring conditions, which correspond largely to IEC 60401, apply for the material properties given in the table:

Properties (valid only for ring cores of sizes R 10 to R 36)			Measuring conditions			
			Frequency kHz	Field strength (material-dependent) kA/m	Max. flux density mT	Temper-ature °C
Initial permeability	μ_i		≤ 10		≤ 0,25	25
Flux density near to saturation	B	mT	≤ 10	≥ 1,2		25; 100
Coercive field strength	H_c	A/m kA/m	≤ 10	≥ 1,2	near saturation	25; 100
Relative loss factor	tan δ/μ_i		–		≤ 0,25	25
Hysteresis material constant	η_B	mT^{-1}	 10 ($\mu_i \geq 500$) 100 ($\mu_i < 500$)		B_1 B_2 1,5 3,0 0,3 1,2	25
Curie temperature	T_c	°C	≤ 10		≤ 0,25	
Relative temperature coefficient	α_F	10^{-6}/K	≤ 10		≤ 0,25	5 … 25 25 … 55
Density		kg/m^3				25
Disaccommodation factor	DF	10^{-6}	≤ 10		≤ 0,25	25; 60 [1)]
Resistivity	ρ	Ωm	DC			25

The following properties are given only for materials for power applications:

Power loss	P_V	kW/m^3	25 100 300 500 1000		200 200 100 50 50	100

1) Higher temperature than specified by IEC (40 °C)

4 Specific material data

DC magnetic bias

$$H_{\_} = \frac{I_{\_} \cdot N}{l_e}$$

$H_{\_}$ = DC field strength [A/m]
$I_{\_}$ = Direct current [A]
N = Number of turns
l_e = Effective magnetic path length [m]

The curves of $\mu_{rev} = f(H_{\_})$ allow an approximate calculation of the variation in reversible permeability (μ_{rev}) and A_L value caused by magnetic bias. These curves are of particular interest for cores for transformers and chokes, since magnetic bias should be avoided if possible with inductors requiring high stability (filter inductors etc.). In the case of geometrically similar cores (i.e. in particular the same A_{min}/A_e ratio) the effective permeability of the core in question in conjunction with the given curves suffices to determine the reversible permeability to a close approximation.

Relative loss factor versus frequency
(measured with ring cores, measuring flux density $\hat{B} \leq 0{,}25$ mT)

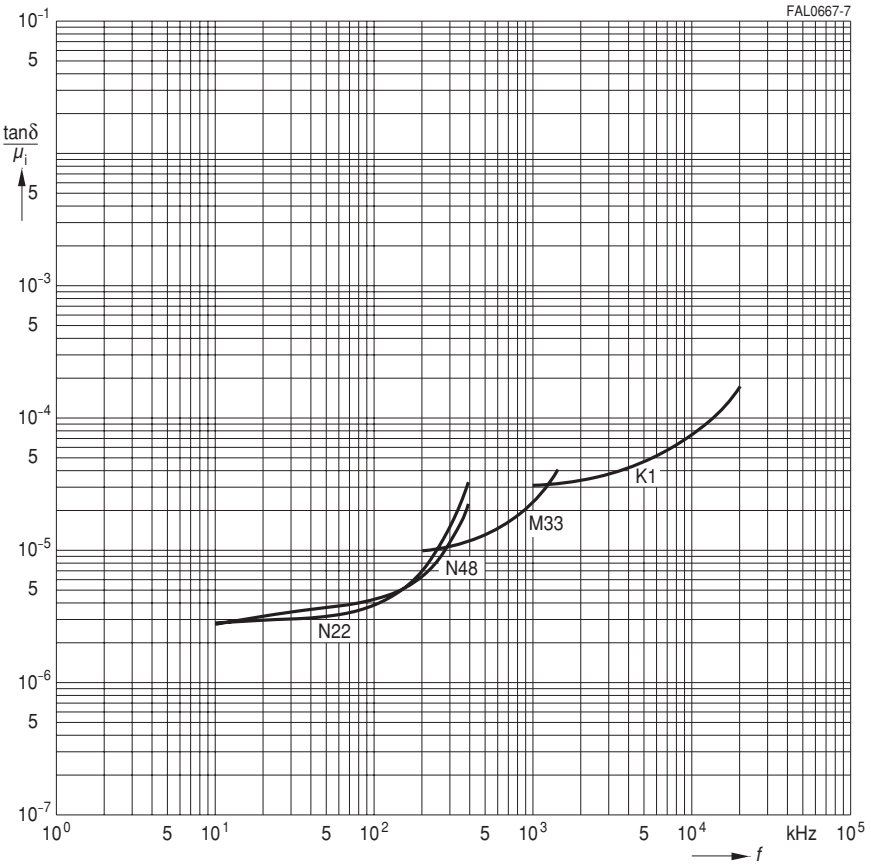

Relative inductance component versus frequency
(measured with ring cores, measuring flux density $\hat{B}$ ≤0,25 mT)

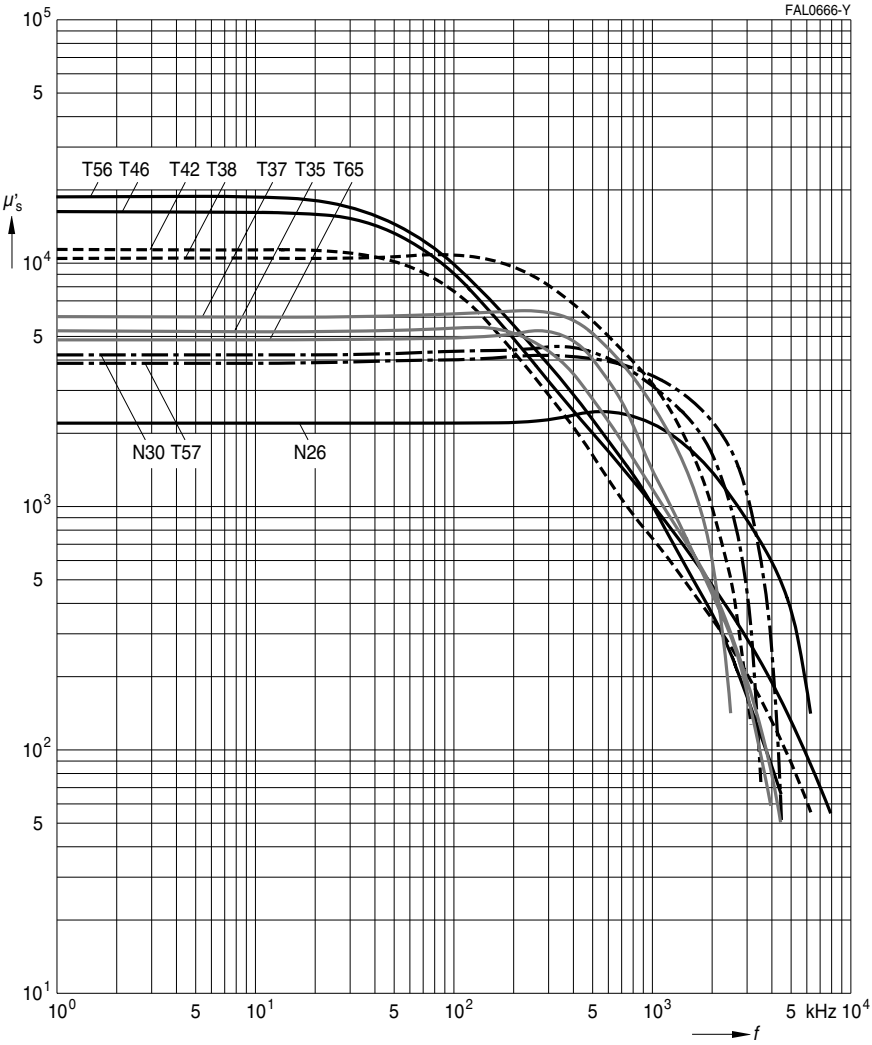

Performance factor versus frequency
(measured with ring cores R29, T = 100 °C, P_V = 300 kW/m³)

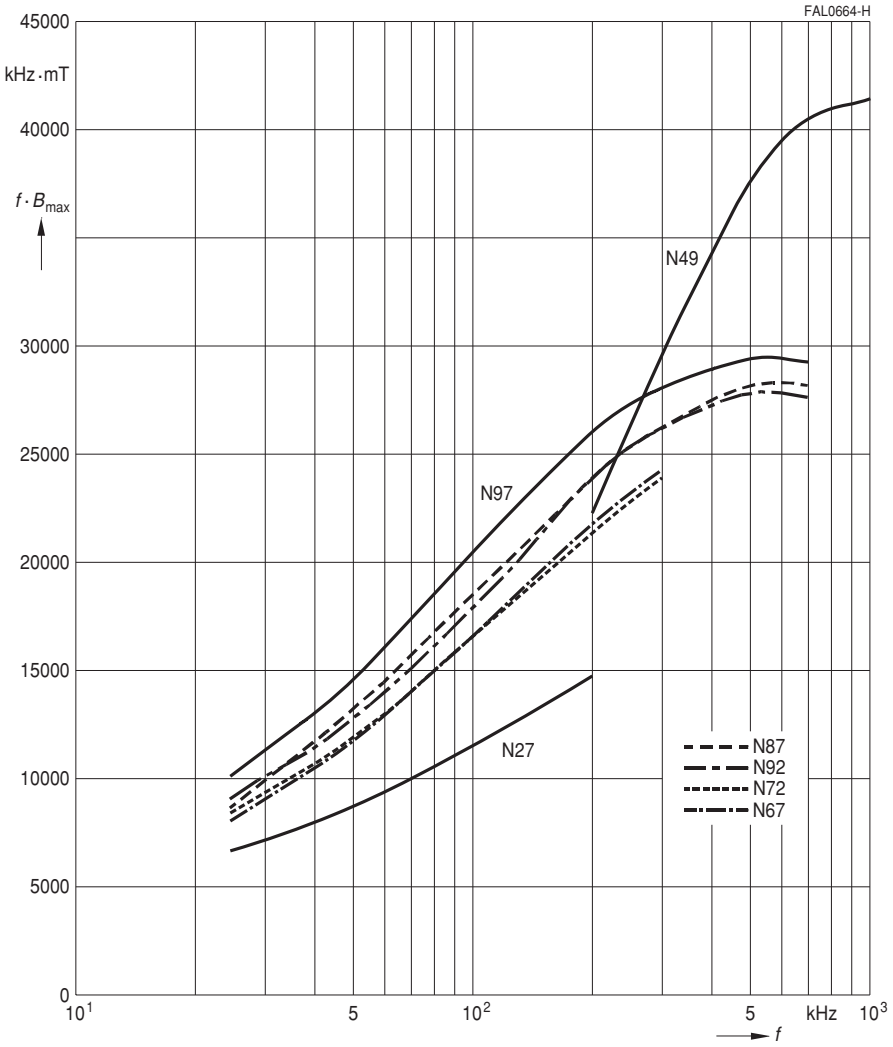

For definition of performance factor see page 116.

Standardized hysteresis material constant versus temperature

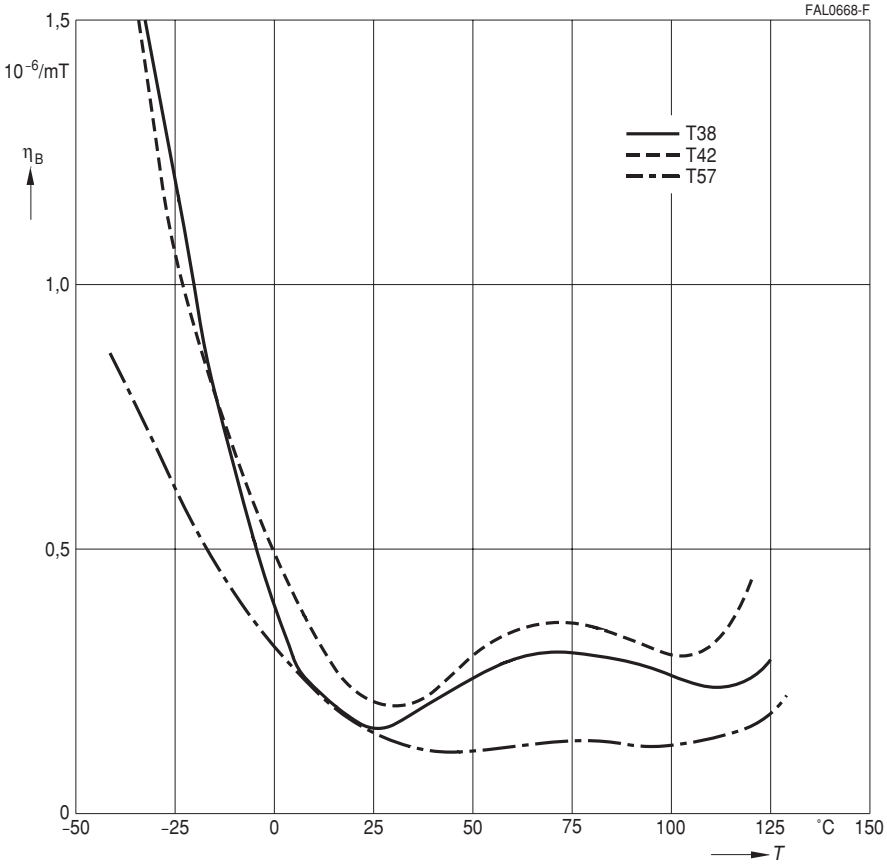

Normalized Impedance

K 1

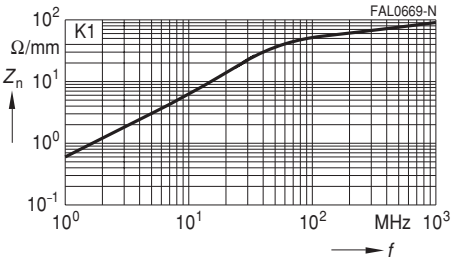

K 6

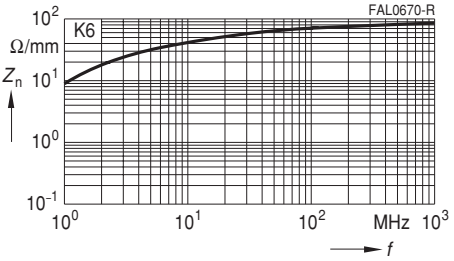

K 7

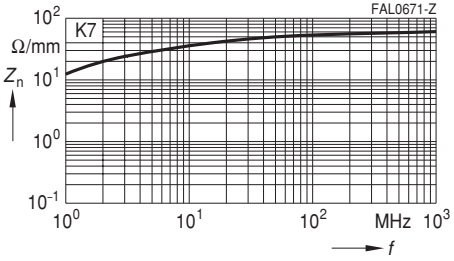

K 8

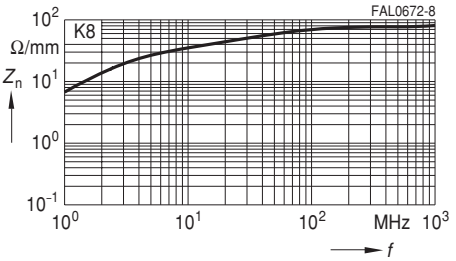

K 10

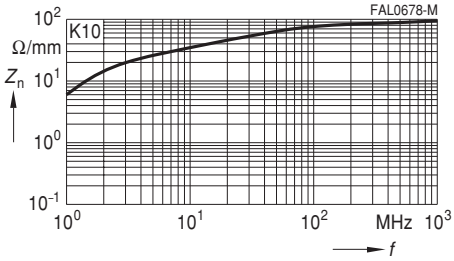

M 13

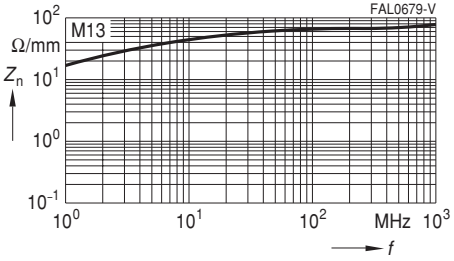

For explanation of Z_n see page 133.

Complex permeability versus frequency
(measured on R20/10 toroids, $\hat{B} \leq 0{,}25$ mT)

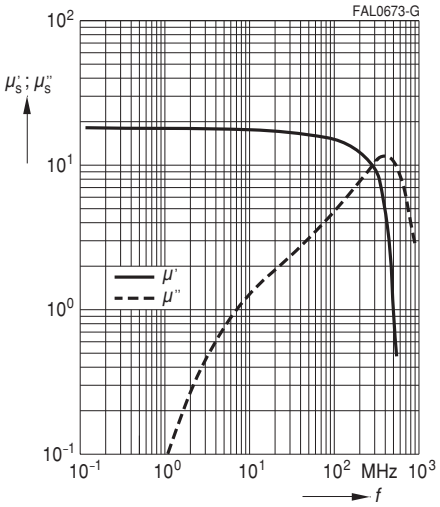

Relative loss factor versus frequeny
(measured on R20/10 toroids, $\hat{B} \leq 0{,}25$ mT)

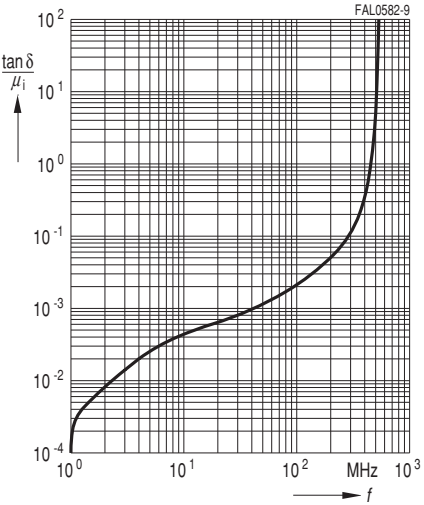

Complex permeability
versus frequency
(measured on R10 toroids, $\hat{B} \leq 0{,}25$ mT)

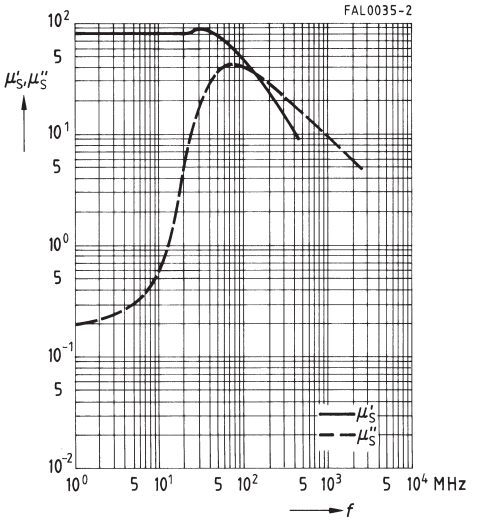

Initial permeability μ_i and relative loss factor
$\tan \delta / \mu_i$ versus temperature
(measured on R10 toroids, $\hat{B} \leq 0{,}25$ mT)

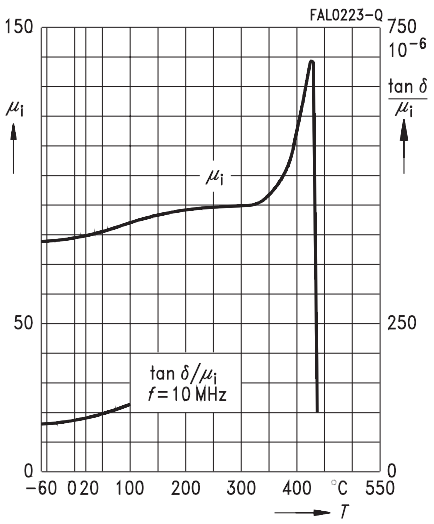

Permeability factor versus temperature
(measured on P and RM cores,
$\hat{B} \leq 0{,}25$ mT), $\mu_i \approx 80$

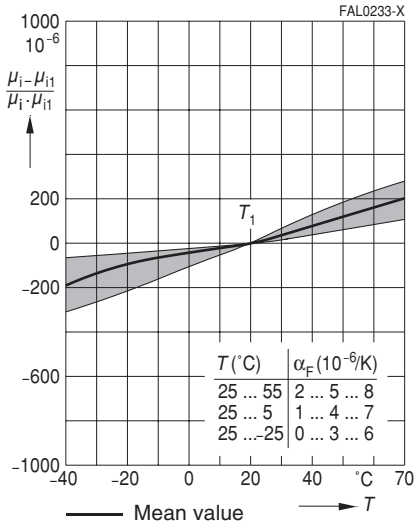

Dynamic magnetization curves
(typical values)
(f = 10 kHz, T = 25 °C)

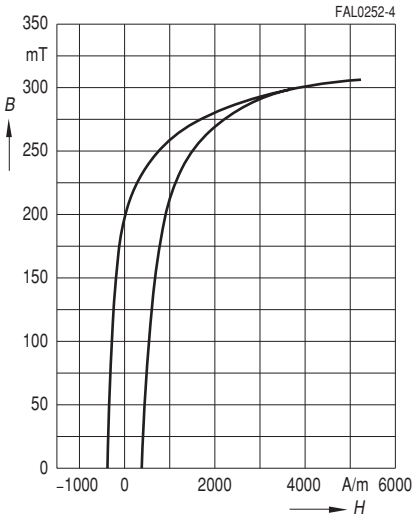

Dynamic magnetization curves
(typical values)
(f = 10 kHz, T =100 °C)

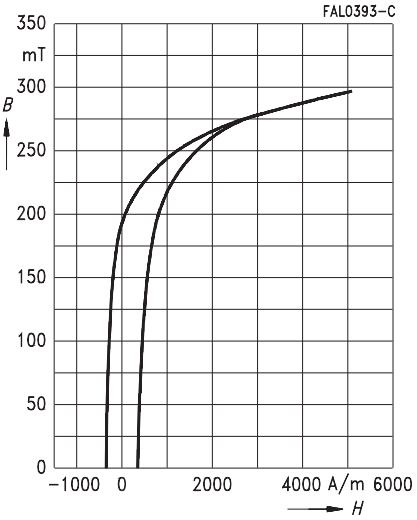

Complex permeability
versus frequency
(measured on R17 toroids, $\hat{B} \leq 0{,}25$ mT)

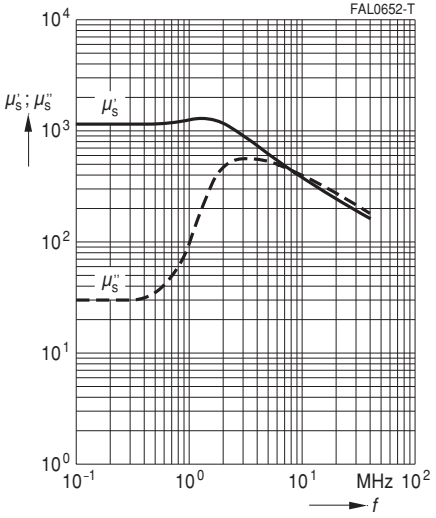

Initial permeability μ_i and relative loss factor
$\tan \delta / \mu_i$ versus temperature
(measured on R17 toroids, $\hat{B} \leq 0{,}25$ mT)

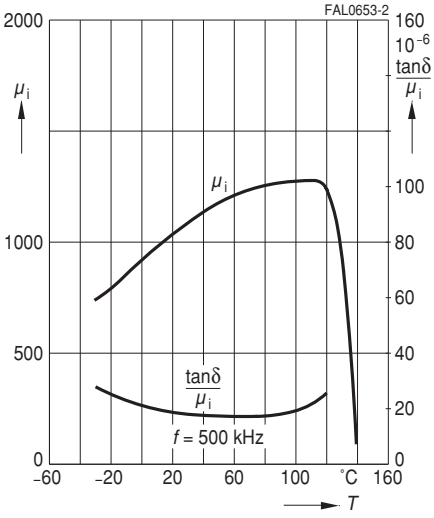

Dynamic magnetization curves
(typical values)
(f = 10 kHz, T = 25 °C)

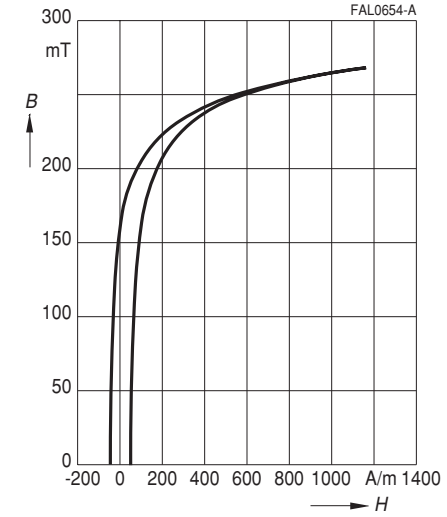

Dynamic magnetization curves
(typical values)
(f = 10 kHz, T =100 °C)

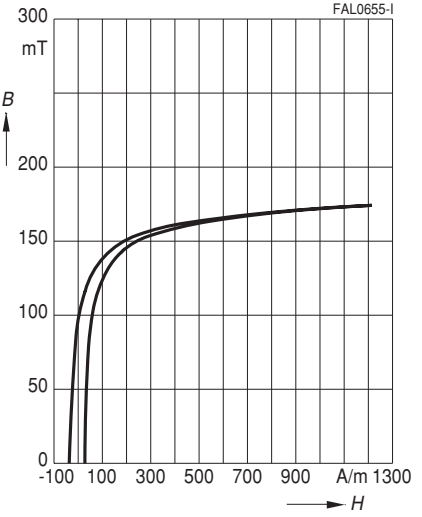

Complex permeability
versus frequency
(measured on R17 toroids, $\hat{B} \leq 0{,}25$ mT)

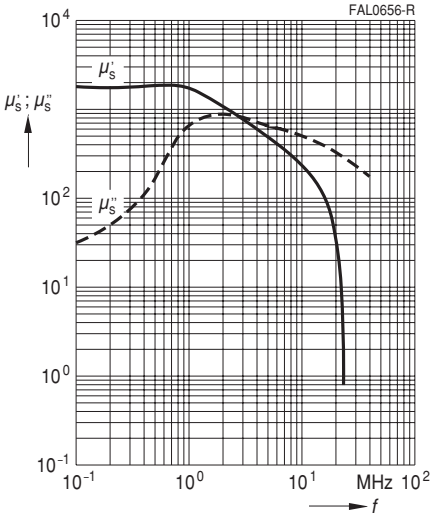

Initial permeability μ_i and relative loss factor
$\tan \delta / \mu_i$ versus temperature
(measured on R17 toroids, $\hat{B} \leq 0{,}25$ mT)

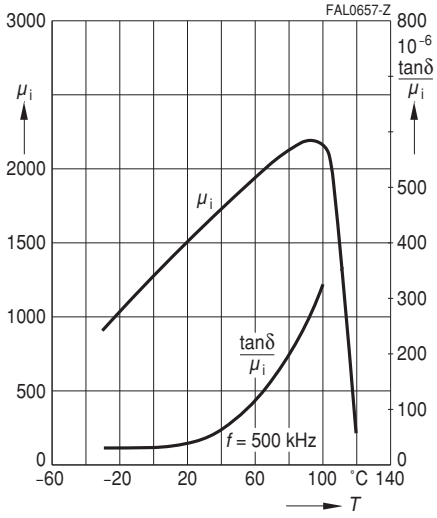

Dynamic magnetization curves
(typical values)
(f = 10 kHz, T = 25 °C)

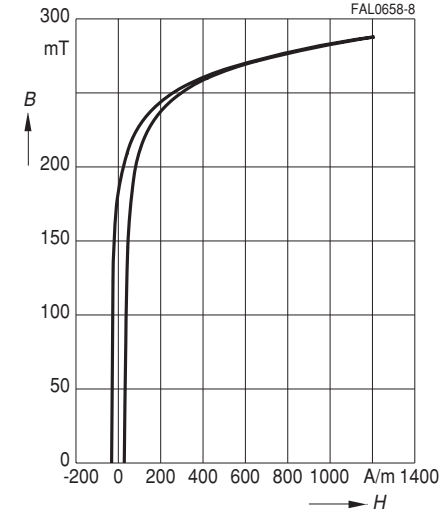

Dynamic magnetization curves
(typical values)
(f = 10 kHz, T =100 °C)

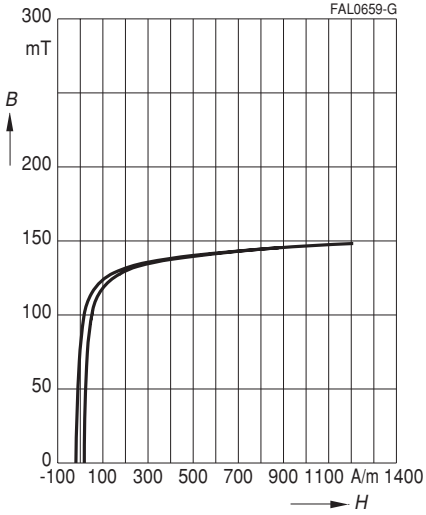

Complex permeability
versus frequency
(measured on R17 toroids, $\hat{B} \leq 0{,}25$ mT)

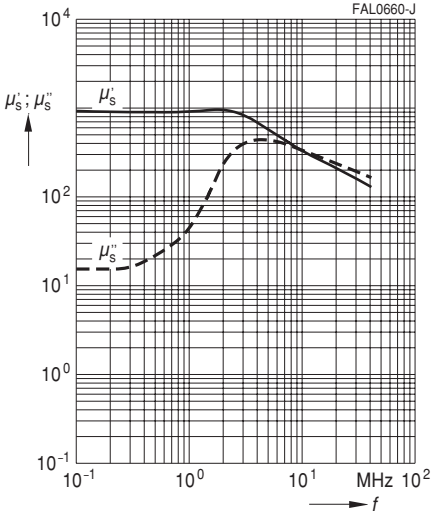

Initial permeability μ_i and relative loss factor
$\tan \delta/\mu_i$ versus temperature
(measured on R17 toroids, $\hat{B} \leq 0{,}25$ mT)

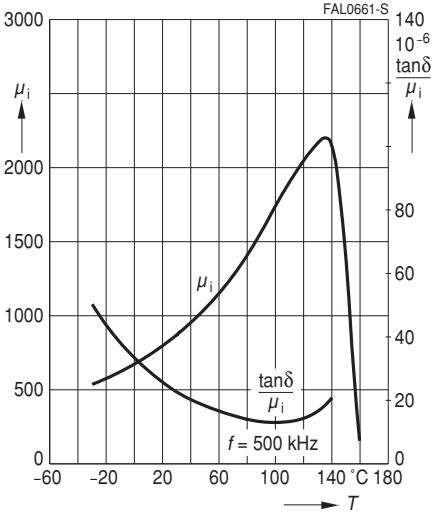

Dynamic magnetization curves
(typical values)
(f = 10 kHz, T = 25 °C)

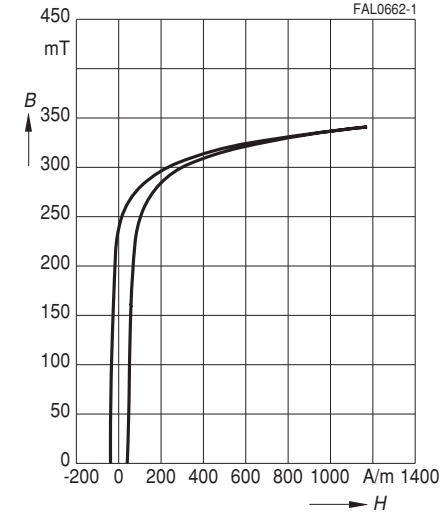

Dynamic magnetization curves
(typical values)
(f = 10 kHz, T =100 °C)

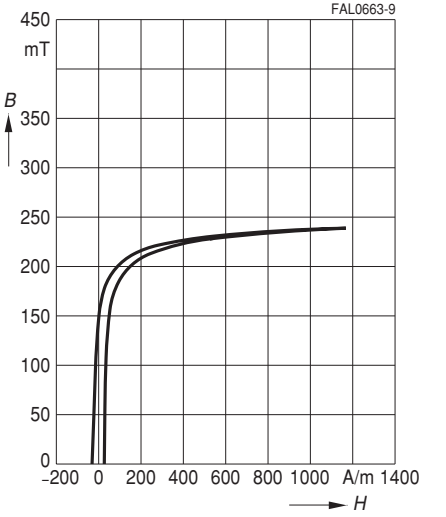

Complex permeability
versus frequency
(measured on R10 toroids, $\hat{B} \leq 0{,}25$ mT)

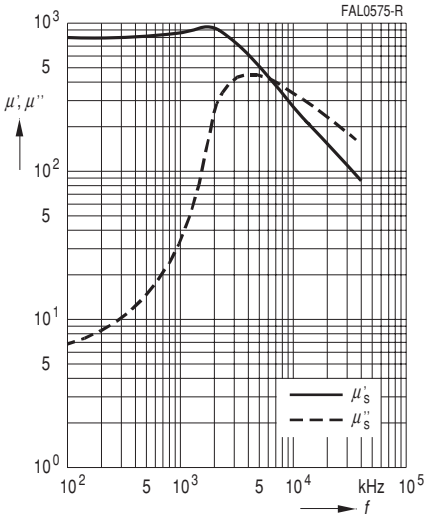

Initial permeability μ_i and relative loss factor
$\tan \delta / \mu_i$ versus temperature
(measured on R10 toroids, $\hat{B} \leq 0{,}25$ mT)

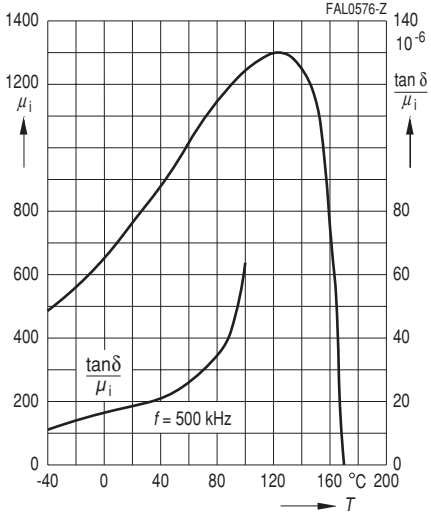

Dynamic magnetization curves
(typical values)
(f = 10 kHz, T = 25 °C)

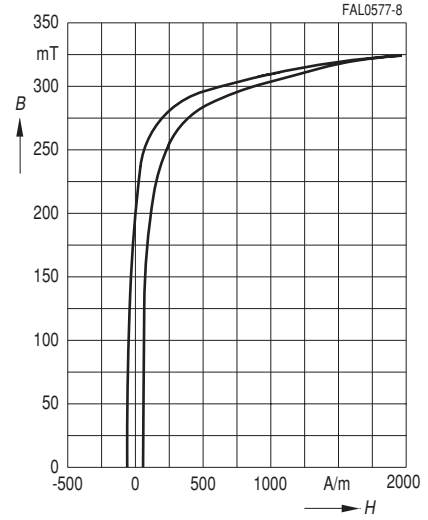

Dynamic magnetization curves
(typical values)
(f = 10 kHz, T = 100 °C)

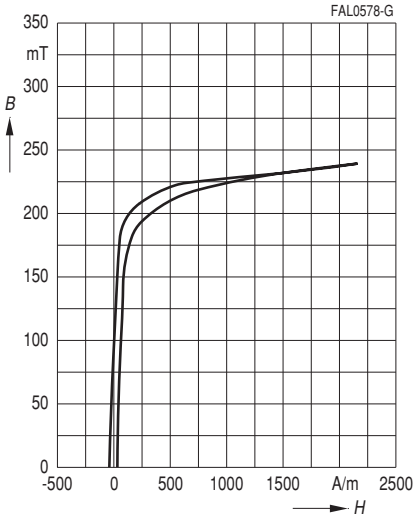

Complex permeability
versus frequency
(measured on R10 toroids, $\hat{B} \leq 0{,}25$ mT)

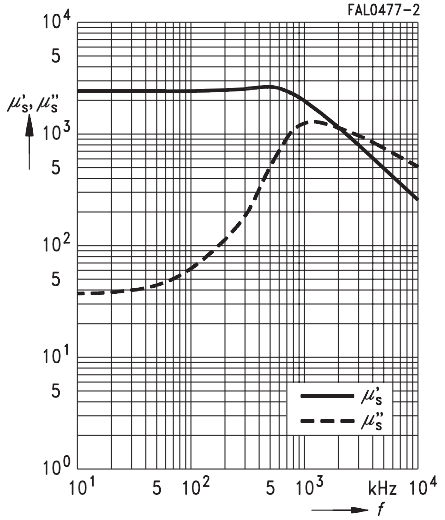

Initial permeability μ_i and relative loss factor
$\tan \delta/\mu_i$ versus temperature
(measured on R25 toroids, $\hat{B} \leq 0{,}25$ mT)

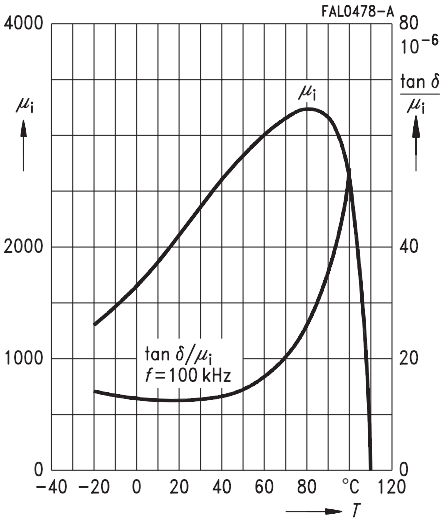

Dynamic magnetization curves
(typical values)
(f = 10 kHz, T = 25 °C)

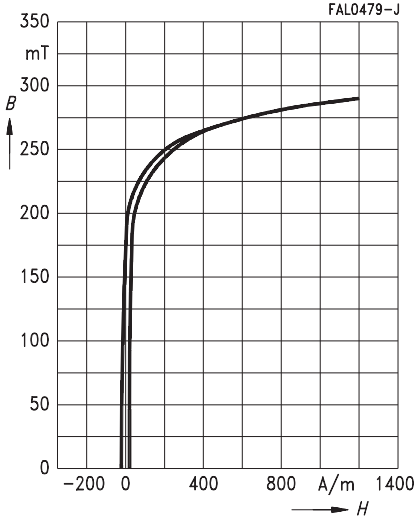

Dynamic magnetization curves
(typical values)
(f = 10 kHz, T = 100 °C)

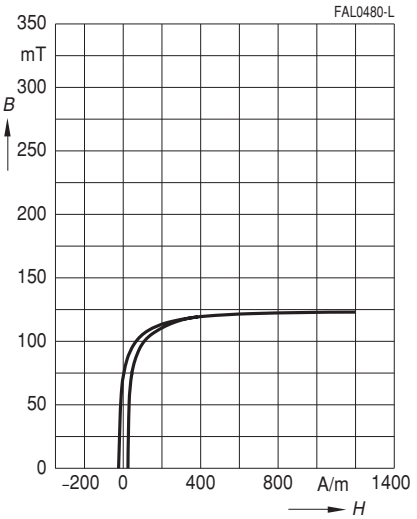

Complex permeability
versus frequency
(measured on R10 toroids, $\hat{B} \leq 0{,}25$ mT)

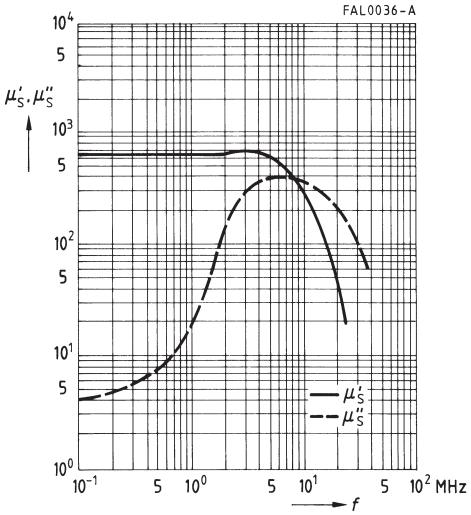

Initial permeability μ_i and relative loss factor
$\tan \delta/\mu_i$ versus temperature
(measured on R10 toroids, $\hat{B} \leq 0{,}25$ mT)

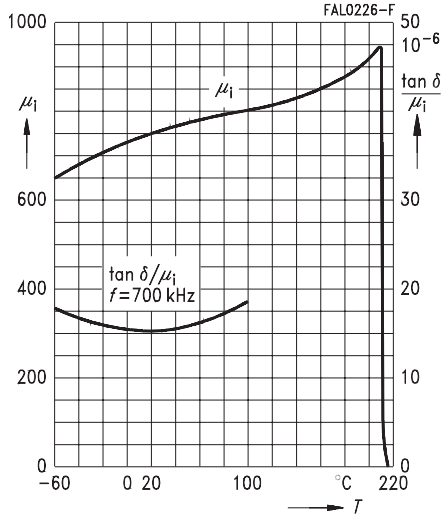

Permeability factor versus temperature
(measured on P and RM cores,
$\hat{B} \leq 0{,}25$ mT), $\mu_i \approx 750$

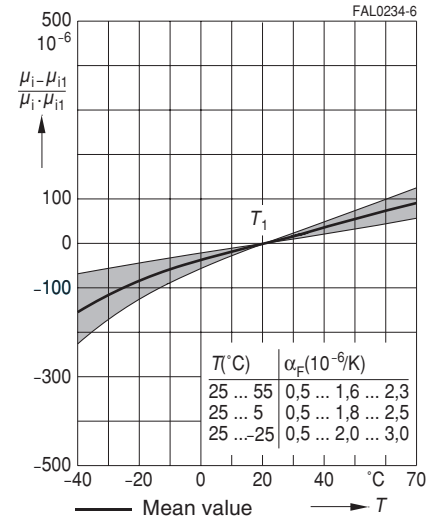

DC magnetic bias of P and RM cores
(typical values)
($\hat{B} \leq 0{,}25$ mT, f = 10 kHz, T = 25 °C)

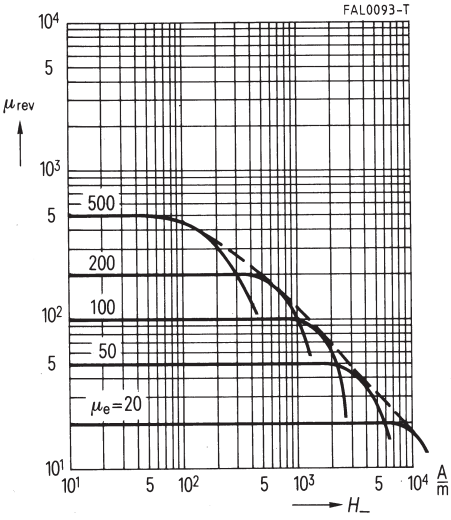

Dynamic magnetization curves
(typical values)
(f = 10 kHz, T = 25 °C)

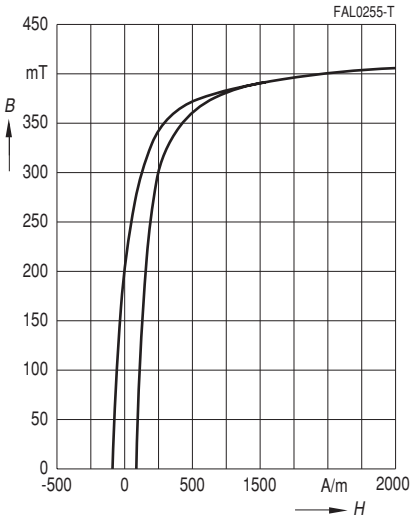

Dynamic magnetization curves
(typical values)
(f = 10 kHz, T = 100 °C)

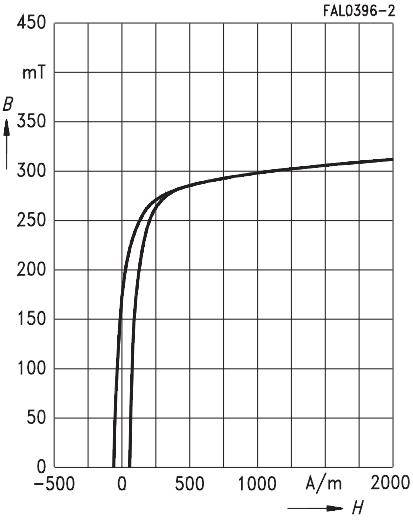

Complex permeability
versus frequency
(measured on R10 toroids, $\hat{B} \leq 0{,}25$ mT)

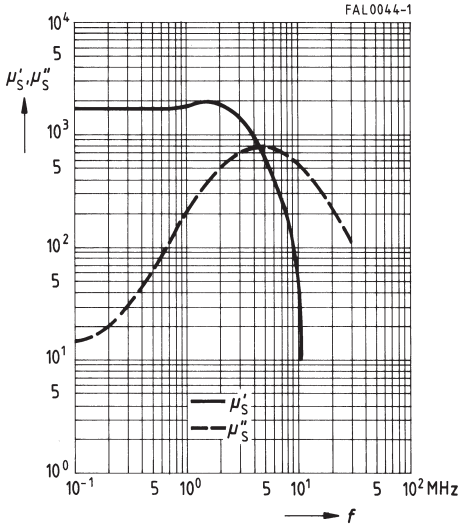

Initial permeability μ_i and relative loss factor
$\tan \delta / \mu_i$ versus temperature
(measured on R10 toroids, $\hat{B} \leq 0{,}25$ mT)

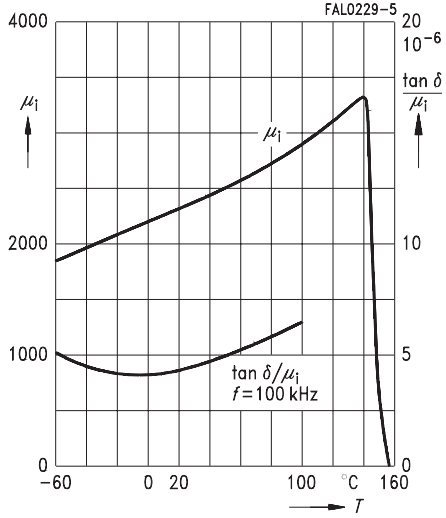

Dynamic magnetization curves
(typical values)
(f = 10 kHz, T = 25 °C)

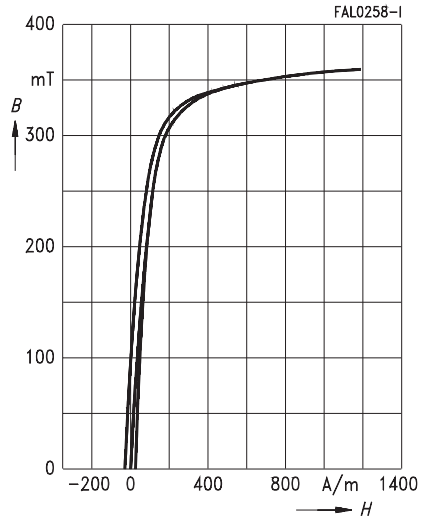

Dynamic magnetization curves
(typical values)
(f = 10 kHz, T = 100 °C)

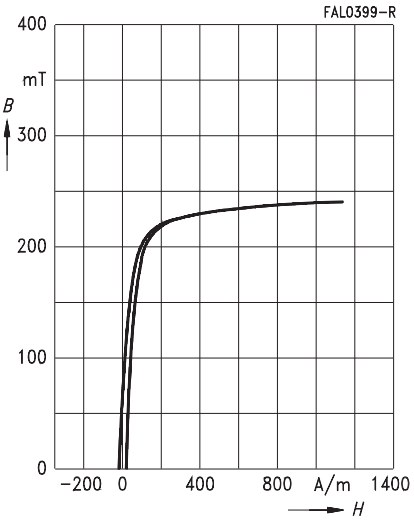

Complex permeability
versus frequency
(measured on R10 toroids, $\hat{B} \leq 0{,}25$ mT)

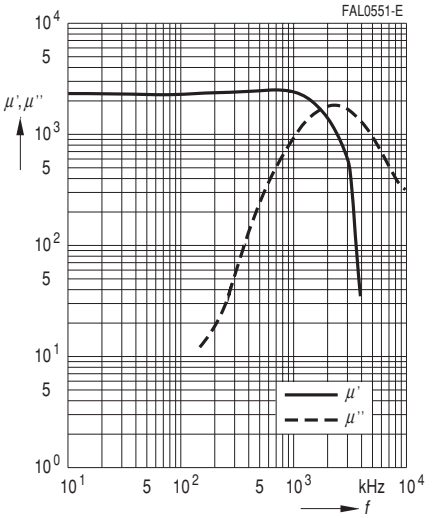

Initial permeability μ_i and relative los factor
$\tan \delta / \mu_i$ versus temperature
(measured on R10 toroids, $\hat{B} \leq 0{,}25$ mT)

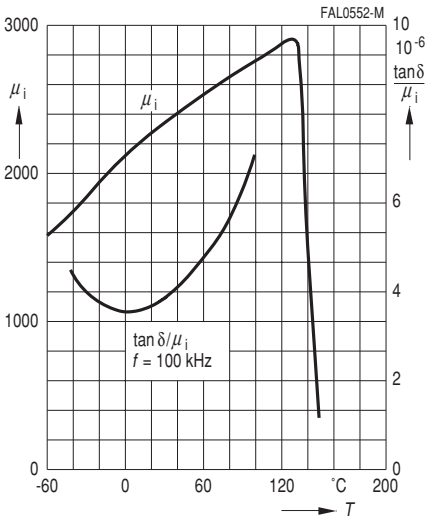

Permeability factor
versus temperature
(measured on R10 toroids, $\hat{B} \leq 0{,}25$ mT)

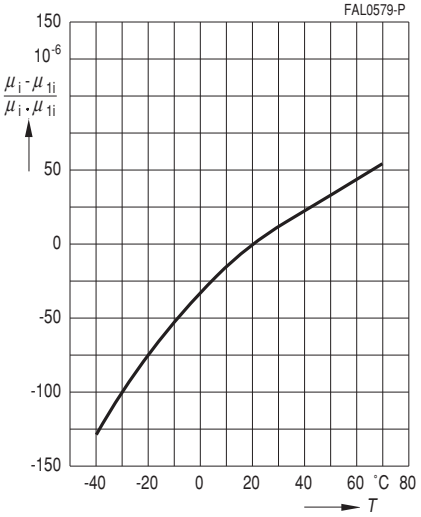

Relative loss factor
versus frequency
(measured on R14 toroids, $\hat{B} \leq 0{,}25$ mT)

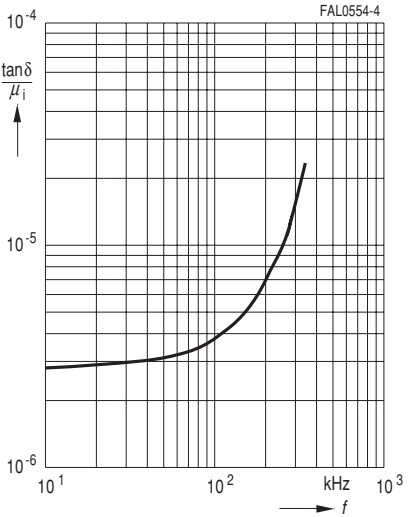

Dynamic magnetization curves
(typical values)
(f = 10 kHz, T = 25 °C)

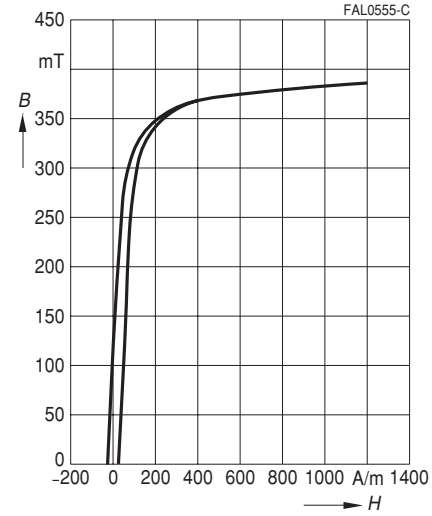

Dynamic magnetization curves
(typical values)
(f = 10 kHz, T = 100 °C)

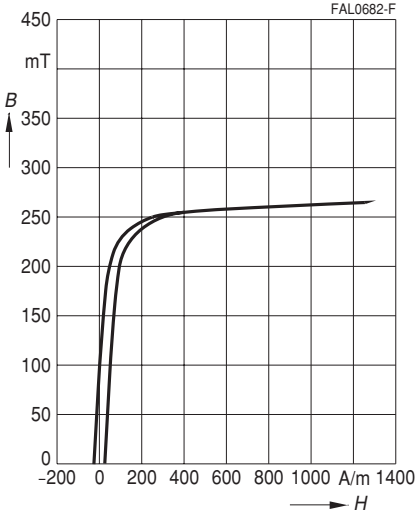

DC magnetic bias of P and RM cores
(typical values)
($\hat{B} \leq$ 0,25 mT, f = 10 kHz, T = 25 °C)

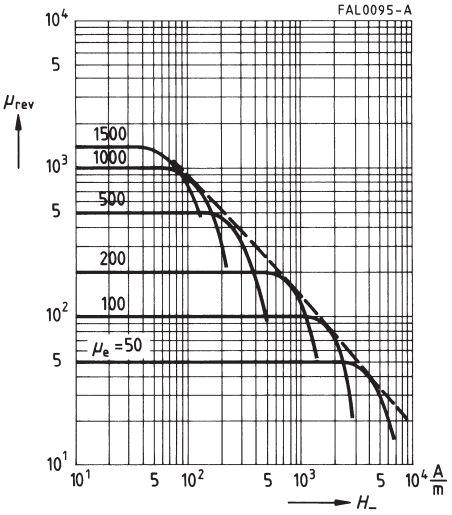

Complex permeability
versus frequency
(measured on R10 toroids, $\hat{B} \leq 0{,}25$ mT)

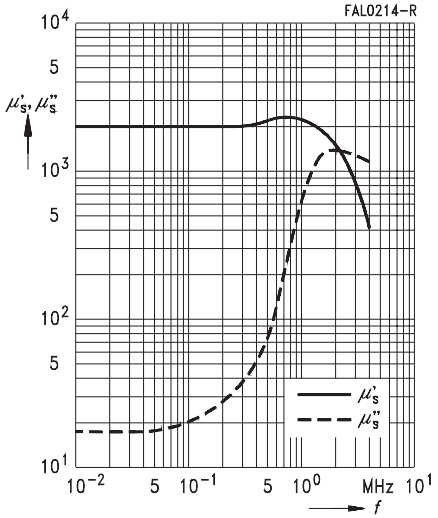

Initial permeability μ_i
versus temperature
(measured on R10 toroids, $\hat{B} \leq 0{,}25$ mT)

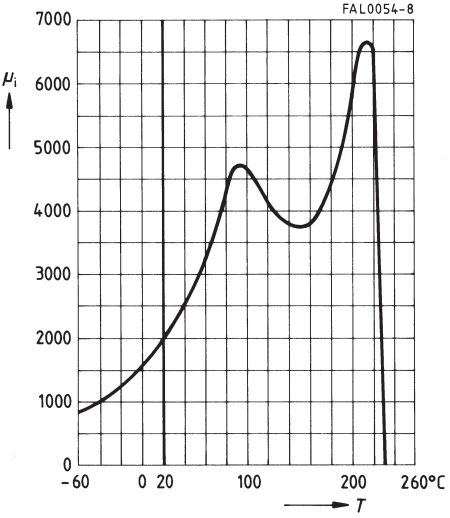

Amplitude permeability versus AC field
flux density
(measured on ungapped E cores)

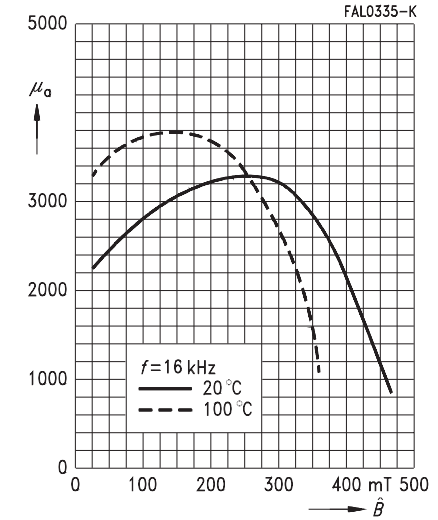

Dynamic magnetization curves
(typical values)
(f = 10 kHz, T = 25 °C)

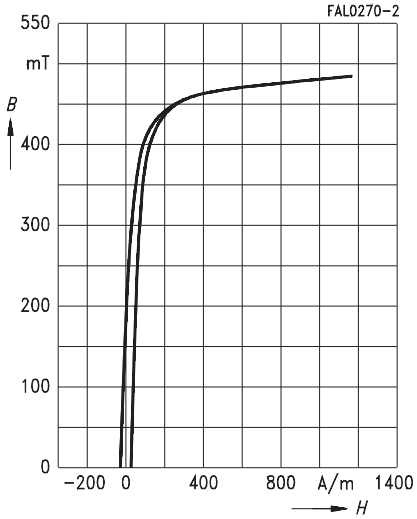

Dynamic magnetization curves
(typical values)
(f = 10 kHz, T = 100 °C)

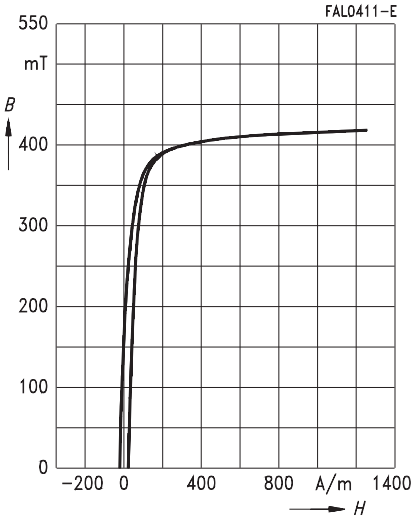

DC magnetic bias
measured on ETD cores
($\hat{B} \leq$ 0,25 mT, f = 10 kHz, T = 25 °C)

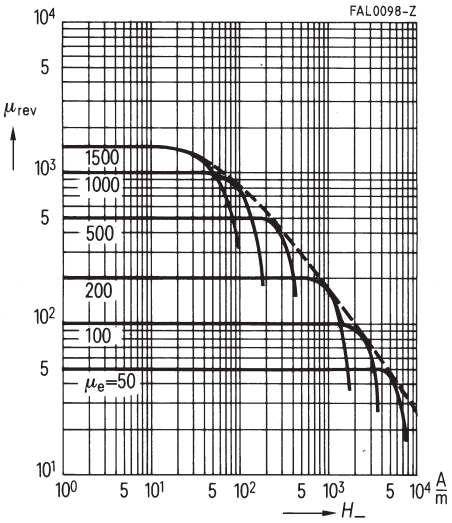

Relative core losses versus AC field flux density
(measured on R16 toroids)

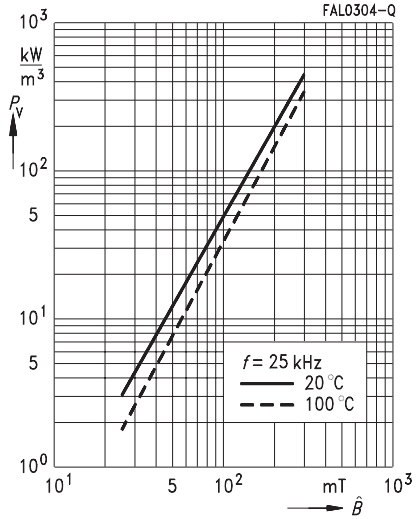

Relative core losses versus temperature
(measured on R16 toroids)

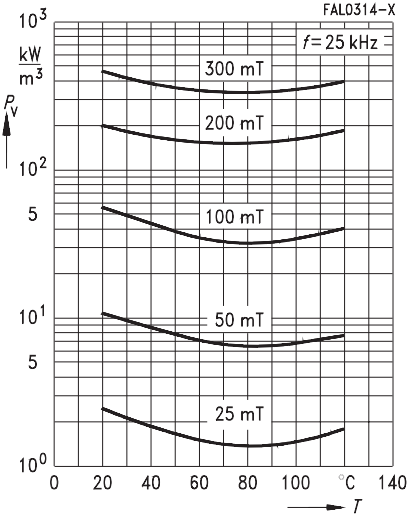

Relative core losses versus frequency
(measured on R16 toroids)

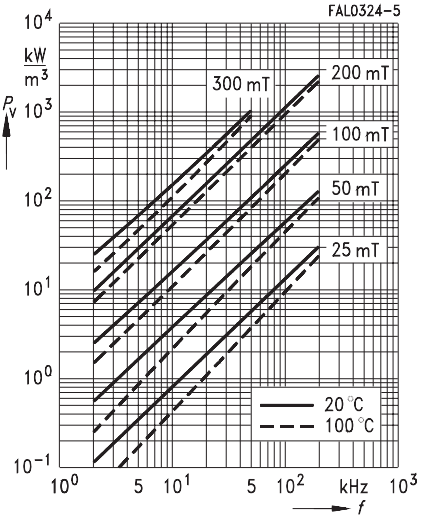

Complex permeability
versus frequency
(measured on R10 toroids, $\hat{B} \leq 0{,}25$ mT)

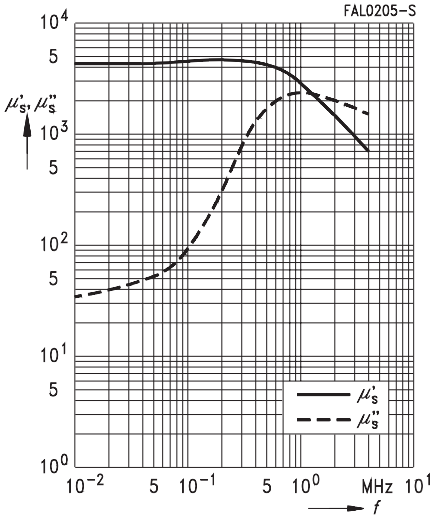

Initial permeability μ_i
versus temperature
(measured on R10 toroids, $\hat{B} \leq 0{,}25$ mT)

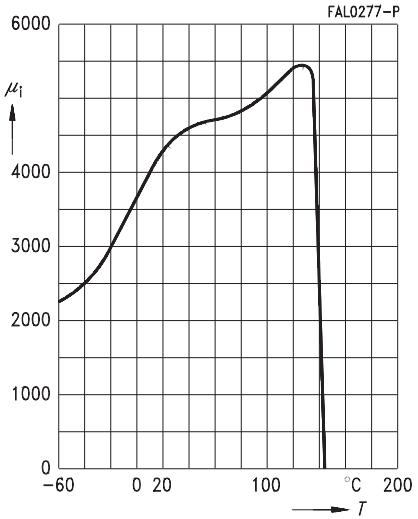

Variation of initial permeability
with temperature
(measured on R10 toroids, $\hat{B} \leq 0{,}25$ mT)

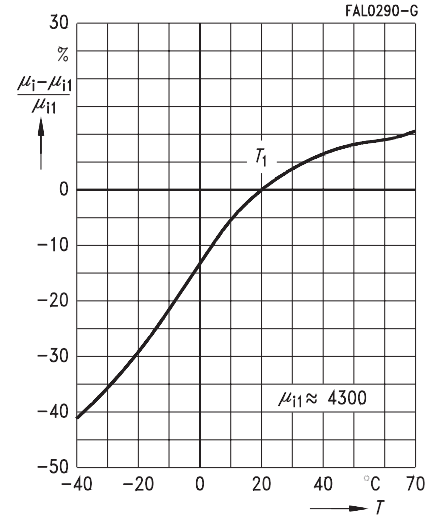

Relative loss factor
versus frequency
(measured on R20 toroids, $\hat{B} \leq 0{,}25$ mT)

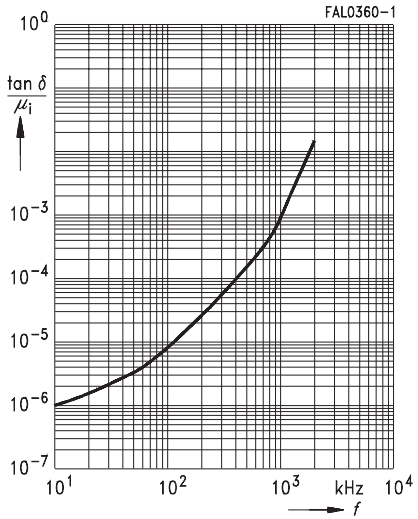

Dynamic magnetization curves
(typical values)
(f = 10 kHz, T = 25 °C)

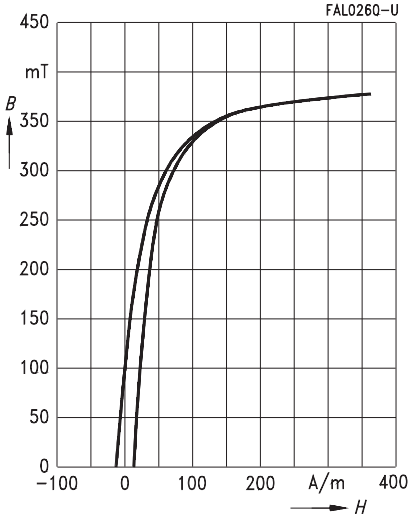

Dynamic magnetization curves
(typical values)
(f = 10 kHz, T = 100 °C)

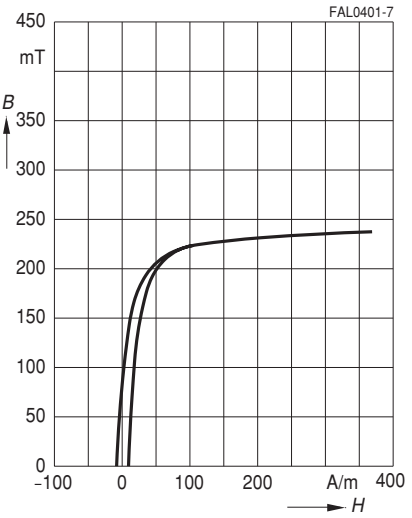

DC magnetic bias of RM cores
(typical values)
($\hat{B} \leq$ 0,25 mT, f = 10 kHz, T = 25 °C)

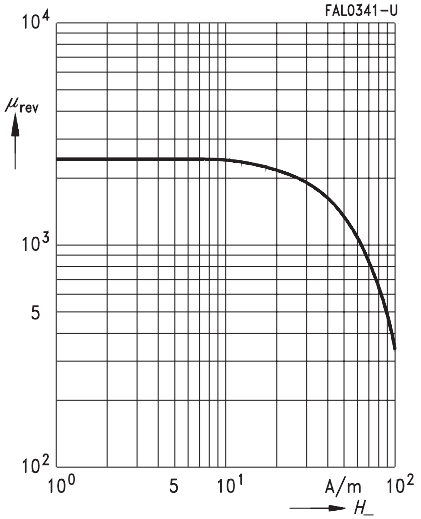

Complex permeability
versus frequency
(measured with R10 ring cores, $\hat{B} \leq 0{,}25$ mT)

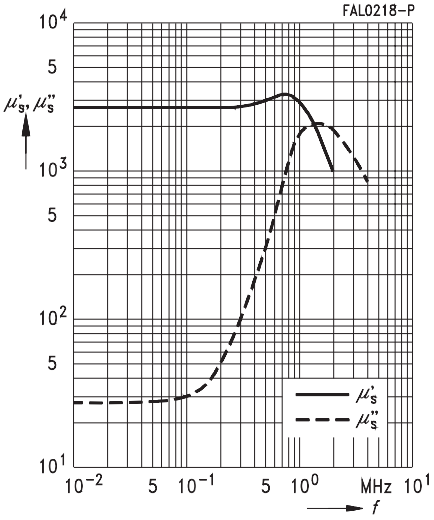

Initial permeability μ_i
versus temperature
(measured with R10 ring cores, $\hat{B} \leq 0{,}25$ mT)

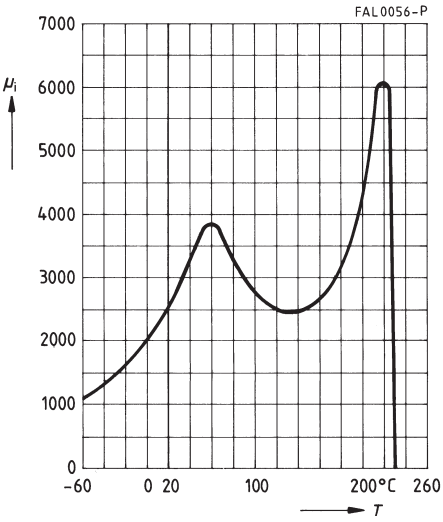

Amplitude permeability
versus AC field flux density
(measured on ungapped E cores)

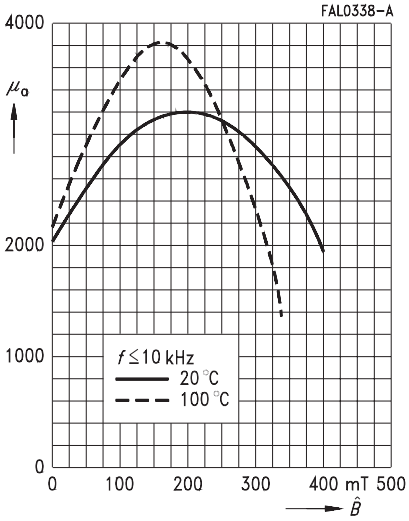

Dynamic magnetization curves
(typical values)
(f = 10 kHz, T = 25 °C)

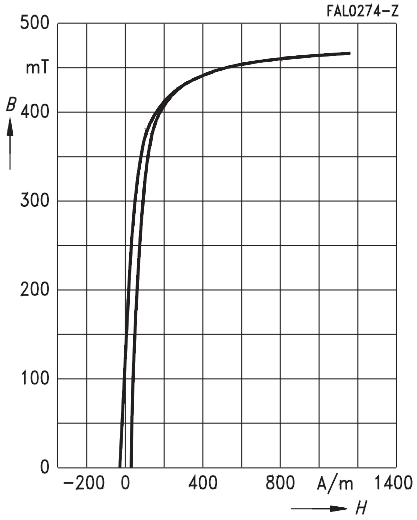

Dynamic magnetization curves
(typical values)
(f = 10 kHz, T = 100 °C)

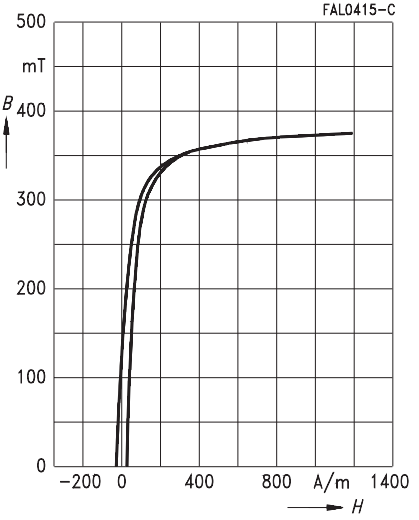

DC magnetic bias
of P and RM cores
($\hat{B} \leq$ 0,25 mT, f = 10 kHz, T = 25 °C)

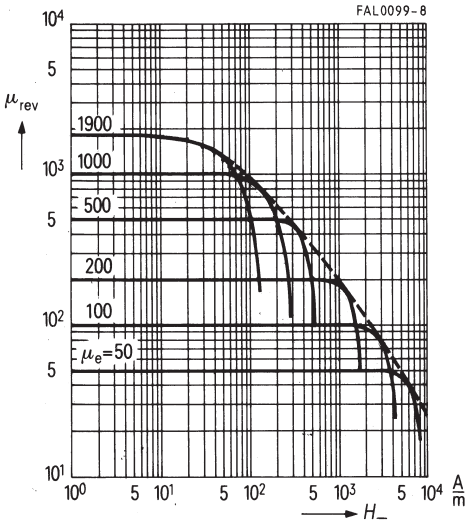

Relative core losses
versus AC field flux density
(measured on R16 toroids)

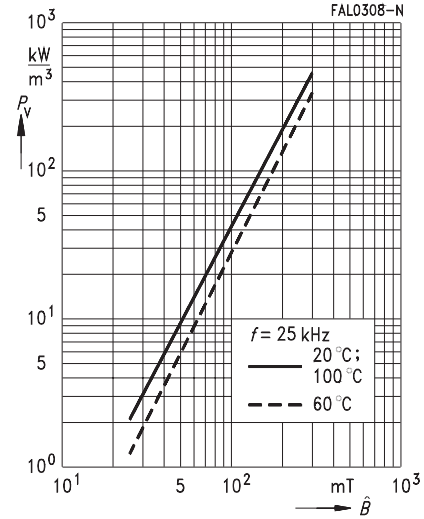

Relative core losses
versus temperature
(measured on R16 toroids)

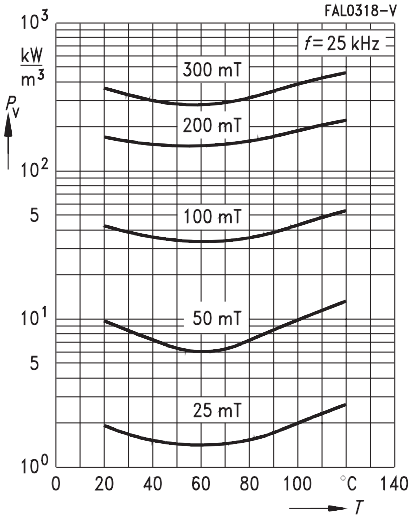

Relative core losses
versus frequency
(measured on R16 toroids)

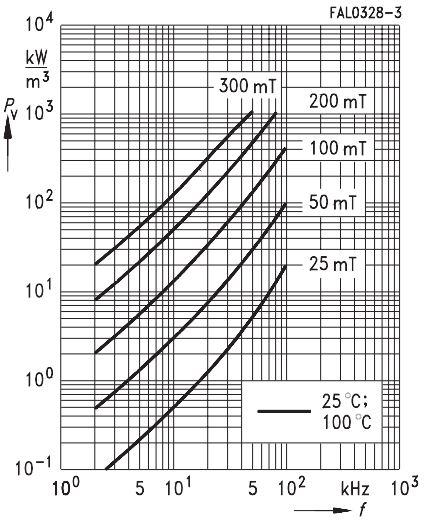

Complex permeability
versus frequency
(measured on R10 toroids, $\hat{B} \leq 0{,}25$ mT)

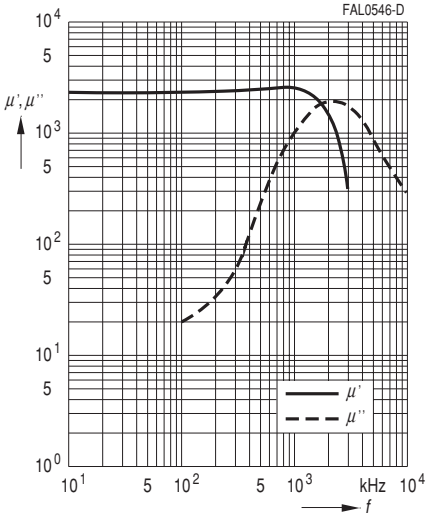

Initial permeability μ_i and relative loss factor
$\tan \delta/\mu_i$ versus temperature
(measured on R10 toroids, $\hat{B} \leq 0{,}25$ mT)

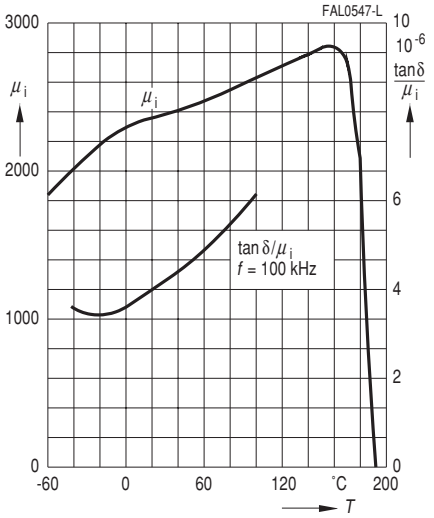

Permeability factor versus temperature
(measured on P and RM cores,
$\hat{B} \leq 0{,}25$ mT), $\mu_i \approx 2300$

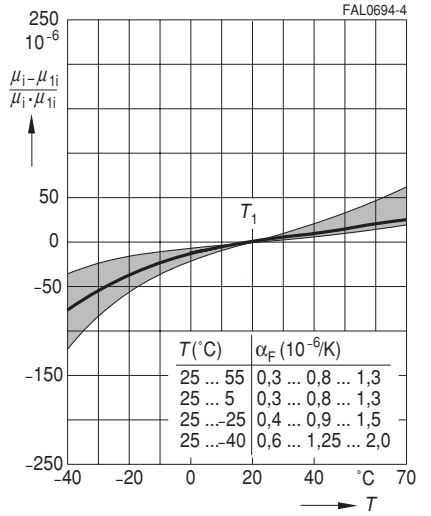

Relative loss factor tan δ/μ_i
versus frequency
(measured on R29 toroids)

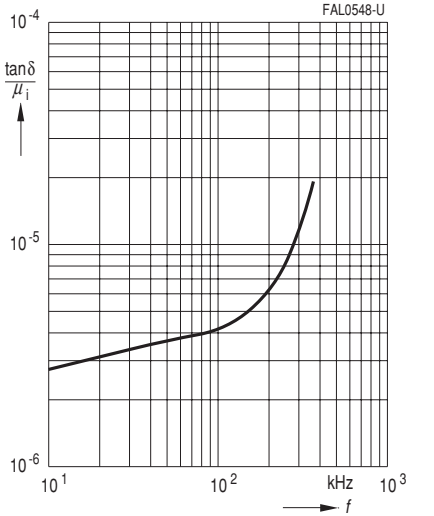

Dynamic magnetization curves
(typical values)
(f = 10 kHz, T = 25 °C)

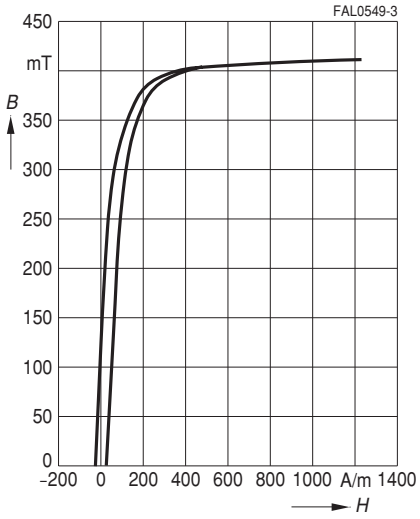

Dynamic magnetization curves
(typical values)
(f = 10 kHz, T = 100 °C)

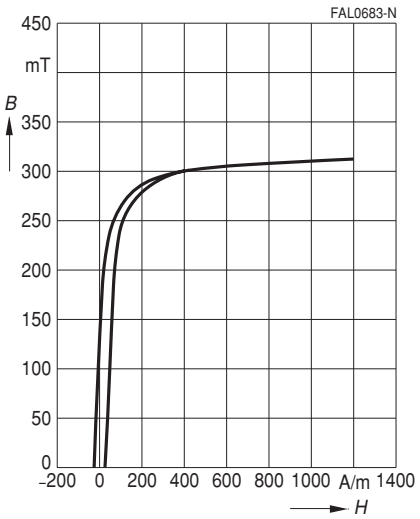

DC magnetic bias
(measured on ETD cores, typical values)
($\hat{B} \leq$ 0,25 mT, f = 10 kHz, T = 25 °C)

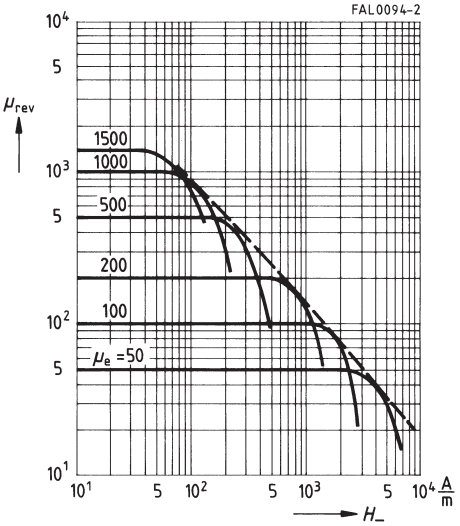

Complex permeability
versus frequency
(measured on R34 toroids, $\hat{B} \leq 0{,}25$ mT)

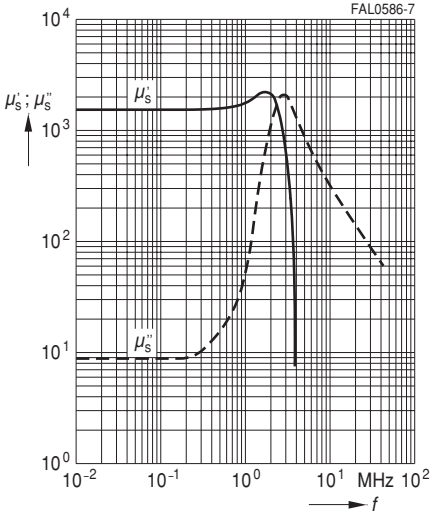

Initial permeability μ_i
versus temperature
(measured on R34 toroids, $\hat{B} \leq 0{,}25$ mT)

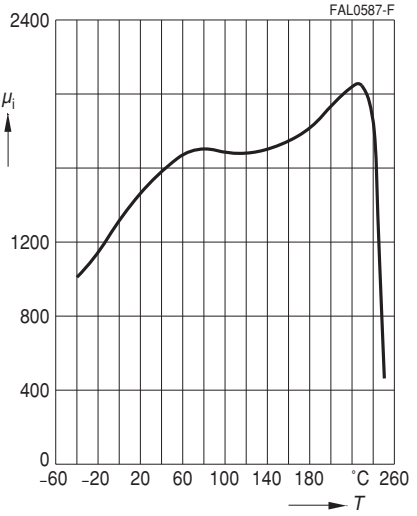

Amplitude permeability
versus AC field flux density
(measured on R34 toroids, $\hat{B} \leq 0{,}25$ mT)

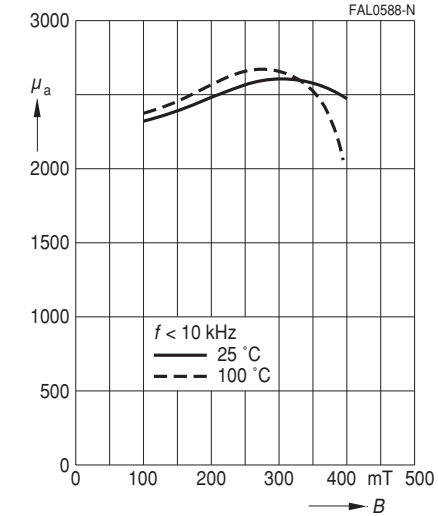

Dynamic magnetization curves
(typical values)
(f = 10 kHz, T = 25 °C)

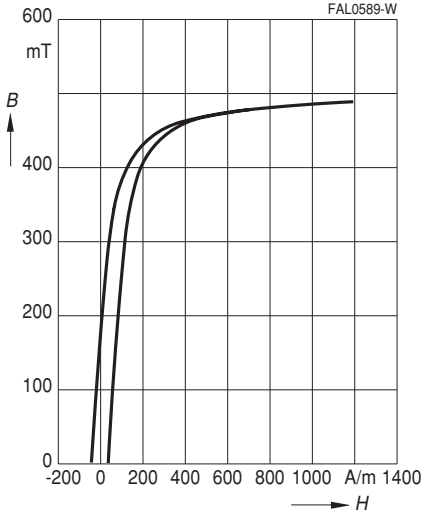

Dynamic magnetization curves
(typical values)
(f = 10 kHz, T = 100 °C)

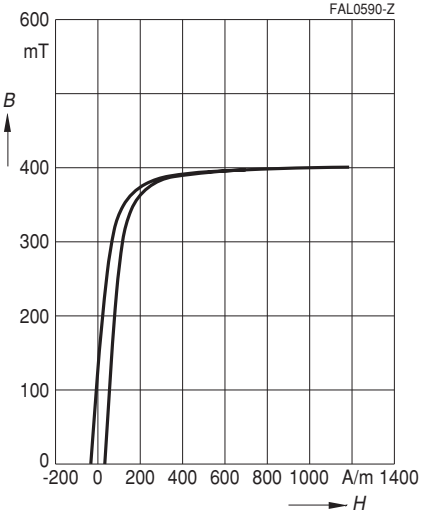

DC magnetic bias
measured on ETD cores
($\hat{B} \leq$ 0,25 mT, f = 10 kHz, T = 25 °C)

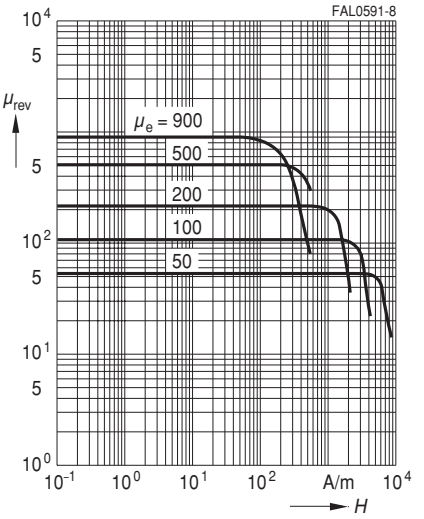

DC magnetic bias
measured on ETD cores
($\hat{B} \leq$ 0,25 mT, f = 10 kHz, T = 100 °C)

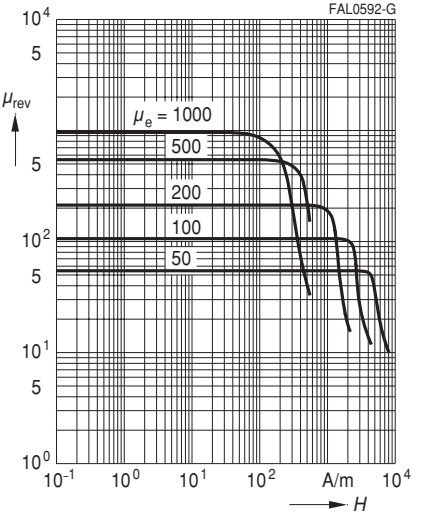

Relative core losses
versus AC field flux density
(measured on R34 toroids)

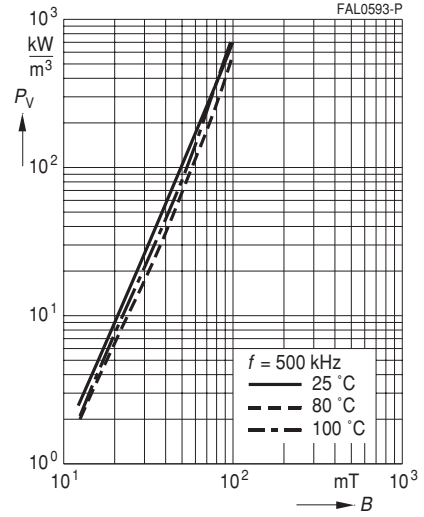

Relative core losses
versus temperature
(measured on R34 toroids)

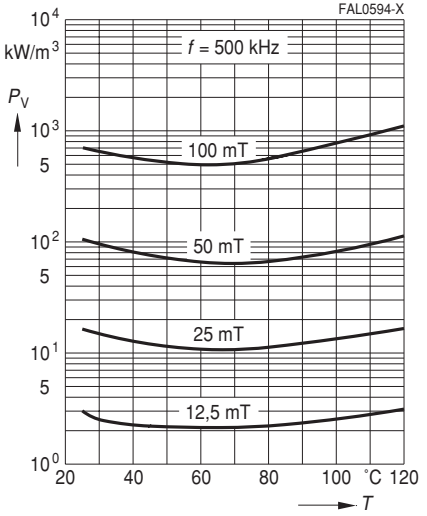

Relative core losses
versus frequency
(measured on R34 toroids)

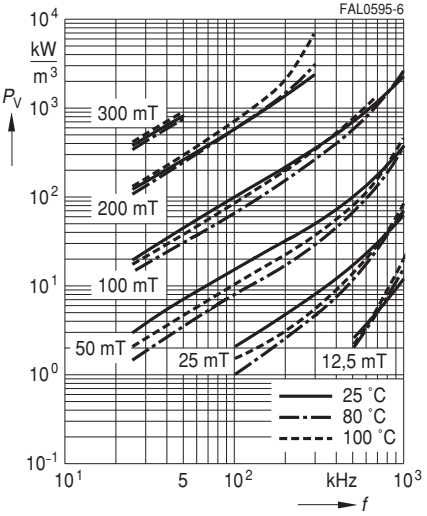

Not for new design

Complex permeability
versus frequency
(measured on R10 toroids, $\hat{B} \leq 0{,}25$ mT)

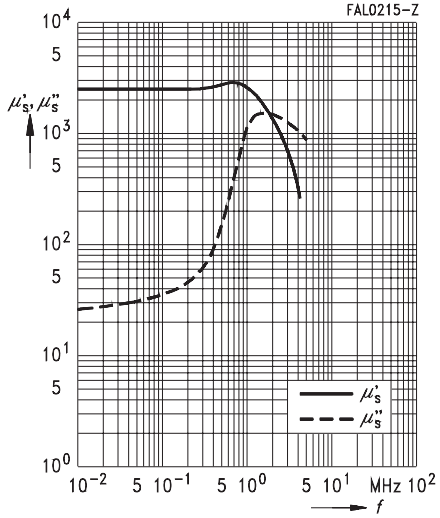

Initial permeability μ_i
versus temperature
(measured on R10 toroids, $\hat{B} \leq 0{,}25$ mT)

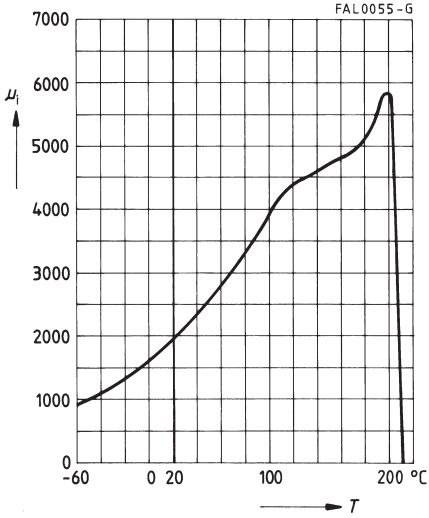

Amplitude permeability versus AC field
flux density
(measured on ungapped E cores)

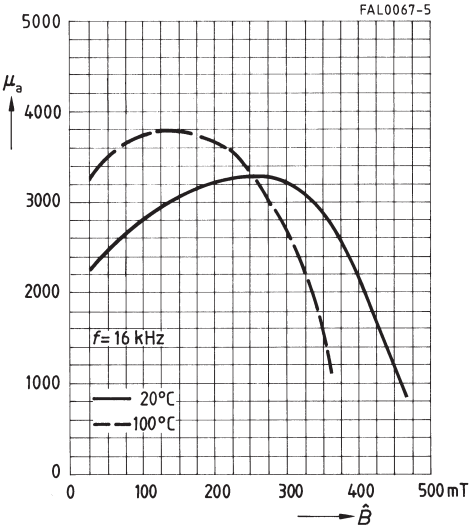

Not for new design

Dynamic magnetization curves
(typical values)
(f = 10 kHz, T = 25 °C)

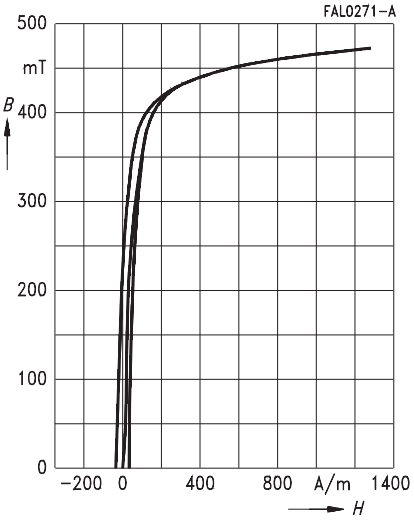

Dynamic magnetization curves
(typical values)
(f = 10 kHz, T = 100 °C)

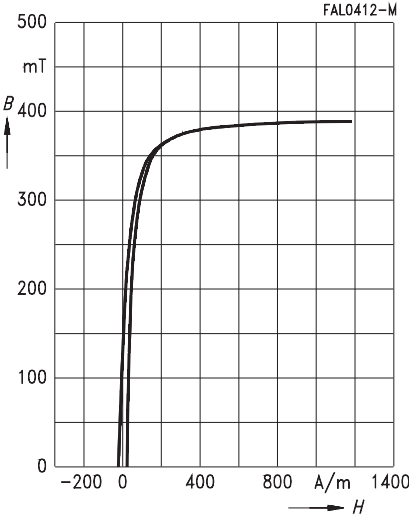

DC magnetic bias
of P, RM, PM and E cores
($\hat{B} \leq$ 0,25 mT, f = 10 kHz, T = 25 °C)

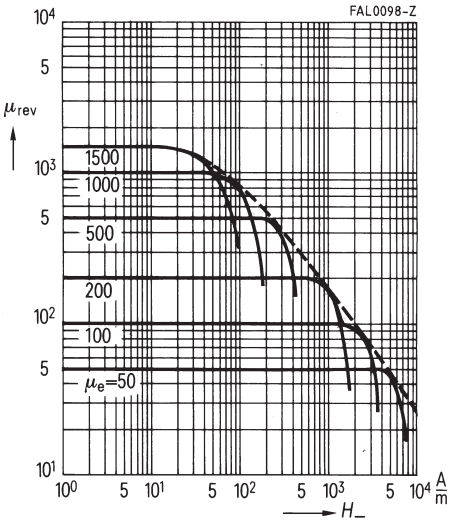

Not for new design

Relative core losses versus AC field flux density
(measured on R16 toroids)

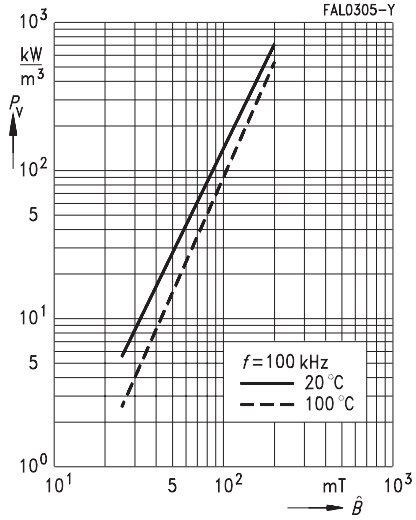

Relative core losses versus temperature
(measured on R16 toroids)

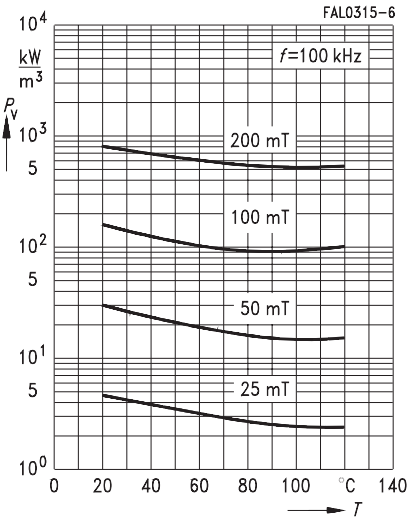

Relative core losses versus frequency
(measured on R16 toroids)

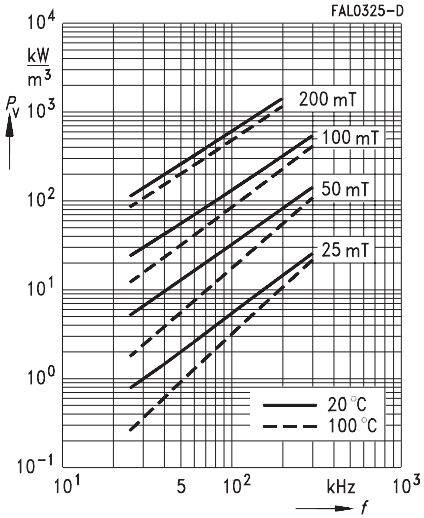

Complex permeability
versus frequency
(measured on R29 toroids, $\hat{B} \leq 0{,}25$ mT)

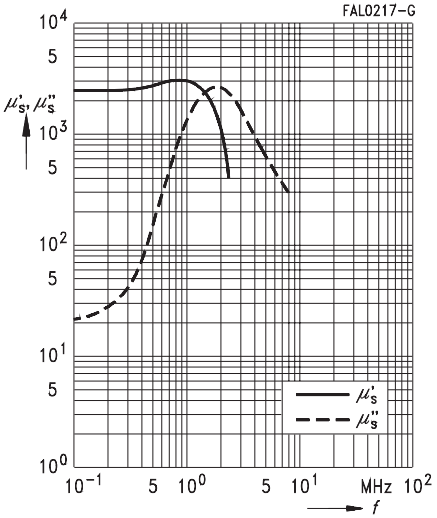

Initial permeability μ_i
versus temperature
(measured on R29 toroids, $\hat{B} \leq 0{,}25$ mT)

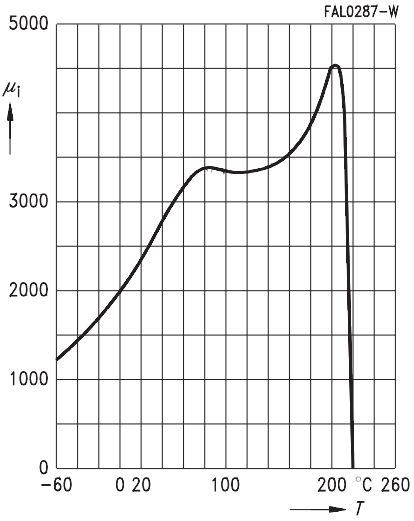

Amplitude permeability versus AC field
flux density
(measured on ungapped U cores)

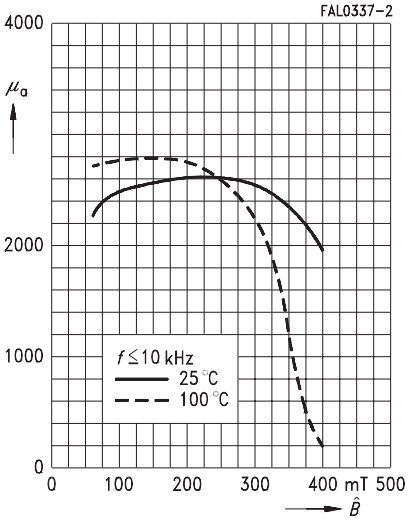

Dynamic magnetization curves
(typical values)
(f = 10 kHz, T = 25 °C)

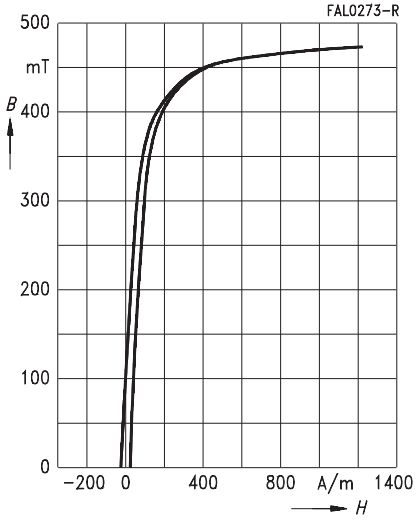

Dynamic magnetization curves
(typical values)
(f = 10 kHz, T = 100 °C)

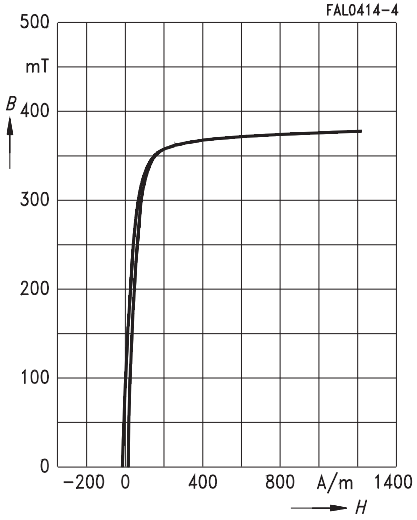

DC magnetic bias of E cores
($\hat{B} \leq$ 0,25 mT, f = 10 kHz, T = 25 °C)

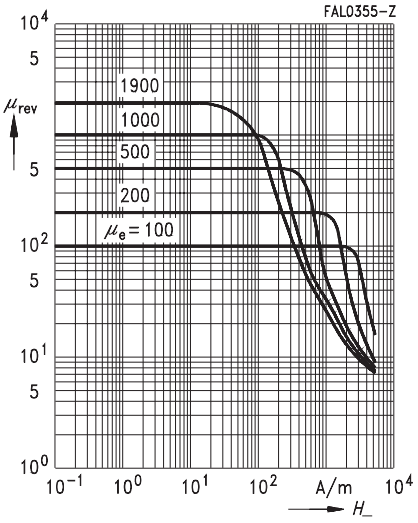

DC magnetic bias of E cores
($\hat{B} \leq$ 0,25 mT, f = 10 kHz, T = 100 °C)

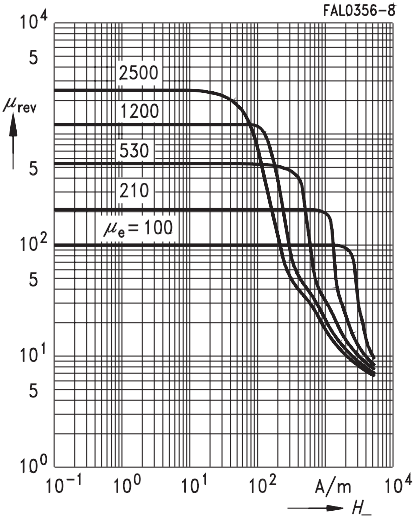

Relative core losses versus AC field flux density
(measured on R29 toroids)

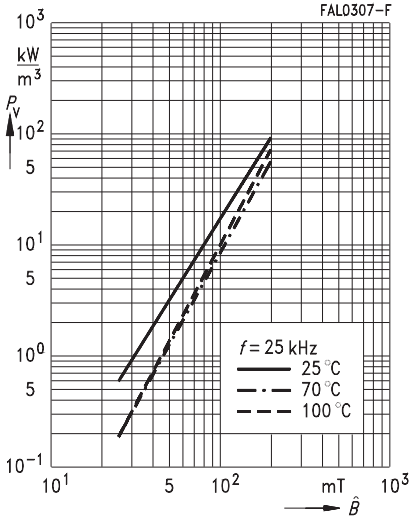

Relative core losses versus temperature
(measured on R29 toroids)

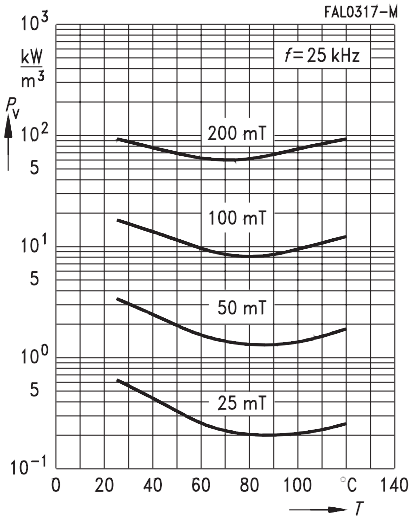

Relative core losses versus frequency
(measured on R29 toroids)

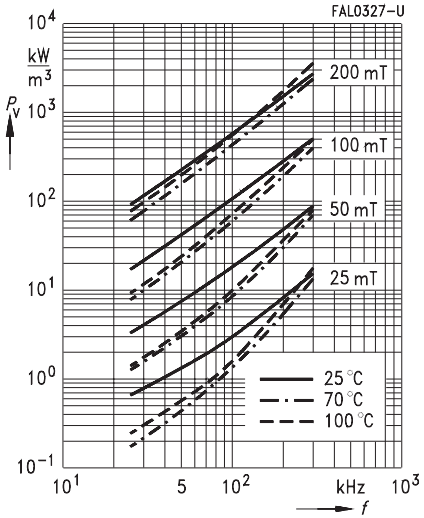

Complex permeability
versus frequency
(measured on R34 toroids, $\hat{B} \leq 0{,}25$ mT)

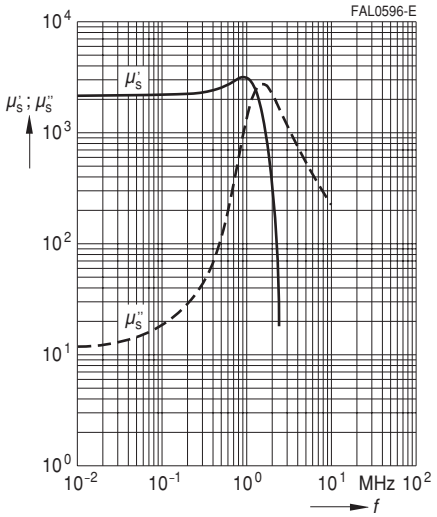

Initial permeability μ_i
versus temperature
(measured on R34 toroids, $\hat{B} \leq 0{,}25$ mT)

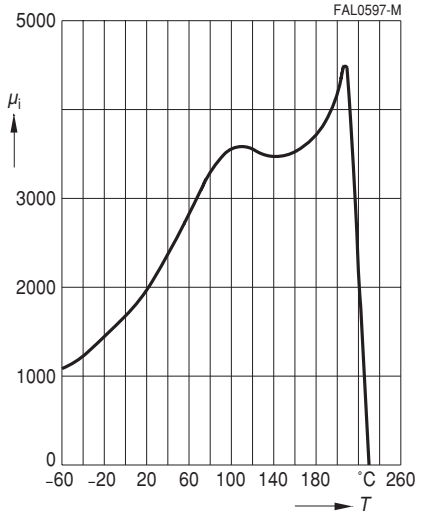

Amplitude permeability
versus AC field flux density
(measured on R34 toroids, $\hat{B} \leq 0{,}25$ mT)

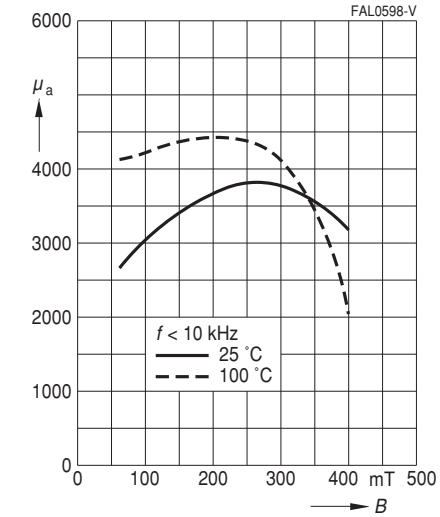

Dynamic magnetization curves
(typical values)
(f = 10 kHz, T = 25 °C)

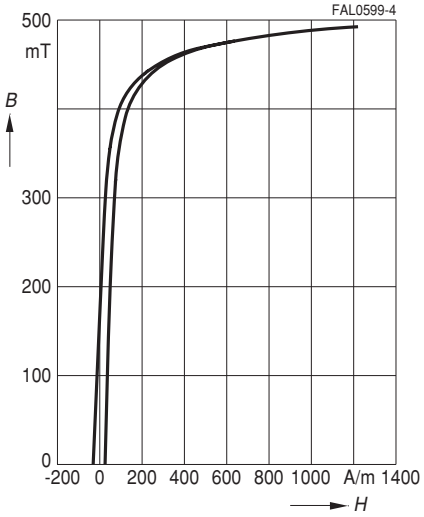

Dynamic magnetization curves
(typical values)
(f = 10 kHz, T = 100 °C)

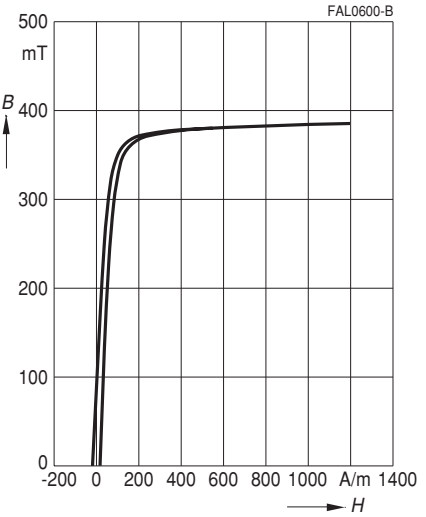

DC magnetic bias
of P, RM, PM and E cores
($\hat{B} \leq$ 0,25 mT, f = 10 kHz, T = 25 °C)

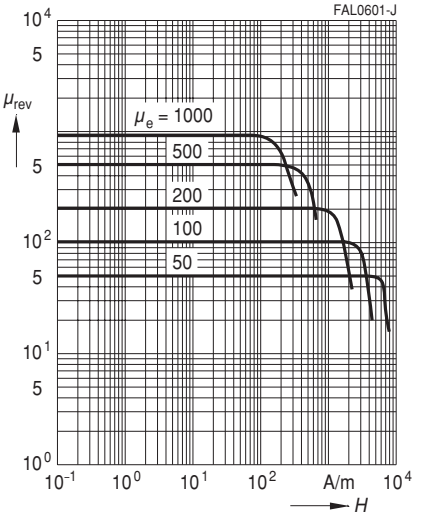

DC magnetic bias
of P, RM, PM and E cores
($\hat{B} \leq$ 0,25 mT, f = 10 kHz, T = 100 °C)

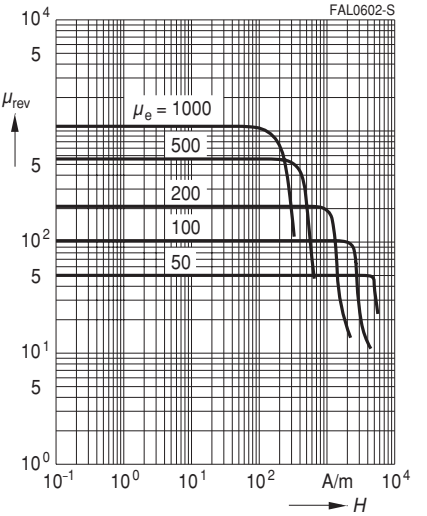

Relative core losses
versus AC field flux density
(measured on R34 toroids)

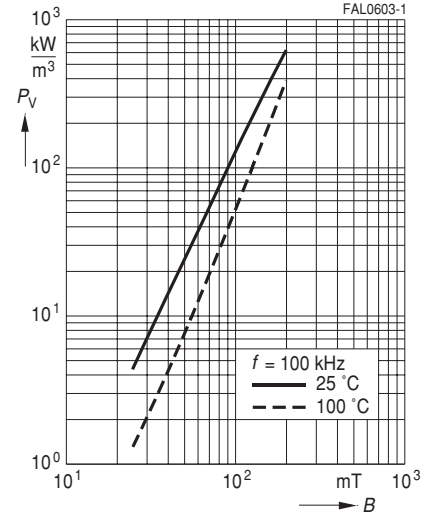

Relative core losses
versus temperature
(measured on R34 toroids)

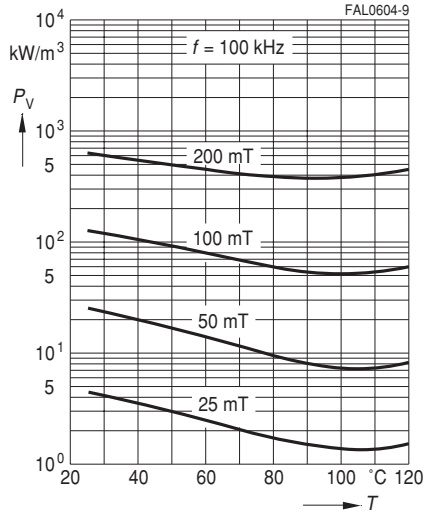

Relative core losses
versus frequency
(measured on R34 toroids)

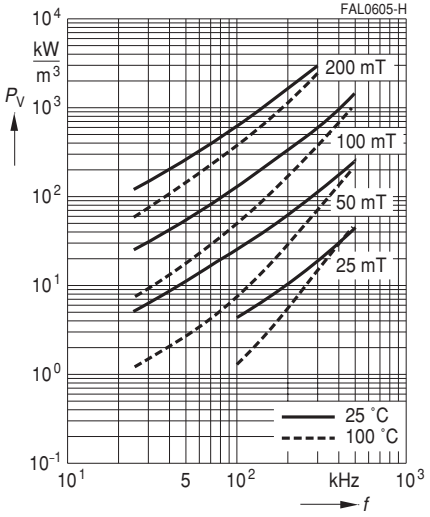

Complex permeability
versus frequency
(measured on R34 toroids, $\hat{B} \leq 0{,}25$ mT)

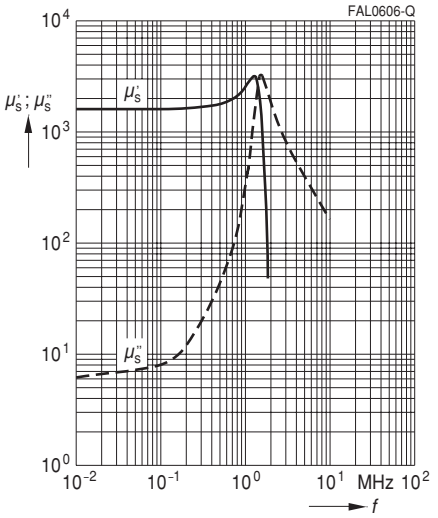

Initial permeability μ_i
versus temperature
(measured on R34 toroids, $\hat{B} \leq 0{,}25$ mT)

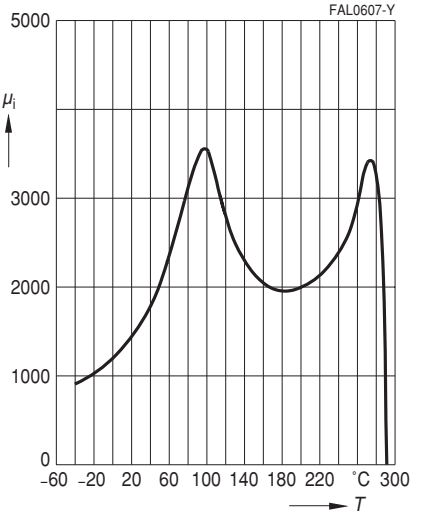

Amplitude permeability
versus AC field flux density
(measured on R34 toroids, $\hat{B} \leq 0{,}25$ mT)

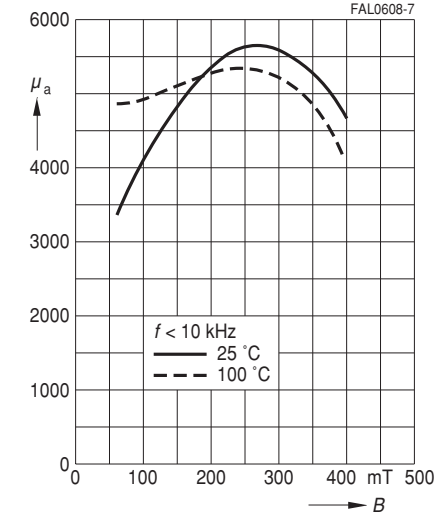

Dynamic magnetization curves
(typical values)
(f = 10 kHz, T = 25 °C)

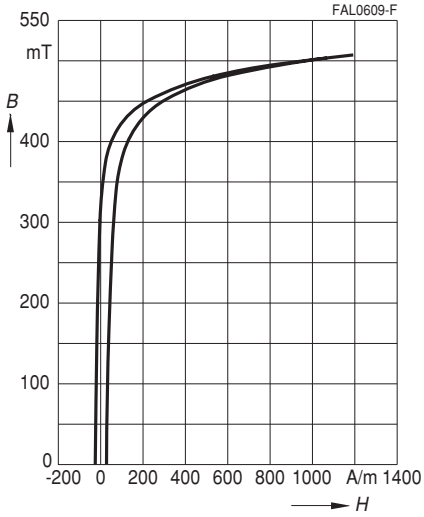

Dynamic magnetization curves
(typical values)
(f = 10 kHz, T = 100 °C)

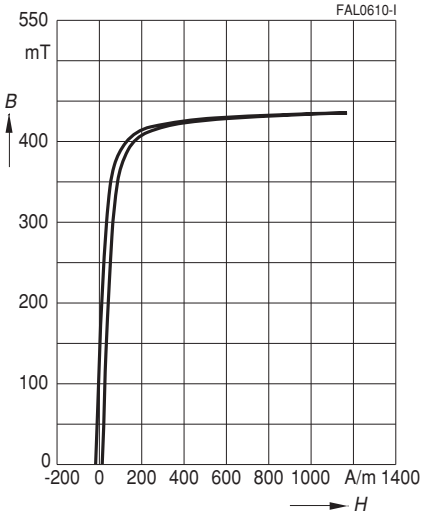

DC magnetic bias
measured on ETD cores
($\hat{B} \leq$ 0,25 mT, f = 10 kHz, T = 25 °C)

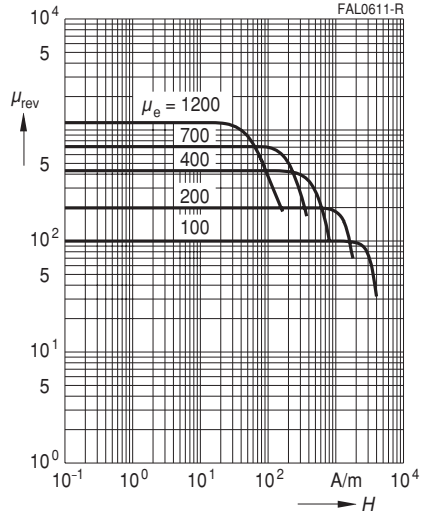

DC magnetic bias
measured on ETD cores
($\hat{B} \leq$ 0,25 mT, f = 10 kHz, T = 100 °C)

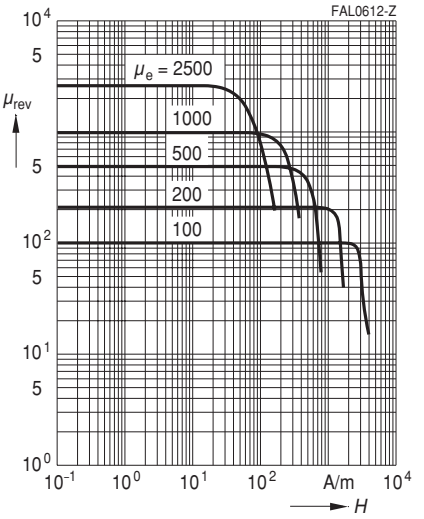

Relative core losses
versus AC field flux density
(measured on R34 toroids)

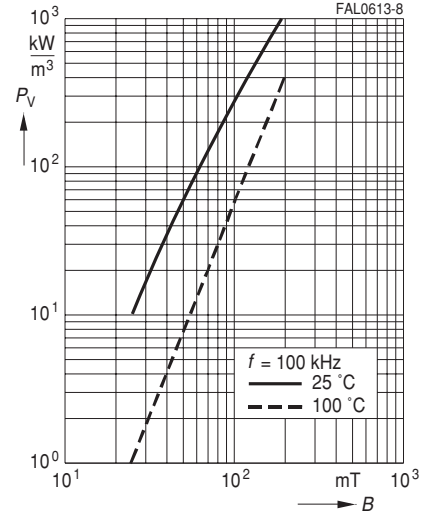

Relative core losses
versus temperature
(measured on R34 toroids)

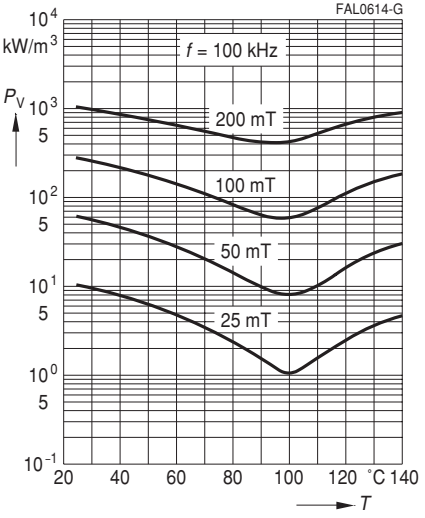

Relative core losses
versus frequency
(measured on R34 toroids)

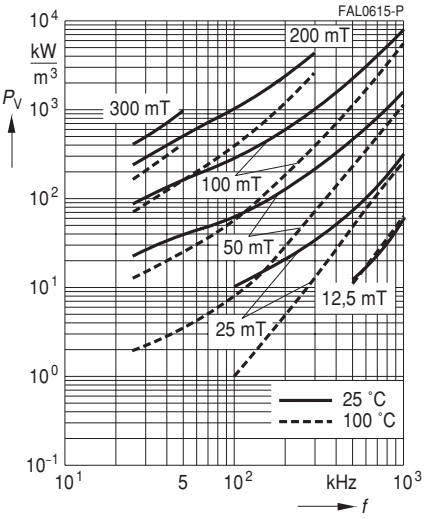

Complex permeability
versus frequency
(measured on R34 toroids, $\hat{B} \leq 0{,}25$ mT)

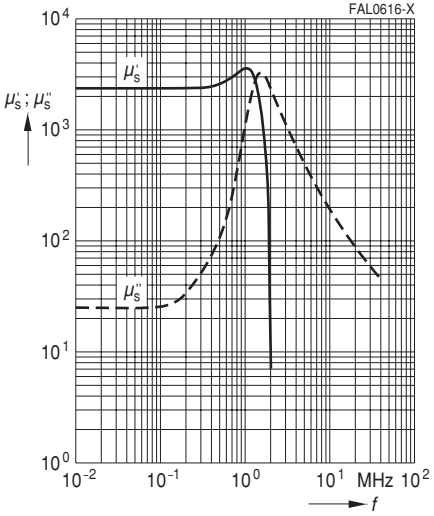

Initial permeability μ_i
versus temperature
(measured on R34 toroids, $\hat{B} \leq 0{,}25$ mT)

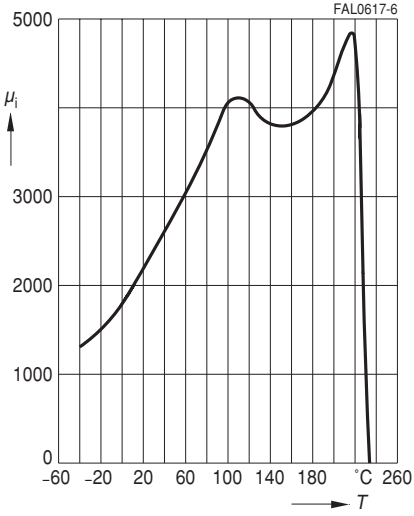

Amplitude permeability
versus AC field flux density
(measured on R34 toroids, $\hat{B} \leq 0{,}25$ mT)

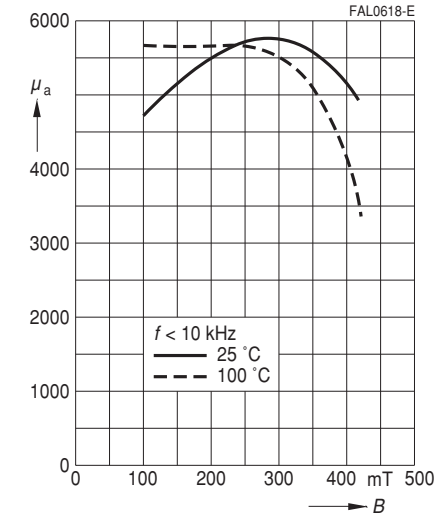

Dynamic magnetization curves
(typical values)
(f = 10 kHz, T = 25 °C)

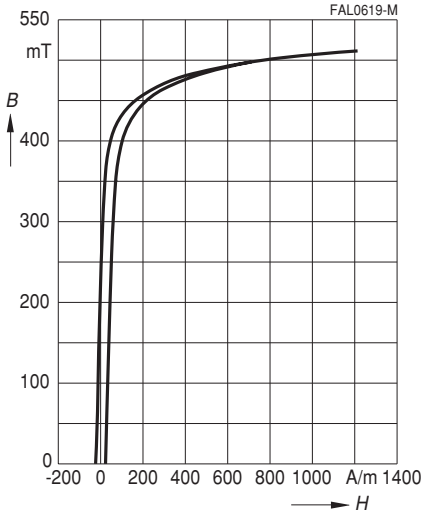

Dynamic magnetization curves
(typical values)
(f = 10 kHz, T = 100 °C)

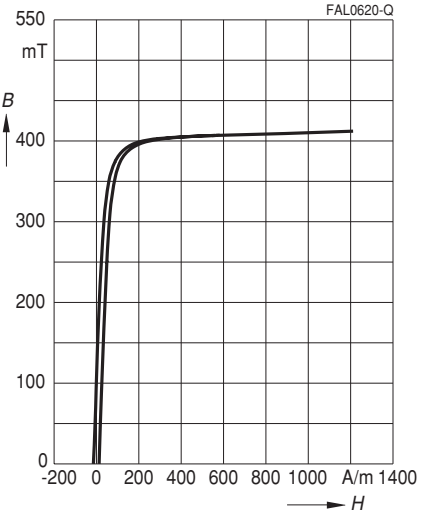

DC magnetic bias
measured on ETD cores
($\hat{B} \leq$ 0,25 mT, f = 10 kHz, T = 25 °C)

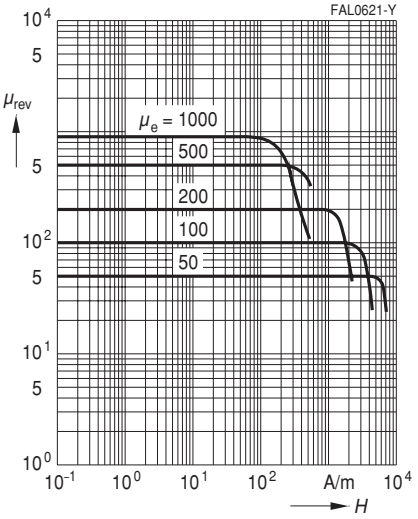

DC magnetic bias
measured on ETD cores
($\hat{B} \leq$ 0,25 mT, f = 10 kHz, T = 100 °C)

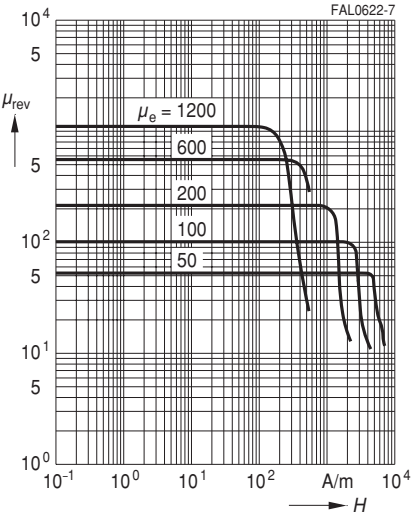

Relative core losses
versus AC field flux density
(measured on R34 toroids)

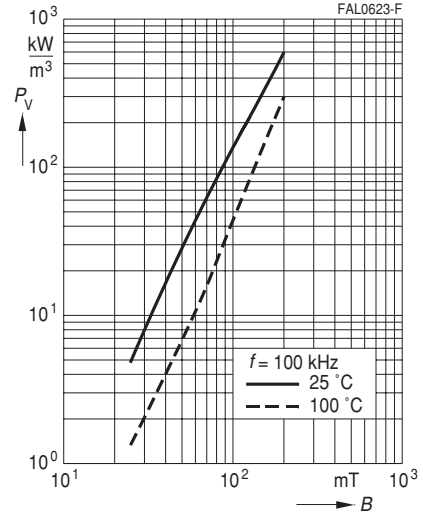

Relative core losses
versus temperature
(measured on R34 toroids)

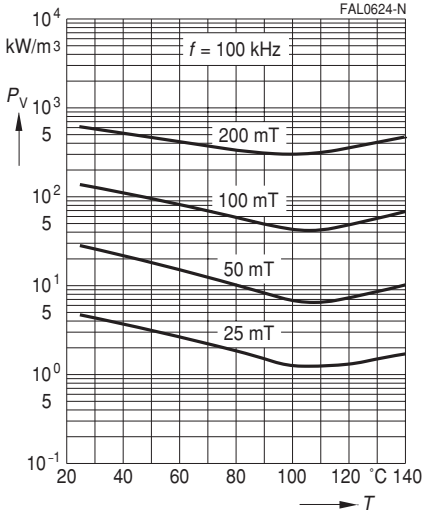

Relative core losses
versus frequency
(measured on R34 toroids)

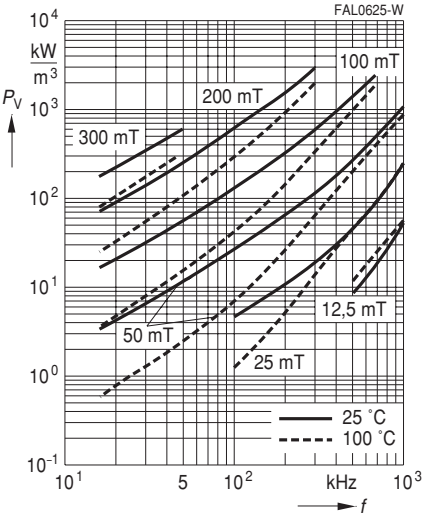

Complex permeability
versus frequency
(measured on R10 toroids, $\hat{B} \leq 0{,}25$ mT)

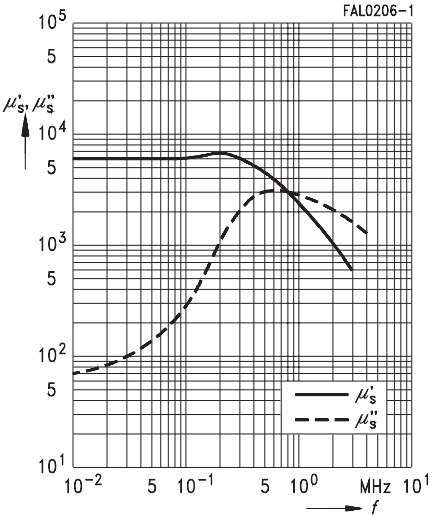

Initial permeability μ_i
versus temperature
(measured on R16 toroids, $\hat{B} \leq 0{,}25$ mT)

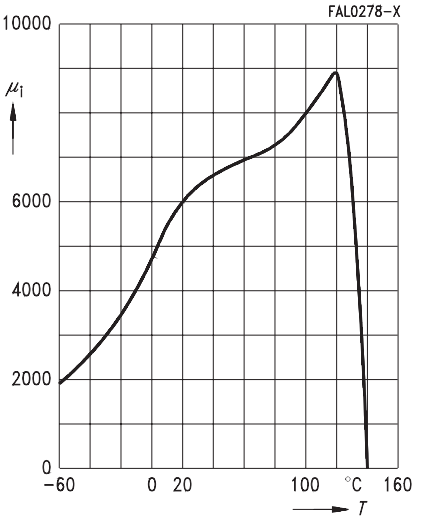

Variation of initial permeability
with temperature
(measured on R16 toroids, $\hat{B} \leq 0{,}25$ mT)

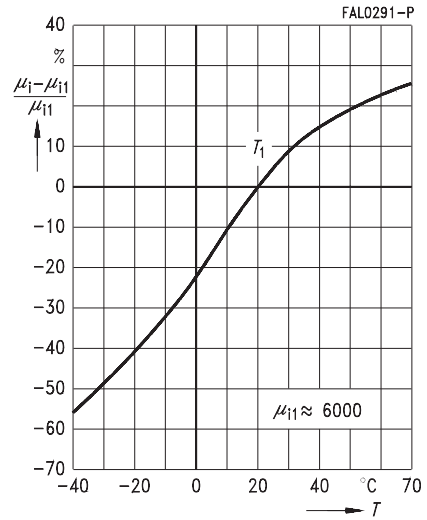

Relative loss factor
versus frequency
(measured on R16 toroids, $\hat{B} \leq 0{,}25$ mT)

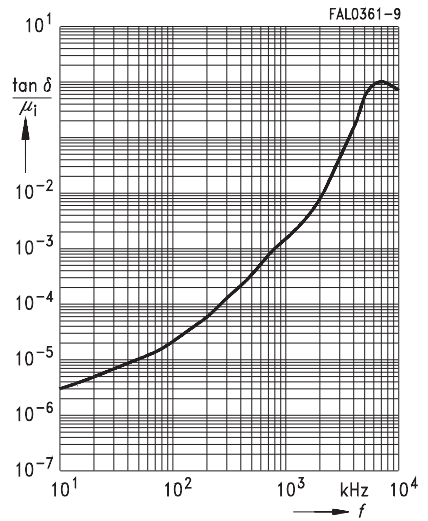

Dynamic magnetization curves
(typical values)
(f = 10 kHz, T = 25 °C)

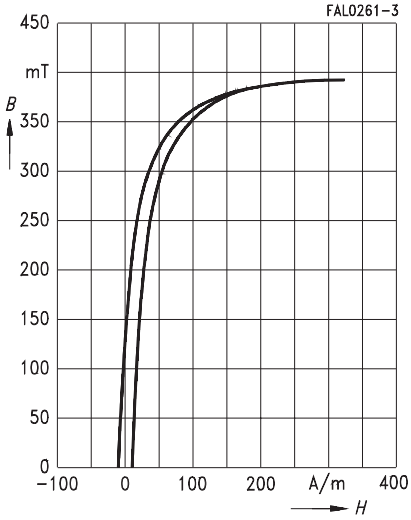

Dynamic magnetization curves
(typical values)
(f = 10 kHz, T = 100 °C)

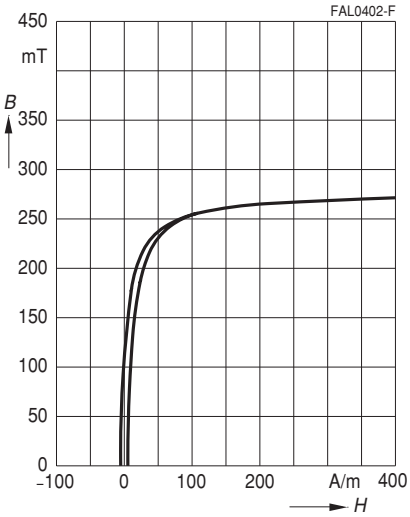

DC magnetic bias
(measured on RM cores, typical values)
($\hat{B} \leq$ 0,25 mT, f = 10 kHz, T = 25 °C)

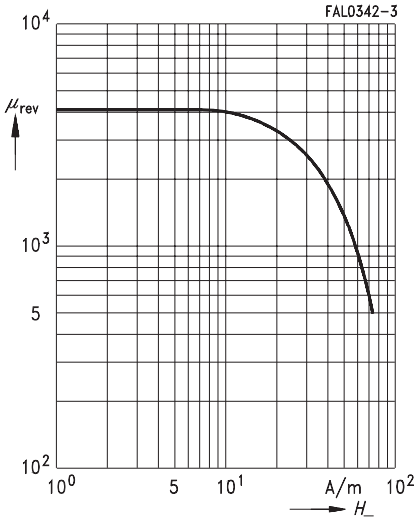

Complex permeability
versus frequency
(measured on R16 toroids, $\hat{B} \leq 0{,}25$ mT)

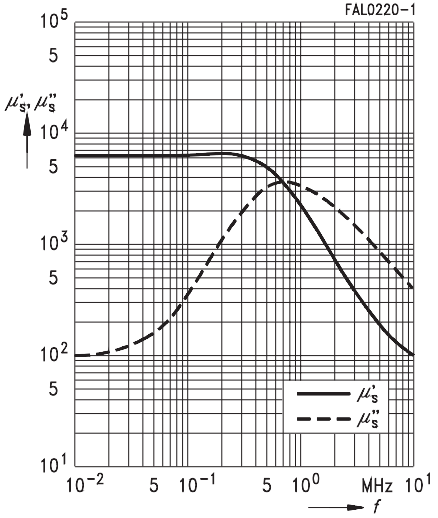

Initial permeability μ_i
versus temperature
(measured on R22 toroids, $\hat{B} \leq 0{,}25$ mT)

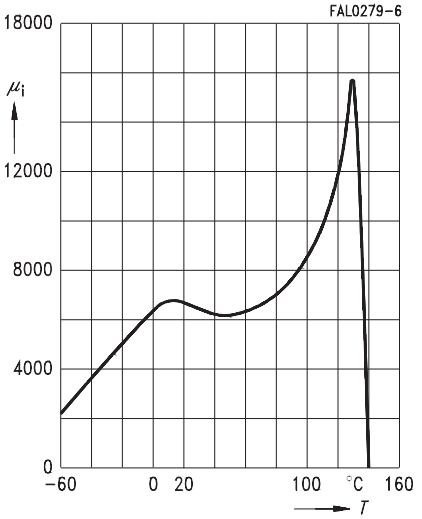

Variation of initial permeability
with temperature
(measured on R22 toroids, $\hat{B} \leq 0{,}25$ mT)

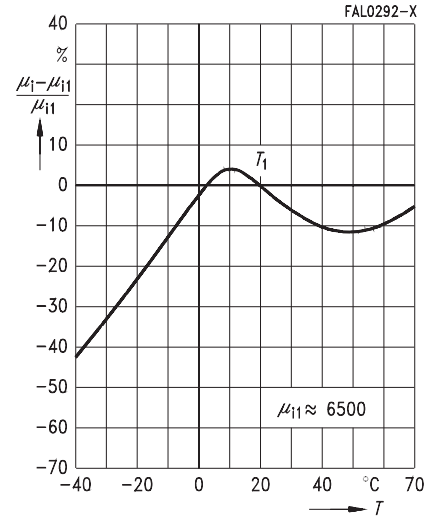

Relative loss factor
versus frequency
(measured on R16 toroids, $\hat{B} \leq 0{,}25$ mT)

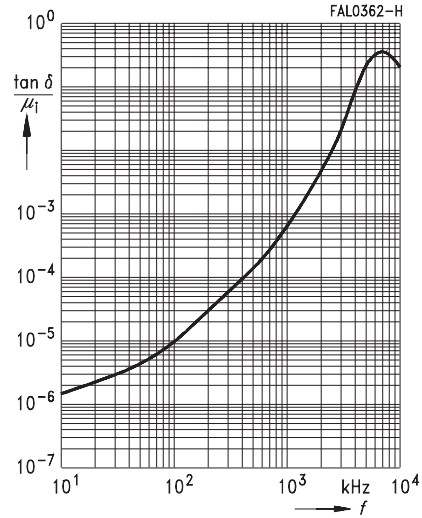

Dynamic magnetization curves
(typical values)
(f = 10 kHz, T = 25 °C)

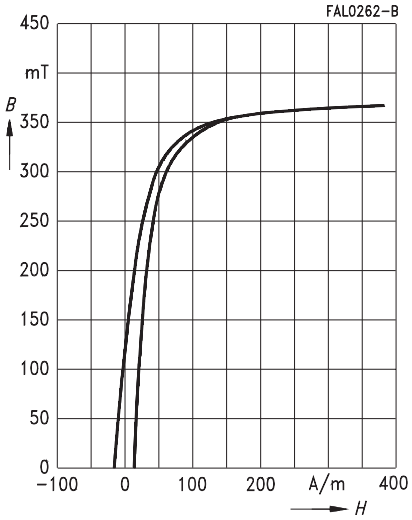

Dynamic magnetization curves
(typical values)
(f = 10 kHz, T = 100 °C)

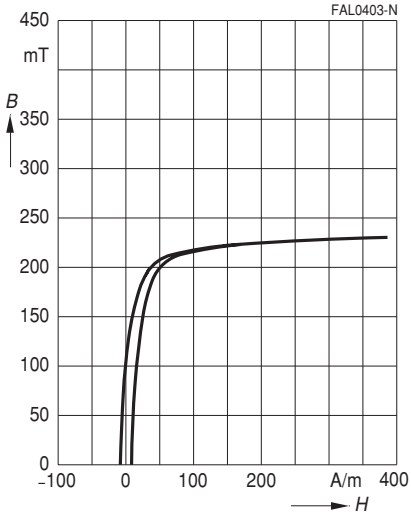

DC magnetic bias
(measured on RM cores, typical values)
($\hat{B} \leq$ 0,25 mT, f = 10 kHz, T = 25 °C)

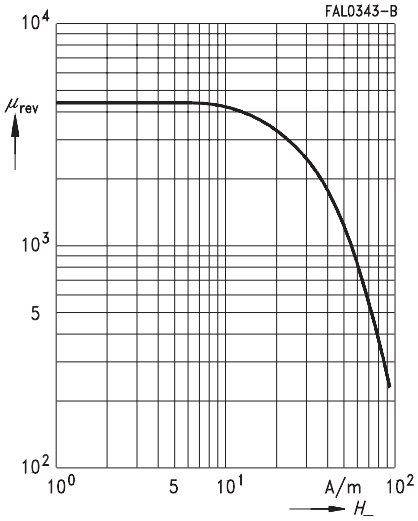

Complex permeability
versus frequency
(measured on R10 toroids, $\hat{B} \leq 0{,}25$ mT)

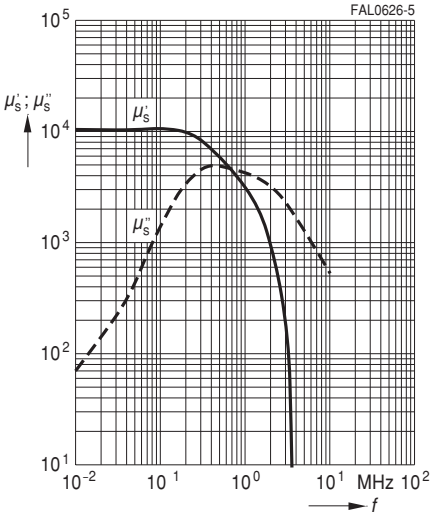

Initial permeability μ_i
versus temperature
(measured on R10 toroids, $\hat{B} \leq 0{,}25$ mT)

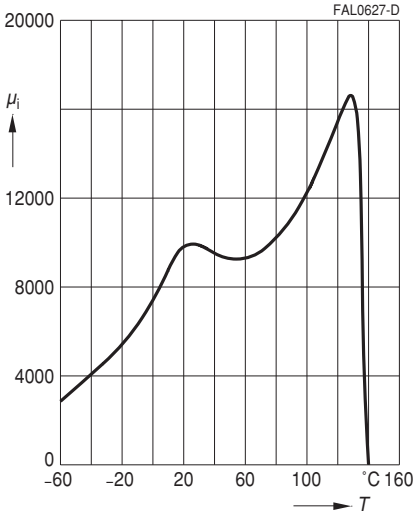

Variation of initial permeability
with temperature
(measured on R10 toroids, $\hat{B} \leq 0{,}25$ mT)

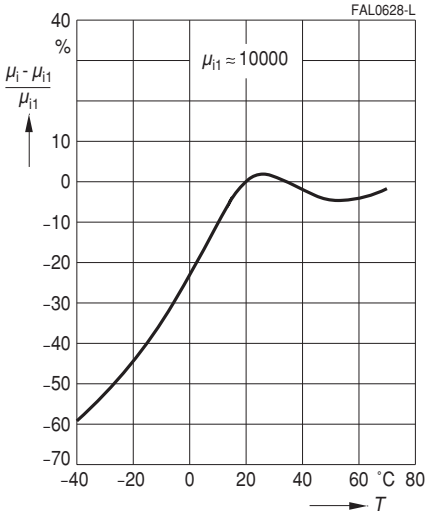

Relative loss factor
versus frequency
(measured on R10 toroids, $\hat{B} \leq 0{,}25$ mT)

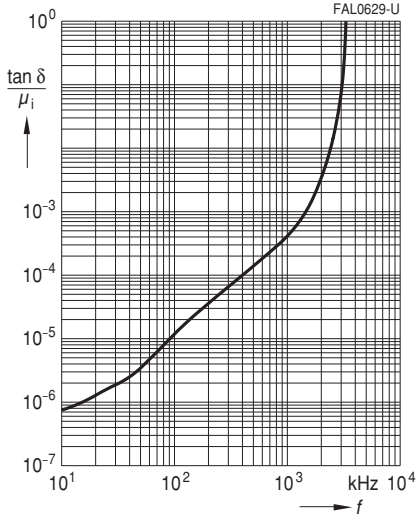

Dynamic magnetization curves
(typical values)
(f = 10 kHz, T = 25 °C)

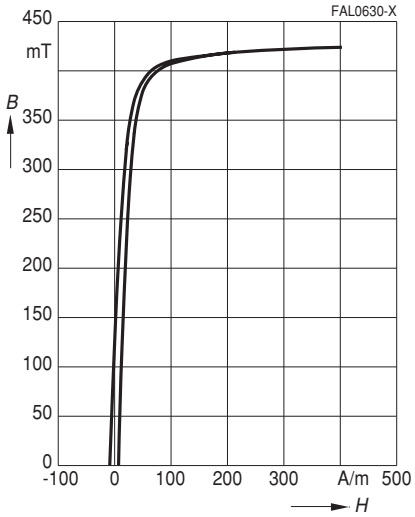

Dynamic magnetization curves
(typical values)
(f = 10 kHz, T = 100 °C)

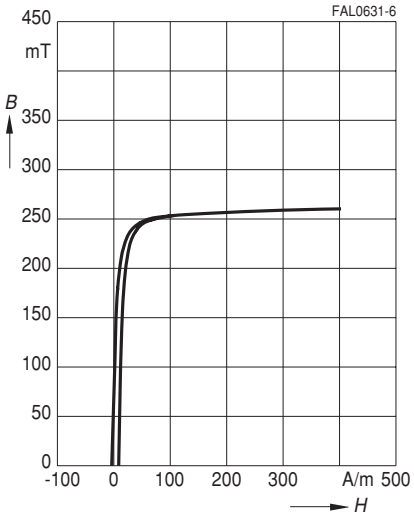

DC magnetic bias
(measured on RM cores, typical values)
($\hat{B} \leq$ 0,25 mT, f = 10 kHz, T = 25 °C)

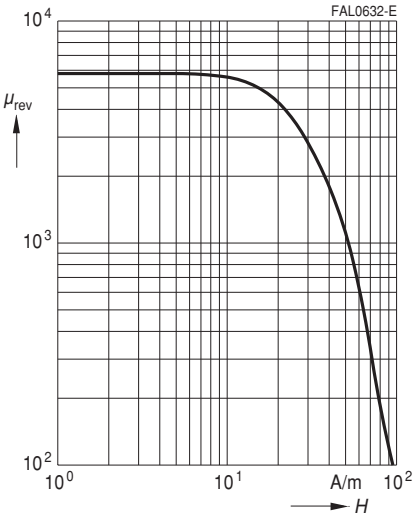

Complex permeability
versus frequency
(measured on R9,5 toroids, $\hat{B} \leq 0{,}25$ mT)

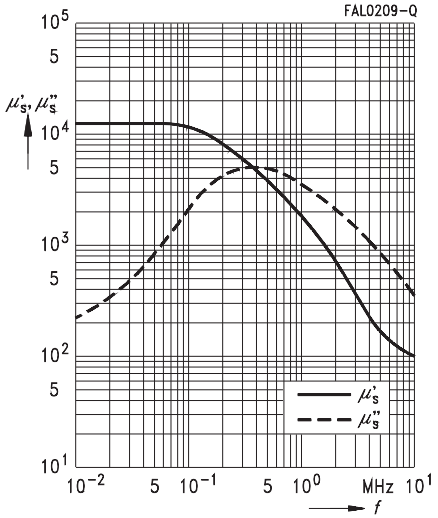

Initial permeability μ_i
versus temperature
(measured on R9,5 toroids, $\hat{B} \leq 0{,}25$ mT)

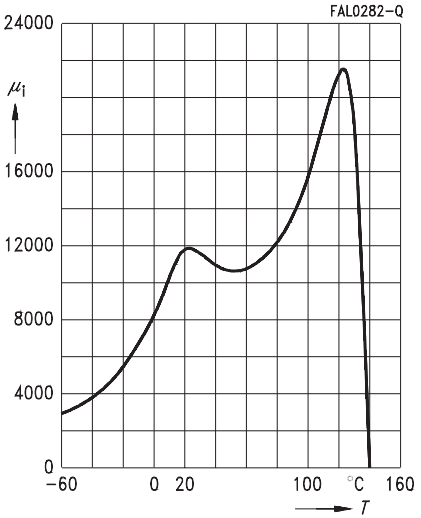

Variation of initial permeability
with temperature
(measured on R9,5 toroids, $\hat{B} \leq 0{,}25$ mT)

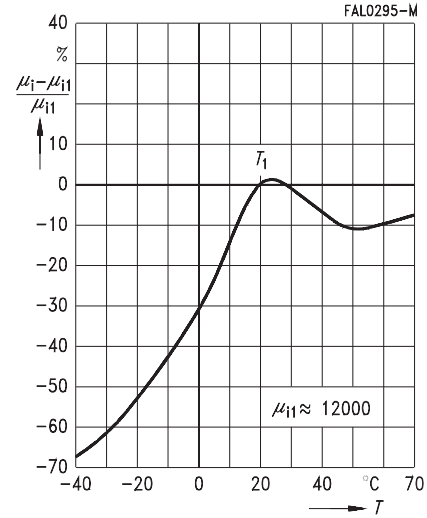

Relative loss factor
versus frequency
(measured on R9,5 toroids, $\hat{B} \leq 0{,}25$ mT)

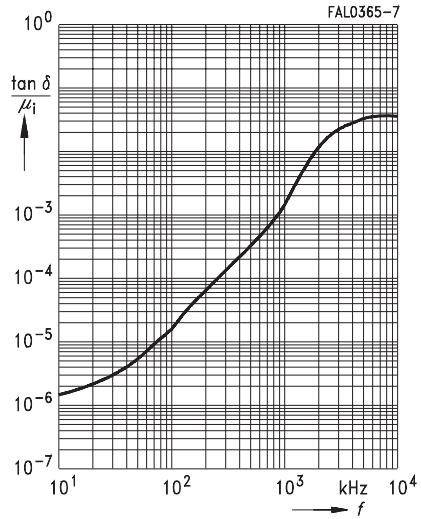

Dynamic magnetization curves
(typical values)
(f = 10 kHz, T = 25 °C)

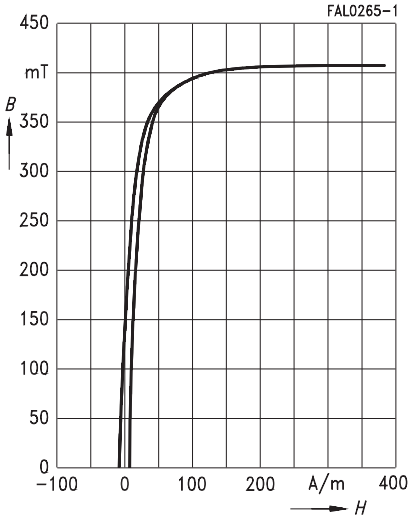

Dynamic magnetization curves
(typical values)
(f = 10 kHz, T = 100 °C)

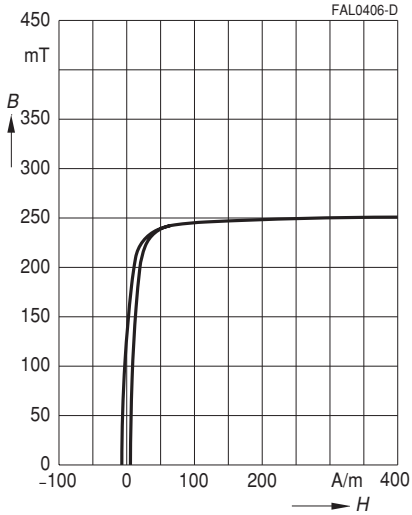

DC magnetic bias
(measured on RM cores, typical values)
($\hat{B} \leq$ 0,25 mT, f = 10 kHz, T = 25 °C)

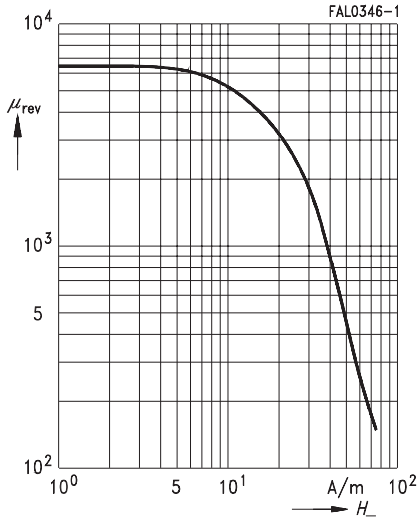

Complex permeability
versus frequency
(measured on R10 toroids, $\hat{B} \leq 0{,}25$ mT)

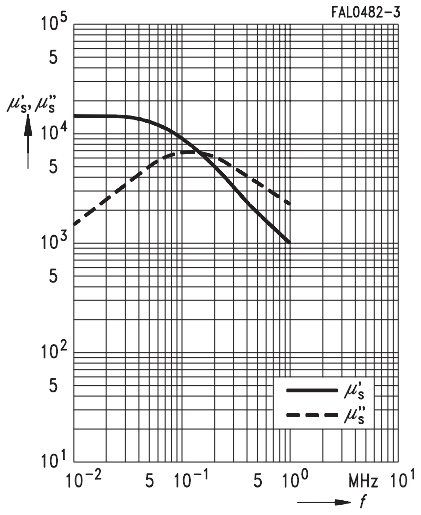

Initial permeability μ_i
versus temperature
(measured on R10 toroids, $\hat{B} \leq 0{,}25$ mT)

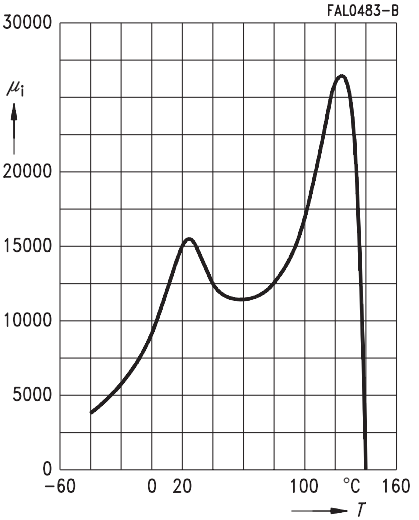

Variation of initial permeability
with temperature
(measured on R10 toroids, $\hat{B} \leq 0{,}25$ mT)

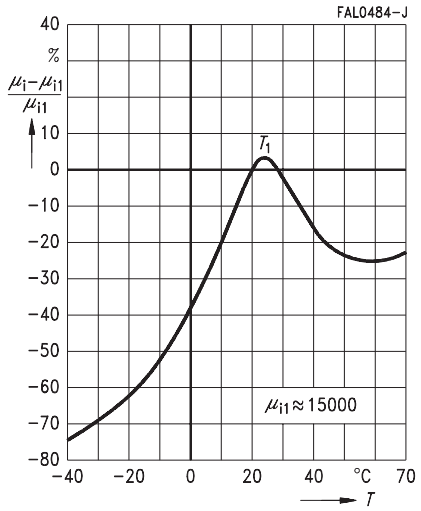

Relative loss factor
versus frequency
(measured on R10 toroids, $\hat{B} \leq 0{,}25$ mT)

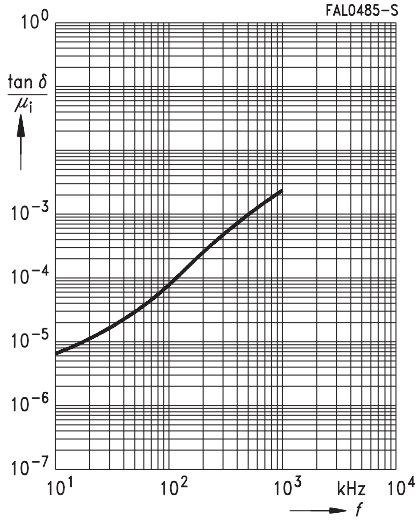

Dynamic magnetization curves
(typical values)
(f = 10 kHz, T = 25 °C)

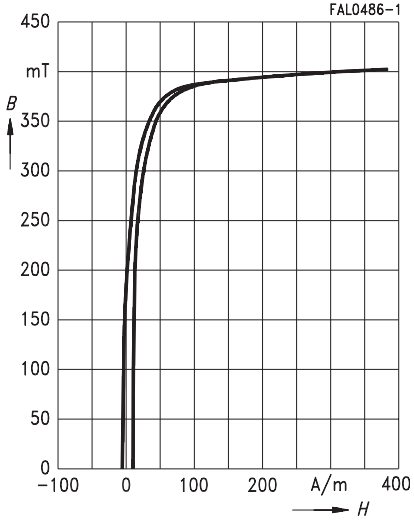

Dynamic magnetization curves
(typical values)
(f = 10 kHz, T = 100 °C)

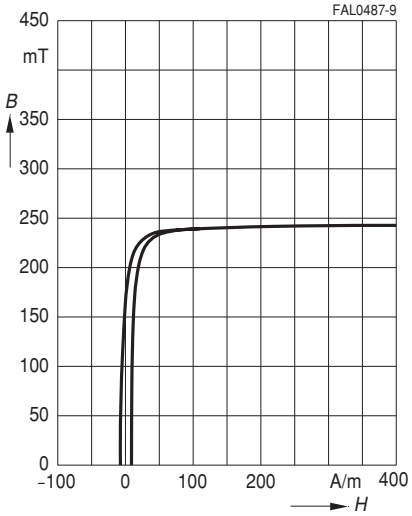

Complex permeability
versus frequency
(measured on R12,5 toroids, $\hat{B} \leq 0{,}25$ mT)

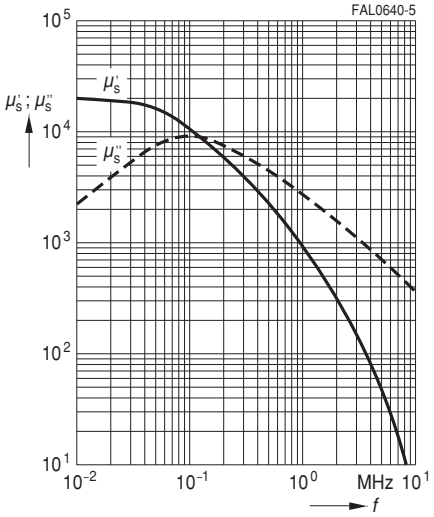

Initial permeability μ_i
versus temperature
(measured on R12,5 toroids, $\hat{B} \leq 0{,}25$ mT)

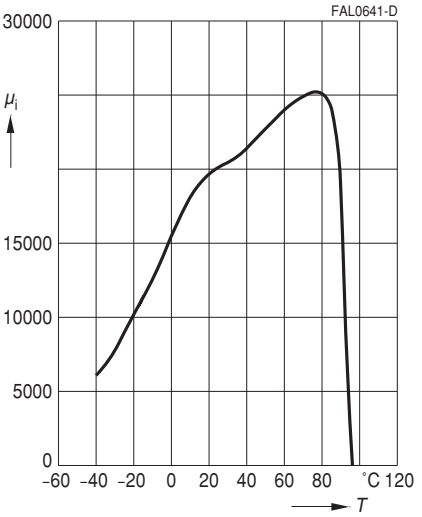

Variation of initial permeability
with temperature
(measured on R12,5 toroids, $\hat{B} \leq 0{,}25$ mT)

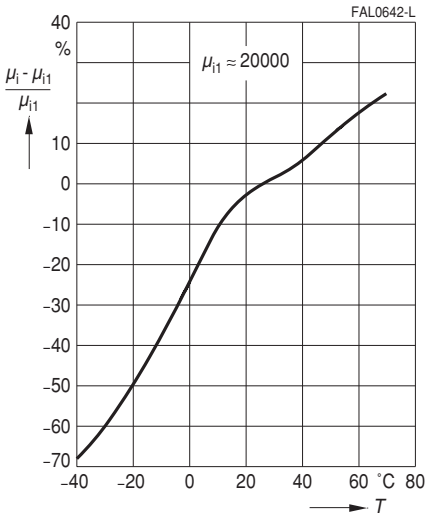

Relative loss factor
versus frequency
(measured on R12,5 toroids, $\hat{B} \leq 0{,}25$ mT)

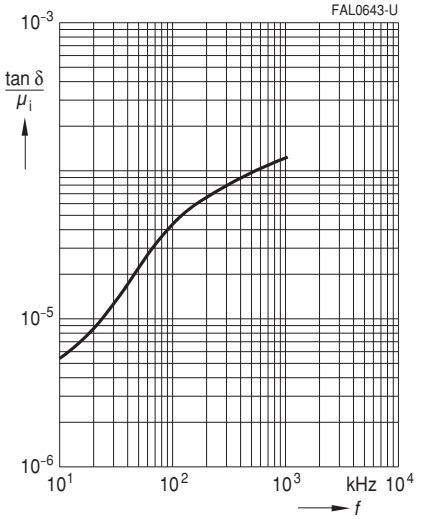

Dynamic magnetization curves
(typical values)
(f = 10 kHz, T = 25 °C)

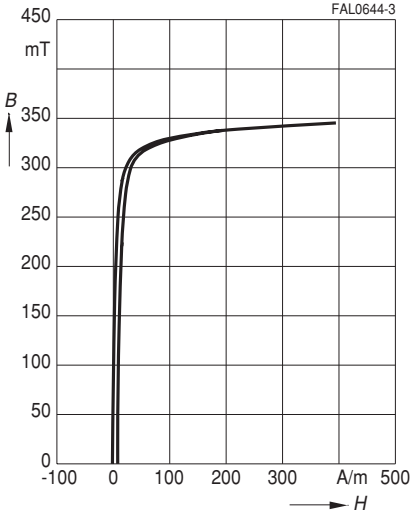

Complex permeability
versus frequency
(measured on R17 toroids, $\hat{B} \leq 0{,}25$ mT)

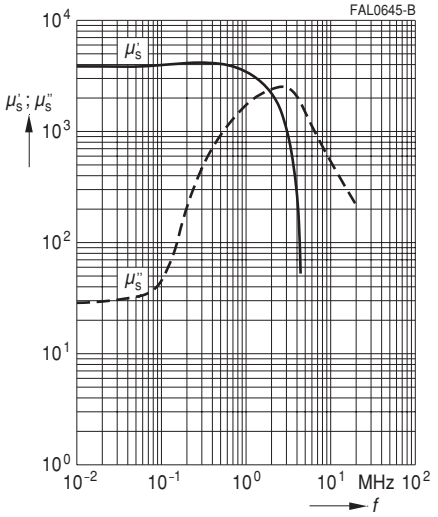

Initial permeability μ_i
versus temperature
(measured on R17 toroids, $\hat{B} \leq 0{,}25$ mT)

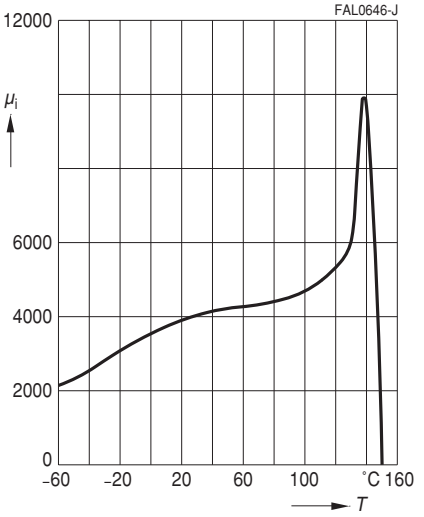

Variation of initial permeability
with temperature
(measured on R17 toroids, $\hat{B} \leq 0{,}25$ mT)

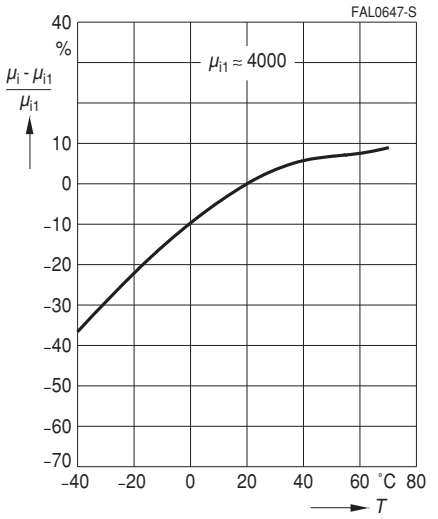

Relative loss factor
versus frequency
(measured on R17 toroids, $\hat{B} \leq 0{,}25$ mT)

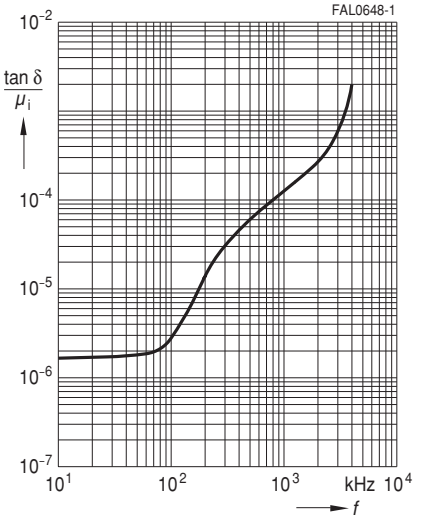

Dynamic magnetization curves
(typical values)
(f = 10 kHz, T = 25 °C)

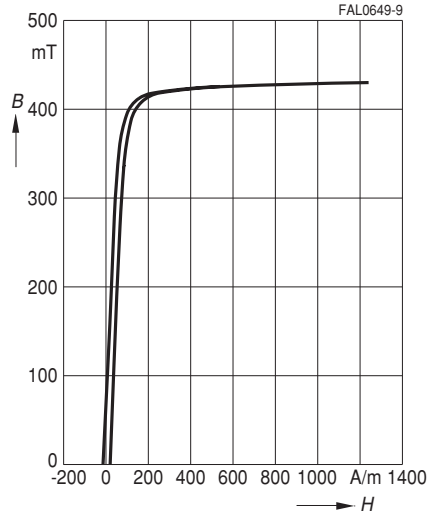

Dynamic magnetization curves
(typical values)
(f = 10 kHz, T = 100 °C)

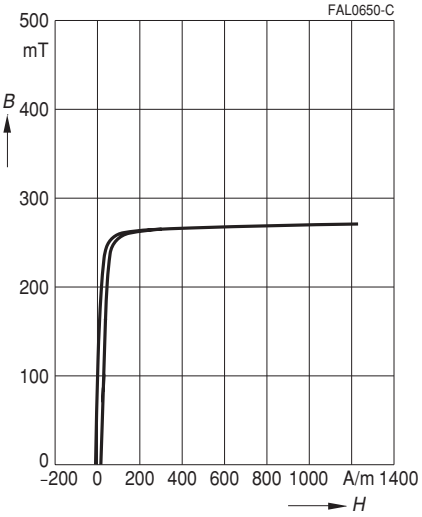

Reversible permeability versus temperature
(measured on toroids at f = 100 kHz,
HDC = 27,5 A/m, $\hat{B}$ = 6 mT)

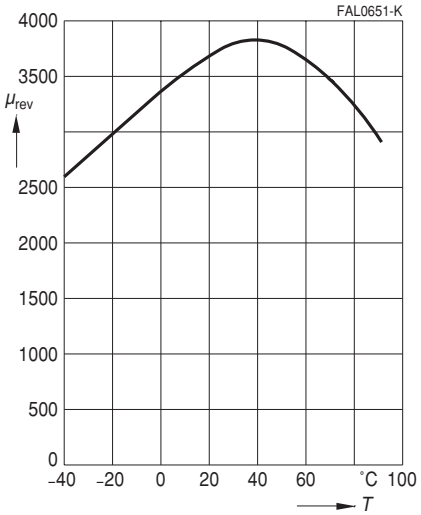

Complex permeability
versus frequency
(measured on R29 toroids, $\hat{B} \leq 0{,}25$ mT)

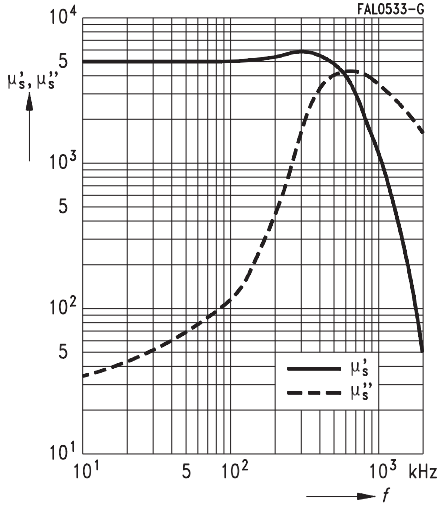

Initial permeability μ_i
versus temperature
(measured on R29 toroids, $\hat{B} \leq 0{,}25$ mT)

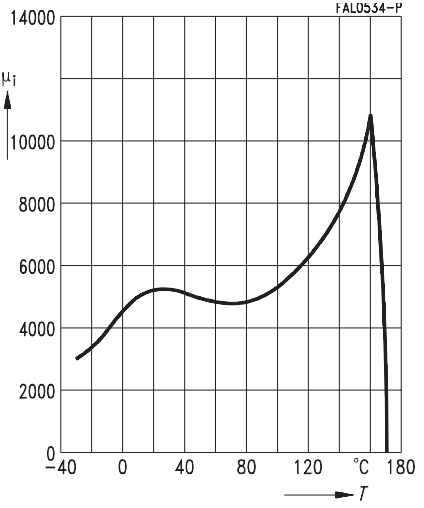

Variation of initial permeability
with temperature
(measured on R29 toroids, $\hat{B} \leq 0{,}25$ mT)

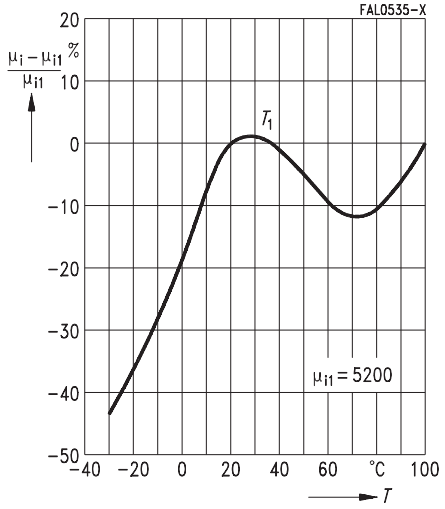

Relative loss factor
versus frequency
(measured on R29 toroids, $\hat{B} \leq 0{,}25$ mT)

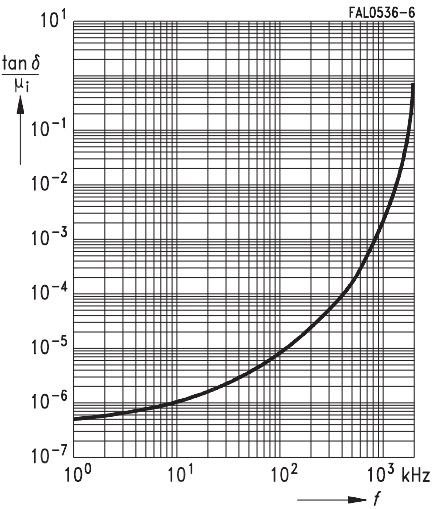

Dynamic magnetization curves
(typical values)
(f = 10 kHz, T = 25 °C)

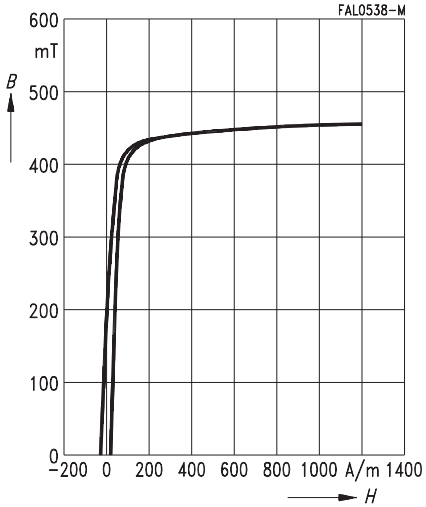

Dynamic magnetization curves
(typical values)
(f = 10 kHz, T = 100 °C)

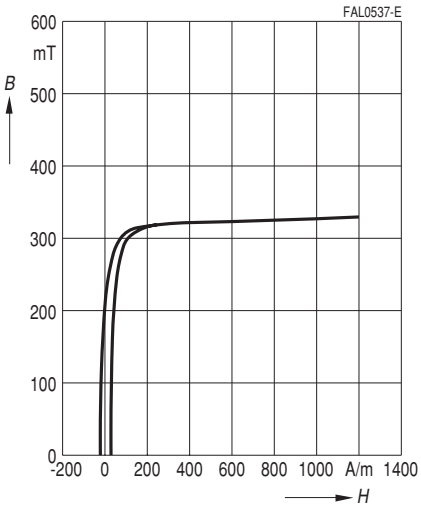

DC magnetic bias
(measured on RM cores, typical values)
($\hat{B} \leq$ 0,25 mT, f = 10 kHz, T = 25 °C)

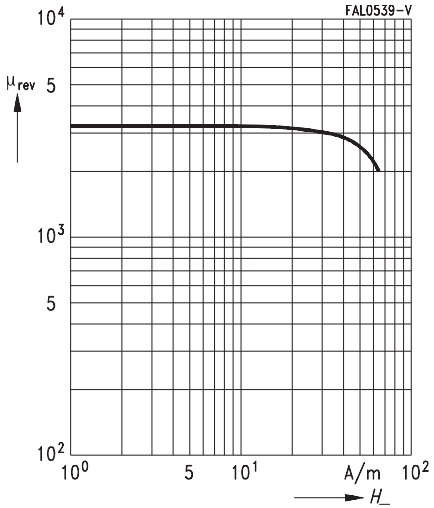

5 Plastic materials, manufacturers and UL numbers

- RM coil formers of thermosetting plastic, color code blue (molded-in pins):
  Bakelite UP 3420® [E 61040 (M)]; Bakelite
- RM, EP and EFD coil formers of thermosetting plastic, color code black (post-inserted pins):
  Sumikon PM 9630® [E41429 (M)]; Sumitomo Bakelite
- RM, EP and EFD coil formers of thermosetting plastic, color code green (post-inserted pins):
  Vyncolit/X611® [E167521 (M)]; Vyncolit NV
- EP7 special coil former of thermosetting plastic:
  AMC 2568® [E 48036 (M)], blue; Synres-Almoco BV
- RM power, P, PM, E, ETD, ER coil formers
  and terminal carriers P7×4, P9×5, P11×7, P36×22 (Polyterephthalate):
  Valox 420-SE0® [E 45329 (M)], black; General Electric Plastics
  Vestodur GF30-FR1® [E66645 (M)], black; Degussa Hüls
  Crastin CE 7931® [E 69578 (M)], black; DuPont
  Pocan 4235® [E 41613 (M)], black; Bayer
  Arnite TV4264SN® [E 47960 (M)], black; DSM
  Rynite FR 530® [E 69578 (M)], black; DuPont
- Terminal carrier P4,6×4,1 (Polyether Ketone):
  Luvocom 1105/GF/20/EM® [---], natural; Lehmann u. Voss & Co.
- Terminal carriers P14×8, P18×11, P22×13, P26×16, P30×19 (Polyterephthalate):
  Pocan 4235® [E 41613 (M)], grey; Bayer
- SMD coil formers (Liquid cristal polymer):
  Sumika Super E4008® [E 54705 (M)], black; Sumitomo Chemical
  Zenite 7130® [E 123598 (M)], black; DuPont
  Vectra C 130 [E 83005 (M)], black; Ticona
- Insulating washers:
  Makrofol KL 3 – 1005/1 [E 41613 (M)], natural; Bayer
  Pokalon SN [E 167358 (M)], natural; LOFO HIGH TECH FILM

Rights to change material reserved.
Further information is given on the packing label.
The trade names are registered trademarks of the listed manufacturers.

Further information to the UL certifications are available in the internet under http//:www.UL.com
Here you get the newest update of the yellow card.

EPCOS is an assigned molder with the UL file no. E 178623 (M).
The assigned designation is A 1770.

1 Hysteresis

The special feature of ferromagnetic and ferrimagnetic materials is that spontaneous magnetization sets in below a material-specific temperature (Curie point). The elementary atomic magnets are then aligned in parallel within macroscopic regions. These so-called Weiss' domains are normally oriented so that no magnetic effect is perceptible. But it is different when a ferromagnetic body is placed in a magnetic field and the flux density B as a function of the magnetic field strength H is measured with the aid of a test coil. Proceeding from $H = 0$ and $B = 0$, the so-called initial magnetization curve is first obtained. At low levels of field strength, those domains that are favorably oriented to the magnetic field grow at the expense of those that are not. This produces what are called wall displacements. At higher field strength, whole domains overturn magnetically – this is the steepest part of the curve – and finally the magnetic moments are moved out of the preferred states given by the crystal lattice into the direction of the field until saturation is obtained, i.e. until all elementary magnets in the material are in the direction of the field. If H is now reduced again, the B curve is completely different. The relationship shown in the hysteresis loop (Fig. 1) is obtained.

1.1 Hysteresis loop

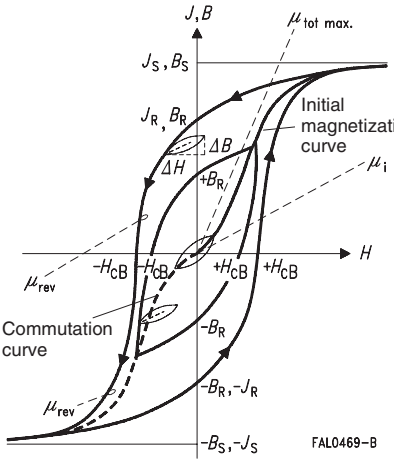

Fig. 1
Magnetization curve
(schematic)

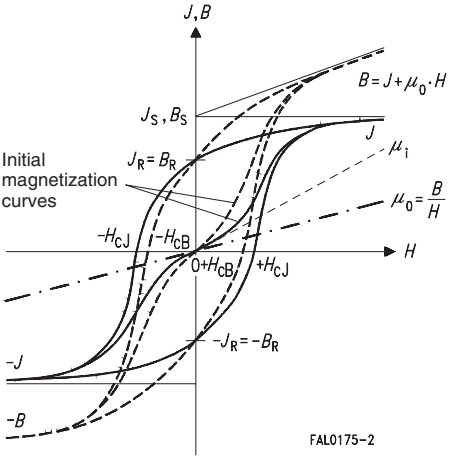

Fig. 2
Hysteresis loops for different
excitations and materials

Magnetic field strength $H = \frac{I \cdot N}{l} = \frac{\text{ampere-turns}}{\text{length in m}}$ $\left[\frac{\text{A}}{\text{m}}\right]$

Magnetic flux density $B = \frac{\phi}{A} = \frac{\text{magnetic flux}}{\text{permeated area}}$ $\left[\frac{\text{Vs}}{\text{m}^2}\right] = [\text{T } \textit{(Tesla)}]$

Polarization J $\quad J = B - \mu_0 H \quad \mu_0 \cdot H \ll J \Rightarrow B \approx J$

General relationship between B and H:

$B = \mu_0 \cdot \mu_r(H) \cdot H$

μ_0 = *magnetic field constant*

$\mu_0 = 1{,}257 \cdot 10^{-6} \left[\frac{Vs}{Am}\right]$

μ_r = *relative permeability*

In a vacuum, $\mu_r = 1$; in ferromagnetic or ferrimagnetic materials the relation $B(H)$ becomes nonlinear and the slope of the hysteresis loop $\mu_r \gg 1$.

1.2 Basic parameters of the hysteresis loop

1.2.1 Initial magnetization curve

The initial magnetization curve describes the relationship $B = \mu_r \mu_0 H$ for the first magnetization following a complete demagnetization. By joining the end points of all "sub-loops" , from $H = 0$ to $H = H_{max}$, (as shown in Figure 1), we obtain the so-called commutation curve (also termed normal or mean magnetization curve), which, for magnetically soft ferrite materials, coincides with the initial magnetization curve.

1.2.2 Saturation magnetization B_S

The saturation magnetization B_S is defined as the maximum flux density attainable in a material (i.e. for a very high field strength) at a given temperature; above this value B_S, it is not possible to further increase $B(H)$ by further increasing H.

Technically, B_S is defined as the flux density at a field strength of $H = 1200$ A/m. As is confirmed in the actual magnetization curves in the chapter on "Materials", the $B(H)$ characteristic above 1200 A/m remains roughly constant (applies to all ferrites with high initial permeability, i.e. where $\mu \geq 100$).

1.2.3 Remanent flux density $B_R(H)$

The remanent flux density (residual magnetization density) is a measure of the degree of residual magnetization in the ferrite after traversing a hysteresis loop. If the magnetic field H is subsequently reduced to zero, the ferrite still has a material-specific flux density $B_R \neq 0$ (see Fig. 1: intersection with the ordinate $H = 0$).

1.2.4 Coercive field strength H_C

The flux density B can be reduced to zero again by applying a specific opposing field $-H_C$ (see Fig. 1: intersection with the abscissa $B = 0$).

The demagnetized state can be restored at any time by:

a) traversing the hysteresis loop at a high frequency and simultaneously reducing the field strength H to $H = 0$.
b) by exceeding the Curie temperature T_C.

2 Permeability

Different relative permeabilities μ are defined on the basis of the hysteresis loop for the various electromagnetic applications.

2.1 Initial permeability μ_i

$$\mu_i = \frac{1}{\mu_0} \cdot \frac{\Delta B}{\Delta H} \qquad (\Delta H \to 0)$$

The initial permeability μ_i defines the relative permeability at very low excitation levels and constitutes the most important means of comparison for soft magnetic materials. According to IEC 60401, μ_i is defined using closed magnetic circuits (e.g. a closed ring-shaped cylindrical coil) for $f \leq 10$ kHz, $B < 0{,}25$ mT, $T = 25$ °C.

2.2 Effective permeability μ_e

Most core shapes in use today do not have closed magnetic paths (Only ring, double E or double-aperture cores have closed magnetic circuits.), rather the circuit consists of regions where $\mu_i \neq 1$ (ferrite material) and $\mu_i = 1$ (air gap). Fig. 3 shows the shape of the hysteresis loop of a circuit of this type.

In practice, an effective permeability μ_e is defined for cores with air gaps.

$$\mu_e = \frac{1}{\mu_0} \frac{L}{N^2} \sum \frac{l}{A}$$

$\sum \frac{l}{A}$ = *form factor*

L = inductance
N = number of turns

It should be noted, for example, that the loss factor tan δ and the temperature coefficient for gapped cores reduce in the ratio μ_e/μ_i compared to ungapped cores.

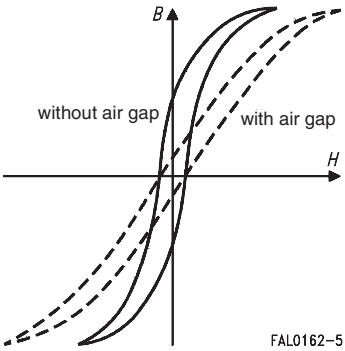

Fig. 3
Comparison of hysteresis loops for a core with and without an air gap

The following approximation applies for an air gap $s \ll l_e$:

$$\mu_e = \frac{\mu_i}{1 + \frac{s}{l_e} \cdot \mu_i}$$

s = width of air gap
l_e = effective magnetic path length

For more precise calculation methods, see for example E.C. Snelling, “Soft ferrites”, 2nd edition.

2.3 Apparent permeability μ_{app}

$$\mu_{app} = \frac{L}{L_0} = \frac{\textit{inductance with core}}{\textit{inductance without core}}$$

The definition of μ_{app} is particularly important for specification of the permeability for coils with tubular, cylindrical and threaded cores, since an unambiguous relationship between initial permeability μ_i and effective permeability μ_e is not possible on account of the high leakage inductances. The design of the winding and the spatial correlation between coil and core have a considerable influence on μ_{app}. A precise specification of μ_{app} requires a precise specification of the measuring coil arrangement.

2.4 Complex permeability $\overline{\mu}$

To enable a better comparison of ferrite materials and their frequency characteristics at very low field strengths (in order to take into consideration the phase displacement between voltage and current), it is useful to introduce μ as a complex operator, i.e. a complex permeability $\overline{\mu}$, according to the following relationship:

$\overline{\mu} = \mu_s' - j \cdot \mu_s''$
where, in terms of a series equivalent circuit, (see Fig. 5)
μ_s' is the relative real (inductance) component of $\overline{\mu}$
and μ'' is the relative imaginary (loss) component of $\overline{\mu}$.

Using the complex permeability $\overline{\mu}$, the (complex) impedance of the coil can be calculated:
$\overline{Z} = j\,\omega\,\overline{\mu}\,L_0$
where L_0 represents the inductance of a core of permeability $\mu_r = 1$, but with unchanged flux distribution.
(cf. also section 4.1: information on tan δ)

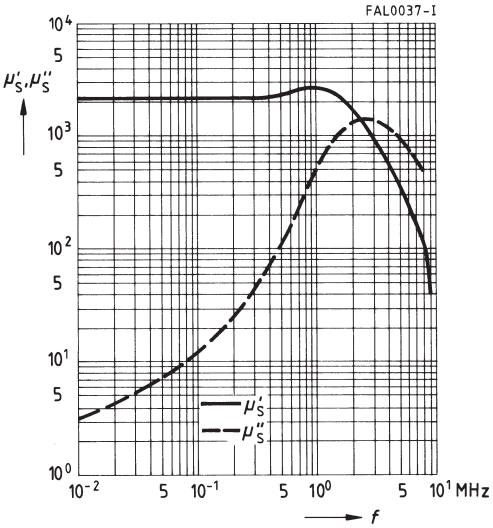

Fig. 4
Complex permeability versus frequency
(measured on R10 toroids, N 48 material, measuring flux density $\hat{B} \leq 0{,}25$ mT)

Fig. 4 shows the characteristic shape of the curves of μ_s' and μ_s" as functions of the frequency, using N 48 material as an example. The real component μ_s' is constant at low frequencies, attains a maximum at higher frequencies and then drops in approximately inverse proportion to *f*. At the same time, μ" rises steeply from a very small value at low frequencies to attain a distinct maximum and, past this, also drops as the frequency is further increased.

The region in which μ' decreases sharply and where the μ" maximum occurs is termed the cut-off frequency f_{cutoff}. This is inversely proportional to the initial permeability of the material (Snoek's law).

2.5 Reversible permeability μ_{rev}

$$\mu_{rev} = \frac{1}{\mu_0} \cdot \lim_{\Delta H \to 0} \left(\frac{\Delta B}{\Delta H}\right)_{H\_}$$

(Permeability with superimposed DC field $H\_$)

In order to measure the reversible permeability μ_{rev}, a small measuring alternating field is superimposed on a DC field. In this case μ_{rev} is heavily dependent on $H\_$, the core geometry and the temperature.

Important application areas for DC field-superimposed, i.e. magnetically biased coils are broadband transformer systems (feeding currents with signal superimposition) and power engineering (shifting the operating point) and the area known as "nonlinear chokes" (cf. chapter on RM cores). For the magnetic bias curves as a function of the excitation $H\_$ see the chapter on "SIFERRIT materials".

2.6 Amplitude permeability μ_a, A_{L1} value

$$\mu_a = \frac{\hat{B}}{\mu_0 \hat{H}}$$ (Permeability at high excitation)

$\hat{B}$ = peak value of flux density
$\hat{H}$ = peak value of field strength

For frequencies well below cut-off frequency, μ_a is not frequency-dependent but there is a strong dependence on temperature. The amplitude permeability is an important definition quantity for power ferrites. It is defined for specific core types by means of an A_{L1} value for $f \leq 10$ kHz, $B = 320$ mT (or 200 mT), $T = 100$ °C.

$$A_{L1} = \frac{\mu_0 \cdot \mu_a}{\sum \frac{l}{A}}$$

3 Magnetic core shape characteristics

Permeabilities and also other magnetic parameters are generally defined as material-specific quantities. For a particular core shape, however, the magnetic data are influenced to a significant extent by the geometry. Thus, the inductance of a slim-line ring core coil is defined as:

$$L = \mu_r \cdot \mu_0 \cdot N^2 \cdot \frac{A}{l}$$

Due to their geometry, soft magnetic ferrite cores in the field of such a coil change the flux parameters in such a way that it is necessary to specify a series of effective core shape parameters in each data sheet. The following are defined:

l_e	effective magnetic length
A_e	effective magnetic cross section
A_{min}	min. magnetic cross section of the core (required to calculate the max. flux density)
$V_e = A_e \bullet l_e$	effective magnetic volume

With the aid of these parameters, the calculation for ferrite cores with complicated shapes can be reduced to the considerably more simple problem of an imaginary ring core with the same magnetic properties. The basis for this is provided by the methods of calculation according to IEC 60205, IEC 60205A and IEC 60205B, which allow the following factors $\Sigma l/A$ and A_L to be calculated:

3.1 Form factor

$$\sum \frac{l}{A} = \frac{l_e}{A_e}$$

The inductance *L* can then be calculated as follows:

$$L = \frac{\mu_e \cdot \mu_0 \cdot N^2}{\sum \frac{l}{A}}$$

where μ_e denotes the effective permeability or another permeability μ_{rev} or μ_a (or μ_i for cores with a closed magnetic path) adapted for the *B*/*H* range in question.

3.2 Inductance factor, A_L value

$$A_L = \frac{L}{N^2} = \frac{\mu_e \cdot \mu_0}{\sum \frac{l}{A}}$$

A_L is the inductance referred to number of turns = 1. Therefore, for a defined number of turns *N*:

$$L = A_L \cdot N^2$$

3.3 Tolerance code letters

The tolerances of the A_L are coded by the letters in the third block of the ordering code in conformity with IEC 60062.

Code letter	Tolerance of A_L value	Code letter	Tolerance of A_L value
A	± 3 %	K	± 10 %
B	± 4 %	L	± 15 %
C	± 6 %	M	± 20 %
D	± 8 %	Q	+ 30 / – 10 %
E	± 7 %	R	+ 30 / – 20 %
G	± 2 %	U	+ 80 / – 0 %
H	± 12 %	X	filling letter
J	± 5 %	Y	+ 40 / – 30 %

The tolerance values available are given in the individual data sheets.

4 Definition quantities in the small-signal range

4.1 Loss factor tan δ

Losses in the small-signal range are specified by the loss factor tan δ.

Based on the impedance $\underline{Z}$ (cf. also section 2.4), the loss factor of the core in conjunction with the complex permeability $\underline{\mu}$ is defined as

$$tan\delta_s = \frac{\mu_s''}{\mu_s'} = \frac{R_s}{\omega L_s} \quad \text{and} \quad tan\delta_p = \frac{\mu_p''}{\mu_p'} = \frac{\omega \cdot L_p}{R_p}$$

where R_s and R_p denote the series and parallel resistance and L_s and L_p the series and parallel inductance respectively.

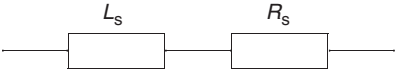

Fig. 5
Lossless series inductance L_s with loss resistance R_s resulting from the core losses.

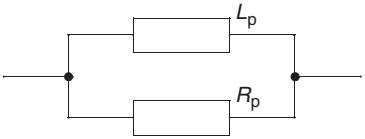

Fig. 6
Lossless parallel inductance L_p with loss resistance R_p resulting from the core losses.

From the relationships between series and parallel circuits we obtain:

$$\mu'_p = \mu'_s \cdot (1 + (tan\delta)^2)$$

$$\mu''_p = \mu''_s \cdot \left(1 + \left(\frac{1}{tan\ \delta}\right)^2\right)$$

4.2 Relative loss factor tan δ/μ_i

In gapped cores the material loss factor tan δ is reduced by the factor μ_e/μ_i. This results in the relative loss factor tan δ_e (cf. also section 2.2):

$$tan\delta_e = \frac{tan\delta}{\mu_i} \cdot \mu_e$$

The table of material properties lists the relative loss factor tan δ/μ_i. This is determined in accordance with IEC 60401 at f = 10 kHz, B = 0,25 mT, T = 25 °C.

4.3 Quality factor *Q*

The ratio of reactance to total resistance of an induction coil is known as the quality factor *Q*.

$$Q = \frac{\omega L}{R_L} = \frac{reactance}{total\ resistance}$$

The total quality factor *Q* is the reciprocal of the total loss factor tan δ of the coil; it is dependent on the frequency, inductance, temperature, winding wire and permeability of the core.

4.4 Hysteresis loss resistance R_h and hysteresis material constant η_B

In transformers, in particular, the user cannot always be content with very low saturation. The user requires details of the losses which occur at higher saturation, e.g. where the hysteresis loop begins to open.

Since this hysteresis loss resistance R_h can rise sharply in different flux density ranges and at different frequencies, it is measured in accordance with IEC 60401 for μ_i values greater than 500 at B_1 = 1,5 and B_2 = 3 mT (ΔB = 1,5 mT), a frequency of 10 kHz and a temperature of 25 °C (for μ_i < 500: f = 100 kHz). The hysteresis loss factor tan δ_h can then be calculated from this.

$$tan\delta_h = \frac{R_h}{\omega \cdot L} = tan\delta(B_2) - tan\delta(B_1)$$

For the hysteresis material constant η_B we obtain:

$$\eta_B = \frac{tan\delta_h}{\mu_e \cdot \Delta\hat{B}}$$

The hysteresis material constant, η_B, characterizes the material-specific hysteresis losses and is a quantity independent of the air gap in a magnetic circuit.

The hysteresis loss factor of an inductor can be reduced, at a constant flux density, by means of an (additional) air gap

$$tan\delta_h = \eta_B \cdot \Delta\hat{B} \cdot \mu_e$$

For further details on the measurement techniques see IEC 60367-1.

5 Definition quantities in the high-excitation range

While in the small-signal range ($H \leq H_c$), i.e. in filter and broadband applications, the hysteresis loop is generally traversed only in lancet form (Fig. 2), for power applications the hysteresis loop is driven partly into saturation. The defining quantities are then

μ_{rev} reversible permeability in the case of superimposition with a DC signal (operating point for power transformers)
μ_a amplitude permeability and
P_V core losses.

5.1 Core losses P_V

The losses of a ferrite core or core set P_V is proportional to the area of the hysteresis loop in question. It can be divided into three components:

$$P_V = P_{V,\ hysteresis} + P_{V,\ eddycurrent} + P_{V,\ residual}$$

Owing to the high specific resistance of ferrite materials, the eddy current losses in the frequency range common today (1 kHz - 2 MHz) may be practically disregarded except in the case of core shapes having a large cross-sectional area.

The power loss P_V is a function of the temperature T, the frequency f, the flux density B and is of course dependent on ferrite material and core shape.

The temperature dependence can generally be approximated by means of a third-order polynomial, while

$$P_V(f) \sim f^{(1+x)} \qquad 0 \le x \le 1$$

applies for the frequency dependence and

$$P_V(B) \sim B^{(2+y)} \qquad 0 \le y \le 1$$

for the flux density dependence. The coefficients x and y are dependent on core shape and material, and there is a mutual dependence between the coefficients of the definition quantity (e.g. T) and the relevant parameter set (e.g. f, B).

In the case of cores which are suitable for power applications, the total core losses P_V are given explicitly for a specific frequency f, flux density B and temperature T in the relevant data sheets.

When determining the total power loss for an inductive component, the winding losses must also be taken into consideration in addition to the core-specific losses.

$$P_{V\ tot} = P_{V\ core} + P_{V\ winding}$$

where, in addition to insulation conditions in the given frequency range, skin effect and proximity effect must also be taken into consideration for the winding.

5.2 Performance factor ($PF = f \cdot B_{max}$)

The performance factor is a measure of the maximum power which a ferrite can transmit, whereby it is generally assumed that the loss does not exceed 300 kW/m^3. Heat dissipation values of this order are usually assumed when designing small and medium-sized transformers. Increasing the performance factor will either enable an increase of the power that can be transformed by a core of identical design, or a reduction in component size if the transformed power is not increased.

If the performance factors of different power transformer materials are plotted as a function of frequency, only slight differences are observed at low frequencies (< 300 kHz), but these differences become more pronounced with increasing frequency. This diagram can be used to determine the optimum material for a given frequency range (for diagram see page 46).

6 Influence of temperature

6.1 $\mu(T)$ curve, Curie temperature T_C

The initial permeability μ_i as a function of T is given for all materials (see chapter on SIFERRIT materials). Important parameters for a $\mu(T)$ curve are the position of the **s**econdary **p**ermeability **m**aximum (SPM) and the Curie temperature. Minimum losses occur at the SPM temperature.

Above the Curie temperature T_C ferrite materials lose their ferrimagnetic properties, i.e. μ_i drops to $\mu_i = 1$. This means that the parallel alignment of the elementary magnets (spontaneous magnetization) is destroyed by increasing thermal activation. This phenomenon is reversible, i.e. when the temperature is reduced below T_C again, the ferrimagnetic properties are restored.

6.2 Temperature coefficient of permeability α

By definition the temperature coefficient α represents a straight line of average gradient between the reference temperatures T_1 and T_2. If the $\mu(T)$ curve is approximately linear in this temperature range, this is a good approximation; in the case of heavily pronounced maxima, as occur particularly with highly permeable broadband ferrites, however, this is less true. The following applies:

$$\alpha = \frac{\mu_{i2} - \mu_{i1}}{\mu_{i1}} \cdot \frac{1}{T_2 - T_1}$$

μ_{i1} = initial permeability μ_i at T_1 = 25 °C
μ_{i2} = the initial permeability μ_i associated with the temperature T_2

6.3 Relative temperature coefficient α_F

$$\alpha_F = \frac{\alpha}{\mu_i} = \frac{\mu_{i2} - \mu_{i1}}{\mu_{i2} \cdot \mu_{i1}} \cdot \frac{1}{T_2 - T_1}$$

In a magnetic circuit with an air gap and the effective permeability μ_e the temperature coefficient is reduced by the factor μ_e/μ_i (cf. also section 2.4).

6.4 Permeability factor

The first factor in the equation for determining the relative temperature coefficient $\frac{\mu_{i2} - \mu_{i1}}{\mu_{i2} \cdot \mu_{i1}}$ is known as the permeability factor.

In the case of SIFERRIT materials for resonant circuits, the temperature dependence of the permeability factor can be seen from the relevant diagram.

6.5 Effective temperature coefficient α_e

$$\alpha_e = \frac{\mu_e}{\mu_i} \cdot \alpha$$

In the case of the ferrite materials for filter applications, the α/μ_i values for the ranges 25 ... 55°C and 5 .... 25°C are given in the table of material properties.

The effective permeability μ_e is required in order to calculate α_e; therefore this is given for each core in the individual data sheets.

6.6 Relationship between the change in inductance and the permeability factor

The relative change in inductance between two temperature points can be calculated as follows:

$$\frac{L_2 - L_1}{L_1} = \frac{\alpha}{\mu_i} \cdot (T_2 - T_1) \cdot \mu_e$$

$$\frac{L_2 - L_1}{L_1} = \frac{\mu_{i2} - \mu_{i1}}{\mu_{i2} \cdot \mu_{i1}} \mu_e$$

6.7 Temperature dependence of saturation magnetization

The saturation magnetization B_S drops monotonically with temperature and at T_C has fallen to $B_S = 0$ mT. The drop for $B_S(25°C)$ and $B_S(100°C)$, i.e. the main area of application for the ferrites, can be taken from the table of material properties.

6.8 Temperature dependence of saturation-dependent permeability (amplitude permeability)

It can be seen from the $\mu_a(B)$ curves for the different materials that μ_a exhibits a more pronounced maximum with increasing temperature and drops off sooner on account of decreasing saturation.

7 Disaccommodation

Ferrimagnetic states of equilibrium can be influenced by mechanical, thermal or magnetic changes (shocks). Generally, an increase in permeability occurs when a greater mobility of individual magnetic domains is attained through the external application of energy. This state is not temporally stable and returns logarithmically with time to the original state.

7.1 Disaccommodation coefficient *d*

$$d = \frac{\mu_{i1} - \mu_{i2}}{\mu_{i1} \cdot (lg\, t_2 - lg\, t_1)}$$

where μ_{i1} = permeability at time t_1
μ_{i2} = permeability at time t_2 and $t_2 > t_1$

7.2 Disaccommodation factor *DF*

$$DF = \frac{d}{\mu_{i1}}$$

Accordingly, a change in inductance can be calculated with the aid of *DF*:

$$\frac{L_1 - L_2}{L_1} = DF \cdot \mu_e \cdot log \frac{t_2}{t_1}$$

8 General mechanical, thermal, electrical and magnetic properties of ferrites

Typical figures for the mechanical and thermal properties of ferrites

Tensile strength	approx. 30 MPa/mm^2
Compressive strength	approx. 800 MPa/mm^2
Vickers hardness HV_{15}	approx. 600 MPa/mm^2
Modulus of elasticity	approx. 150000 N/mm^2
Fracture toughness K_{1c}	approx. 0,8 ... 1,1 MPam$^{1/2}$
Thermal conductivity	approx. 4 ... 7·10^{-3} J/mm·s·K
Coefficient of linear expansion	approx. 7 ... 10 ·10^{-6} 1/K
Specific heat	approx. 0,7 J/g·K

8.1 Mechanical properties

Ferrite cores have to meet mechanical requirements during assembling and for a growing number of applications. Since ferrites are ceramic materials one has to be aware of the special behavior under mechanical load.

As valid for any ceramic material, ferrite cores are brittle and sensitive to any shock, fast changing or tensile load. Especially high cooling rates under ultrasonic cleaning and high static or cyclic loads can cause cracks or failure of the ferrite cores.

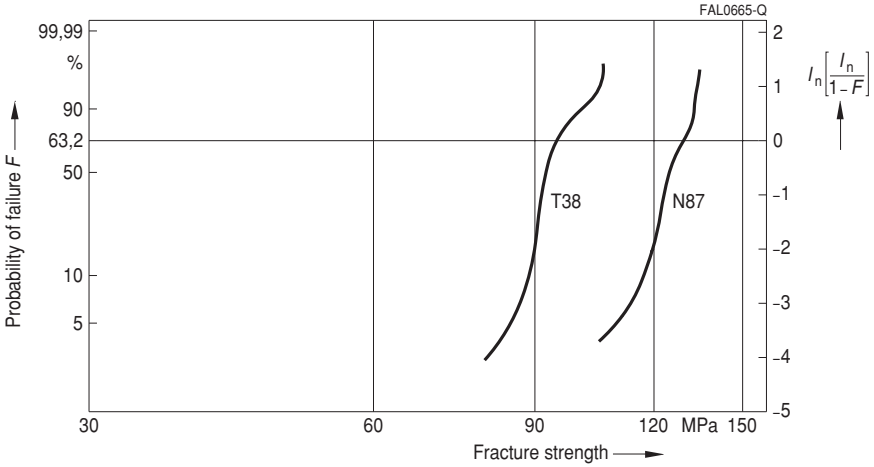

Fig. 7
Weibull plot of fracture strength values of the materials T38 and N87

There are two modes of crack growth: fast (critical) or slow (subcritical) crack propagation. In the first case spontaneous breakdown occurs. In the second case the crack propagates slowly during static or cycling loading, and then the sample can only fail if a critical crack length is achieved. According to the linear elastic fracture mechanics these two mechanisms could be described in terms of stress intensity factors. For life time predictions the knowledge of subcritical crack growth and R- (respectively K_R–) curve behavior of the material is essential.

The reduction of the material strength by temperature induced propagating microstructural cracks can be described as follows:

$$\sigma = \alpha \cdot \Delta T \frac{E_0}{1 + 2\pi N l^2}$$

σ	effective strength
α	Coefficient of thermal expansion (7 … 12 · 10^{-6} 1/K)
E_0	Modulus of elasticity
N	Number of temperature changes
l	Crack length

The brittleness of ferrite materials can be quantified by means of the fracture toughness. High fracture toughness values indicate decreased material brittleness. The quantity of the fracture toughness is a measure for the stress in the core necessary for a propagating crack. For the crack propagation it is required that the stress intensity factor exceeds the fracture toughness.

$$K_1 \geq K_{1C} \quad \text{with} \quad K_1 = \sigma_{appl}\sqrt{l \cdot Y} \quad \text{and} \quad K_{1C} = \sqrt{G_C E}$$

K_1	Stress intensity facture
K_{1C}	Fracture toughness
σ_{appl}	applied stress
Y	Factor for fracture/sample geometry
G_C	Critical fracture area energy
E	Modulus of elasticity

Typical fracture toughness values can be obtained from the table on page 119.

Ferrite materials have a pronounced R-curve behavior, i. e. the fracture toughness increases with propagating crack length. In practice there is a rather tolerant behavior towards moderate single stress events.

8.2 Stress sensitivity of magnetic properties

Stresses in the core affect not only the mechanical but also the magnetic properties. It is apparent that the initial permeability is dependent on the stress state of the core. With

$$\mu_i \cong \frac{1}{\frac{1}{\mu_{io}} + k \cdot \sigma_T}; \qquad k \approx 30 \cdot 10^{-6} \cdot \frac{1}{\text{MPa}}$$

where μ_{io} is the initial permeability of the unstressed material, it can be shown that the higher the stresses are in the core, the lower is the value for the initial permeability. Embedding the ferrite cores (e.g. in plastic) can induce these stresses. A permeability reduction of up to 50% and more can be observed, depending on the material. In this case, the embedding medium should have the greatest possible elasticity.

8.3 Magnetostriction

Linear magnetostriction is defined as the relative change in length of a magnetic core under the influence of a magnetic field. The greatest relative variation in length $\lambda = \Delta l/l$ occurs at saturation magnetization. The values of the saturation magnetostriction (λ_s) of our ferrite materials are given in the following table (negative values denote contraction).

SIFFERIT material	K 12	K 1	N 48
λ_s in 10^{-6}	– 21	– 18	– 1,5

Magnetostrictive effects are of significance principally when a coil is operated in the frequency range < 20 kHz and then undesired audible frequency effects (distortion etc.) occur.

8.4 Resistance to radiation

SIFERRIT materials can be exposed to the following radiation without significant variation ($\Delta L/L \leq 1\%$ for ungapped cores):

gamma quanta:	10^9 rad
quick neutrons	$2 \cdot 10^{20}$ neutrons/m^2
thermal neutrons	$2 \cdot 10^{22}$ neutrons/m^2

8.5 Resistivity ρ, dielectric constant ε

At room temperature, ferrites have a resistivity in the range 1 Ωm to 10^5 Ωm; this value is usually higher at the grain boundaries than in the grain interior. The temperature dependence of the core resistivity corresponds to that of a semiconductor:

$$\rho \sim e^{\frac{E_a}{k \cdot T}}$$

E_a Activation energy (0,1 ... 0,5 eV)
k Boltzmann constant
T Absolute temperature [K]

Thus the resistivity at 100 °C is one order of magnitude less than at 25 °C, which is significant, particularly in power applications, for the magnitude of the eddy-current losses.

Similarly, the resistivity decreases with increasing frequency.

Example: Material N 48

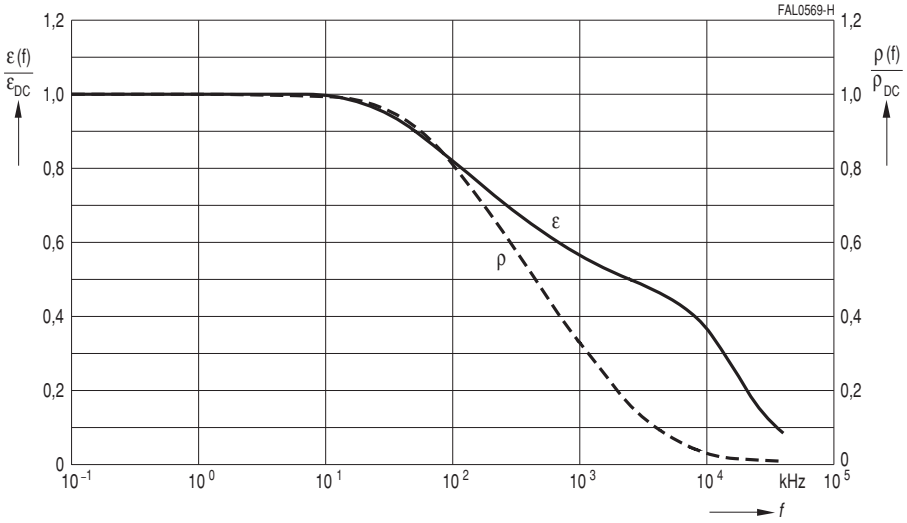

Fig. 8
Resistivity and dielectric constant versus frequency

The different resistivity values for grain interior and grain boundary result in high (apparent) dielectric constants ε at low frequencies. The dielectric constant ε for all ferrites falls to values around 10 … 20 at very high frequencies. NiZn ferrites already reach this value range at frequencies around 100 kHz.

SIFFERIT material	Resistivity (approx.)	Dielectric constant ε at (approximate values)				
	Ωm	10 kHz	100 kHz	1 MHz	100 MHz	300 MHz
K1 (NiZn)	10^5	30	15	12	11	11
N 48 (MnZn)	1	$140 \cdot 10^3$	$115 \cdot 10^3$	$80 \cdot 10^3$		

Magnetostrictive effects are of significance principally when a coil is operated in the frequency range < 20 kHz and then undesired audible frequency effects occur.

9 Coil characteristics

Resistance factor A_R

The resistance factor A_R, or A_R value, is the DC resistance R_{Cu} per unit turn, analogous to the A_L value.

$$A_R = \frac{R_{Cu}}{N^2}$$

When the A_R value and number of turns N are given, the DC resistance can be calculated from $R_{CU} = A_R N^2$.

From the winding data etc. the A_R value can be calculated as follows:

$$A_R = \frac{\rho \cdot l_N}{f_{Cu} \cdot A_N}$$

where ρ = resistivity (for copper: 17,2 $\mu\Omega$ mm), l_N = average length of turn in mm, A_N = cross section of winding in mm^2, f_{Cu} = copper space factor. If these units are used in the equation, the A_R value is obtained in $\mu\Omega = 10^{-6}\ \Omega$. For calculation of l_N and A_N the middle dimensions are used.

For coil formers, A_R values are given in addition to A_N and l_N. They are based on a copper filling factor of $f_{Cu} = 0{,}5$. This permits the A_R value to be calculated for any filling factor f_{Cu}:

$$A_{R(f_{Cu})} = A_{R(0,5)} \cdot \frac{0{,}5}{f_{Cu}}$$

For rough estimation a copper filling factor of $f_{Cu} = 0{,}5$ is sufficient. Else is given in the filling factor out of DIN 46435.

1 Cores for filter applications

1.1 Gapped cores for filter/resonant circuits

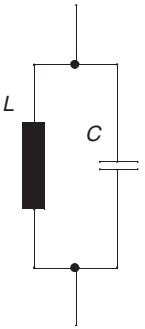

Basic requirements:

- low tan δ
- close tolerance for A_L value
- close tolerance for temperature coefficient
- low disaccommodation factor *DF*
- wide adjustment range

Gapped cores are therefore always used in high quality circuits (for materials see application survey, page 32).

In the case of small air gaps (max. 0,2 mm) the air gap can be ground into only one core half. In this case the half with the ground air gap bears the stamp. The other half is blank.

The air gap enables the losses in the small-signal area and the temperature coefficient to be reduced by a factor of μ_e/μ_i in the small-signal area. More important, however, is that close A_L value tolerances can be achieved.

The rated A_L values for cores with ground air gap can be obtained from the individual data sheets. The data for the individual cores also include the effective permeability μ_e used to approximately determine the effective loss factor tan δ_e and the temperature coefficient of the effective permeability α_e from the ring core characteristics (see table of material properties).

It should be noted at this point that in cores with a larger air gap the stray field in the immediate vicinity of the air gap can cause additional eddy current losses in the copper winding. If the coil quality must meet stringent requirements, it is therefore advisable to wind several layers of polystyrene, nylon tape or even FPC film under the wire in the part of the winding that is in the proximity of the air gap; with a 3-section coil former this would be the part of the center section near the air gap.

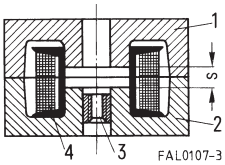

Fig. 9
Schematic drawing showing the construction of a P or RM core set with a total air gap *s*, comprising 2 core halves (1 and 2), threaded part (3) and padded winding (4)

1.2 P and RM cores with threaded sleeves

P and RM cores are supplied with a glued-in threaded sleeve. EPCOS uses automatic machines featuring high reliability in dosing of the adhesive and in positioning the threaded sleeve in the core.

The tight fit of the threaded sleeve is regularly checked – including a humid atmosphere of 40 °C/93 % r.h. (in accordance with IEC 60068-2-3) over 4 days – and also by periodic tests over 3 weeks. The usual bonding strengths of 20 N for ∅ 2 mm holes (e.g. for P 11 × 7, RM 5) and 30 N for ∅ 3 mm holes (e.g. for P 14 × 11, RM 6) are greatly exceeded, reaching an average of > 100 N. The threaded sleeve is continuously checked for proper centering. Overall, the controlled automated procedure guarantees higher reliability than manual gluing with its unavoidable inadequacies. Owing to the porosity of the ferrite, tension of the ferrite structure due to hardened adhesive that has penetrated cannot always be avoided. Hence, the relative temperature coefficient α_F may be increased by approximately $0{,}2 \cdot 10^{-6}$/K.

1.3 Typical calculation of a resonant circuit inductor

The following example serves to illustrate the dependencies to be considered when designing a resonant circuit inductor:

A SIFERRIT pot core inductor is required with an inductance of L = 640 µH and a minimum quality factor Q = 400 ($\tan \delta_L = 1/Q = 2{,}5 \cdot 10^{-3}$) for a frequency of 500 kHz. The temperature coefficient α_e of this inductor should be $100 \cdot 10^{-6}$/K in the temperature range + 5 to + 55 °C.

a) Choice of material

According to the table of material properties and the tan δ/μ_i curves (see chapter “SIFERRIT materials”) the material M 33, for example, can be used for 500 kHz.

b) Choice of A_L value

The Q and temperature coefficient requirements demand a gapped pot core. The relative temperature coefficient α_F of SIFERRIT M 33 according to the table of material properties is on average about $1{,}6 \cdot 10^{-6}$/K. Since the required α_e value of the gapped P core should be about $100 \cdot 10^{-6}$/K, the effective permeability is

$$\alpha_F = \frac{\alpha_e}{\mu_e} \quad \Rightarrow \quad \mu_e = \frac{\alpha_e}{\alpha/\mu_i} = 100 \cdot 10^{-6}/K \cdot \frac{1}{1,6 \cdot 10^{-6}/K} = 62{,}5$$

With pot core P 18 × 11 (B65651): μ_e = 47,9 for A_L = 100 nH.
With pot core P 22 × 13 (B65661): μ_e = 39,8 for A_L = 100 nH.

c) Choice of winding material

RF litz wire 20×0,05 with single natural silk covering is particularly suitable for frequencies around 500 kHz. The overall diameter of the wire including insulation of 0,367 mm and the average resistivity of 0,444 Ω/m are obtained from the litz-wire table (refer to pertinent standard). It is recommended that the actual overall diameter always be measured, and this value used for the calculation.

d) Number of turns and type of core

For an A_L value of 100 nH and an inductance of 640 µH the equation $N = (L/A_L)^{1/2}$ yields 80 turns. The nomogram for coil formers on page 155 shows that for a wire with an external diameter of 0,367 mm the two-section former for core type P 18 × 11 80 can easily take 80 turns. This type can therefore be used with a two-section former.

e) Length of wire and DC resistance

The length of an average turn l_N on the above former is 35,6 mm. The length of litz wire necessary for the coil is therefore 80 · 35,6 mm = 2848 mm plus say 2 · 10 cm for the connections, giving a total length of 3,04 m. The average resistivity of this wire is 0,444 Ω/m; the total DC resistance is thus 3,04 m · 0,444 Ω/m ≈ 1,35 Ω. It should be noted that the length of an average turn l_N given in the individual data sheets always refers to the fully wound former. If the former is not fully wound, the length of an average turn must be corrected according to the extent of the winding.

f) Quality test

The mathematical calculation of the total loss, i.e. the losses of the core and windings is very laborious and only approximate. At the specified frequency of 500 kHz considerable dielectric and eddy-current losses occur. The quality is therefore checked on a sample coil wound as specified above, in this case the value being about 550 as shown in the Q factor characteristics for P 18 × 11 in the data sheet.

g) Checking the temperature coefficient

The core P 18 × 11 with A_L = 100 nH has an effective permeability μ_e = 47,9. SIFERRIT M 33 has a relative temperature coefficient $\alpha_F \approx 1{,}6 \cdot 10^{-6}$/K; therefore the following temperature coefficient can be calculated

$$\alpha_e = \mu_e \cdot \alpha_F = 47{,}9 \cdot 1{,}6 \cdot 10^{-6}/\mathrm{K} = 76{,}6 \cdot 10^{-6}/\mathrm{K}$$

Actual measurement yielded 90 · 10^{-6}/K.

It should be pointed out that with pot cores the temperature coefficient of the unwound coil has almost no influence since the flux density lies primarily in the core.

For effective permeabilities μ_e < 80, however, due to the influence of the winding an additional temperature coefficient of approx. (10 … 30) · 10^{-6}/K must be included in the calculation.

2 Cores for broadband transformers

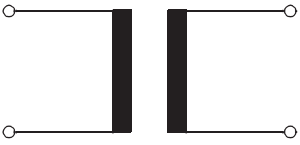

General requirements:

- high A_L values (≙ high effective permeability) to restrict number of turns
- good broadband properties, i.e. high impedance up to highest possible frequencies
- low total harmonic distortion (≙ low hysteresis material constant η_B)
- low sensitivity to superimposed DC currents (≙ highest possible values for T_C and B_S)
- low tan δ for high-frequency applications

2.1 Precision-ground, ungapped cores for broadband transformers

For fields of application such as matching transformers in digital telecommunication networks or pulse signal transformers, either cores which form a closed magnetic circuit (toroids, double E or double-aperture cores) or paired core sets without air gap are used. In order to achieve the highest possible effective permeability here, these cores are precision ground with residual air gaps $s \sim 1$ µm. By selecting the low-profile core types, the A_L value can be further increased, and the number of turns reduced.

For this reason, RM and pot cores made of materials N 30, T 38, T 42 and T 46 are especially suitable for these applications. For high-frequency applications, N 26, M 33 and K 1 are suitable.

2.2 Fundamentals for broadband transformers in the range 10 kHz to over 1 GHz – an example

Broadband transformers are constructed primarily using closed core shapes, i.e. toroids and double-aperture cores. Divided core designs such as P/RM cores or small E/ER cores, which allow more simple winding, are particularly suitable for transformers up to approximately 200 MHz.

The bandwidth $\Delta f = f_{oG} - f_{uG}$ (f_{oG} = upper cut-off frequency, f_{uG} = lower cut-off frequency) is considered the most important transformer characteristic.

Cut-off frequency: Frequency at which the voltage at the transformer drops by 3 dB (≙ – 30%)

The following holds true for circuit quality Q > 10 (typical value):

$$\Delta f = \frac{f_r}{R_i} \cdot \sqrt{\frac{L_H}{C_0}}$$

f_r = Resonance frequency
R_i = Internal resistance of generator (normally, R_i << loss resistance of ferrite)
L_H = Main inductance
C_0 = Winding capacitance

Transmission loss curve

$$\alpha = ln\frac{U}{U_r}$$

U_r = voltage at f_r
α = attenuation when matched with line impedance (e.g. 50 Ω)

Example: 1 : 1 transformer based on E6,3/T38 with 2 ×10 turns

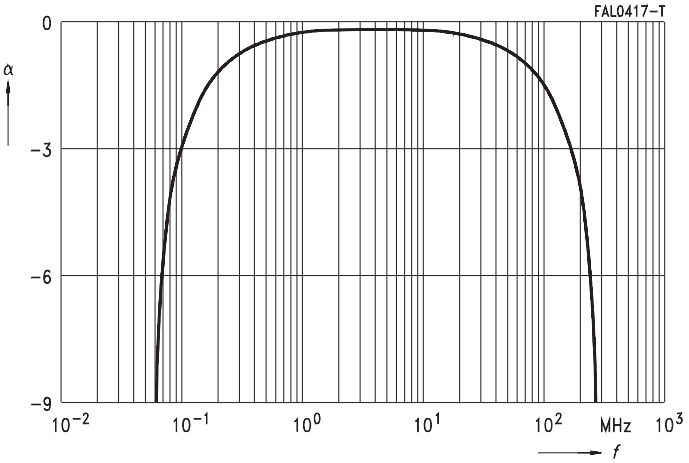

Fig. 10
Transmission loss curve for transformer E6,3/T38 with 2 ×10 turns (parallel)

2.3 Low-distortion transformers for digital data transmission (ISDN, xDSL)

The new digital transmission technologies over copper like ISDN, HDSL (high-rate digital subscriber line) and ADSL (asymmetric digital subscriber line) require very small harmonic distortion in order to maintain maximal line length. This requirement can be calculated from material parameters for the third harmonic distortion with the Rayleigh model for small-signal hysteresis (sinusoidal current).

$$k_3 = \frac{u_3}{u_1} = 0,6 \cdot tan\delta_h = 0,6 \cdot \mu_e \cdot \eta_B \cdot \hat{B}$$

For a typical design a transformer has to be matched to a chipset via the turn ratios $N1 : N2 : N3$ …, the inductances L_1, L_2, L_3 … and the maximum dc resistances R_1, R_2, R_3 …

The third harmonic distortion for winding j can then be calculated as

$$k_3 = \frac{0,6}{\mu_0} \cdot \underbrace{\eta_B}_{\text{Material}} \cdot \underbrace{\frac{\hat{U}}{2\pi f}}_{\text{Circuit conditions}} \cdot \underbrace{L_j \cdot \left[\frac{\rho}{f_{Cu} \sum_{j=1} \left(\frac{N_j}{N_1}\right)^2 \cdot \frac{1}{R_j}}\right]^{3/2}}_{\text{Design constraints}} \cdot \underbrace{\frac{\sum_i l_i}{l_e} \cdot \frac{l_e}{A_e^2}}_{\text{Core}} \cdot \underbrace{\frac{l_N^{3/2}}{A_N^{3/2}}}_{\text{Coil former}}$$

Geometry

This equation shows the contribution of the various design parameters:

– The material is characterized by the hysteresis material constant η_B. Limit values for this parameter are given in the SIFERRIT material tables. The actual level for η_B varies for different cores. In order to select the best material for an application, the normalized temperature dependence $\eta_B(T)/\eta_B(25\ °C)$ is of great help (cf. graph on page 47). Being mainly composition-dependent, these curves are thus material-specific.

– The geometry can be taken into account by a core distortion factor (*CDF*) defined as

$$CDF = \frac{\sum l_i}{l_e} \cdot \frac{l_e}{A_e^2} \cdot \frac{l_N^{3/2}}{A_N^{3/2}}$$

The factor $\Sigma l_i / l_e$ is the closer to 1, the less the core section varies along the magnetic path (homogeneous core shape). The values for *CDF* are given in the following table for the core shapes preferred for these applications.

Cores w/o hole	*CDF* (mm $^{-4,5}$)	Cores w. hole	*CDF* (mm $^{-4,5}$)	EP cores	*CDF* (mm $^{-4,5}$)
P 9 × 5	1,25	P 3,3 × 2,6	85,9	EP 5	10,6
P 11 × 7	0,644	P 4,6 × 4,1	46,7	EP 7	1,68
P 14 × 8	0,164	P 7 × 4	4,21	EPX 7/9	0,749
P 18 × 11	0,0470	P 9 × 5	1,72	EP 10	0,506
P 22 × 13	0,0171	P 11 × 7	0,790	EPX 10	0,329
P 26 × 16	0,00723	P 14 × 8	0,217	EP 13	0,191
P 30 × 19	0,00311	P 18 × 11	0,0545	EPO 13	0,172
P 36 × 22	0,00149	P 22 × 13	0,0220	EP 17	0,0619
RM 4	0,498	P 26 × 16	0,0099	EP 20	0,00945
RM 5	0,184	P 30 × 19	0,00366	EFD 10	3,919
RM 6	0,0576	P 36 × 22	0,00166	EFD 15	0,376
RM 7	0,0339	P 41 × 25	0,00112	EFD 20	0,0837
RM 8	0,0162	RM 4	0,814	EFD 25	0,0231
RM 10	0,00676	RM 5	0,243	EFD 30	0,0161
RM 12	0,00215	RM 6	0,0779	ER 9,5	2,557
RM14	0,00100	RM 7	0,0415	ER 11	1,453
TT/PR 14 × 8	0,205	RM 8	0,0235		
TT/PR 18 × 11	0,0561	RM 10	0,00906		
TT/PR 23 × 11	0,0217				
TT/PR 23 × 18	0,0119				
TT/PR 30 × 19	0,00465				

The values of this parameter indicate that roughly

$$CDF \sim \frac{1}{V_e^{3/2}}$$

I.e. the larger the core, the smaller is the distortion. Due to space restriction, however, the choice has to be made among the core shapes of a given size.

– The circuit conditions, i.e. voltage amplitude $\hat{u}$ and frequency f affect directly the flux density in the core. For increasing flux density, a deviation of the absolute value of k_3 from the calculated test value is expected, since the tan δ_h vs. $\hat{B}$ curve deviates from linear.
– The distortion k_{3c} for a transformer in a circuit with given impedance conditions can be obtained from the following formula:

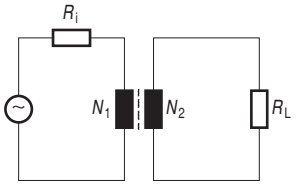

$$k_{3c} = \frac{k_3}{\sqrt{1 + \left[3\omega L_1 \cdot \left(\frac{1}{R_i} + \left(\frac{N_2}{N_1}\right)^2 \cdot \frac{1}{R_L}\right)\right]^2}}$$

R_i = internal resistance of generator
R_L = load resistance
L_1 = primary inductance

The actual circuit distortion k_{3c} will in general be smaller than the calculated sinusoidal current value k_3.

3 Cores for LAN applications

LAN (**L**ocal **A**rea **N**etwork) is a connection of local computers in most cases inside a building. The transfer rate values between 10 Mbit/s and 100 Mbit/s. The transmission rates are 10 Mbit/s (10 Base T), 100 Mbit/s (100 Base T) and 1 Gbit/s (Gigabit Ethernet).

3.1 Signal transformers

To design the signal 1:1 transformer small toroids are typically used. Its functions are impedance matching and network termination. Due to space restriction the core has to be the smallest possible, that still meets the inductance requirement under the given working conditions (100 kHz).

The mostly used core sizes are beginning from outer/inner diameters of 2,54/1,27 mm (0,1/0,05 inch) up to 3,94/2,24 mm (0,155/0,088 inch) with different variations of inner diameter and core height (refer also to chapter *"Toroids"*, page 529 ff).

The multi-level coding of the digital waveform is not always symmetrical to the zero line. This imbalance results in an effective dc current, which is allowed to value 8 mA max. Therefore the inductance of the ferrite toroid is specified under a constant dc current of 8 mA. The saturation flux density values 430 mT at 25 °C and the initial permeability is 4000 (fig. 11).

For indoor application the temperature range is 0 to 70 °C. To use the LAN technology also in outdoor application the temperature range needs to be extended from – 40 to + 85 °C without changing the electrical specification.

The recently developed material T 57 enables design in both temperature ranges.

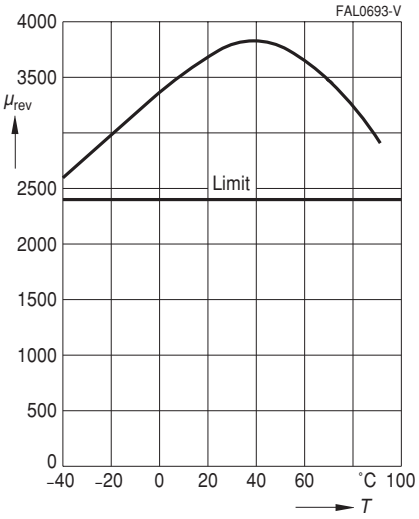

Fig. 11
μ_{rev} versus temperature, measured on toroid R 3,43/1,78/2,11; material T 57 f = 100 kHz, $\hat{B}$ = 6 mT, N = 26, H_{dc} = 27 A/m. (I_{dc} = 8mA)

3.2 Common-mode chokes

For the suppression of common-mode interference in the frequency range from about 30 MHz to 300 MHz it is necessary to use current-compensated chokes in the LAN network.

The corresponding ferrite material is K 10, which is a NiZn material with a permeability of approx. 700 for small Parylene coated cores. The impedance versus frequency curve of K 10 is ideally adapted to the suppression requirement in the LAN network (fig. 12).

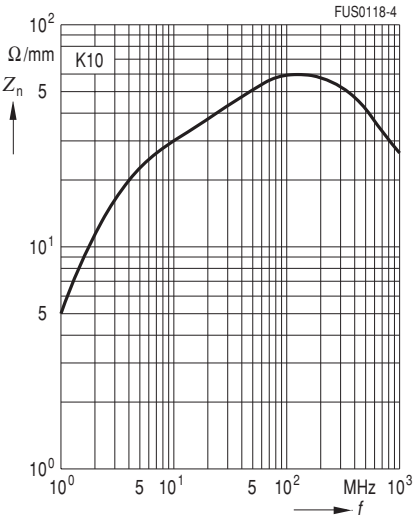

Fig. 12
Normalized impedance curve, measured on toroid R 10 (N = 2 turns)

To complete the materials for common-mode chokes, EPCOS has developed three new NiZn materials:

- K 8 (μ_i = 860, T_C approx. 160 °C)
- K 6 (μ_i = 1000, T_C approx. 130 °C)
- K 7 (μ_i = 1500, T_C approx. 110 °C)

3.3 Coating to ensure highest insulation resistance

Typically the toroid has to withstand 1 kV Hipot test. Therefore the toroids needs to be coated with Parylene (Galxy) which ensures highest insulation resistance. With 12,5 µm (0,0005 inch) a breakdown voltage of 2,7 kV can be achieved. The coating will also protect the wire during winding operation. The material data sheet specifies a breakdown voltage of 2,7 kV, if coated 12,5 µm.

4 Cores for EMI applications

4.1 Ring cores to suppress line interference

With the ever-increasing use of electrical and electronic equipment, it becomes increasingly important to be able to ensure that all facilities will operate simultaneously in the context of electromagnetic compatibility (EMC) without interfering with each others' respective functions. The EMC legislation which came into force at the beginning of 1996 applies to all electrical and electronic products marketed in the EU, both new and existing ones. So the latter may have to be modified so that they are neither susceptible to electromagnetic interference, nor emit spurious radiation. Ferrite cores are ideally suited for this purpose since they are able to suppress interference over a wide frequency range.

At frequencies above 1 MHz, ferrite rings slipped over a conductor lead to an increase in the impedance of this conductor. The real component of this impedance absorbs the interference energy.

A ferrite material's suitability for suppressing interference within a specific frequency spectrum depends on its magnetic properties, which vary with frequency. Before the right material can be selected, the impedance $|Z|$ must be known as a function of frequency.

The curve of impedance as a function of frequency is characterized by the sharp increase in loss at resonance frequency.

Measurement results:

The measurements shown here were made at room temperature (25 ± 3 °C) using an HP 4191A RF impedance analyzer with a flux density of $\hat{B} \leq 1$ mT.

The maximum of the impedance curve shifts to lower frequencies as the number of turns increases; this is due to the capacitive effect of the turns (figure 12, using R25/15 as an example).

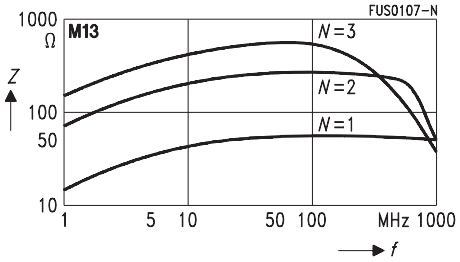

Fig. 12

The impedance curves of different materials are summarized on page 48 for direct comparison. The normalized impedance $|Z|_n = |Z| / N^2 \times \Sigma (l_e / A_e)$ were used to display material properties only. The geometry factor was calculated on the basis of the core dimensions.

These normalized impedance curves are guide values, mostly measured using toroidal core R 10 with a number of turns N = 1 (wire diameter 0,7 mm); they may vary slightly, depending on the geometry.

4.2 Common-mode chokes

Compact electrical and electronic equipment primarily generates common-mode interference. In order to be able to meet the safety requirements (keeping within the leakage current limits), chokes with a high asymmetrically effective inductance must be used. Current-compensated chokes with a closed core topology are especially suitable for this purpose. The problem of core material saturation due to the useful current is solved in these designs by winding two coils with equal number of turns on the core. These coils are connected in such a way that the magnetic flux induced by the upper coil is compensated by the lower coil.

The new Magnetic Design Tool of EPCOS contains the normalized impedance versus frequency curves of all ferrite materials, which are suitable for EMI applications.

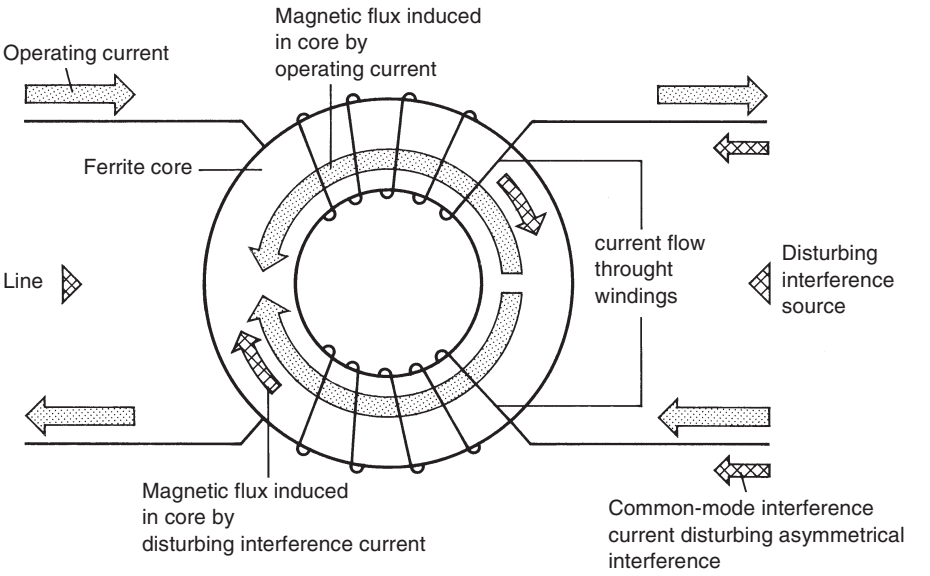

Fig. 13

Current-compensated toroid choke; double choke shown as an example.

4.3 NiZn ferrites

Toroidal cores of NiZn ferrites are especially suitable for the suppression of high frequency interference, because of the high ohmic resistance of these materials (ca. 10^5 Ωm). Therefore the negative effect of eddy current is negligible and the usage of these materials allow relatively high impedance values even at frequency well above 100 MHz. There is limiting factor to create NiZn ferrites with higher initial permeability, because with increasing permeability the Curie temperature decreases. For example the Curie temperature for a NiZn ferrite of μi = 2300 (M 13) is specified > 105 °C, which is at the limit for many applications.

An applicacion example in the automotive sector is the CAN-Bus choke, where core sizes from outer diameter 2,5 mm to 6,3 mm (0,1 to 0,29 inch) in material K 6, K 7, K 8 and K 10 are used. As the transmission frequencies in the telecom industry are rising, it is also expected, that the demand for NiZn ferrites will grow.

Another application example for NiZn ferrite toroids is the usage of cores alone on component leads or in board level circuitry either

– to prevent any parasitic oscillations or
– to attenuate unwanted signal pickup or transmissions which might travel along component leads or interconnecting wires, traces, or cables.

4.4 MnZn ferrites

For the application as current-compensated chokes MnZn ferrites are widely used in the whole range of sizes. The advantage of the MnZn materials is the much higher permeability, which can be realised together with a sufficiently high Curie temperature. For example our material T 56 has an outstanding permeability of 20 000 and a Curie temperature of > 90 °C. Using very high permeability ferrites reduces the number of turns, which are necessary to reach a certain inductance. This avoids the negative impact of a high number of turns like dc resistance or parasitic capacitance and not at least costs.

Small cores R 2,5 up to R 12,5 in the materials N 30, T 38, T 46, T 56 can be used for example in Telecom Networks like ISDN.

Cores of mid range sizes from R 13,3 to R 26 are used as choke in power lines usually in electronic ballasts in lamps, switch-mode power supplies in TV sets, washing machines and chargers. Ferrite materials: N 30, T 65, T 35, T 37, T 38, T 46.

The usage for core sizes R 34 and bigger are in industrial applications, in filters for frequency converters (lifts, pumps, traction systems, conveyer systems, air conditioning systems), general-purpose application in power electronics, UPS and wind-driven power plants. Especially for high temperarure or/and high current application in these fields our material T 65 is the most suitable because of its high saturation flux density of 460 mT and high Curie temperature of > 160 °C. The initial permeability on big cores is about 4500 to 5000.

If there is not especially high current or high temperature applied, we recommend to use our materials N 30 (μ_i = 4300) and T 37 (μ_i approx. 5500 to 6000 on big cores). The choice of material depends on the frequency range, which has to be covered by the attenuation. This is determined by the characteristic of permeability.

5 Cores for inductive sensors

The proximity switch, widely used in automation engineering, is based on the damping of a high-frequency LC oscillator by the approach of a metal. The oscillator inductor consists of a cylindrical coil and a ferrite core half whose open side forms what is known as the active area. The function of the ferrite core consists in spatially aligning the magnetic field so as to restrict the interaction area.

The oscillator design must take into account that the inductor forms a magnetically open circuit. The inductance and quality are decisively dependent on the coil design, unlike in the case of closed circuits. The initial permeability plays a subordinate role here, as is shown by the following example:

Core: P9 × 5 (B65517-D …)
Coil: 100 turns, 0,08 CuL
Current: 1 mA
Frequency: 100 kHz

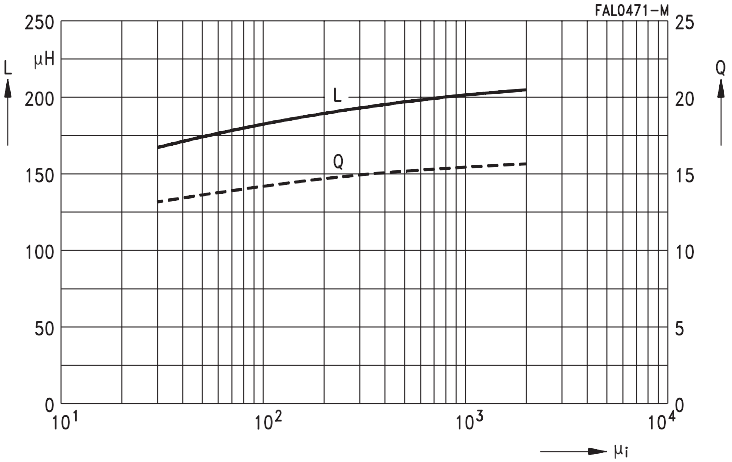

Fig. 14
Inductance and quality versus initial permeability
P9,3 × 2,7, *N* = 100, *f* = 100 kHz, *I* = 1 mA

Decisive for this application is the attainment of as high a Q as possible, with the lowest possible dependence on temperature at the oscillator frequency. When the distance between the damping lug and the active area changes, the oscillator Q should however change as strongly as possible.

If the relative change in Q $\Delta Q/Q$ exceeds a predefined threshold, e.g. 10 %, a switching operation is initiated at the so-called operating distance. Attainment of the target values depends on appropriate coil dimensioning and can generally only be performed empirically.

6 Cores for power applications

6.1 Core shapes and materials

The enormously increased diversity of application in power electronics has led to a considerable expansion not only in the spectrum of core shapes but also in the range of materials.

To satisfy the demands of higher-frequency applications, the EFD cores have been developed in sizes EFD 10, 15, 20, 25 and EFD 30. These are characterized by an extremely flat design, optimized cross-sectional distribution and optimized winding shielding.

For many standard applications up to 100 kHz, materials N 27, N 41 and N 72 can be used. For the range up to 500 kHz, materials N 92, N 87 and N 97 are suitable. N 49 covers the range from 300 kHz to 1 MHz e.g. for DC/DC (resonance) converters.

For detailed information on core shapes see the individual data sheets, for general information on materials see the chapter on SIFERRIT materials.

6.2 Low-profile cores for planar magnetics

The design of planar devices has attracted the attention of magnetic design engineers, since this type of devices has interesting advantages over conventional wound components (cf. Fig. 15):

- low total height
- outstanding reproducibility of electrical parameters
- excellent thermal performance
- high degree of integration

a) Conventional magnetics b) Planar magnetics

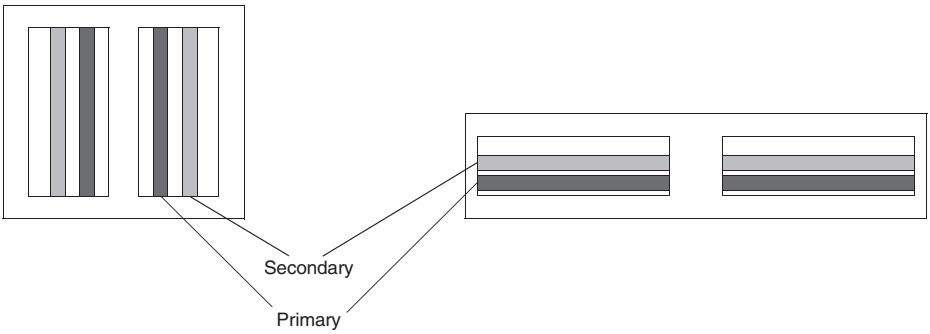

Fig. 15

In order to fulfill the requirements of this technology, suitable cores are needed. The most common designs of low-profile cores have been adopted in a new IEC standard (61860) to offer geometrically compatible cores for this application. These cores cover RM 4 LP through RM 14 LP, ER 9,5, ER 11, ER 14,5/6 and ELP cores. A common denominator of these cores is that the length of the core is larger than both its total height and its width.

The advantages of this core design are:

- high A_L values
- high core surface to volume ratio
- large core surface to contact heat sink

The preferred materials used in combination with low-profile cores are N 87, N 97, N 92 and N 49 for power applications as well as T 38 and T 42 for applications requiring high inductance values.

6.3 Correlation: Applications – core shape/material

6.3.1 Step-down converters

Typical circuit diagram (Fig. 16)

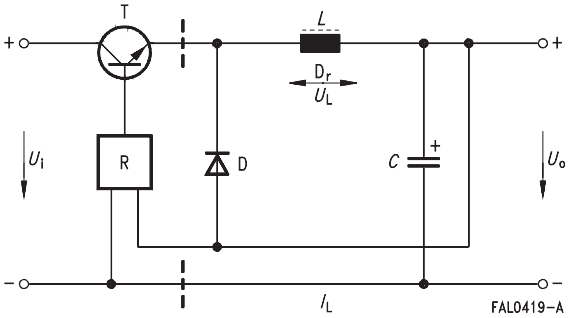

Advantages

- only one choke required
- high efficiency
- low radio interference

Disadvantages

- only one output voltage
- restricted short-circuit withstand capability (no line isolation)

Application areas

- providing a constant output voltage, isolated from input voltage
- regulation in a forward converter
- regulated voltage inversion
- sinusoidal line current draw

Core/material requirements

- Standard requirements regarding losses and saturation

EPCOS recommendations for core shape/material

- E/ETD/U/RM cores made of
  N 27 (standard)
  N 87, N 97 (low losses, high saturation)
  N 92 (very high saturation)

6.3.2 Single-ended flyback converter

Typical circuit diagram (Fig. 17)

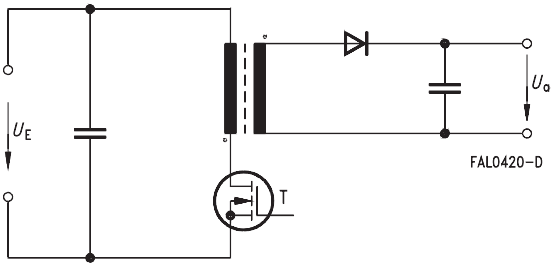

Advantages

- simple circuit variant (low cost)
- low component requirement
- only one inductive component
- low leakage losses
- several easily regulatable output voltages

Disadvantages

- close coupling of primary and secondary sides
- high eddy current losses in the air gap area
- large transformer core with air gap restricts possible applications
- average radio interference
- exacting requirements on the components

Application areas

- low and medium powers up to max. 200 W with wide output voltage range
- maximum operating frequency approx. 100 kHz

Core/material requirements

- low power losses at high temperature
- very high saturation with low dependence on temperature
- gapped cores (recently also with A_L value guarantee)

EPCOS recommendations for core shape/material

- E/U cores in
  N 27 (standard)
  N 87, N 92 (low losses, high saturation)

6.3.3 Single-ended forward converter

Typical circuit diagram (Fig. 18)

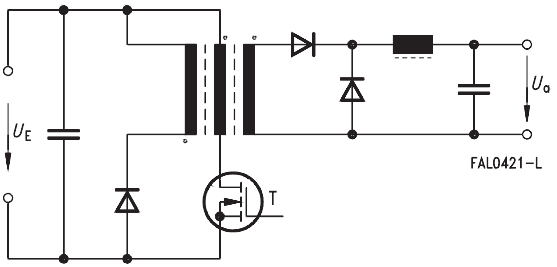

Advantages

- higher power range than flyback converter
- lower demands on circuit components
- high efficiency

Disadvantages

- 2 inductive components
- large choke
- demagnetization winding
- high radio interference suppression complexity
- increased component requirement, particularly with several regulated output voltages

Application areas

- medium and high powers (up to 500 W) especially in the area of low output voltages
- PWM (pulse width) modulation up to approx. 500 kHz

Core/material requirements

- low losses at high temperatures and at high frequencies (low eddy-current losses)
- generally, ungapped cores

EPCOS recommendations for core shape/material

- E/ETD, small EFD cores, RM/PM cores made of
  N 27, N 41 (up to 100 kHz)
  N 87, N 97 (up to 500 kHz)
  N 49 (up to 1 MHz)

6.3.4 Push-pull converter

Typical circuit diagram (Fig. 19)

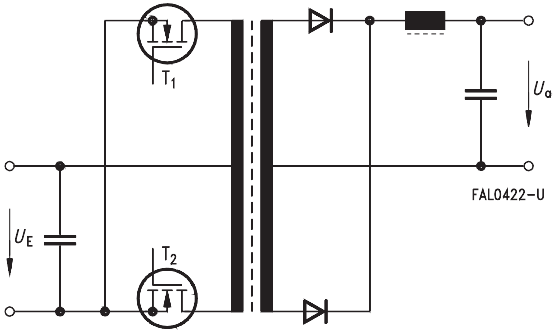

Advantages

- powers up to the kW range
- small choke
- high efficiency
- low radio interference suppression complexity

Disadvantages

- 2 inductive components
- complex winding
- high component requirement, particularly with several regulated output voltages

Application areas

- high powers (>>100 W), also at high output voltages
- PWM (pulse width) modulation up to 500 kHz

Core/material requirements

- low losses at high temperatures
- low eddy-current losses since application areas is up to 500 kHz and above
- generally, ungapped cores

EPCOS recommendations for core shape/material

- large E/ETD, RM/PM cores made of
  N 27, N 97, N 87 (with large core cross sections ($A_e \geq 250$ mm^2), on account of eddy-current losses N 87 must be used even where $f < 100$ kHz)

6.3.5 Electronic lamp ballast device

Typical circuit diagram (Fig. 20)

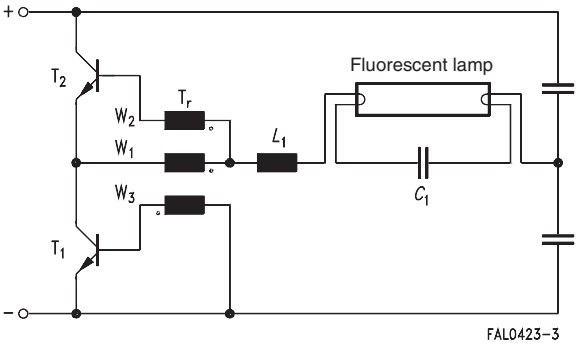

Advantages

- considerably reduced size compared to 50 Hz line solution
- significantly higher efficiency than line voltage regulator

Disadvantages

- high component requirement

Application areas

- control unit for fluorescent lamps

Core/material requirements

- low losses in the range 50 – 80 °C
- pulse power requirements
- gapped and ungapped E cores
- ring cores with defined pulse characteristic

EPCOS recommendations for core shape/material

- E/ETD/EFD cores made of N 72 for L_1

6.4 Selection of switch-mode power supply transformer cores

The previous section (Correlation: Applications – core shape/material) provides a guide for the rough selection of core shape and material.

The following procedure should be followed when selecting the actual core size and material:

1) Definition of requirements
– range of power capacities P_{trans}
– specification of the SMPS type
– specification of pulse frequency and maximum temperature rise
– specification of the maximum volume

2) Selection of "possible" core shapes/materials on the basis of the "Power capacity" tables starting on page 146.

These tables associate core shape/material combinations (and the volume V) with the power capacity of the different converter types at a "typical" frequency f_{typ} and a "cut-off frequency" f_{cutoff}.

The typical frequency specified here is a frequency for which specific applications are known, or which serves as the base frequency for the specified core loss values.

The cut-off frequency is selected such that the advantages of other materials predominate above this frequency and that it is therefore advisable to switch to a different material which is better optimized for this range.

3) Final selection of core shape/material

The core shapes/materials selected as possibilities under 2) must now be compared with the relevant data sheets for the specific core types and the material data (typical curves), taking the following points into consideration:

– volume
– accessories (power coil former)
– A_L values of ungapped core
– A_L values/air gap specifications
– temperature minimum for losses, Curie temperature T_C, saturation magnetization B_S, magnetic bias characteristic, amplitude permeability characteristic

Core shape/material combinations which are not contained in the individual data sheets can be requested from EPCOS.

6.5 Selection tables: Power capacities

In order to calculate the transmissible power, the following relationship is used (transformer with two equal windings):

$$P_{trans} = C \Delta B f A_e \cdot A_N \cdot j$$

where C is a coefficient characterizing the converter topolgy[1)], i.e.

$C = 1$: push-pull converter
$C = 0{,}71$: single-ended converter
$C = 0{,}62$: flyback converter

Both the core losses associated with the flux swing ΔB and the copper losses due to the current density j result in a temperature increase ΔT. Assuming that both loss contributions are equal and that $P_V \sim B^2$, the power capacity can be approximated by

$$P_{trans} \approx C \cdot \underbrace{\frac{PF}{\sqrt{P_V}}}_{\text{Material}} \cdot \underbrace{\frac{\Delta T}{R_{th}}}_{\text{Thermal design}} \cdot \underbrace{\sqrt{\frac{f_{Cu}}{\rho_{Cu}}}}_{\text{Winding}} \cdot \underbrace{\sqrt{\frac{A_N \cdot A_e}{l_N \cdot l_e}}}_{\text{Geometry}}$$

The equation shows how the different aspects in the design contribute to the power capacity:

– The material term is the performance factor *PF* divided by the square root of the specific core loss level for which it was derived (cf. page 46 and page 116). For a given core shape deviations from this value are possible as given by its data sheet.

– The values for ΔT are associated with the material according to the following table.

	ΔT_{max} K
N 27	30
N 41	30
N 49	20
N 72	40
N 87	50
N 92	50
N 97	50

– The thermal resistance is defined as

$$R_{th} = \frac{\Delta T}{P_{Vcore} + P_{Vcopper}}$$

– These values should be regarded as typical for a given core shape. They were determined by measurement under the condition of free convection in air and are given in the table on page 150 ff.

1) G. Roespel, “Effect of the magnetic material on the shape and dimensions of transformers and chokes in switched-mode power supplies”, J. of Magn. and Magn. Materials 9 (1978) 145-49

For actual designs the actual values for R_{th} should be determined and the tabulated P_{trans} values adjusted accordingly.

– The winding design was taken into account in the calcualtions by f_{Cu} = 0,4 and ρ_{Cu} for DC. In actual design large deviations of the dc resistance due to high frequency effects (skin effect, proximity effect) occur, unless special wire types such as litz wires are used. If the R_{AC}/R_{DC} ratio for a given winding is known, this can be used to correct the tabulated power capacities accordingly.
– The geometry term is related to the core shape and size. However, note that the thermal resistance is also size-dependent via the empirical relation (cf. figure 21):

$$R_{th} \sim \frac{1}{\sqrt{V_e}}$$

The tabulated power capacities provide a means for making a selection among cores, although the absolute values will not be met in practice for the reasons explained before.

In the calculation of power capacities the following conditions were also applied:

– The application area for flyback converters was restricted to $f < 150$ kHz.
– The power specifications for N 49 should be read as applicable to DC/DC (quasi) resonance converters (single-ended forward operation).
– The maximum flux densities were defined as follows:
For flyback converters: $\Delta B \leq 200$ mT ($\Delta B \leq 50$ mT for material N 49)
For push-pull converters: $\Delta B \leq 400$ mT.

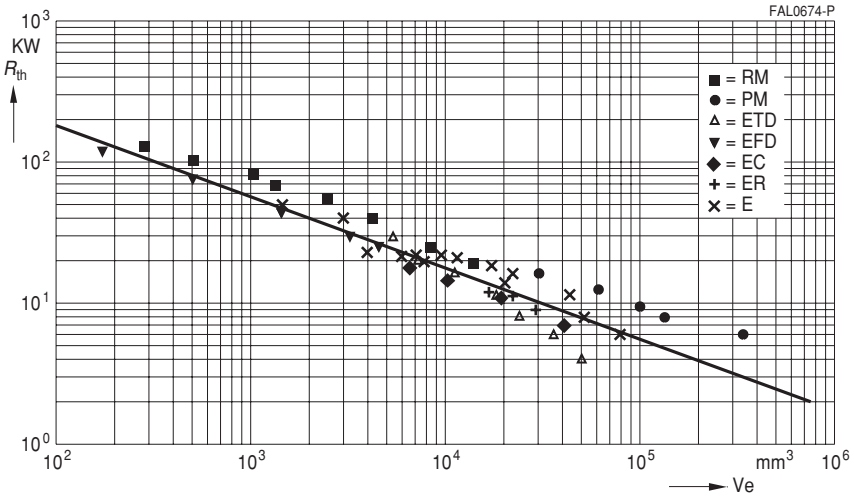

Fig. 21
Thermal resistance versus core effective volume

P_{trans} of cores for wound transformers (f_{Cu} = 0,4)

	N 27	N 41	N 49	N 72	N 87	N 92	N 97
$f_{typ\ [kHz]}$	25	25	500	25	100	100	100
RM 4 LP			19		20	18	
RM 4			22		24		31
RM 5 LP			29		35	32	
RM 5		9	38		48		61
RM 6 LP			45		56	51	
RM 6		17	64		79		101
RM 7 LP			67		82	75	
RM 7		23	86		107		137
RM 8 LP			97		121	111	
RM 8		35	131		162		207
RM 10 LP			173		214	196	
RM 10		63	234		289		370
RM 12 LP			366		453	416	
RM 12		136	503		622		796
RM 14 LP			611		756	694	
RM 14		229	846		1046		1339
PM 50/39	391				1742		
PM 62/49	673				2999		
PM 74/59	1131				5036		
PM 87/70	1567						
PM 114/93	2963						
EP 7					13		
EP 10					25		
EP 13					55		
EP 17					114		
EP 20					329		
P 9 × 5							
P 11 × 7					25		
P 14 × 8		12			62		
P 18 × 11					133		
P 22 × 13					232		
P 26 × 16					394		
P 30 × 19					613		

P_{trans} of cores for wound transformers (f_{Cu} = 0,4)

	N 27	N 41	N 49	N 72	N 87	N 92	N 97
$f_{typ\ [kHz]}$	25	25	500	25	100	100	100
TT/PR 14 × 8					52		
TT/PR 18 × 11					117		
TT/PR 23 × 11					204		
TT/PR 23 × 18					217		
TT/PR 30 × 19					540		
E 5					1,7		
E 6,3					2,4		
E 8,8					5,0		
E 13/7/4	5				28		
E 14/8/4	7	13					
E 16/6/5	9						
E 16/8/5	13	13,2			67		
E 19/8/5	16				82		
E 20/10/6	26				118		
E 21/9/5	15						
E 25/13/7	49				218		
E 25,4/10/7	42				189		
E 30/15/7	94				418		
E 32/16/9	118				525		
E 32/16/11					566		
E 34/14/9	118						
E 36/18/11	146				652		
E 40/16/12	172			574	768		
E 42/21/15	214				952		
E 42/21/20	289				1290		
E 47/20/16	304				1350		
E 55/28/21	538				2396		
E 55/28/25	763				3400		
E 56/24/19	532						
E 65/32/27	1091				4860		
E 70/33/32	1453				6500		
E 80/38/20	1503				6700		
ER 9,5					9		
ER 11/5			15		14		

P_{trans} of cores for wound transformers (f_{Cu} = 0,4)

	N 27	N 41	N 49	N 72	N 87	N 92	N 97
$f_{typ\ [kHz]}$	25	25	500	25	100	100	100
ER 14,5/6			15		12	11	
ER 28/17/11				290			
ER 35/20/11	309						
ER 42/22/15	384						
ER 46/17/18	376						
ER 49/27/17	636						
ER 54/18/18	482						
ETD 29/16/10	96				428		548
ETD 34/17/11	151				674		863
ETD 39/20/13	230				1023		1309
ETD 44/22/15	383				1708		2186
ETD 49/25/16	594				2645		3385
ETD 54/28/19	897				3998		5116
ETD 59/31/22	1502				6692		8564
EC 35/17/10	145						
EC 41/20/12	220						
EC 52/24/14	402						
EC 70/35/16	907						
EFD 10/5/3			13		12		
EFD 15/8/5			38		42		
EFD 20/10/7			93		115		
EFD 25/13/9			198		245		
EFD 30/15/9			258		319		
EV 15/9/7	175				231		
EV 25/13/13	316				685		
EV 30/16/13	482				1050		
UI 93/104/16	1028						
UU 93/152/16	1413						
UI 93/104/20	1283						
UU 93/152/20	1780						
UI 93/104/30	1784				7950		
UU 93/152/30	2874				12800		
U 101/76/30	4400						
U 141/78/30	4300						

P_{trans} of low-profile cores for planar transformers (f_{Cu} = 0,1)

	N 49	N 87	N 92
RM 4 LP	9,5	10	
RM 5 LP	14	17,5	
RM 6 LP	22	28	
RM 7 LP	33	41	
RM 8 LP	48	60	
RM 10 LP	86	107	
RM 12 LP	183	226	
RM 14 LP	305	378	
ER 9,5		4,5	
ER 11/5	7,5	7	
ER 14,5/6	13	12	11
EILP 14	12	11	10
EELP 14	16	17	16
EILP 18	30	37	34
EELP 18	44	55	50
EILP 22	78	96	88
EELP 22	109	134	123
EILP 32	143	177	
EELP 32	203	252	
EILP 38	262	323	
EELP 38	380	470	
EILP 43	360	445	
EELP 43	500	619	
EILP 58		731	
EELP 58		1046	
EILP 64	800	991	
EELP 64	1130	1397	

6.6 Thermal resistance for the main power transformer core shapes

Core shapes	R_{th} (K/W)	Core shapes	R_{th} (K/W)	Core shapes	R_{th} (K/W)
RM 4	120	E 5	308	ER 9,5	164
RM 4 LP	135	E 6,3	283	ER 11/5	134
RM 5	100	E 8,8	204	ER 14,5/6	99
RM 5 LP	111	E 13/7/4	94	ER 28/17/11	22
RM 6	80	E 14/8/4	79	ER 35/20/11	18
RM 6 LP	90	E 16/6/5	76	ER 42/22/15	14
RM 7	68	E 16/8/5	65	ER 46/17/18	13
RM 7 LP	78	E 19/8/5	60	ER 49/27/17	9
RM 8	57	E 20/10/6	46	ER 54/18/18	11
RM 8 LP	65	E 21/9/5	59		
RM 10	40	E 25/13/7	40	ETD 29/16/10	28
RM 10 LP	45	E 25,4/10/7	41	ETD 34/17/11	20
RM 12	25	E 30/15/7	23	ETD 39/20/13	16
RM 12 LP	29	E 32/16/9	22	ETD 44/22/15	11
RM 14	18	E 32/16/11	21	ETD 49/25/16	8
RM 14 LP	21	E 34/14/9	23	ETD 54/28/19	6
		E 36/18/11	18	ETD 59/31/22	4
PM 50/39	15	E 40/16/12	20		
PM 62/49	12	E 42/21/15	19	EC 35/17/10	18
PM 74/59	9,5	E 42/21/20	15	EC 41/20/12	15
PM 87/70	8	E 47/20/16	13	EC 52/24/14	11
PM 114/93	6	E 55/28/21	11	EC 70/35/16	7
		E 55/28/25	8		
EP 7	141	E 56/24/19	9,5	EFD 10/5/3	120
EP 10	122	E 65/32/27	6,5	EFD 15/8/5	75
EP 13	82	E 70/33/32	5,5	EFD 20/10/7	45
EP 17	58	E 80/38/20	7	EFD 25/13/9	30
EP 20	32	EI LP 14	116	EFD 30/15/9	25
		EE LP 14	105		
P 9 × 5	142	EI LP 18	61	EV 15/9/7	55
P 11 × 7	106	EE LP 18	56	EV 25/13/13	27
P 14 × 8	73	EI LP 22	38	EV 30/16/13	21
P 18 × 11	51	EE LP 22	35		
P 22 × 13	37	EI LP 32	26	UU 93/152/16	4,5
P 26 × 16	27	EE LP 32	24	UI 93/104/16	5
P 30 × 19	22	EI LP 38	20	UU 93/152/20	4
P 36 × 22	17	EE LP 38	18	UI 93/104/20	4,5
		EI LP 43	16	UU 93/152/30	3
TT/PR 14 × 8	77	EE LP 43	15	UI 93/104/30	4
TT/PR 18 × 11	54	EI LP 58	12	U 101/76/30	3,3
TT/PR 23 × 11	39	EE LP 58	11	U 141/78/30	2,5
TT/PR 23 × 18	31	EI LP 64	9,5		
TT/PR 30 × 19	24	EE LP 64	9		

1 Gapped and ungapped ferrite cores

Even with the best grinding methods known today, a certain degree of roughness on ground surfaces cannot be avoided, so that the usual term “without air gap” or “ungapped” does not imply no air gap at all. The A_L values quoted allow for a certain amount of roughness of the ground faces. The tolerance of the A_L value for ungapped cores is – 20 to + 30 % or – 30 to + 40 %. Closer tolerances are not available for several reasons. The spread in the A_L values of ungapped cores practically equal the spread in ring core permeability (± 20 % … ± 30 %), and the A_L value largely depends on the grinding quality of the matching surfaces.

The following are normally defined:

precision-ground/lapped cores	$s_{resid} \approx 1\ \mu m$
normally ground cores	$s_{resid} \approx 10\ \mu m$
gapped cores	$s \geq 10\ \mu m$

The residual air gap s_{resid} here is the total of the residual air gaps at the leg or centerpost contact surfaces.

With increasing material permeability the influence of the inevitable residual air gap grows larger. The spreads in the A_L value may also be increased by the mode of core assembly. Effects of mounting and gluing can result in a reduction of the A_L value.

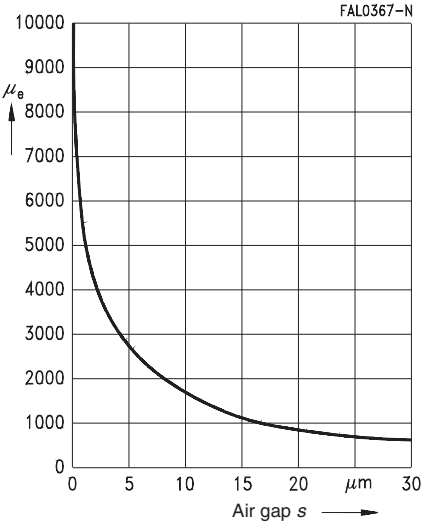

Fig. 18
Relationship between permeability μ_e and air gap s for an RM 4/T 38 ferrite core

2 Processing notes for the manufacture of wound products for small-signal and power applications

2.1 Winding design

For the most common core types the maximum number of turns for the individual coil formers can be seen from the following nomograms. The curves have been derived from the equation

$$N = \frac{A_N}{A_{wire}} \cdot f_{Cu}$$

where

N = max. number of turns
A_N = winding cross section in mm^2
A_{wire} = wire cross section in mm^2
f_{CU} = copper space factor versus wire diameter
(f_{CU} approx. 0,55 for wire diameter 0,05)

Common wires and litz wires are specified in the pertinent standards (IEC 60317-11; IEC 60182-1, IEC 60182-2).

As can be seen from Fig. 19, as high a winding level as possible should be employed because at low μ_e values in particular a low winding level (h/H ratio) can cause an A_L drop of up to 10% compared to the maximum value with full winding. (By our standards, the A_L values are always related to fully wound 100-turn coils.)

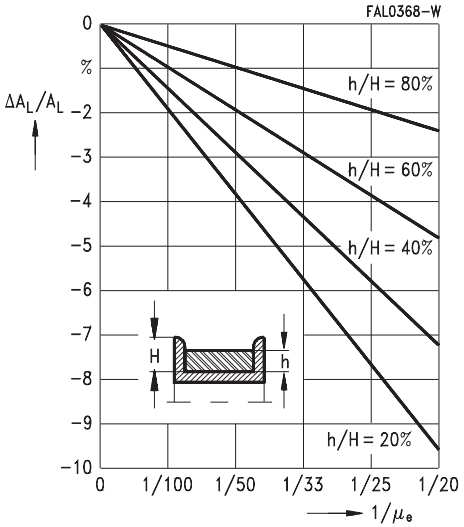

Fig. 19
Percentage change in A_L value versus relative winding height h/H

RM cores

Maximum number of turns *N* for coil formers

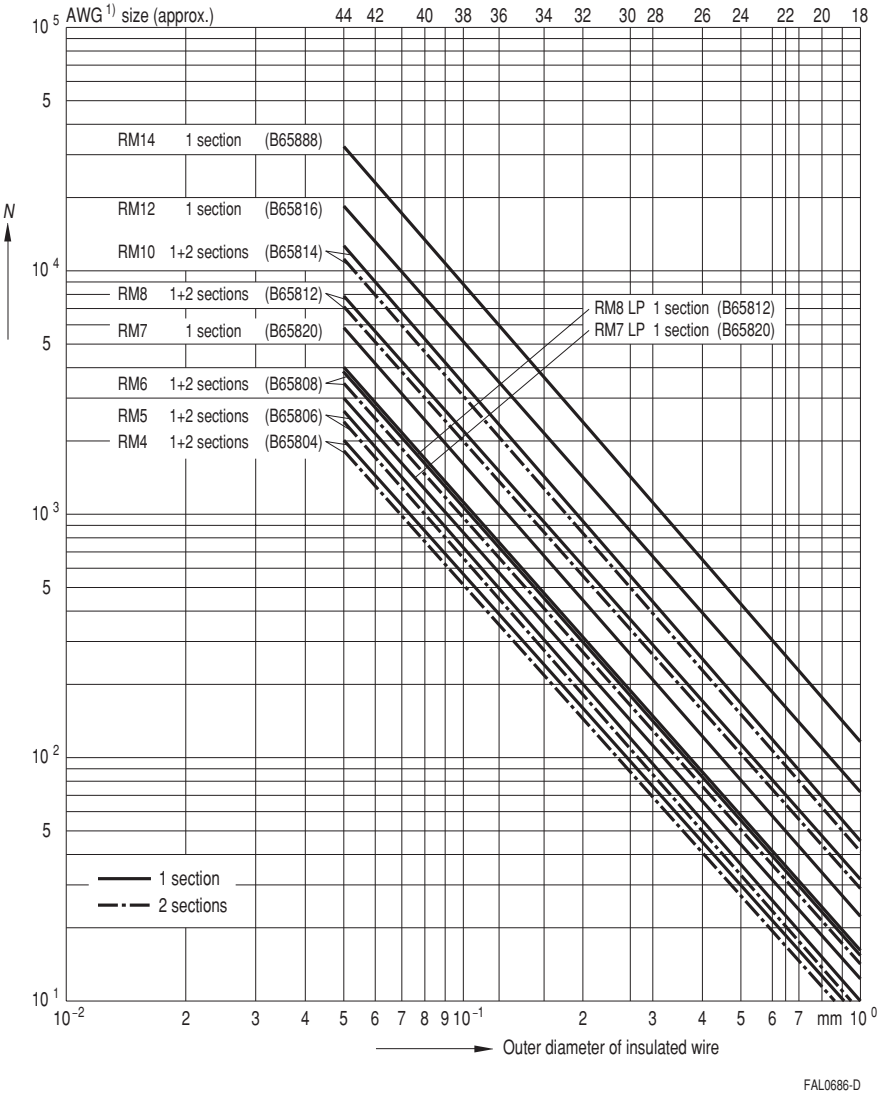

FAL0686-D

1) American Wire Gauge (AWG)

PM cores

Maximum number of turns *N* for coil formers

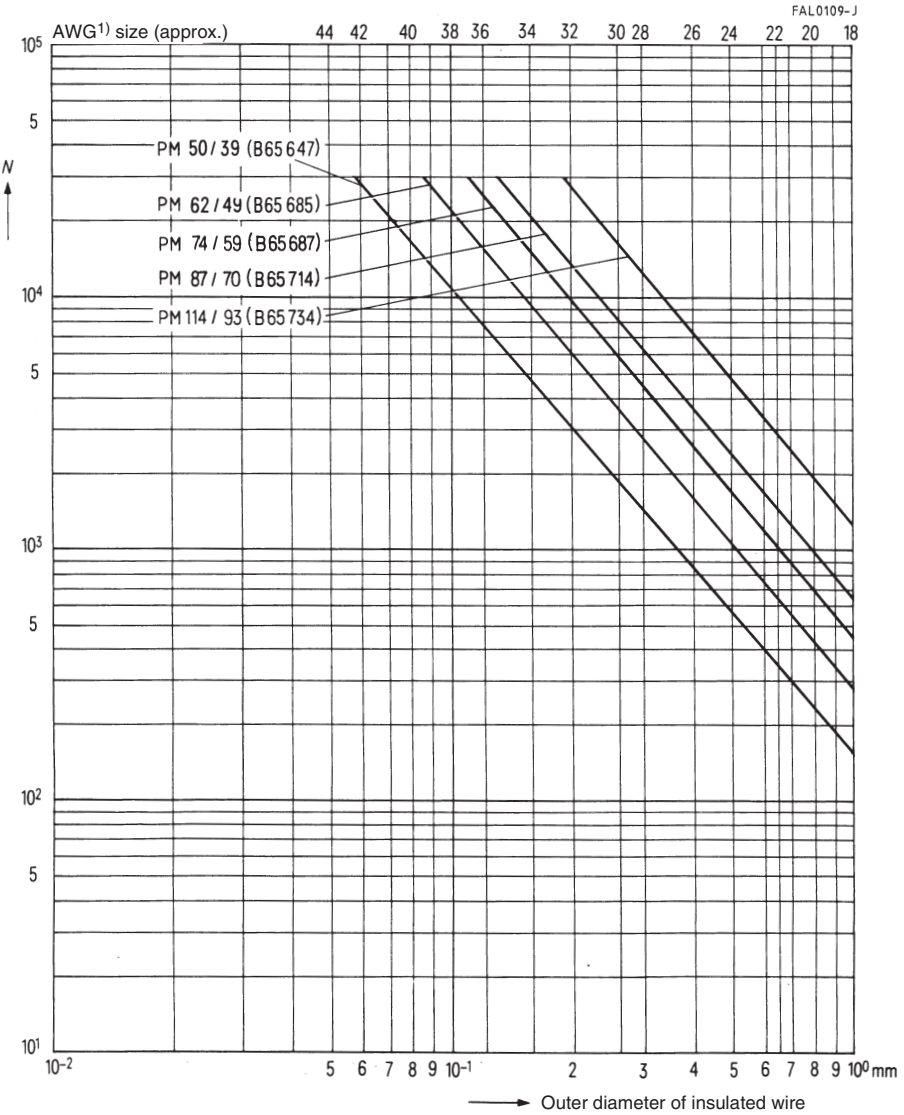

1) American Wire Gauge (AWG)

P cores

Maximum number of turns *N* for coil formers

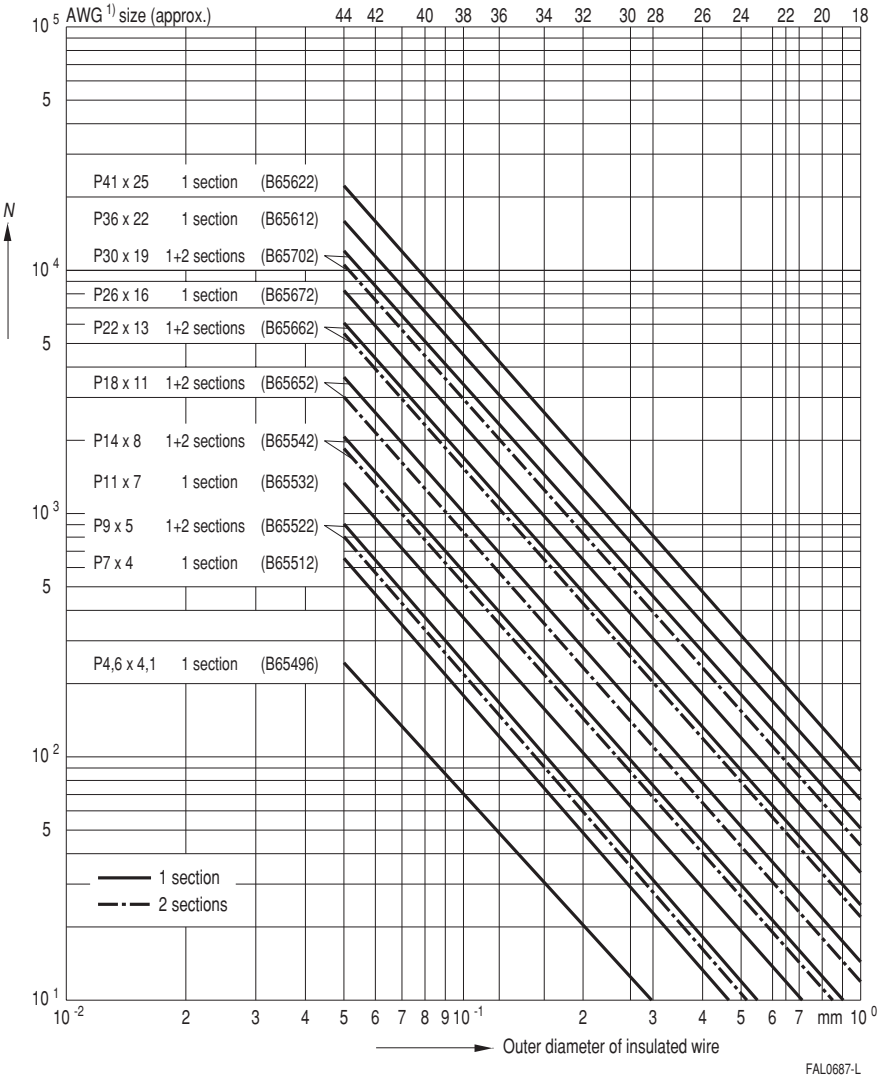

1) American Wire Gauge (AWG)

EP cores

Maximum number of turns *N* for coil formers

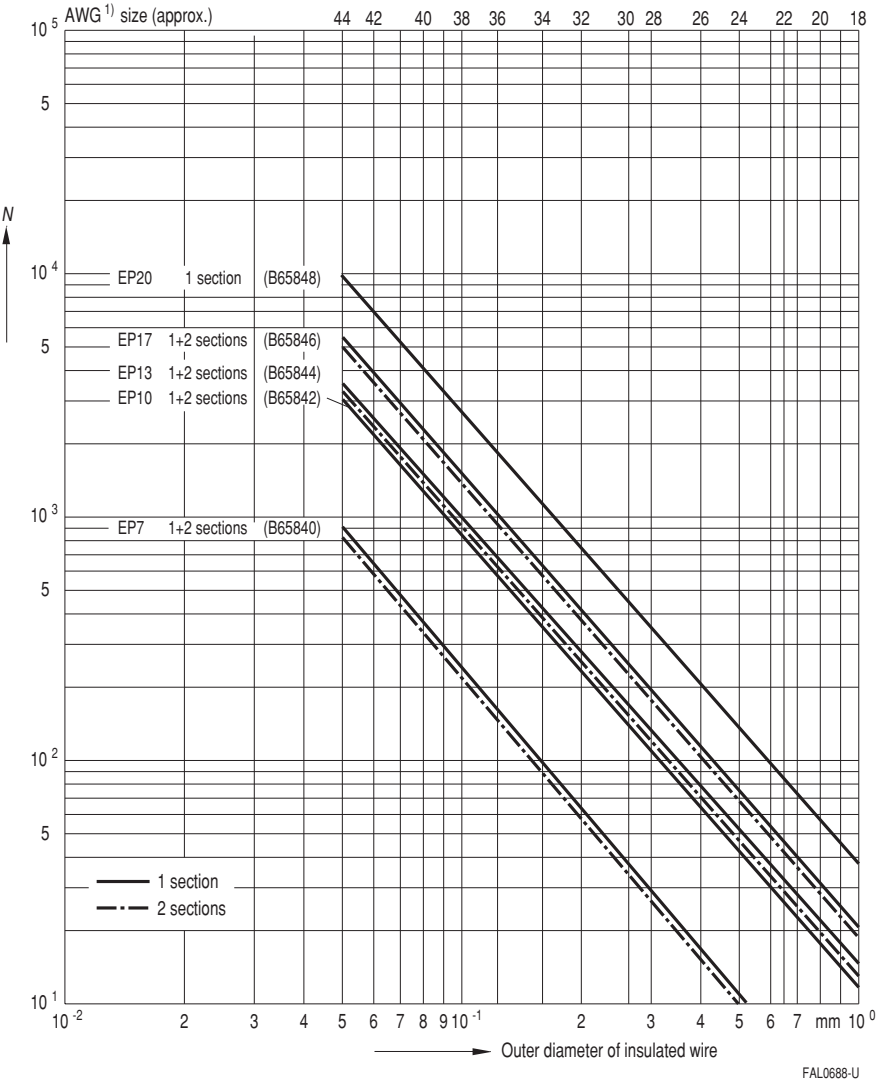

1) American Wire Gauge (AWG)

EFD cores

Maximum number of turns *N* for coil formers

FAL0427-1

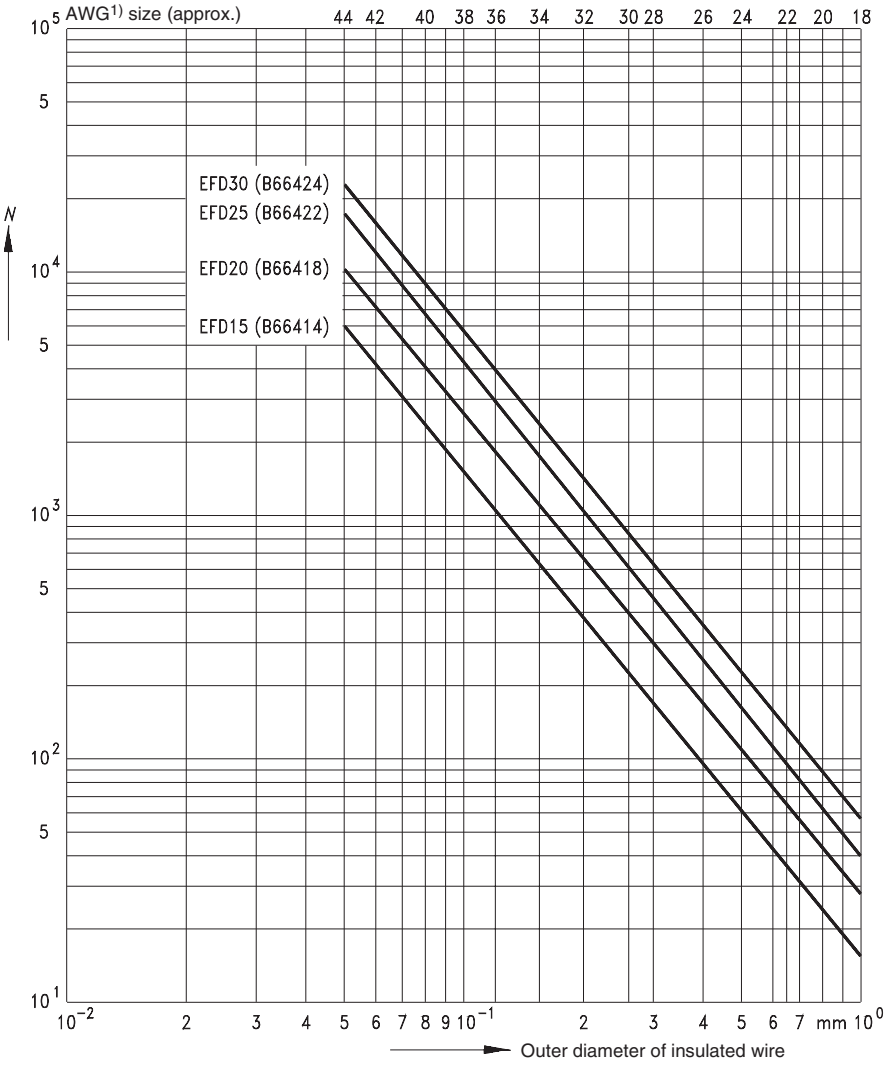

1) American Wire Gauge (AWG)

ETD and ER cores

Maximum number of turns *N* for coil formers

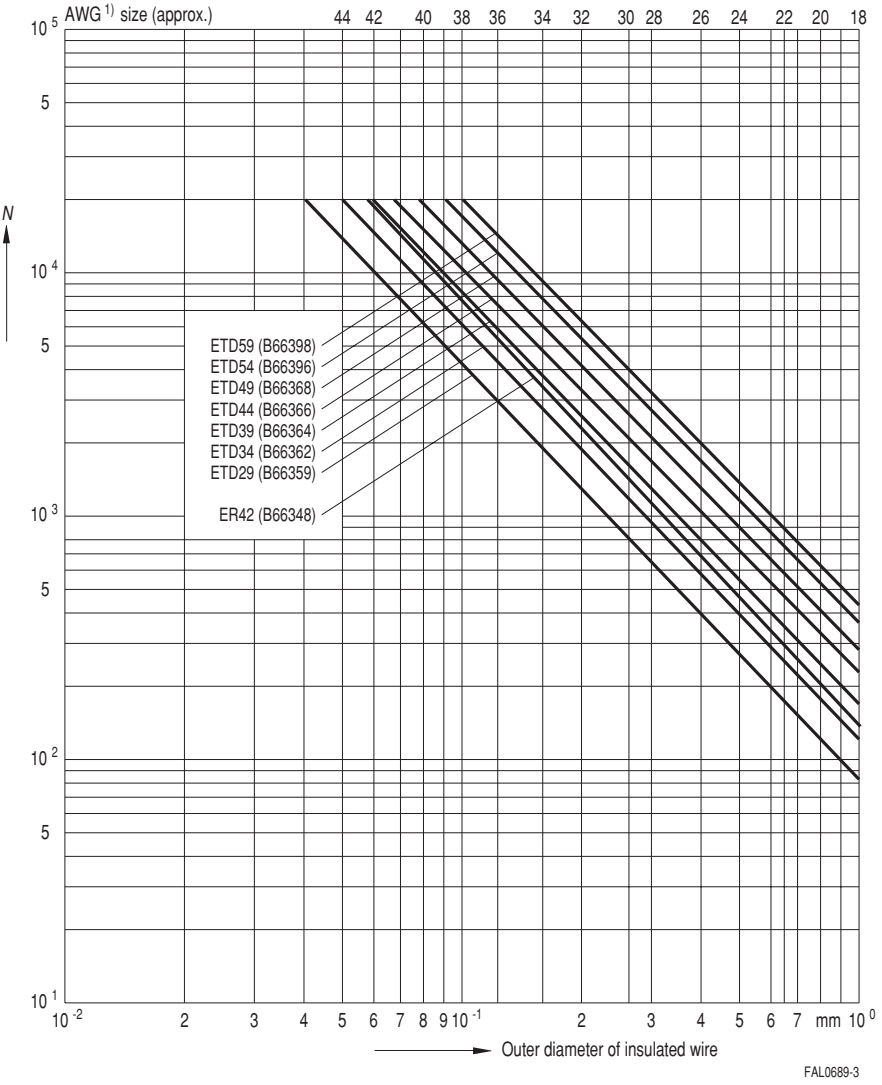

1) American Wire Gauge (AWG)

E cores

Maximum number of turns *N* for coil formers

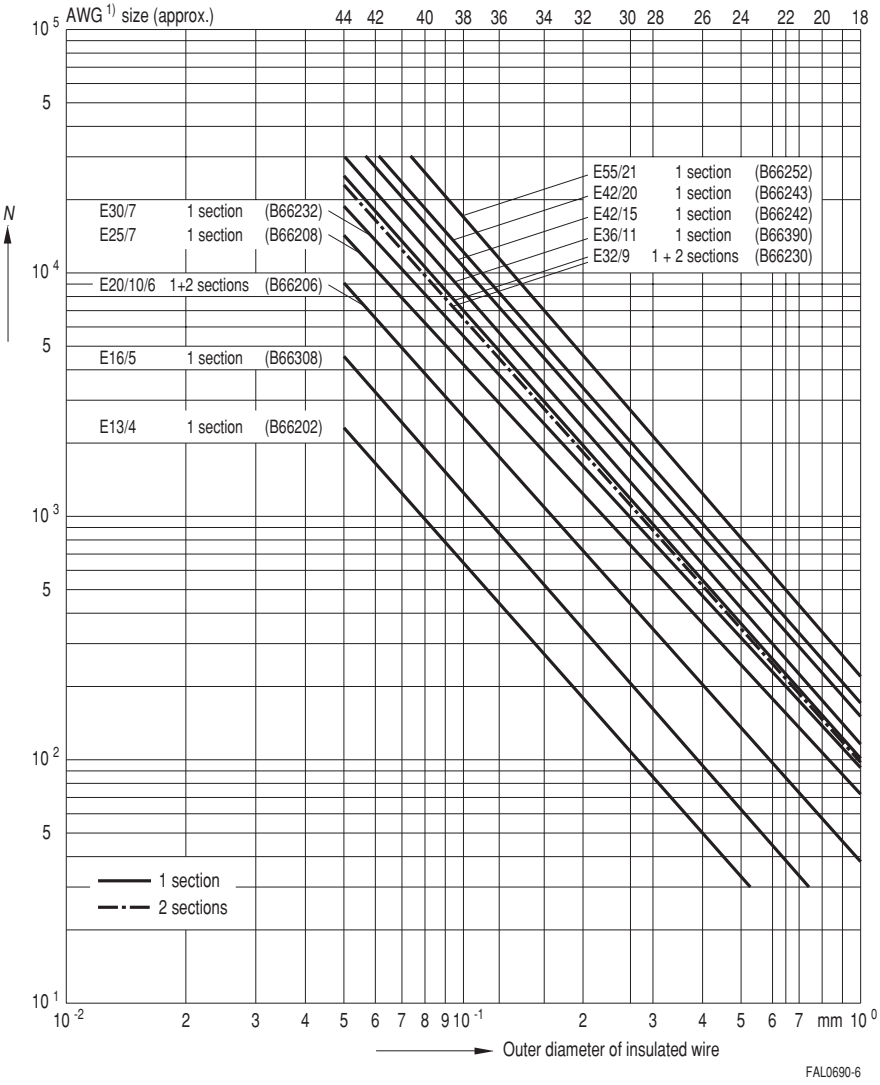

1) American Wire Gauge (AWG)

SMD types

Maximum number of turns *N* for coil formers

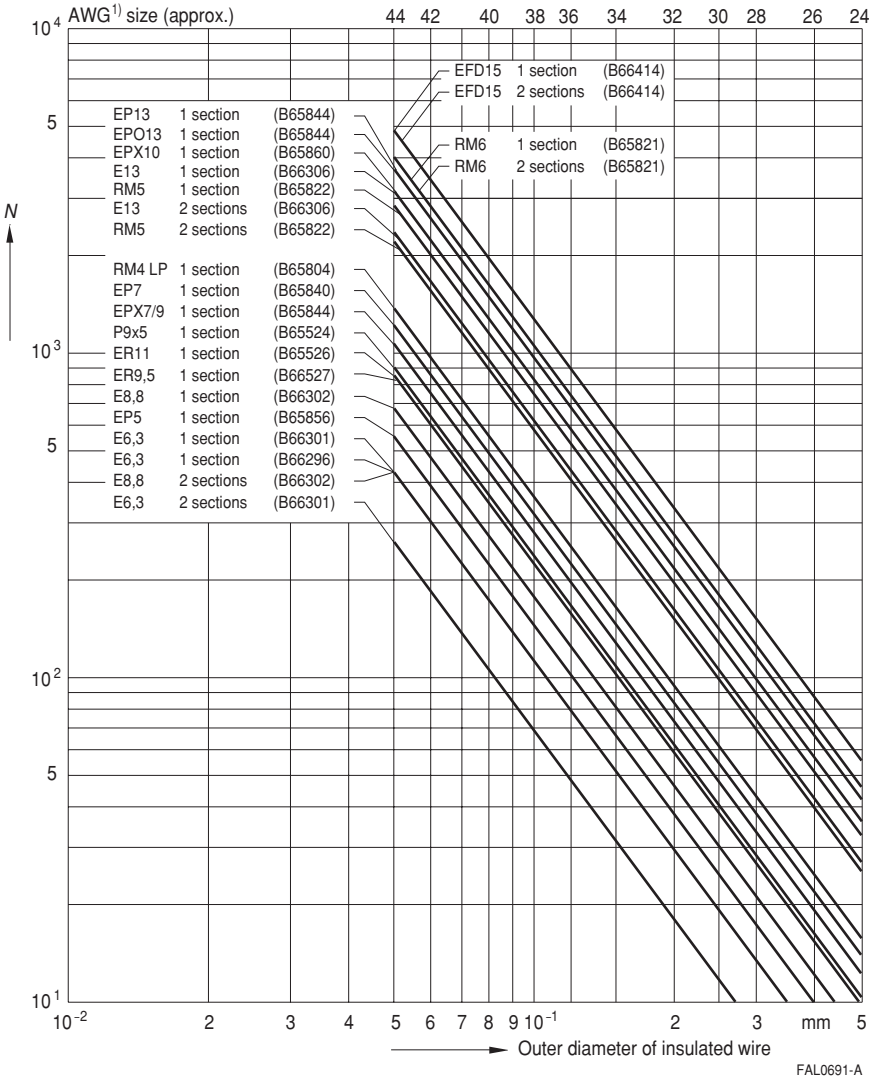

1) American Wire Gauge (AWG)

2.2 Soldering/Inductor assembly

The winding wires are preferably connected to the pins by dip soldering. Note the following when soldering:

– Prior to every dip soldering process the oxide film must be removed from the surface of the solder bath.
– 2 to 3 turns of the wire are dipped into the solder bath; the coil former must not be allowed to come too close to the solder or remain there for too long (see diagram).
– Typical values are: Bath temperature: 400 °C, soldering time: 1 s.

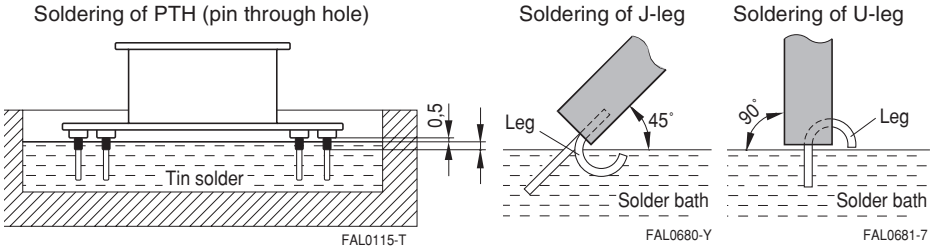

For inductor assembly, it is advisable to clamp the cores with the associated relevant mounting assemblies for the coil formers and cores. In this way it is possible to avoid the effects of external mechanical stress.

2.3 Design and processing information for SMD components

2.3.1 Automatic placement

EPCOS ferrite accessories are suitable for automatic placement. Many automatic placement machines pick up the components with suction probes and pliers, so the inductive components should have simple and clear contours as well as a sufficiently large and flat surface. Ferrite cores with a perpendicular magnetic axis, e.g. RM and ER cores, have a smooth surface and the flange for the coil former is styled right for the purpose. For cores with a horizontal magnetic axis, e.g. E cores and toroids, we provide cover caps to meet these requirements.

2.3.2 Coplanarity

Coplanarity means the maximum spacing between a terminal and a plane surface. If inductive components are fabricated with coplanarity of < 0,2 mm for example, then one or more terminals may be spaced maximally 0,2 mm from a plane surface.
Inductive components are fabricated to standard with coplanarity of < 0,2 mm. Coplanarity is influenced by a number of factors:

a) Coil former specification
The coplanarity of the coil former is < 0,1 mm for manufacturing reasons.

b) Winding wire
Use of thick winding wire (e.g. 0,25 mm diameter in model ER 11) leads to considerable mechanical strain on the terminal during winding, and this can degrade coplanarity.

c) Soldering temperature and duration
When winding wire is soldered to a terminal, the coil former is subjected to high thermal stress. If thick wires have to be soldered, the soldering temperature and/or duration increase and thus the thermal stress on the coil former too. This also degrades coplanarity.

Consequently the use of thick wires degrades coplanarity in two ways: greater mechanical strain when winding, and greater thermal stress during soldering.

If electrical requirements call for the use of thick wires, either the manufacturing effort is greater (it takes longer and the costs are higher), or a terminal geometry has to be chosen that is suitable for the use of thick wires. EPCOS offers three different SMD lead geometries: gullwings, J terminals and molded-in U terminals.

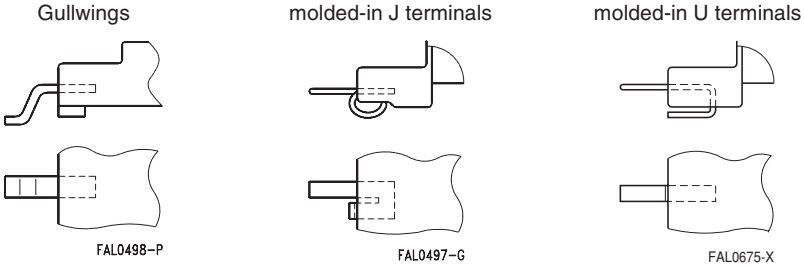

With gullwings the wire is wound direct on the terminal, which is then soldered on the circuit board. With J terminals the wire is wound on a separate pin, and the J terminal is soldered to the circuit board. With U terminals the wire is wound on a separate pin and the lower pin is soldered to the circuit board.

So gullwings are suitable for applications with thin wire (up to approx. 0,18 mm in diameter), and J and U terminals for use with thick wire (upwards from 0,18 mm in diameter). These figures for wire diameter are only intended as guidelines. Depending on wire diameter, the winding arrangement, the pinning and electrical requirements, one has to decide from case to case which solution is best for the particular application.

2.3.3 Solder paste application

Coplanarity has to be considered when determining the thickness of the solder paste. If coplanarity is < 0,2 mm for example, the solder paste has to be applied at least 0,2 mm thick to ensure proper soldering.

2.3.4 Solderability

EPCOS accessories are suitable for wave and reflow soldering. To ensure proper soldering on the circuit board, EPCOS accessories satisfy solderability as specified in IEC 60068-2-20. In deviation to this soldering temperature is 350 °C ± 5 °C, 1 s as the bobbins used to be dipped in a solder bath (T > 350 °C) for soldering the wire to the pins.

2.4 Gluing

The mating surfaces must be free of dust, grease and fibers. From the numerous adhesives available, epoxy resins with appropriate hardeners have proved particularly suitable. The following adhesives can be recommended:

a) for cores:
100 g Araldite AY 103
16 g hardener HY 956
Pot life 1 hour max.
Curing 3 hours at 60 °C
Thermal stability of the glued joint 60 °C
(for a short period 90 °C)

b) for cores:
100 g Araldite AY 103
40 g hardener HY 991
Pot life 1 hour
Curing 60 minutes at 80 °C
Thermal stability of the glued joint 80 °C

c) for cores:
100 g Araldite AY 105-1
50 g hardener HY 991
Pot life approx. 1 hour
Curing 45 minutes at 80 °C
Thermal stability of the glued joint 100 °C

d) for coil formers:
100 g adhesive a)
200 cm^3 filler Aerosil 200
Curing same as a)

e) for external gluing:
Single-component adhesive AV 118
Open pot life
Curing 10 minutes 180 °C
20 minutes 160 °C
45 minutes 140 °C
Thermal stability of the glued joint 120 °C

(Manufacturer of adhesives a) – e): Vantico (former Ciba Geigy)

2.5 Adhesive application and core mating

A quantity of adhesive appropriate to the area in question is applied to the cleaned surface of the core's side walls. The centerpost must remain free of adhesive. The two core halves without coil former are then placed on a mandrel and rotated against each other two or three times to spread the adhesive. A slight ring of adhesive exuding around the edges indicates that sufficient adhesive has been applied.

On porous, low-permeability SIFERRIT materials (K) the adhesive should be applied and spread twice.

The next step should follow immediately since the adhesive film easily attracts dust and absorbs moisture. Therefore, the core pair with adhesive already applied is opened for a short time and the wound coil is inserted without touching the mating surfaces.

The wound coil is then fixed into position. This can be done by using resilient spacers which must be inserted before applying the adhesive. Appropriate spacers are available on request.

The coil former can also be fixed by gluing, e.g. using adhesive d), but only at one spot on the core bottom to avoid any mechanical stress caused by the difference in thermal expansion of core and coil former.

Adhesive e) is suitable for external gluing, which implies only four dots of adhesive at the joints on both sides of the openings. Because of the somewhat lower torsional strength, it should be noted that this kind of gluing should only be used with mounted cores.

2.6 Holding jigs

The core assembly is cured under pressure in a centering jig. The core center hole – where present – is used for centering, and two to eight coils can be held in one jig with a pressure spring. Spacers will ensure that the pressure is only exerted on the side walls of the core.

Single jigs facilitate the coil inductance measurement, which has proved useful for checking cores with small air gaps before the adhesive has hardened. Small inductance corrections can be made by slightly turning the core halves relative to each other.

2.7 Final adjustment

(possible only with adjustable cores)

With all assembled ferrite cores, a magnetic activation takes place as a result of mounting influences such as clamping, gluing and soldering, i.e. a disaccommodation process commences. Therefore the final adjustment for high-precision inductors should take place no earlier than one day after assembly; preferably, one week should first elapse.

2.8 Hole arrangement

For drilling the through-holes into the PC board we recommend the dimensions given in the hole arrangement for each coil former, which depend on the distance of the pins on the pin outlet level.

2.9 Creepage and clearance

For telecom transformers the clearance and creepage distances and the thickness of insulation must be considered acc. EN 60 950 subclause 2.9.

Survey of packing modes

Ferrites

	Type	Packing	Para.	
RM cores	RM 4 to RM 10 RM 12, RM 14	Blister tapes Standard trays	3.2 2.2.1	170 168
PM cores	PM 50/39 to PM 114/93	Standard trays	2.2.1	168
P cores	all P cores P 9 × 5 to P 22 × 13	Standard trays Blister tapes on request	2.2.1 3.2	168 170
P core halves	7,35 × 3,6 to 150 × 30	Standard trays	2.2.1	168
TT/PR cores		Standard trays	2.2.1	168
EP cores	EP 5 to EP 20 EPX 7/9, EPX 10, EPO 13	Standard trays Blister tapes on request	2.2.1 3.2	168 170
E cores	E 5 to E 10 E 6,3 and E 8,8 Core length 12,6 … 36 mm Core length > 36 mm	Standard trays Tape on reel Block packing Standard trays	2.2.1 3.3 2.2.2 2.2.1	168 170 168 168
ELP cores ER cores ETD cores EC cores EFD cores EV cores DE cores		Standard trays	2.2.1	168
U and I cores		Standard trays	2.2.1	168
Toroids (ring cores)	Packing depends on size and version (coated/uncoated)	Standard trays Boxes Bags	2.2.1 2.3.2 2.3.1	168 169 169
Double-aperture cores		Bags	2.3.1	169

Accessories

Coil formers with pins	Polystyrene boards	2.2.3	169
Coil formers	Boxes	2.3.2	169
Mounting assemblies	Boxes	2.3.2	169
Clamps	Bags (individual clamps)	2.3.1	169
Insulating washers	Bags (individual washers), Boxes	2.3.1	169

Packing

1 General information

Our product packaging modes ensure maximum protection against damage during transportation. Moreover, our packing materials are selected with environmental considerations in mind. They are marked with the appropriate recycling symbols.

Because of the large variety of types and sizes, we use five basic kinds of packing, which are described in points 2 and 3 below:

- blister tape
- tray
- container
- reel
- magazine

The packing units are based on the following system:

1.1 Packing unit (PU)

Usually, a packing unit is a collection of a number of basic packages. The size of the packing unit is stated for the particular components in their data sheets. When ordering, please state complete packing units if possible. We reserve the right to round the ordered quantity accordingly.

1.2 Dispatch unit

A number of packing units are combined to form a dispatch unit. Standard dispatch units for large quantities are a Europallet or pallet carton. For small quantities, folding corrugated cardboard boxes are used in standard sizes. In the case of small quantities a dispatch unit may also include packages with other components.

1.3 Bar-code standard label

On the product packing label (standard label) we include bar-code information in addition to plain text. In addition to benefits relating to the internal flow of goods, this provides above all a more rapid and error-free means of identification checking for the customer.

Examples of barcode labels with production ID (1P), lot number (1T), date code (10D), production number (30P) and quantity (Q)

Example for core label

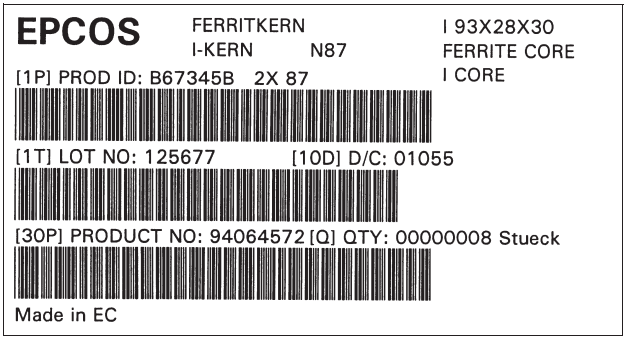

FAL0685-5

Example for accessories label

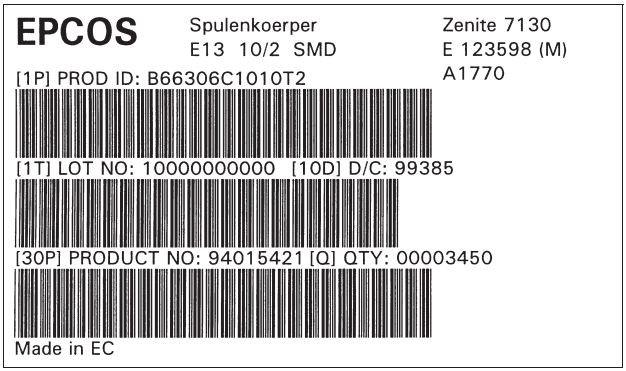

FAL0684-W

Example of a customer-specific barcode label

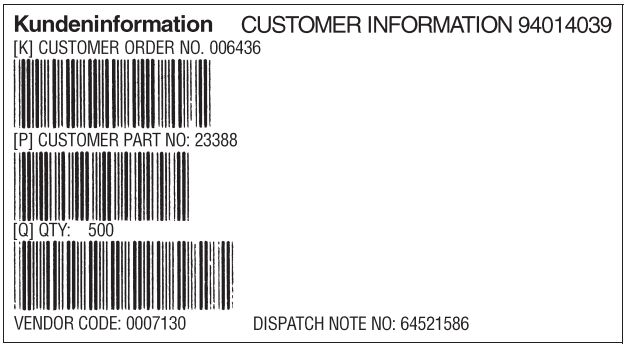

FAL0698-2

2 Modes of packing

2.1 Blister tape

Blister packing was specially devised for handling by automatic systems but has also proved to be very good for conventional handling, especially where small quantities are concerned. See point 3.2 for a detailed description and a list of the core types that can be supplied in this type of packing.

2.2 Tray (pallet)

2.2.1 Standard tray

The polystyrene tray (basic package) is the standard packing for most types of core. The area of 200 mm × 300 mm corresponds to the module dimensions of DIN 55 510 and is based on the area of the 800 mm × 1200 mm Europallet. Depending on the overall height of the trays and the numbers contained, several trays will be stacked to form a packing unit and provided with a corrugated cardboard cover. For the protection of the cores the entire stack is also shrink-wrapped in polyethylene film.

Each core is enclosed in a separate compartment. When P cores and similar types are packed in sets, the halves of the core pairs are packed so that their pole faces are opposite one another. As a rule their association is identified by markings in the polystyrene (recessed webs, thinner webs). In the case of P3,3 × 2,6 and P4,6 × 4,1 cores the halves of a set are not located in a single tray but in different trays of a packing unit.

2.2.2 Block packing

For E and U core we prefer block packing in trays with the dimensions 200 mm × 300 mm. The symmetry, position, length and spacing of the blocks are always the same. The height of the tray is dependent on the size of the core. For the makeup of a packing unit see point 2.2.1.

Block packing can be supplied in boxes of corrugated cardboard (special packing unit!) on request.

Block packing permits highly rationalized handling and is designed for automatic processing.

Packing unit for standard or block packing

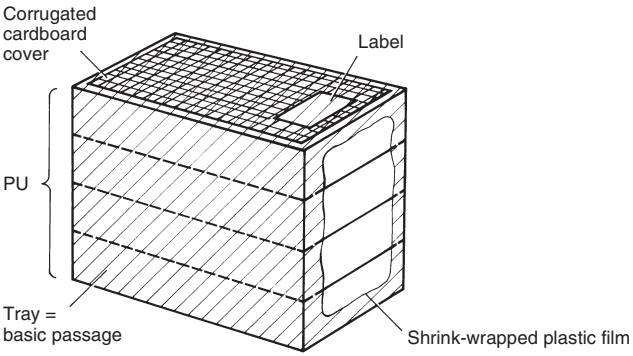

2.2.3 Board for coil formers with pins

For coil formers with pins, a polystyrene board is generally used. The coil formers are inserted in the board with the pins downwards. A number of stacked boards (packing unit) are enclosed in a jacket of cardboard, or packed in a folding box, and in some cases are shrink-wrapped in plastic.

2.3 Container

2.3.1 Bag

Small ferrite parts are packed in flat polyethylene bags. The number per bag depends on the volume of the parts. Generally four bags in a corrugated cardboard box form a packing unit.

Small accessories (clamps, mounting assemblies, and also pinless and SMD coil formers) are also packed in this way. The size of the bag depends on the volume of the parts (packing unit).

2.3.2 Box

Coated ring cores of medium size are packed in cardboard boxes with cardboard or polyethylene foam inlays. The number per box depends on the volume of the cores.

Accessories (large mounting assemblies, coil formers, clamps, washers etc.) are packed in boxes of cardboard or corrugated cardboard.

3 Delivery modes for automatic processing

3.1 General information on inductor production

The inductor parts described in the following can be handled by automatic manufacturing systems. In addition to automatic winding machines - which can be combined with wrapping, fluxing and soldering stations - flexible, high-performance automatic assembly lines are available. Design and packing of the individual parts (ferrite cores, coil formers, clamps, insulating washers and adjusting screws) have been optimized for automatic processing and permit easy feeding to the various stations of production lines.

We supply RM cores up to RM10 (P and EP cores on request) blister-taped in dispenser boxes. By inserting a plate-shaped resilient insulating washer between core and coil former, gluing can be dispensed with.

We also provide consulting services with examples of implementations to customers planning to introduce automatic production lines.

Production sequence

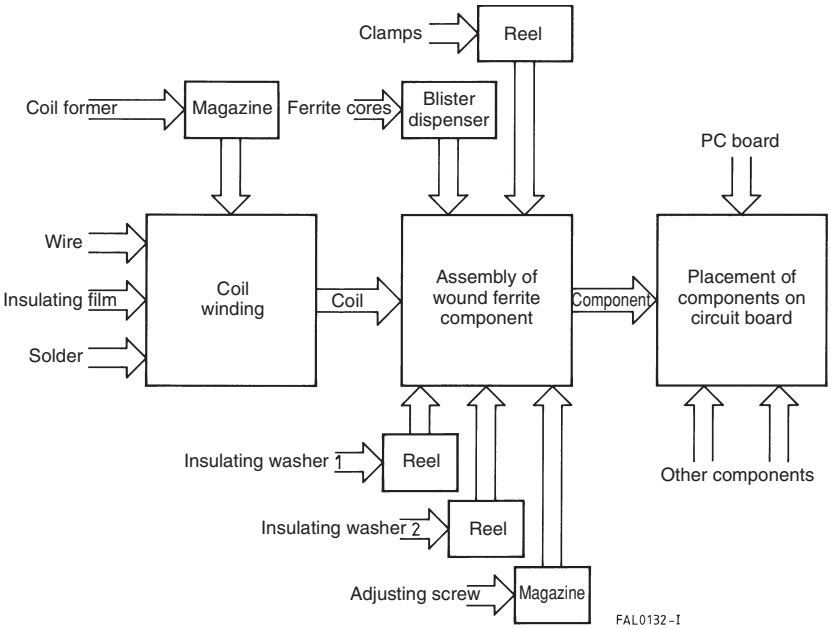

3.2 Cores in blister tape (strips)

The cores are packed in sets ready for assembly, i.e. a stamped core with the base upwards and an unstamped core (possibly with a threaded sleeve) with the pole face upwards. The blister tapes have a hole at one end for orientation purposes (see also illustration). The tapes are sealed with a paper cover. Looking at a tape with the hole on the left and the paper cover on top, then after removing the paper cover the stamped cores will be in the upper row and the unstamped cores of the sets in the lower row.

Several blister tapes are combined in a box with a perforated tear-off cover (dispenser pack) to form a packing unit. The tapes are packed so that the orientation hole appears in the dispenser opening. The box is shrink-wrapped in polyethylene film.

3.3 Cores in blister tape (reeled)

E 5 and E 6,3 cores can also be supplied taped and reeled as per IEC 60286-3, optionally in conductive or non-conductive tapes. The cores are oriented for automatic feeding. The tapes are sealed with a transparent cover tape and wound on 330-mm polystyrol reels. Each reel is identified with a bar code label and a release label.

Packing

The following table lists the core types which are available in blister tape:

Type	Dimensions of blister tape $l \times b \times d$ mm	Spacing mm	Spacing upper/ lower row mm	Dimensions of dispenser pack $l \times b \times h$ mm	Sets/ tape	Tapes/ box	Sets/ box	Approx. net weight g
RM cores								
RM 4	340 × 60 × 6,6	17,0	27,5	349 × 63 × 203	20	30	600	1000
RM 4 LP	340 × 60 × 5,0	17,0	27,5	349 × 63 × 203	20	40	800	
RM 5	340 × 60 × 8,0	17,0	27,5	349 × 63 × 203	20	25	500	1550
RM 6	340 × 60 × 8,0	17,0	27,5	349 × 63 × 203	20	25	500	2550
R 6	340 × 60 × 8,0	17,0	27,5	349 × 63 × 203	20	25	500	2550
RM 7	295 × 82 × 9,4	29,5	38,5	301 × 85 × 240	10	25	400	1925
RM 8	295 × 82 × 11,8	29,5	38,5	301 × 85 × 240	10	20	200	2600
RM 10	295 × 82 × 11,8	29,5	38,5	301 × 85 × 240	10	20	200	4600
RM 10 LP	295 × 82 × 9,4	29,5	38,5	301 × 85 × 240	10	25	250	
EP cores (on request)								
EP 7	340 × 60 × 5,0	17,0	27,5	349 × 63 × 203	20	40	800	1260
EP 10	340 × 60 × 8,0	17,0	27,5	349 × 63 × 203	20	25	500	1375
EP 13	340 × 60 × 8,0	17,0	27,5	349 × 63 × 203	20	25	500	2550
EP 17	295 × 82 × 11,8	29,5	38,5	301 × 85 × 240	10	20	200	2220
EP 20	295 × 82 × 11,8	29,5	38,5	301 × 85 × 240	10	20	200	5640
P cores (on request)								
P 9 × 5	340 × 60 × 4,0	17,0	27,5	349 × 63 × 203	20	50	1000	800
P 11 × 7	340 × 60 × 4,0	17,0	27,5	349 × 63 × 203	20	50	1000	1700
P 14 × 8	295 × 82 × 5,9	29,5	38,5	301 × 85 × 240	10	40	400	1280
P 18 × 11	295 × 82 × 9,4	29,5	38,5	301 × 85 × 240	10	25	250	1500
P 22 × 13	295 × 82 × 9,4	29,5	38,5	301 × 85 × 240	10	25	250	3250
E cores (on request)					Pieces/reel		Pieces/box	
E 5	27000 × 12 × 2,7	4,0	4,0	370 × 340 × 100	6500		32500	
E 6,3	27000 × 12 × 2,7	4,0	8,0	370 × 340 × 100	3400		17000	
E 8,8	33000 × 16 × 3,0	4,0	10,0	370 × 340 × 100	2100		10500	

For ordering codes refer to the individual data sheets.
Dimensions are nominal; tolerances given in design drawings.

3.4 Blister tapes

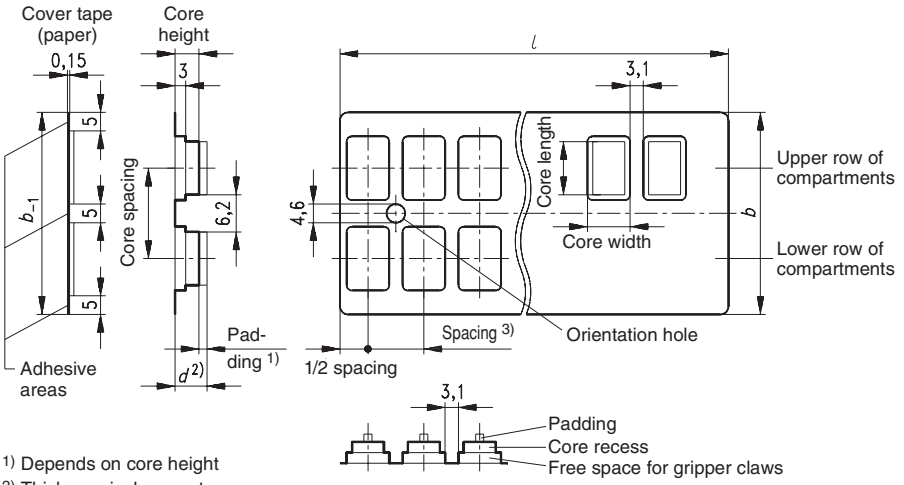

The blister compartments always comprise the following function spaces: a free space for the gripper claws, the recess in which the core rests and the padding.

The free space enables the cores to be removed by mechanical grippers. On the reverse side of the blister, these free spaces lead to a regular grid arrangement with a spacing of 6,2 mm and 3,1 mm. The blisters should be guided and stopped at these intervals. A hanging arrangement is to be preferred, because this avoids problems arising in case the blister height or padding thickness varies.

The core recess centers the core in the blister compartment.

The padding serves as protection during transport and as spacing to achieve correct filling of the dispenser pack. The shape and position of the padding may vary, depending on the production method used. All padding dimensions given must therefore be considered to be subject to change at any time.

3.5 Dispenser pack

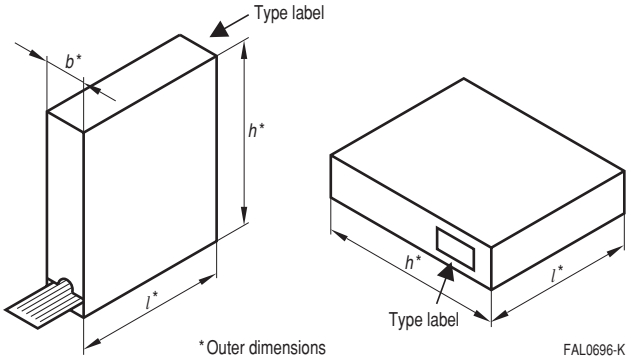

To open a blister tape manually, peel back the paper cover tape smoothly but not too quickly, along the axis of the tape as shown in the following illustration.

When opening a blister tape automatically, it is advisable not to completely remove the paper cover. Rather, the cover paper should be divided up by means of 4 longitudinal cuts so that the mating surfaces remain on the blister (cf. blister tape illustration). The paper strips produced above the two rows of compartments can then be easily lifted. This avoids malfunctions resulting from fluctuations in the adhesive properties of the paper sealing tape.

3.6 Skin packing

Skin packing is a new and very compact packing method.

Several cores are placed on a cardboard pallet and sealed in GLTE film by heat shrinking. The various pallets are then stacked in a cardboard box.

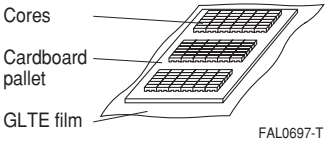

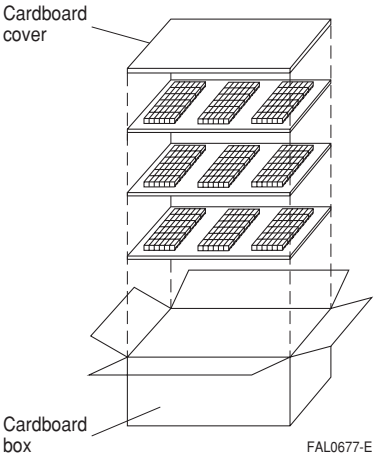

Advantages

- Environmentally friendly solution with easy-to-recycle materials
- Suitable for all cores larger than E30
- Good protection of mating surface
- Film can be peeled back very easily
- Code numbers printed on cores can be read through transparent film

Cores for which skin packing is used:

E 47, ELP 43, I 43; special types on request.

1 Production sequence and quality assurance during ferrite manufacture (schematic)

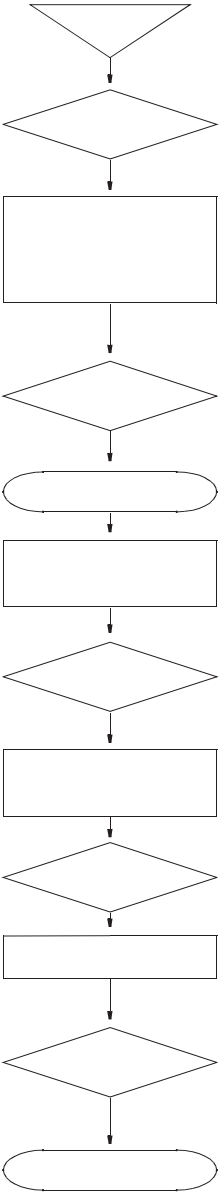

	Quality records Traceability
Raw materials (powder)	
Incoming inspection Analysis of chemical comp. (X-ray fluorescence analysis)	X-ray fluorescence analysis reports
Granulate production Weighing, mixing, presintering, grinding, stirring in binder. Homogenization, spraying incl. process control checks	
Bulk mix release Chemical analysis Manufacture and testing of sample cores	Bulk mix release report
Granulate storage	
Parts production Pressing, decarbonizing, sintering incl. process control checks	
Sinter check Testing of electrical and mechanical properties	Sinter check test report
Parts processing e.g. surface grinding, AL grinding, etc. incl. process control checks	
Final inspection/Monitoring Testing electr./mech. properties	Final inspection reports
Packing in PU (factory packing)	
Delivery release, Outgoing inspection, checking of reports and finish Labeling with “FER QS Freigabe” (FER QA release label)	FER QA release label or date code on packing
Sales warehouse	

2 General information

2.1 Ferrites quality objectives

Quality plays a central role in the competition for the better and more favorable product. As a guiding principle for the continual improvement of product and service quality, the Ferrites Division has set quality objectives which are regularly updated and successively extended to all products. These serve as target criteria for new developments and are similarly required of current products.

To realize the objectives for existing products, projects involving teams of staff from all areas are working on product and process improvements without regard to departmental boundaries.

2.2 Total Quality Management

The aim of Total Quality Management (TQM) is to gear the entire organization to optimally satisfying customer requirements.

Following the principle of “quality from the very start”, everyone in our company is involved in realizing this objective. Systematic planning, careful selection of our suppliers and mastery of the development and production processes are the most important guarantors for maintaining a high quality level.

Internal measures to promote quality, such as training courses, quality group work, working committees and Q audits, strengthen the sense of responsibility of every employee and help to recognize and avoid errors.

Modern quality instruments such as FMEA[1)] and SPC[2)] supplement and support our quality assurance and enhancement measures.

3 Ferrites quality assurance system

The documented QA system of the Ferrites Division forms the basis for all quality assurance activities. At all locations the Ferrites QA systems satisfy the international QA standard ISO 9000, as witnessed by certificates from the DNV (Det Norske Veritas), LRQA (Lloyd’s Register Quality Assurance), KPMG Quality Registrar or the AFAQ (Association Française pour l‘Assurance de la Qualité).

3.1 Quality assurance for incoming goods

To ensure the quality of raw materials and bought-in parts, the ferrite plants of EPCOS work only with suppliers who can establish proof of both a high quality product and an effective quality assurance system.

Where it is necessary for process control – as in the case of the iron oxide for example – the plants perform their own incoming inspections.

3.2 Quality assurance in production

The production processes are monitored and controlled by constant examination of the process parameters and (intermediate) products. These inspections are included in the company-wide statistical process control (SPC).

At the conclusion of each major production stage a release inspection (“quality control gate”) is performed to establish proof of the quality.

1) FMEA Failure Mode and Effects Analyses
2) SPC Statistical Process Control

3.3 Traceability

By recording the lot or batch numbers on the documentation accompanying the process, complete traceability is maintained in the production sequence.

After delivery, traceability to the internal release inspections (“quality control gates”) is ensured by the date code which is printed on the label (see page 167).

4 Delivery quality

The quality level of the products released for delivery is constantly monitored, recorded and evaluated. These data for ferrite cores are available on request.

5 Classification of defects

A product is considered defective if it does not comply with the specifications given in the data sheets or in the agreed technical purchase specification.

Use of the sampling plan according to IEC 60410/DIN ISO 2859 (previously DIN 40 080, contents identical to MIL STD 105 D) is recommended where incoming inspections are carried out by the user.

5.1 Electrical properties

The measuring conditions can be found in the chapter “General – Definitions”. The product data and relevant tolerance limits are defined in the respective data sheets. The material data given in the chapter “SIFERRIT materials” are to be understood as typical values.

Measuring conditions deviating from the data book require agreement between the customer and the EPCOS Ferrites Division.

5.2 Dimensions

The dimensioned drawings in the individual data sheets are definitive for the dimensions.

5.3 Finish

Assessment of the finish of ferrite cores is performed in accordance with EPCOS finish specifications. These are based on IEC 60424. Detailed drawings, which are available on request, specify the maximum permissible limit values for damage which can never be totally excluded with ceramic components. Assessment of the solderability of terminal pins for coil formers and clamps is carried out in accordance with IEC 60068 2-20, test Ta, method 1 (aging 3).

5.4 AQL values

Within the framework of our quality goals, we are gradually tightening the AQL values which are intended for use in the customer's incoming goods inspection, currently the value AQL 0,25 is applicable.

1 IEC standards

Please refer also the latest CO publications (www.iec.ch)

Publication	Title
IEC 60133 Ed. 4.0	Dimensions of pot cores made of magnetic oxides and associated parts
IEC 60205 Ed. 1.0	Calculation of the effective parameters of magnetic piece parts
IEC 60205 Amd. 1 Ed. 1.0	Amendment No. 1
IEC 60205 Amd. 2 Ed. 1.0	Amendment No. 2
IEC 60205 A Ed. 1.0	First Supplement
IEC 60205 B Ed. 1.0	Second Supplement
IEC 60367-1 Ed. 2.0	Cores for inductors and transformers for telecommunications. Part 1: Measuring methods
IEC 60367-1 Amd. 1 Ed. 2.0	Amendment No. 1
IEC 60367-1 Amd. 2 Ed. 2.0	Amendment No. 2
IEC 60367-2 Ed. 1.0	Cores for inductors and transformers for telecommunications. Part 2: Guides for the drafting of performance specifications
IEC 60367-2 Amd.1 Ed. 1.0	Amendment No. 1
IEC 60367-2 A Ed. 1.0	Cores for inductors and transformers for telecommunications. Part 2: Guides for the drafting of performance specifications – First Supplement
IEC 60401 Ed. 2.0	Ferrite materials – Guide on the format of data appearing in manufacturers' catalogues of transformer and inductor cores
IEC 60424-1 Ed. 1.0	Ferrite cores – Guide on the limits of surface irregularities. Part 1: General specification
IEC 60424-2 Ed. 1.0	Guidance on the limits of surface irregularities of ferrite cores. Part 2: RM cores
IEC 60424-3 Ed. 1.0	Ferrite cores – Guide on the limits of surface irregularities Part 3: ETD cores and E cores
IEC 60431 Ed. 2.0	Dimensions of square cores (RM cores) made of magnetic oxides and associated parts
IEC 60431 Amd. 1 Ed. 2.0	Amendment No. 1
IEC 60431 Amd. 2 Ed. 2.0	Amendment No. 2
IEC 60647 Ed. 1.0	Dimensions for magnetic oxide cores intended for use in power supplies (EC cores)
IEC60723-1 Ed. 1.0	Inductor and transformer cores for telecommunications. Part 1: Generic specification
IEC 60723-2 Ed. 1.0	Inductor and transformer cores for telecommunications. Part 2: Sectional specification. Magnetic oxide cores for inductor applications
IEC 60723-2 Amd. 1 Ed. 1.0	Amendment No. 1

Publication	Title
IEC 60723-2-1 Ed. 1.0	Inductor and transformer cores for telecommunications. Part 2: Blank detail specification. Magnetic oxide cores for inductor applications. Assessment level A
IEC 60723-3 Ed. 1.0	Inductor and transformer cores for telecommunications. Part 3: Sectional specification: Magnetic oxide cores for broad-band transformers
IEC 60723-3-1 Ed. 1.0	Inductor and transformer cores for telecommunications. Part 3: Blank detail specification: Magnetic oxide cores for broad-band transformers. Assessment levels A and B
IEC 60723-4 Ed. 1.0	Inductor and transformer cores for telecommunications. Part 4: Sectional specification: Magnetic oxide cores for transformers and chokes for power applications
IEC 60723-4-1 Ed. 1.0	Inductor and transformer cores for telecommunications. Part 4: Blank detail specification: Magnetic oxide cores for transformers and chokes for power applications. Assessment level A
IEC 60723-5 Ed. 1.0	Inductor and transformer cores for telecommunications. Part 5: Sectional specification: Adjusters used with magnetic oxide cores for use in adjustable inductors and transformers
IEC 60723-5-1 Ed. 1.0	Inductor and transformer cores for telecommunications. Part 5: Sectional specification: Adjusters used with magnetic oxide cores for use in adjustable inductors and transformers. Section 1: Blank detail specification. Assessment level A
IEC 61185 Ed. 1.0	Magnetic oxide cores (ETD cores) intended for use in power supply applications – Dimensions
IEC 61185 Amd. 1 Ed. 1.0	Amendment No. 1
IEC 61246 Ed. 1.0	Magnetic oxide cores (E cores) of rectangular cross-section and associated parts – Dimensions
IEC 61247 Ed. 1.0	PM cores made of magnetic oxides and associated parts – Dimensions
IEC 61332 Ed. 1.0	Soft ferrite material classification
IEC 61333 Ed. 1.0	Marking on U and E ferrite cores
IEC 61596 Ed. 1.0	Magnetic oxide EP cores and associated parts for use in inductors and transformers – Dimensions
IEC 61604 TR 3 Ed. 1.0	Dimensions of uncoated ring cores of magnetic oxides
IEC 61860 Ed. 1.0	Dimensions of low-profile cores made of magnetic oxides
IEC 62044-3 Ed. 1.0	Cores made of soft magnetic materials – Measuring methods. Part 3: Magnetic properties at high excitation level

2 Quality assessment

The IEC standards mainly specify dimensions, designations and magnetic characteristics, whereas the European system of quality assessment CECC and the harmonized DIN-CECC standards additionally define methods of measurement and quality levels.

Since 1982 the IEC has been establishing the so-called IEC Q-system, which will have worldwide applicability. German DIN IEC standards are being harmonized with this quality system.

CECC and IEC-Q standards have a similar structure: they are subdivided into generic specifications (GS), sectional specifications (SS) and blank detail specifications (BDS). The numbering system of QC is analogous to that of CECC.

The detail specifications of CECC and IEC do not fully correspond to each other.

A quality assessment system of “Capability Approval” for the production of ferrite parts is being established.

Our product line includes a wide range of toroids with finely graded diameters ranging from 2,5 to 200 mm.

Other core heights can be supplied on request. All cores are available in the usual materials.

Applications

- Toroids are primarily used as EMC chokes for suppressing RF interference in the MHZ region and in signal transformers.

  Typical applications for toroids of NiZn ferrites are LAN chokes. One of the materials available for this purpose is K10; other materials upon request.

  The following high-permeability MnZn materials are available for interference suppression:

  – R2,5 through R12,5 for telecommunications, e.g. ISDN (N30, T38, T46, T56)
  – R13,3 through R26 for power line chokes (N30, T65, T35 to T56)
  – > R34 for chokes and filters in industrial use (T65)

- Toroids are also increasingly used for power applications. Here, the typical values for amplitude permeability and power loss, as summarized in the section on "*SIFERRIT Materials*" (page 31), are applicable to the special power materials.

Coating

Toroids are available in different coating versions, thus offering the appropriate solution for every application. The coating not only offers protection for the edges but also provides an insulation function.

For small ring cores, we have introduced a parylene coating (Galxyl) which features a low coating thickness and high dielectric strength.

Coatings of ring cores

Version	Epoxy (blue)	Galxyl (Parylene)
Main application	Medium/big sizes (≥ R9,53)	Small sizes (≤ R9,53)
Layer thickness	< 0,4 mm	0,012 or 0,025 mm
Breakdown voltage (minimum values)	> 1,0 kV (for R9,53; R10) > 1,5 kV (for R12,5 thru R20) > 2,0 kV (for > R20)	> 1 kV (standard value)
Mechanical quality	High firmness	Smooth surface
Maximum temperature (short-time)	approx. 180 °C	approx. 130 °C
Advantage	Low influence on A_L value	Very low thickness
UL rating	UL 94 V-0	UL 94 V-0
Ordering code	B64290-**L**…	B64290-**P**…

Dielectric strength test

The following test setup is used to test the dielectric strength of the insulating coating: A copper ring is pressed to the top edge of the ring. It touches the ferrite ring at the edges (see diagram).

The test duration is 2 seconds.

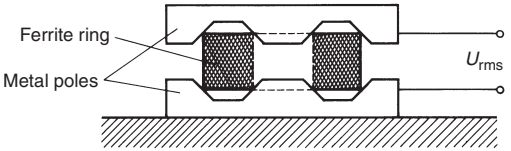

FUS0021-H

Chamfer

Large toroidal cores use thick wires that are partially subjected to high mechanical stress during winding. This can damage the wire insulation as well as the coating of the cores, thus reducing the breakdown voltage. To avoid this, EPCOS toroids with diameters of more than 26 mm have a chamfer. This prevents any insulation damage, and produces uniform coating thickness at the same time.

Successively EPCOS will apply chamfers to all toroids with diameter ≥ 10 mm.

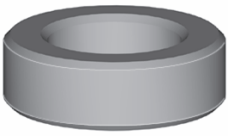

FUS0127-3

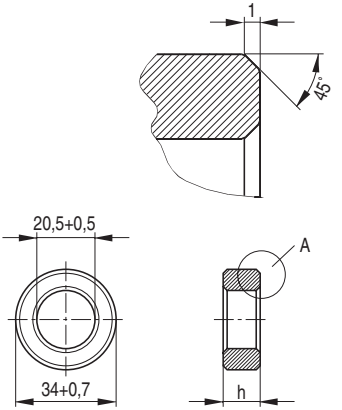

FUS0125-L

Compilation of the ordering code

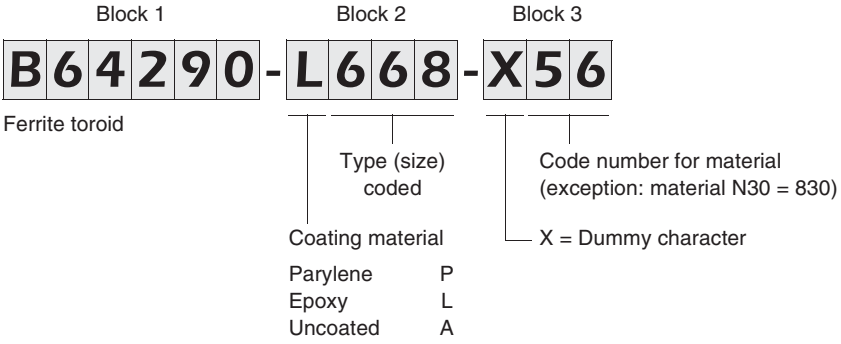

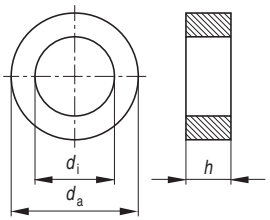

FUS0017-P

Overview of available sizes

Type Toroid size ($d_a \times d_i \times h$) mm	inch	Chamfer	Type code (ordering code, block 2)	Page
R 2,50 × 1,50 × 1,00	R 0,098 × 0,059 × 0,039		-P35	534
R 2,54 × 1,27 × 1,27	R 0,100 × 0,050 × 0,050		-P734	534
R 3,05 × 1,27 × 1,27	R 0,120 × 0,050 × 0,050		-P683	535
R 3,05 × 1,27 × 2,54	R 0,120 × 0,050 × 0,100		-P739	535
R 3,05 × 1,78 × 2,03	R 0,120 × 0,070 × 0,080		-P733	536
R 3,43 × 1,78 × 1,78	R 0,135 × 0,070 × 0,070		-P731	536
R 3,43 × 1,78 × 2,03	R 0,135 × 0,070 × 0,080		-P745	537
R 3,43 × 1,78 × 2,11	R 0,135 × 0,070 × 0,083		-P709	537
R 3,94 × 1,78 × 1,78	R 0,155 × 0,070 × 0,070		-P732	538
R 3,94 × 2,24 × 1,30	R 0,155 × 0,088 × 0,051		-P61	538
R 4,00 × 2,40 × 1,60	R 0,157 × 0,094 × 0,063		-P36	539
R 5,84 × 3,05 × 3,00	R 0,230 × 0,120 × 0,118		-P687	539
R 6,30 × 3,80 × 2,50	R 0,248 × 0,150 × 0,098		-P37	540
R 9,53 × 4,75 × 3,17	R 0,375 × 0,187 × 0,125		-L62	540
R 10,0 × 6,00 × 4,00	R 0,394 × 0,236 × 0,157		-L38	541
R 12,5 × 7,50 × 5,00	R 0,492 × 0,295 × 0,197		-L44	541
R 12,7 × 7,90 × 6,35	R 0,500 × 0,311 × 0,250		-L742	542
R 13,3 × 8,30 × 5,00	R 0,524 × 0,327 × 0,197		-L644	542
R 14,0 × 9,00 × 5,00	R 0,551 × 0,354 × 0,197		-L658	543
R 15,0 × 10,4 × 5,30	R 0,591 × 0,409 × 0,209		-L623	543
R 15,8 × 8,90 × 4,70	R 0,622 × 0,350 × 0,185		-L743	544
R 16,0 × 9,60 × 6,30	R 0,630 × 0,378 × 0,248		-L45	544
R 17,0 × 10,7 × 6,80	R 0,669 × 0,421 × 0,268		-L652	545
R 18,4 × 5,90 × 5,90	R 0,724 × 0,232 × 0,232		-L697	545

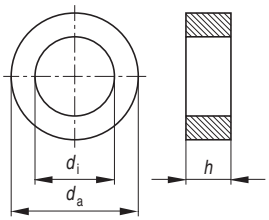

FUS0017-P

Overview of available sizes (continued)

Type Toroid size ($d_a \times d_i \times h$) mm	inch	Chamfer	Type code (ordering code, block 2)	Page
R 20,0 × 10,0 × 7,00	R 0,787 × 0,394 × 0,276		-L632	546
R 22,1 × 13,7 × 6,35	R 0,870 × 0,539 × 0,250		-L638	546
R 22,1 × 13,7 × 7,90	R 0,870 × 0,539 × 0,311		-L719	547
R 22,1 × 13,7 × 12,5	R 0,870 × 0,539 × 0,492		-L651	547
R 22,6 × 14,7 × 9,20	R 0,890 × 0,579 × 0,362		-L626	548
R 25,3 × 14,8 × 10,0	R 0,996 × 0,583 × 0,394		-L618	548
R 25,3 × 14,8 × 20,0	R 0,996 × 0,583 × 0,787		-L616	549
R 29,5 × 19,0 × 14,9	R 1,142 × 0,748 × 0,587	×	-L647	549
R 30,5 × 20,0 × 12,5	R 1,201 × 0,787 × 0,492	×	-L657	550
R 34,0 × 20,5 × 10,0	R 1,339 × 0,807 × 0,394	×	-L58	550
R 34,0 × 20,5 × 12,5	R 1,339 × 0,807 × 0,492	×	-L48	551
R 36,0 × 23,0 × 15,0	R 1,417 × 0,906 × 0,591	×	-L674	551
R 38,1 × 19,05 × 12,7	R 1,500 × 0,750 × 0,500	×	-L668	552
R 40,0 × 24,0 × 16,0	R 1,575 × 0,945 × 0,630	×	-L659	552
R 41,8 × 26,2 × 12,5	R 1,646 × 1,031 × 0,492	×	-L22	553
R 50,0 × 30,0 × 20,0	R 1,969 × 1,181 × 0,787	×	-L82	553
R 58,3 × 40,8 × 17,6	R 2,283 × 1,606 × 0,693	×	-L40	554
R 63,0 × 38,0 × 25,0	R 2,480 × 1,496 × 0,984	×	-L699	554
R 68,0 × 48,0 × 13,0	R 2,677 × 1,890 × 0,512		-L696	555
R 87,0 × 54,3 × 13,5	R 3,425 × 2,138 × 0,531	×	-L730	555
R 102 × 65,8 × 15,0	R 4,016 × 2,591 × 0,591		-L84	556
R 140 × 103 × 25,0	R 5,512 × 4,055 × 0,984		-A705	556
R 202 × 153 × 25,0	R 7,953 × 6,024 × 0,984		-A711	557

■ Parylene coating

R 2,50 × 1,50 × 1,00 (mm)
R 0,098 × 0,059 × 0,039 (inch)

Dimensions

d_a (mm)	d_i (mm)	Height (mm)	d_a (inch)	d_i (inch)	Height (inch)	
2,50 ± 0,12	1,50 ± 0,1	1,00 ± 0,1	0,098 ± 0,005	0,059 ± 0,004	0,039 ± 0,004	uncoated[1)]
Coating thickness 0,012 mm						coated

Characteristics and ordering codes

Material	A_L value nH	μ_i (approx.)	Ordering code	Magnetic characteristics			
				$\Sigma l/A$ mm^{-1}	l_e mm	A_e mm^2	V_e mm^3
K10	70 ± 25 %	700	B64290-P35-X10	12,30	6,02	0,49	3,00
T57	410 ± 25 %	4000	B64290-P35-X57				
T65	470 ± 30 %	4600	B64290-P35-X65				
T38	1020 ± 30 %	10000	B64290-P35-X38				
T46	1530 ± 30 %	15000	B64290-P35-X46				
T56	2040 + 30 / – 40 %	20000	B64290-P35-X56				

■ Parylene coating

R 2,54 × 1,27 × 1,27 (mm)
R 0,100 × 0,050 × 0,050 (inch)

Dimensions

d_a (mm)	d_i (mm)	Height (mm)	d_a (inch)	d_i (inch)	Height (inch)	
2,54 ± 0,12	1,27 ± 0,12	1,27 ± 0,12	0,100 ± 0,005	0,050 ± 0,005	0,050 ± 0,005	uncoated[1)]
Coating thickness 0,012 mm						coated

Characteristics and ordering codes

Material	A_L value nH	μ_i (approx.)	Ordering code	Magnetic characteristics			
				$\Sigma l/A$ mm^{-1}	l_e mm	A_e mm^2	V_e mm^3
K10	120 ± 25 %	700	B64290-P734-X10	7,14	5,53	0,77	4,29
T57	690 ± 25 %	3900	B64290-P734-X57				
T65	800 ± 30 %	4500	B64290-P734-X65				
T38	1760 ± 30 %	10000	B64290-P734-X38				
T46	2640 ± 30 %	15000	B64290-P734-X46				
T56	3520 + 30 / – 40 %	20000	B64290-P734-X56				

1) Upon request

■ Parylene coating

R 3,05 × 1,27 × 1,27 (mm)
R 0,120 × 0,050 × 0,050 (inch)

Dimensions

d_a (mm)	d_i (mm)	Height (mm)	d_a (inch)	d_i (inch)	Height (inch)	
3,05 ± 0,12	1,27 ± 0,12	1,27 ± 0,12	0,120 ± 0,005	0,050 ± 0,005	0,050 ± 0,005	uncoated[1)]
Coating thickness 0,012 mm						coated

Characteristics and ordering codes

Material	A_L value nH	μ_i (approx.)	Ordering code	Magnetic characteristics			
				$\Sigma l/A$ mm^{-1}	l_e mm	A_e mm^2	V_e mm^3
K10	160 ± 25 %	700	B64290-P683-X10	5,65	5,99	1,06	6,4
T57	830 ± 25 %	3700	B64290-P683-X57				
T65	1000 ± 30 %	4500	B64290-P683-X65				
T38	2200 ± 30 %	9900	B64290-P683-X38				
T46	3340 ± 30 %	15000	B64290-P683-X46				
T56	4400 + 30 / – 40 %	20000	B64290-P683-X56				

■ Parylene coating

R 3,05 × 1,27 × 2,54 (mm)
R 0,120 × 0,050 × 0,100 (inch)

Dimensions

d_a (mm)	d_i (mm)	Height (mm)	d_a (inch)	d_i (inch)	Height (inch)	
3,05 ± 0,12	1,27 ± 0,12	2,54 ± 0,12	0,120 ± 0,005	0,050 ± 0,005	0,100 ± 0,005	uncoated[1)]
Coating thickness 0,012 mm						coated

Characteristics and ordering codes

Material	A_L value nH	μ_i (approx.)	Ordering code	Magnetic characteristics			
				$\Sigma l/A$ mm^{-1}	l_e mm	A_e mm^2	V_e mm^3
K10	330 ± 25 %	700	B64290-P739-X10	2,82	5,99	2,12	12,7
T57	1700 ± 25 %	3800	B64290-P739-X57				
T65	2000 ± 30 %	4500	B64290-P739-X65				
T38	4200 ± 30 %	9400	B64290-P739-X38				
T46	6500 ± 30 %	15000	B64290-P739-X46				
T56	8700 + 30 / – 40 %	20000	B64290-P739-X56				

1) Upon request

■ Parylene coating

R 3,05 × 1,78 × 2,03 (mm)
R 0,120 × 0,070 × 0,080 (inch)

Dimensions

d_a (mm)	d_i (mm)	Height (mm)	d_a (inch)	d_i (inch)	Height (inch)	
3,05 ± 0,12	1,78 ± 0,12	2,03 ± 0,12	0,120 ± 0,005	0,070 ± 0,005	0,080 ± 0,005	uncoated[1)]
Coating thickness 0,012 mm						coated

Characteristics and ordering codes

Material	A_L value nH	μ_i (approx.)	Ordering code	Magnetic characteristics			
				$\Sigma l/A$ mm^{-1}	l_e mm	A_e mm^2	V_e mm^3
K10	160 ± 25 %	700	B64290-P733-X10	5,75	7,23	1,26	9,10
T57	870 ± 25 %	4000	B64290-P733-X57				
T65	1000 ± 30 %	4600	B64290-P733-X65				
T38	2150 ± 30 %	9900	B64290-P733-X38				
T46	3250 ± 30 %	15000	B64290-P733-X46				
T56	4300 + 30 / – 40 %	20000	B64290-P733-X56				

■ Parylene coating

R 3,43 × 1,78 × 1,78 (mm)
R 0,135 × 0,070 × 0,070 (inch)

Dimensions

d_a (mm)	d_i (mm)	Height (mm)	d_a (inch)	d_i (inch)	Height (inch)	
3,43 ± 0,12	1,78 ± 0,12	1,78 ± 0,12	0,135 ± 0,005	0,070 ± 0,005	0,070 ± 0,005	uncoated[1)]
Coating thickness 0,012 mm						coated

Characteristics and ordering codes

Material	A_L value nH	μ_i (approx.)	Ordering code	Magnetic characteristics			
				$\Sigma l/A$ mm^{-1}	l_e mm	A_e mm^2	V_e mm^3
K10	160 ± 25 %	700	B64290-P731-X10	5,38	7,63	1,42	10,7
T57	930 ± 25 %	4000	B64290-P731-X57				
T65	1050 ± 30 %	4500	B64290-P731-X65				
T38	2300 ± 30 %	10000	B64290-P731-X38				
T46	3400 ± 30 %	15000	B64290-P731-X46				
T56	4600 + 30 / – 40 %	20000	B64290-P731-X56				

1) Upon request

■ Parylene coating

R 3,43 × 1,78 × 2,03 (mm)
R 0,135 × 0,070 × 0,080 (inch)

Dimensions

d_a (mm)	d_i (mm)	Height (mm)	d_a (inch)	d_i (inch)	Height (inch)	
3,43 ± 0,12	1,78 ± 0,12	2,03 ± 0,12	0,135 ± 0,005	0,070 ± 0,005	0,080 ± 0,005	uncoated[1)]
Coating thickness 0,012 mm						coated

Characteristics and ordering codes

Material	A_L value nH	μ_i (approx.)	Ordering code	Magnetic characteristics			
				$\Sigma l/A$ mm^{-1}	l_e mm	A_e mm^2	V_e mm^3
K10	190 ± 25 %	700	B64290-P745-X10	4,72	7,63	1,62	12,2
T57	1060 ± 25 %	4000	B64290-P745-X57				
T65	1200 ± 30 %	4500	B64290-P745-X65				
T38	2650 ± 30 %	10000	B64290-P745-X38				
T46	4000 ± 30 %	15000	B64290-P745-X46				
T56	5300 + 30 / – 40 %	20000	B64290-P745-X56				

■ Parylene coating

R 3,43 × 1,78 × 2,11 (mm)
R 0,135 × 0,070 × 0,083 (inch)

Dimensions

d_a (mm)	d_i (mm)	Height (mm)	d_a (inch)	d_i (inch)	Height (inch)	
3,43 ± 0,12	1,78 ± 0,12	2,11 ± 0,12	0,135 ± 0,005	0,070 ± 0,005	0,083 ± 0,005	uncoated[1)]
Coating thickness 0,012 mm						coated

Characteristics and ordering codes

Material	A_L value nH	μ_i (approx.)	Ordering code	Magnetic characteristics			
				$\Sigma l/A$ mm^{-1}	l_e mm	A_e mm^2	V_e mm^3
K10	200 ± 25 %	700	B64290-P709-X10	4,54	7,63	1,68	12,7
T57	1100 ± 25 %	4000	B64290-P709-X57				
T65	1300 ± 30 %	4700	B64290-P709-X65				
T38	2770 ± 30 %	10000	B64290-P709-X38				
T46	4000 ± 30 %	15000	B64290-P709-X46				
T56	5500 + 30 / – 40 %	20000	B64290-P709-X56				

1) Upon request

■ Parylene coating

R 3,94 × 1,78 × 1,78 (mm)
R 0,155 × 0,070 × 0,070 (inch)

Dimensions

d_a (mm)	d_i (mm)	Height (mm)	d_a (inch)	d_i (inch)	Height (inch)	
3,94 ± 0,12	1,78 ± 0,12	1,78 ± 0,12	0,155 ± 0,005	0,070 ± 0,005	0,070 ± 0,005	uncoated[1)]
Coating thickness 0,012 mm						coated

Characteristics and ordering codes

Material	A_L value nH	μ_i (approx.)	Ordering code	Magnetic characteristics			
				$\Sigma l/A$ mm^{-1}	l_e mm	A_e mm^2	V_e mm^3
K10	200 ± 25 %	700	B64290-P732-X10	4,44	8,10	1,82	14,8
T57	1100 ± 25 %	3900	B64290-P732-X57				
T65	1350 ± 30 %	4800	B64290-P732-X65				
T38	2830 ± 30 %	10000	B64290-P732-X38				
T46	4200 ± 30 %	15000	B64290-P732-X46				
T56	5600 + 30 / – 40 %	20000	B64290-P732-X56				

■ Parylene coating

R 3,94 × 2,24 × 1,30 (mm)
R 0,155 × 0,088 × 0,051 (inch)

Dimensions

d_a (mm)	d_i (mm)	Height (mm)	d_a (inch)	d_i (inch)	Height (inch)	
3,94 ± 0,12	2,24 ± 0,12	1,30 ± 0,12	0,155 ± 0,005	0,088 ± 0,005	0,051 ± 0,005	uncoated[1)]
Coating thickness 0,012 mm						coated

Characteristics and ordering codes

Material	A_L value nH	μ_i (approx.)	Ordering code	Magnetic characteristics			
				$\Sigma l/A$ mm^{-1}	l_e mm	A_e mm^2	V_e mm^3
K10	100 ± 25 %	700	B64290-P61-X10	8,56	9,21	1,08	9,90
T57	550 ± 25 %	3800	B64290-P61-X57				
T65	700 ± 30 %	4800	B64290-P61-X65				
T38	1470 ± 30 %	10000	B64290-P61-X38				
T46	2200 ± 30 %	15000	B64290-P61-X46				
T56	2900 + 30 / – 40 %	20000	B64290-P61-X56				

1) Upon request

■ Parylene coating

R 4,00 × 2,40 × 1,60 (mm)
R 0,157 × 0,094 × 0,063 (inch)

Dimensions

d_a (mm)	d_i (mm)	Height (mm)	d_a (inch)	d_i (inch)	Height (inch)	
4,00 ± 0,12	2,40 ± 0,1	1,60 ± 0,1	0,157 ± 0,005	0,094 ± 0,004	0,063 ± 0,004	uncoated[1)]
Coating thickness 0,012 mm						coated

Characteristics and ordering codes

Material	A_L value nH	μ_i (approx.)	Ordering code	Magnetic characteristics			
				$\Sigma l/A$ mm^{-1}	l_e mm	A_e mm^2	V_e mm^3
N30	700 ± 25 %	4300	B64290-P36-X830	7,96	9,63	1,25	12,0
T65	750 ± 30 %	4600	B64290-P36-X65				
T38	1630 ± 30 %	10000	B64290-P36-X38				
T46	2450 ± 30 %	15000	B64290-P36-X46				
T56	3250 + 30 / – 40 %	20000	B64290-P36-X56				

■ Parylene coating

R 5,84 × 3,05 × 3,00 (mm)
R 0,230 × 0,120 × 0,118 (inch)

Dimensions

d_a (mm)	d_i (mm)	Height (mm)	d_a (inch)	d_i (inch)	Height (inch)	
5,84 ± 0,12	3,05 ± 0,12	3,00 ± 0,12	0,230 ± 0,005	0,120 ± 0,005	0,118 ± 0,005	uncoated[1)]
Coating thickness 0,012 mm						coated

Characteristics and ordering codes

Material	A_L value nH	μ_i (approx.)	Ordering code	Magnetic characteristics			
				$\Sigma l/A$ mm^{-1}	l_e mm	A_e mm^2	V_e mm^3
N30	1680 ± 25 %	4300	B64290-P687-X830	3,22	13,03	4,04	52,6
T65	1800 ± 30 %	4600	B64290-P687-X65				
T38	3900 ± 30 %	10000	B64290-P687-X38				
T46	5850 ± 30 %	15000	B64290-P687-X46				
T56	7700 + 30 / – 40 %	20000	B64290-P687-X56				

1) Upon request

■ Parylene coating

R 6,30 × 3,80 × 2,50 (mm)
R 0,248 × 0,150 × 0,098 (inch)

Dimensions

d_a (mm)	d_i (mm)	Height (mm)	d_a (inch)	d_i (inch)	Height (inch)	
6,30 ± 0,15	3,80 ± 0,12	2,50 ± 0,12	0,248 ± 0,006	0,150 ± 0,005	0,098 ± 0,005	uncoated[1)]
Coating thickness 0,012 mm						coated

Characteristics and ordering codes

Material	A_L value nH	μ_i (approx.)	Ordering code	Magnetic characteristics			
				$\Sigma l/A$ mm^{-1}	l_e mm	A_e mm^2	V_e mm^3
N30	1090 ± 25 %	4300	B64290-P37-X830	4,97	15,21	3,06	46,5
T65	1160 ± 30 %	4600	B64290-P37-X65				
T38	2530 ± 30 %	10000	B64290-P37-X38				
T46	3600 ± 30 %	14000	B64290-P37-X46				
T56	5000 + 30 / – 40 %	20000	B64290-P37-X56				

■ Epoxy coating

R 9,53 × 4,75 × 3,17 (mm)
R 0,375 × 0,187 × 0,125 (inch)

Dimensions

d_a (mm)	d_i (mm)	Height (mm)	d_a (inch)	d_i (inch)	Height (inch)	
9,53 ± 0,19	4,75 ± 0,12	3,17 ± 0,15	0,375 ± 0,007	0,187 ± 0,005	0,125 ± 0,006	uncoated[1)]
10,5 max.	3,8 min.	4,1 max.	0,413 max.	0,130 min.	0,161 max.	coated

Characteristics and ordering codes

Material	A_L value nH	μ_i (approx.)	Ordering code	Magnetic characteristics			
				$\Sigma l/A$ mm^{-1}	l_e mm	A_e mm^2	V_e mm^3
N30	1900 ± 25 %	4300	B64290-L62-X830	2,85	20,72	7,28	151
T65	2050 ± 30 %	4600	B64290-L62-X65				
T35	2650 ± 25 %	6000	B64290-L62-X35				
T38	4410 ± 30 %	10000	B64290-L62-X38				
T46	6400 ± 30 %	15000	B64290-L62-X46				

1) Upon request

■ Epoxy coating

R 10,0 × 6,00 × 4,00 (mm)
R 0,394 × 0,236 × 0,157 (inch)

Dimensions

d_a (mm)	d_i (mm)	Height (mm)	d_a (inch)	d_i (inch)	Height (inch)	
10,0 ± 0,2	6,0 ± 0,15	4,00 ± 0,15	0,394 ± 0,008	0,236 ± 0,006	0,157 ± 0,006	uncoated[1)]
10,8 max.	5,25 min.	4,75 max.	0,433 max.	0,199 min.	0,195 max.	coated

Characteristics and ordering codes

Material	A_L value nH	μ_i (approx.)	Ordering code	Magnetic characteristics			
				$\Sigma l/A$ mm^{-1}	l_e mm	A_e mm^2	V_e mm^3
N87	900 ± 25 %	2200	B64290-L38-X87	3,07	24,07	7,83	188
N30	1760 ± 25 %	4300	B64290-L38-X830				
T65	1900 ± 30 %	4700	B64290-L38-X65				
T35	2460 ± 25 %	6000	B64290-L38-X35				
T37	2660 ± 25 %	6500	B64290-L38-X37				
T38	4090 ± 30 %	10000	B64290-L38-X38				
T46	6000 ± 30 %	15000	B64290-L38-X46				

■ Epoxy coating

R 12,5 × 7,50 × 5,00 (mm)
R 0,492 × 0,295 × 0,197 (inch)

Dimensions

d_a (mm)	d_i (mm)	Height (mm)	d_a (inch)	d_i (inch)	Height (inch)	
12,5 ± 0,3	7,5 ± 0,2	5,00 ± 0,15	0,492 ± 0,012	0,295 ± 0,008	0,197 ± 0,005	uncoated[1)]
13,6 max.	6,5 min.	5,95 max.	0,535 max.	0,256 min.	0,234 max.	coated

Characteristics and ordering codes

Material	A_L value nH	μ_i (approx.)	Ordering code	Magnetic characteristics			
				$\Sigma l/A$ mm^{-1}	l_e mm	A_e mm^2	V_e mm^3
N87	1120 ± 25 %	2200	B64290-L44-X87	2,46	30,09	12,23	368
N30	2200 ± 25 %	4300	B64290-L44-X830				
T65	2400 ± 30 %	4700	B64290-L44-X65				
T35	3060 ± 25 %	6000	B64290-L44-X35				
T37	3320 ± 25 %	6500	B64290-L44-X37				
T38	5110 ± 30 %	10000	B64290-L44-X38				

1) Upon request

■ Epoxy coating

R 12,7 × 7,90 × 6,35 (mm)
R 0,500 × 0,311 × 0,250 (inch)

Dimensions

d_a (mm)	d_i (mm)	Height (mm)	d_a (inch)	d_i (inch)	Height (inch)	
12,7 ± 0,3	7,9 ± 0,25	6,35 ± 0,2	0,500 ± 0,012	0,311 ± 0,010	0,250 ± 0,008	uncoated[1)]
13,6 max.	7,15 min.	7,15 max.	0,535 max.	0,281 min.	0,281 max.	coated

Characteristics and ordering codes

Material	A_L value nH	μ_i (approx.)	Ordering code	Magnetic characteristics			
				$\Sigma l/A$ mm^{-1}	l_e mm	A_e mm^2	V_e mm^3
N87	1330 ± 25 %	2200	B64290-L742-X87	2,08	31,17	14,96	466
N30	2600 ± 25 %	4300	B64290-L742-X830				
T65	2850 ± 30 %	4700	B64290-L742-X65				
T35	3620 ± 25 %	6000	B64290-L742-X35				
T37	3920 ± 25 %	6500	B64290-L742-X37				
T38	6030 ± 30 %	10000	B64290-L742-X38				

■ Epoxy coating

R 13,3 × 8,30 × 5,00 (mm)
R 0,524 × 0,327 × 0,197 (inch)

Dimensions

d_a (mm)	d_i (mm)	Height (mm)	d_a (inch)	d_i (inch)	Height (inch)	
13,3 ± 0,3	8,3 ± 0,3	5,00 ± 0,15	0,524 ± 0,012	0,327 ± 0,012	0,197 ± 0,005	uncoated[1)]
14,4 max.	7,2 min.	5,95 max.	0,567 max.	0,283 min.	0,234 max.	coated

Characteristics and ordering codes

Material	A_L value nH	μ_i (approx.)	Ordering code	Magnetic characteristics			
				$\Sigma l/A$ mm^{-1}	l_e mm	A_e mm^2	V_e mm^3
N87	1040 ± 25 %	2200	B64290-L644-X87	2,67	32,70	12,27	401
N30	2030 ± 25 %	4300	B64290-L644-X830				
T65	2300 ± 30 %	4900	B64290-L644-X65				
T35	2830 ± 25 %	6000	B64290-L644-X35				
T37	3060 ± 25 %	6500	B64290-L644-X37				
T38	4700 ± 30 %	10000	B64290-L644-X38				

1) Upon request

■ Epoxy coating

R 14,0 × 9,00 × 5,00 (mm)
R 0,551 × 0,354 × 0,197 (inch)

Dimensions

d_a (mm)	d_i (mm)	Height (mm)	d_a (inch)	d_i (inch)	Height (inch)	
14,0 ± 0,3	9,0 ± 0,25	5,00 ± 0,2	0,551 ± 0,012	0,354 ± 0,012	0,197 ± 0,008	uncoated[1)]
15,1 max.	7,95 min.	6,0 max.	0,594 max.	0,313 min.	0,236 max.	coated

Characteristics and ordering codes

Material	A_L value nH	μ_i (approx.)	Ordering code	Magnetic characteristics			
				$\Sigma l/A$ mm^{-1}	l_e mm	A_e mm^2	V_e mm^3
N87	970 ± 25 %	2200	B64290-L658-X87	2,84	34,98	12,30	430
N30	1900 ± 25 %	4300	B64290-L658-X830				
T65	2300 ± 30 %	5200	B64290-L658-X65				
T35	2650 ± 25 %	6000	B64290-L658-X35				
T37	2880 ± 25 %	6500	B64290-L658-X37				
T38	4420 ± 30 %	10000	B64290-L658-X38				

■ Epoxy coating

R 15,0 × 10,4 × 5,30 (mm)
R 0,591 × 0,409 × 0,209 (inch)

Dimensions

d_a (mm)	d_i (mm)	Height (mm)	d_a (inch)	d_i (inch)	Height (inch)	
15,0 ± 0,5	10,4 ± 0,4	5,30 ± 0,3	0,591 ± 0,020	0,409 ± 0,016	0,209 ± 0,012	uncoated[1)]
16,3 max.	9,2 min.	6,4 max.	0,642 max.	0,362 min.	0,252 max.	coated

Characteristics and ordering codes

Material	A_L value nH	μ_i (approx.)	Ordering code	Magnetic characteristics			
				$\Sigma l/A$ mm^{-1}	l_e mm	A_e mm^2	V_e mm^3
N87	850 ± 25 %	2200	B64290-L623-X87	3,24	39,02	12,05	470
N30	1670 ± 25 %	4300	B64290-L623-X830				
T65	2020 ± 30 %	5200	B64290-L623-X65				
T35	2330 ± 25 %	6000	B64290-L623-X35				
T37	2520 ± 25 %	6500	B64290-L623-X37				
T38	3880 ± 30 %	10000	B64290-L623-X38				

1) Upon request

■ Epoxy coating

R 15,8 × 8,90 × 4,70 (mm)
R 0,622 × 0,350 × 0,185 (inch)

Dimensions

d_a (mm)	d_i (mm)	Height (mm)	d_a (inch)	d_i (inch)	Height (inch)	
15,8 ± 0,38	8,9 ± 0,25	4,70 ± 0,13	0,622 ± 0,015	0,350 ± 0,010	0,185 ± 0,005	uncoated[1)]
16,8 max.	8,05 min.	5,45 max.	0,661 max.	0,317 min.	0,215 max.	coated

Characteristics and ordering codes

Material	A_L value nH	μ_i (approx.)	Ordering code	Magnetic characteristics			
				$\Sigma l/A$ mm^{-1}	l_e mm	A_e mm^2	V_e mm^3
N87	1190 ± 25 %	2200	B64290-L743-X87	2,33	36,75	15,78	580
N30	2320 ± 25 %	4300	B64290-L743-X830				
T65	2800 ± 30 %	5200	B64290-L743-X65				
T35	3240 ± 25 %	6000	B64290-L743-X35				
T37	3500 ± 25 %	6500	B64290-L743-X37				
T38	5400 ± 30 %	10000	B64290-L743-X38				

■ Epoxy coating

R 16,0 × 9,60 × 6,30 (mm)
R 0,630 × 0,378 × 0,248 (inch)

Dimensions

d_a (mm)	d_i (mm)	Height (mm)	d_a (inch)	d_i (inch)	Height (inch)	
16,0 ± 0,4	9,6 ± 0,3	6,30 ± 0,2	0,630 ± 0,016	0,378 ± 0,012	0,248 ± 0,008	uncoated[1)]
17,2 max.	8,5 min.	7,3 max.	0,677 max.	0,335 min.	0,287 max.	coated

Characteristics and ordering codes

Material	A_L value nH	μ_i (approx.)	Ordering code	Magnetic characteristics			
				$\Sigma l/A$ mm^{-1}	l_e mm	A_e mm^2	V_e mm^3
N87	1420 ± 25 %	2200	B64290-L45-X87	1,95	38,52	19,73	760
N30	2770 ± 25 %	4300	B64290-L45-X830				
T65	3350 ± 30 %	5200	B64290-L45-X65				
T35	3870 ± 25 %	6000	B64290-L45-X35				
T37	4190 ± 25 %	6500	B64290-L45-X37				
T38	6440 ± 30 %	10000	B64290-L45-X38				

1) Upon request

■ Epoxy coating

R 17,0 × 10,7 × 6,80 (mm)
R 0,669 × 0,421 × 0,268 (inch)

Dimensions

d_a (mm)	d_i (mm)	Height (mm)	d_a (inch)	d_i (inch)	Height (inch)	
17,0 ± 0,4	10,7 ± 0,3	6,80 ± 0,2	0,669 ± 0,016	0,421 ± 0,012	0,268 ± 0,008	uncoated[1)]
18,2 max.	9,6 min.	7,8 max.	0,717 max.	0,378 min.	0,307 max.	coated

Characteristics and ordering codes

Material	A_L value nH	μ_i (approx.)	Ordering code	Magnetic characteristics			
				$\Sigma l/A$ mm^{-1}	l_e mm	A_e mm^2	V_e mm^3
N87	1390 ± 25 %	2200	B64290-L652-X87	2,00	42,00	21,04	884
N30	2710 ± 25 %	4300	B64290-L652-X830				
T65	3250 ± 30 %	5200	B64290-L652-X65				
T35	3770 ± 25 %	6000	B64290-L652-X35				
T37	4080 ± 25 %	6500	B64290-L652-X37				
T38	5700 ± 30 %	9000	B64290-L652-X38				

■ Epoxy coating

R 18,4 × 5,90 × 5,90 (mm)
R 0,724 × 0,232 × 0,232 (inch)

Dimensions

d_a (mm)	d_i (mm)	Height (mm)	d_a (inch)	d_i (inch)	Height (inch)	
18,4 ± 0,4	5,9 ± 0,3	5,90 ± 0,2	0,724 ± 0,016	0,232 ± 0,012	0,232 ± 0,008	uncoated[1)]
19,5 max.	4,8 min.	6,7 max.	0,768 max.	0,189 min.	0,264 max.	coated

Characteristics and ordering codes

Material	A_L value nH	μ_i (approx.)	Ordering code	Magnetic characteristics			
				$\Sigma l/A$ mm^{-1}	l_e mm	A_e mm^2	V_e mm^3
N87	2950 ± 25 %	2200	B64290-L697-X87	0,94	31,03	33,14	1029
N30	5770 ± 25 %	4300	B64290-L697-X830				
T65	6680 ± 30 %	5000	B64290-L697-X65				
T35	8020 ± 25 %	6000	B64290-L697-X35				
T37	8690 ± 25 %	6500	B64290-L697-X37				
T38	12000 ± 30 %	9000	B64290-L697-X38				

1) Upon request

■ Epoxy coating

R 20,0 × 10,0 × 7,00 (mm)
R 0,787 × 0,394 × 0,276 (inch)

Dimensions

d_a (mm)	d_i (mm)	Height (mm)	d_a (inch)	d_i (inch)	Height (inch)	
20,0 ± 0,4	10,0 ± 0,25	7,00 ± 0,4	0,787 ± 0,016	0,394 ± 0,010	0,276 ± 0,016	uncoated[1)]
21,2 max.	8,75 min.	8,1 max.	0,835 max.	0,344 min.	0,319 max.	coated

Characteristics and ordering codes

Material	A_L value nH	μ_i (approx.)	Ordering code	Magnetic characteristics			
				$\Sigma l/A$ mm^{-1}	l_e mm	A_e mm^2	V_e mm^3
N87	2130 ± 25 %	2200	B64290-L632-X87	1,30	43,55	33,63	1465
N30	4160 ± 25 %	4300	B64290-L632-X830				
T65	5050 ± 30 %	5200	B64290-L632-X65				
T35	5000 ± 25 %	5100	B64290-L632-X35				
T37	6280 ± 25 %	6500	B64290-L632-X37				
T38	8500 ± 30 %	8700	B64290-L632-X38				

■ Epoxy coating

R 22,1 × 13,7 × 6,35 (mm)
R 0,870 × 0,539 × 0,250 (inch)

Dimensions

d_a (mm)	d_i (mm)	Height (mm)	d_a (inch)	d_i (inch)	Height (inch)	
22,1 ± 0,4	13,7 ± 0,3	6,35 ± 0,3	0,870 ± 0,016	0,539 ± 0,012	0,250 ± 0,012	uncoated[1)]
23,3 max.	12,6 min.	7,4 max.	0,917 max.	0,496 min.	0,291 max.	coated

Characteristics and ordering codes

Material	A_L value nH	μ_i (approx.)	Ordering code	Magnetic characteristics			
				$\Sigma l/A$ mm^{-1}	l_e mm	A_e mm^2	V_e mm^3
N87	1340 ± 25 %	2200	B64290-L638-X87	2,07	54,15	26,17	1417
N30	2610 ± 25 %	4300	B64290-L638-X830				
T65	3160 ± 30 %	5200	B64290-L638-X65				
T35	3200 ± 25 %	5300	B64290-L638-X35				
T37	3950 ± 25 %	6500	B64290-L638-X37				
T38	5400 ± 30 %	8900	B64290-L638-X38				

1) Upon request

■ Epoxy coating

R 22,1 × 13,7 × 7,90 (mm)
R 0,870 × 0,539 × 0,311 (inch)

Dimensions

d_a (mm)	d_i (mm)	Height (mm)	d_a (inch)	d_i (inch)	Height (inch)	
22,1 ± 0,4	13,7 ± 0,3	7,90 ± 0,3	0,870 ± 0,016	0,539 ± 0,012	0,311 ± 0,012	uncoated[1)]
23,3 max.	12,6 min.	9,0 max.	0,917 max.	0,496 min.	0,354 max.	coated

Characteristics and ordering codes

Material	A_L value nH	μ_i (approx.)	Ordering code	Magnetic characteristics			
				$\Sigma l/A$ mm^{-1}	l_e mm	A_e mm^2	V_e mm^3
N87	1660 ± 25 %	2200	B64290-L719-X87	1,66	54,15	32,55	1763
N30	3250 ± 25 %	4300	B64290-L719-X830				
T65	3930 ± 30 %	5200	B64290-L719-X65				
T35	4000 ± 25 %	5300	B64290-L719-X35				
T37	4900 ± 25 %	6500	B64290-L719-X37				
T38	6500 ± 30 %	8600	B64290-L719-X38				

■ Epoxy coating

R 22,1 × 13,7 × 12,5 (mm)
R 0,870 × 0,539 × 0,492 (inch)

Dimensions

d_a (mm)	d_i (mm)	Height (mm)	d_a (inch)	d_i (inch)	Height (inch)	
22,1 ± 0,4	13,7 ± 0,3	12,5 ± 0,5	0,870 ± 0,016	0,539 ± 0,012	0,492 ± 0,020	uncoated[1)]
23,3 max.	12,6 min.	13,8 max.	0,917 max.	0,496 min.	0,543 max.	coated

Characteristics and ordering codes

Material	A_L value nH	μ_i (approx.)	Ordering code	Magnetic characteristics			
				$\Sigma l/A$ mm^{-1}	l_e mm	A_e mm^2	V_e mm^3
N87	2630 ± 25 %	2200	B64290-L651-X87	1,05	54,15	51,15	2789
N30	5140 ± 25 %	4300	B64290-L651-X830				
T65	6200 ± 30 %	5200	B64290-L651-X65				
T35	6000 ± 25 %	5000	B64290-L651-X35				
T37	7770 ± 25 %	6500	B64290-L651-X37				
T38	10000 ± 30 %	8400	B64290-L651-X38				

1) Upon request

■ Epoxy coating

R 22,6 × 14,7 × 9,20 (mm)
R 0,890 × 0,579 × 0,362 (inch)

Dimensions

d_a (mm)	d_i (mm)	Height (mm)	d_a (inch)	d_i (inch)	Height (inch)	
22,6 ± 0,4	14,7 ± 0,2	9,20 ± 0,2	0,890 ± 0,016	0,579 ± 0,008	0,362 ± 0,008	uncoated[1)]
23,8 max.	13,7 min.	10,2 max.	0,937 max.	0,539 min.	0,402 max.	coated

Characteristics and ordering codes

Material	A_L value nH	μ_i (approx.)	Ordering code	Magnetic characteristics			
				$\Sigma l/A$ mm^{-1}	l_e mm	A_e mm^2	V_e mm^3
N87	1740 ± 25 %	2200	B64290-L626-X87	1,59	56,82	35,78	2033
N30	3420 ± 25 %	4300	B64290-L626-X830				
T65	4100 ± 30 %	5200	B64290-L626-X65				
T35	4200 ± 25 %	5300	B64290-L626-X35				
T37	5170 ± 25 %	6500	B64290-L626-X37				
T38	6700 ± 30 %	8500	B64290-L626-X38				

■ Epoxy coating

R 25,3 × 14,8 × 10,0 (mm)
R 0,996 × 0,583 × 0,394 (inch)

Dimensions

d_a (mm)	d_i (mm)	Height (mm)	d_a (inch)	d_i (inch)	Height (inch)	
25,3 ± 0,7	14,8 ± 0,5	10,0 ± 0,2	0,996 ± 0,028	0,583 ± 0,020	0,394 ± 0,008	uncoated[1)]
26,8 max.	13,5 min.	11,0 max.	1,043 max.	0,531 min.	0,433 max.	coated

Characteristics and ordering codes

Material	A_L value nH	μ_i (approx.)	Ordering code	Magnetic characteristics			
				$\Sigma l/A$ mm^{-1}	l_e mm	A_e mm^2	V_e mm^3
N87	2360 ± 25 %	2200	B64290-L618-X87	1,17	60,07	51,26	3079
N30	4620 ± 25 %	4300	B64290-L618-X830				
T65	5350 ± 30 %	5000	B64290-L618-X65				
T35	5400 ± 25 %	5000	B64290-L618-X35				
T37	6970 ± 25 %	6500	B64290-L618-X37				
T38	9100 ± 30 %	8500	B64290-L618-X38				

1) Upon request

■ Epoxy coating

R 25,3 × 14,8 × 20,0 (mm)
R 0,996 × 0,583 × 0,787 (inch)

Dimensions

d_a (mm)	d_i (mm)	Height (mm)	d_a (inch)	d_i (inch)	Height (inch)	
25,3 ± 0,7	14,8 ± 0,5	20,0 ± 0,5	0,996 ± 0,028	0,583 ± 0,020	0,787 ± 0,020	uncoated[1)]
26,8 max.	13,5 min.	21,3 max.	1,043 max.	0,531 min.	0,839 max.	coated

Characteristics and ordering codes

Material	A_L value nH	μ_i (approx.)	Ordering code	Magnetic characteristics			
				$\Sigma l/A$ mm^{-1}	l_e mm	A_e mm^2	V_e mm^3
N87	4680 ± 25 %	2200	B64290-L616-X87	0,59	60,07	102,5	6157
N30	9160 ± 25 %	4300	B64290-L616-X830				
T65	10600 ± 30 %	5000	B64290-L616-X65				
T35	10700 ± 25 %	5000	B64290-L616-X35				
T37	13800 ± 25 %	6400	B64290-L616-X37				
T38	18000 ± 30 %	8400	B64290-L616-X38				

■ Epoxy coating
■ With chamfer

R 29,5 × 19,0 × 14,9 (mm)
R 1,142 × 0,748 × 0,587 (inch)

Dimensions

d_a (mm)	d_i (mm)	Height (mm)	d_a (inch)	d_i (inch)	Height (inch)	
29,5 ± 0,7	19,0 ± 0,5	14,9 ± 0,4	1,142 ± 0,028	0,748 ± 0,020	0,587 ± 0,016	uncoated[1)]
31,0 max.	17,7 min.	16,1 max.	1,220 max.	0,697 min.	0,634 max.	coated

Characteristics and ordering codes

Material	A_L value nH	μ_i (approx.)	Ordering code	Magnetic characteristics			
				$\Sigma l/A$ mm^{-1}	l_e mm	A_e mm^2	V_e mm^3
N87	2880 ± 25 %	2200	B64290-L647-X87	0,96	73,78	76,98	5680
N30	5630 ± 25 %	4300	B64290-L647-X830				
T65	6800 ± 30 %	5200	B64290-L647-X65				
T37	8500 ± 25 %	6500	B64290-L647-X37				
T38	10500 ± 30 %	8000	B64290-L647-X38				

1) Upon request

■ Epoxy coating
■ With chamfer

R 30,5 × 20,0 × 12,5 (mm)
R 1,201 × 0,787 × 0,492 (inch)

Dimensions

d_a (mm)	d_i (mm)	Height (mm)	d_a (inch)	d_i (inch)	Height (inch)	
30,5 ± 1,0	20,0 ± 0,6	12,5 ± 0,4	1,201 ± 0,039	0,787 ± 0,024	0,492 ± 0,016	uncoated[1)]
32,3 max.	18,2 min.	13,7 max.	1,272 max.	0,717 min.	0,539 max.	coated

Characteristics and ordering codes

Material	A_L value nH	μ_i (approx.)	Ordering code	Magnetic characteristics			
				$\Sigma l/A$ mm^{-1}	l_e mm	A_e mm^2	V_e mm^3
N87	2320 ± 25 %	2200	B64290-L657-X87	1,19	77,02	64,66	4980
N30	4540 ± 25 %	4300	B64290-L657-X830				
T65	5400 ± 30 %	5100	B64290-L657-X65				
T37	6400 ± 25 %	6100	B64290-L657-X37				
T38	8400 ± 30 %	8000	B64290-L657-X38				

■ Epoxy coating
■ With chamfer

R 34,0 × 20,5 × 10,0 (mm)
R 1,339 × 0,807 × 0,394 (inch)

Dimensions

d_a (mm)	d_i (mm)	Height (mm)	d_a (inch)	d_i (inch)	Height (inch)	
34,0 ± 0,7	20,5 ± 0,5	10,0 ± 0,3	1,339 ± 0,028	0,807 ± 0,020	0,394 ± 0,012	uncoated[1)]
35,5 max.	19,2 min.	11,1 max.	1,398 max.	0,756 min.	0,437 max.	coated

Characteristics and ordering codes

Material	A_L value nH	μ_i (approx.)	Ordering code	Magnetic characteristics			
				$\Sigma l/A$ mm^{-1}	l_e mm	A_e mm^2	V_e mm^3
N87	2230 ± 25 %	2200	B64290-L58-X87	1,24	82,06	66,08	5423
N30	4360 ± 25 %	4300	B64290-L58-X830				
T65	5100 ± 30 %	5000	B64290-L58-X65				
T37	6100 ± 25 %	6000	B64290-L58-X37				
T38	8100 ± 30 %	8000	B64290-L58-X38				

1) Upon request

■ Epoxy coating
■ With chamfer

R 34,0 × 20,5 × 12,5 (mm)
R 1,339 × 0,807 × 0,492 (inch)

Dimensions

d_a (mm)	d_i (mm)	Height (mm)	d_a (inch)	d_i (inch)	Height (inch)	
34,0 ± 0,7	20,5 ± 0,5	12,5 ± 0,3	1,339 ± 0,028	0,807 ± 0,020	0,492 ± 0,012	uncoated[1)]
35,5 max.	19,2 min.	13,6 max.	1,398 max.	0,756 min.	0,535 max.	coated

Characteristics and ordering codes

Material	A_L value nH	μ_i (approx.)	Ordering code	Magnetic characteristics			
				$\Sigma l/A$ mm^{-1}	l_e mm	A_e mm^2	V_e mm^3
N87	2790 ± 25 %	2200	B64290-L48-X87	0,99	82,06	82,60	6778
N30	5460 ± 25 %	4300	B64290-L48-X830				
T65	6400 ± 30 %	5000	B64290-L48-X65				
T37	7600 ± 25 %	6000	B64290-L48-X37				
T38	10100 ± 30 %	8000	B64290-L48-X38				

■ Epoxy coating
■ With chamfer

R 36,0 × 23,0 × 15,0 (mm)
R 1,417 × 0,906 × 0,591 (inch)

Dimensions

d_a (mm)	d_i (mm)	Height (mm)	d_a (inch)	d_i (inch)	Height (inch)	
36,0 ± 0,7	23,0 ± 0,5	15,0 ± 0,4	1,417 ± 0,028	0,906 ± 0,020	0,591 ± 0,016	uncoated[1)]
37,5 max.	21,7 min.	16,2 max.	1,476 max.	0,854 min.	0,638 max.	coated

Characteristics and ordering codes

Material	A_L value nH	μ_i (approx.)	Ordering code	Magnetic characteristics			
				$\Sigma l/A$ mm^{-1}	l_e mm	A_e mm^2	V_e mm^3
N87	2940 ± 25 %	2200	B64290-L674-X87	0,94	89,65	95,89	8597
N30	5750 ± 25 %	4300	B64290-L674-X830				
T65	6700 ± 30 %	5000	B64290-L674-X65				
T37	8000 ± 25 %	6000	B64290-L674-X37				
T38	9400 ± 30 %	7000	B64290-L674-X38				

1) Upon request

■ Epoxy coating
■ With chamfer

R 38,1 × 19,05 × 12,7 (mm)
R 1,500 × 0,750 × 0,500 (inch)

Dimensions

d_a (mm)	d_i (mm)	Height (mm)	d_a (inch)	d_i (inch)	Height (inch)	
38,1 ± 0,5	19,05 ± 0,4	12,7 ± 0,3	1,500 ± 0,020	0,750 ± 0,016	0,500 ± 0,012	uncoated[1)]
39,2 max.	18,05 min.	13,6 max.	1,543 max.	0,711 min.	0,535 max.	coated

Characteristics and ordering codes

Material	A_L value nH	μ_i (approx.)	Ordering code	Magnetic characteristics			
				$\Sigma l/A$ mm^{-1}	l_e mm	A_e mm^2	V_e mm^3
N87	3870 ± 25 %	2200	B64290-L668-X87	0,71	82,97	116,2	9644
N30	7570 ± 25 %	4300	B64290-L668-X830				
T65	8800 ± 30 %	5000	B64290-L668-X65				
T37	10500 ± 25 %	6000	B64290-L668-X37				
T38	12300 ± 30 %	7000	B64290-L668-X38				

■ Epoxy coating
■ With chamfer

R 40,0 × 24,0 × 16,0 (mm)
R 1,575 × 0,945 × 0,630 (inch)

Dimensions

d_a (mm)	d_i (mm)	Height (mm)	d_a (inch)	d_i (inch)	Height (inch)	
40,0 ± 1,0	24,0 ± 0,7	16,0 ± 0,4	1,575 ± 0,039	0,945 ± 0,028	0,630 ± 0,016	uncoated[1)]
41,8 max.	22,5 min.	17,2 max.	1,646 max.	0,886 min.	0,677 max.	coated

Characteristics and ordering codes

Material	A_L value nH	μ_i (approx.)	Ordering code	Magnetic characteristics			
				$\Sigma l/A$ mm^{-1}	l_e mm	A_e mm^2	V_e mm^3
N87	3590 ± 25 %	2200	B64290-L659-X87	0,77	96,29	125,3	12070
N30	7000 ± 25 %	4300	B64290-L659-X830				
T65	8200 ± 30 %	5000	B64290-L659-X65				
T37	9800 ± 25 %	6000	B64290-L659-X37				

1) Upon request

■ Epoxy coating
■ With chamfer

R 41,8 × 26,2 × 12,5 (mm)
R 1,646 × 1,031 × 0,492 (inch)

Dimensions

d_a (mm)	d_i (mm)	Height (mm)	d_a (inch)	d_i (inch)	Height (inch)	
41,8 ± 1,0	26,2 ± 0,6	12,5 ± 0,3	1,646 ± 0,039	1,031 ± 0,024	0,492 ± 0,012	uncoated[1)]
43,6 max.	24,8 min.	13,6 max.	1,717 max.	0,976 min.	0,535 max.	coated

Characteristics and ordering codes

Material	A_L value nH	μ_i (approx.)	Ordering code	Magnetic characteristics			
				$\Sigma l/A$ mm^{-1}	l_e mm	A_e mm^2	V_e mm^3
N87	2560 ± 25 %	2200	B64290-L22-X87	1,08	103,0	95,75	9862
N30	5000 ± 25 %	4300	B64290-L22-X830				
T65	5800 ± 30 %	5000	B64290-L22-X65				
T37	7000 ± 25 %	6000	B64290-L22-X37				

■ Epoxy coating
■ With chamfer

R 50,0 × 30,0 × 20,0 (mm)
R 1,969 × 1,181 × 0,787 (inch)

Dimensions

d_a (mm)	d_i (mm)	Height (mm)	d_a (inch)	d_i (inch)	Height (inch)	
50,0 ± 1,0	30,0 ± 0,7	20,0 ± 0,5	1,969 ± 0,039	1,181 ± 0,028	0,787 ± 0,020	uncoated[1)]
51,8 max.	28,5 min.	21,3 max.	2,039 max.	1,122 min.	0,839 max.	coated

Characteristics and ordering codes

Material	A_L value nH	μ_i (approx.)	Ordering code	Magnetic characteristics			
				$\Sigma l/A$ mm^{-1}	l_e mm	A_e mm^2	V_e mm^3
N87	4460 ± 25 %	2200	B64290-L82-X87	0,62	120,4	195,7	23560
N30	8700 ± 25 %	4300	B64290-L82-X830				
T65	10000 ± 30 %	4900	B64290-L82-X65				
T37	12000 ± 25 %	6000	B64290-L82-X37				

1) Upon request

■ Epoxy coating
■ With chamfer

R 58,3 × 40,8 × 17,6 (mm)
R 2,283 × 1,606 × 0,693 (inch)

Dimensions

d_a (mm)	d_i (mm)	Height (mm)	d_a (inch)	d_i (inch)	Height (inch)	
58,3 ± 1,0	40,8 ± 0,8	17,6 ± 0,4	2,283 ± 0,039	1,606 ± 0,031	0,693 ± 0,016	uncoated[1)]
60,1 max.	39,2 min.	18,8 max.	2,366 max.	1,543 min.	0,740 max.	coated

Characteristics and ordering codes

Material	A_L value nH	μ_i (approx.)	Ordering code	Magnetic characteristics			
				$\Sigma l/A$ mm^{-1}	l_e mm	A_e mm^2	V_e mm^3
N87	2760 ± 25 %	2200	B64290-L40-X87	1,00	152,4	152,4	23230
N30	5400 ± 25 %	4300	B64290-L40-X830				
T65	6250 ± 30 %	5000	B64290-L40-X65				
T37	7160 ± 25 %	5700	B64290-L40-X37				

■ Epoxy coating
■ With chamfer

R 63,0 × 38,0 × 25,0 (mm)
R 2,480 × 1,496 × 0,984 (inch)

Dimensions

d_a (mm)	d_i (mm)	Height (mm)	d_a (inch)	d_i (inch)	Height (inch)	
63,0 ± 1,5	38,0 ± 1,2	25,0 ± 0,8	2,480 ± 0,059	1,496 ± 0,047	0,984 ± 0,031	uncoated[1)]
65,3 max.	36,0 min.	26,6 max.	2,571 max.	1,417 min.	1,047 max.	coated

Characteristics and ordering codes

Material	A_L value nH	μ_i (approx.)	Ordering code	Magnetic characteristics			
				$\Sigma l/A$ mm^{-1}	l_e mm	A_e mm^2	V_e mm^3
N87	5000 ± 25 %	2200	B64290-L699-X87	0,50	152,1	305,9	46530
N30	10800 ± 25 %	4300	B64290-L699-X830				
T65	12600 ± 30 %	5000	B64290-L699-X65				
T37	13900 ± 25 %	5500	B64290-L699-X37				

1) Upon request

■ Epoxy coating

R 68,0 × 48,0 × 13,0 (mm)
R 2,677 × 1,890 × 0,512 (inch)

Dimensions

d_a (mm)	d_i (mm)	Height (mm)	d_a (inch)	d_i (inch)	Height (inch)	
68,0 ± 1,2	48,0 ± 1,0	13,0 ± 0,4	2,677 ± 0,047	1,890 ± 0,039	0,512 ± 0,015	uncoated[1)]
60,1 max.	46,2 min.	14,2 max.	2,756 max.	1,819 min.	0,559 max.	coated

Characteristics and ordering codes

Material	A_L value nH	μ_i (approx.)	Ordering code	Magnetic characteristics			
				$\Sigma l/A$ mm^{-1}	l_e mm	A_e mm^2	V_e mm^3
N87	1990 ± 25 %	2200	B64290-L696-X87	1,39	178,6	128,7	22980
N30	3890 ± 25 %	4300	B64290-L696-X830				
T65	4500 ± 30 %	5000	B64290-L696-X65				
T37	5000 ± 25 %	5500	B64290-L696-X37				

■ Epoxy coating
■ With chamfer

R 87,0 × 54,3 × 13,5 (mm)
R 3,425 × 2,138 × 0,531 (inch)

Dimensions

d_a (mm)	d_i (mm)	Height (mm)	d_a (inch)	d_i (inch)	Height (inch)	
87,0 ± 1,5	54,3 ± 1,1	13,5 ± 0,3	3,425 ± 0,059	2,138 ± 0,043	0,531 ± 0,012	uncoated[1)]
89,3 max.	52,4 min.	14,8 max.	3,516 max.	2,063 min.	0,583 max.	coated

Characteristics and ordering codes

Material	A_L value nH	μ_i (approx.)	Ordering code	Magnetic characteristics			
				$\Sigma l/A$ mm^{-1}	l_e mm	A_e mm^2	V_e mm^3
N87	2790 ± 25 %	2200	B64290-L730-X87	0,99	213,9	216,7	46360
N30	5400 ± 25 %	4300	B64290-L730-X830				
T37	7000 ± 25 %	5500	B64290-L730-X37				

1) Upon request

■ Epoxy coating

R 102 × 65,8 × 15,0 (mm)
R 4,016 × 2,591 × 0,591 (inch)

Dimensions

d_a (mm)	d_i (mm)	Height (mm)	d_a (inch)	d_i (inch)	Height (inch)	
102,0 ± 2,0	65,8 ± 1,3	15,0 ± 0,5	4,016 ± 0,079	2,591 ± 0,051	0,591 ± 0,020	uncoated[1)]
104,8 max.	63,7 min.	16,3 max.	4,126 max.	2,508 min.	0,642 max.	coated

Characteristics and ordering codes

Material	A_L value nH	μ_i (approx.)	Ordering code	Magnetic characteristics			
				$\Sigma l/A$ mm^{-1}	l_e mm	A_e mm^2	V_e mm^3
N87	2880 ± 25 %	2200	B64290-L84-X87	0,96	255,3	267,2	68220
N30	5500 ± 25 %	4200	B64290-L84-X830				

■ Without coating

R 140 × 103 × 25,0 (mm)
R 5,512 × 4,055 × 0,984 (inch)

Dimensions

d_a (mm)	d_i (mm)	Height (mm)	d_a (inch)	d_i (inch)	Height (inch)	
140,0 ± 3,0	103 ± 2,0	25,0 ± 1,0	5,512 ± 0,118	4,055 ± 0,079	0,984 ± 0,039	uncoated
143,8 max.	100,2 min.	26,8 max.	5,661 max.	3,945 min.	1,055 max.	coated[1)]

Characteristics and ordering codes

Material	A_L value nH	μ_i (approx.)	Ordering code	Magnetic characteristics			
				$\Sigma l/A$ mm^{-1}	l_e mm	A_e mm^2	V_e mm^3
N30	6200 ± 25 %	4000	B64290-A705-X830	0,82	375,8	458,9	172440

1) Upon request

■ Without coating

R 202,0 × 153 × 25,0 (mm)
R 7,953 × 6,024 × 0,984 (inch)

Dimensions

d_a (mm)	d_i (mm)	Height (mm)	d_a (inch)	d_i (inch)	Height (inch)	
202,0 ± 4,0	153,0 ± 3,0	25,0 ± 1,0	7,953 ± 0,157	6,024 ± 0,118	0,984 ± 0,039	uncoated
206,8 max.	149,2 min.	26,8 max.	8,142 max.	5,874 min.	1,055 max.	coated 1)

Characteristics and ordering codes

Material	A_L value nH	μ_i (approx.)	Ordering code	Magnetic characteristics			
				$\Sigma l/A$ mm^{-1}	l_e mm	A_e mm^2	V_e mm^3
N30	5200 ± 25 %	3700	B64290-A711-X830	0,90	550,5	608,6	335030

1) Upon request

Primarily used for broadband transformers up to high frequencies

Application examples

- SIFERRIT material N30 for low frequencies and for pulse applications
- SIFERRIT material K1 for matching transformers and baluns up to about 250 MHz in antenna feeders or in input circuits of VHF and TV receivers

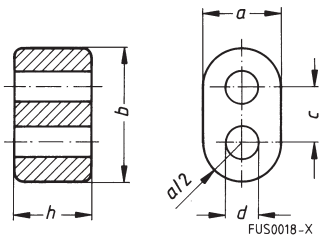

Dimensions[1]					Magnetic characteristics				Weight
h (mm)	*b* (mm)	*a* (mm)	*c* (mm)	*d* (mm)	$\Sigma l/A$[3] mm^{-1}	l_e[3] mm	A_e[3] mm^2	V_e[3] mm^3	g
14,5 – 1,0	14,50 – 1,0	8,5 – 0,5	5,85 ± 0,25	3,4 + 0,80	0,31	15,3	49,7	760	4,0
8,3 – 0,6	14,50 – 1,0	8,5 – 0,5	5,85 ± 0,25	3,4 + 0,60	0,54	15,3	28,4	435	2,5
6,2 – 0,5	7,25 – 0,5	4,2 – 0,4	2,90 ± 0,15	1,7 + 0,30	0,75	7,6	10,2	78	0,4
2,5 – 0,2	3,60 – 0,3	2,1 – 0,3	1,45 ± 0,10	0,8 + 0,15	1,78	3,7	2,1	7,8	0,1
2,0 – 0,2	3,60 – 0,3	2,1 – 0,3	1,45 ± 0,10	0,8 + 0,15	2,20	3,7	1,7	6,3	0,1

Overview of available types

Core height *h* (mm)	Material	A_L value[3] nH (Tol. ± 30 %)	Ordering code[4]
14,5 – 1,0[2]	K1	330	B62152-A1-X1
8,3 – 0,6[2]	K1	190	B62152-A4-X1
	N30	10000	B62152-A4-X30
6,2 – 0,5[2]	K1	140	B62152-A7-X1
	N30	7300	B62152-A7-X30
2,5 – 0,2	K1	60	B62152-A8-X1
	N30	3100	B62152-A8-X30
	M13	1440[5]	B62152-A8-X13
2,0 – 0,2	K1	42	B62152-A27-X1
	N30	2400	B62152-A27-X30
	M13	1100[5]	B62152-A27-X13

1) Cores made of NiZn ferrite may exceed the specified dimensions by up to 5 %.
2) In accordance with DIN 41279, shape G.
3) Magnetic characteristics and A_L value are based on winding of center leg.
4) Double-aperture cores are available with parylene coating on request. In this case the thickness of the coating is approx. 10 to 15 µm. Ordering code for coated version: B62152-P…
5) Preliminary A_L value

Ferrite Polymer Composites

General Information

Ferrite cores are familiar as brittle, rigid and bulky components for high-inductance coils and transformers. The performance of such ferrites depends very much on external influences such as temperature, pressure, electromagnetic fields and frequency.

FPC is a homogeneous mixture of ferrite powder and plastic with outstanding mechanical and magnetic properties. This rugged material can be processed into injection-molded parts or thin, flexible film to open up innovative applications.

The new C351 film is suitable for high-temperature applications up to 200 °C and is UL 94-V0-listed. It is also available with copper coatings of 35 to 75 µm and in various thicknesses from 0,2 to 0,4 mm. FPC film of materials C350 and C351 can also be supplied in self-adhesive versions.

FPC film is ideal for EMC applications, e.g. to shield coils against metals or absorb interference at frequencies of 500 MHz and higher. It opens up many other applications, such as implementation of low-profile coils for identification systems and electronic article surveillance in retailing and logistics, for sensors or contactless smart cards. FPC can also be used for compensation of deflection yoke coils in TV picture tubes and computer monitors. This innovative material is also suitable as spacing between ferrite cores – instead of air gaps or non-magnetic films – to suppress leakage fields, for instance, or to adjust the biasing curve.

Basic features

- Composite material of polymer and ferrite for injection molded parts
- Minor influence of temperature
- High dc magnetic bias capability
- Suitable for a wide frequency range
- High electrical resistance

Technical benefits

- High mechanical stability
- Excellent dimensional stability
- Manufacturing technique: injection molding
  → production of any core shape possible
- Distributed air gap → low winding losses

Applications

- Inductive proximity switches
- Identification systems, e.g. immobilizer in automobiles
- Non-contact power transmission
- Resonance inductors for DC/DC converters

Core shapes on request

Physical properties

Material	Symbol	Unit	C302
Initial permeability; f = 1 MHz	μ_i		17 ± 20 %
Flux density (near saturation) H = 25 kA/m; f = 10 kHz	B_S (25 °C)	mT	330
Remanent flux density H = 25 kA/m; f = 10 kHz	B_r (25 °C)	mT	15
Coercive field strength H = 25 kA/m; f = 10 kHz	H_C (25 °C)	A/m	770
Relative loss factor f = 1 MHz f = 100 MHz	$\tan\delta/\mu_i$		 < 0,0004 < 0,03
Hysteresis material constant	η_B	10^{-3}/mT	< 0,25
Temperature coefficient	$\alpha = \Delta\mu/\mu\Delta T$	1/K	< 0,0002
Density		kg/m^3	3500
Resistivity f = 10 kHz f = 10 MHz	ρ	Ωm	 21 13
Dielectric constant f = 10 kHz f = 10 MHz	ε_r		 280 100
Max. operating temperature	T_{max}	°C	180

Basic features

- FPC is a composite material of polymer and ferrite
- FPC film is a thin, mechanically flexible film

Technical benefits

- Stable magnetic characteristics
- Low weight: FPC film is 40% lower in density than ferrite
- High mechanical strength
- Shaping as required: customer-specific solutions possible
- Economy: easy transport and storage,
  simple, rationalized processing, low mounting volume
- C351 film suitable for high-temperature applications (up to 200 °C)
- Material C351 approved to UL 94-V0 (E 140 693)
- Various film thickness (from 0,2 to 0,4 mm)
- Self-adhesive versions
- C351 film with optional copper coatings 35 to 75 µm thick

Applications

- Implementation of low-profile coils, e.g. for
  – identification systems
  – security tags for electronic article surveillance
  – sensors
  – inductive reading of smart cards
- Electromagnetic shielding of coils from metals to prevent interference
- EMC: absorption of radiated emissions at frequencies ≥ 500 MHz
- Compensation of deflection yokes to correct distortion at the corners of TV screens and monitors
- Spacing between ferrite cores (as a substitute for air gaps or non-magnetic films) for
  – suppression of the leakage field
  – adjustment of the biasing curve

Ordering details

The ordering codes are structured as follows:

1st group Design	2nd group Film thickness/width		3rd group Copper coating[1]/material	
B68450: Film on reel	A: 0,2 mm B: 0,3 mm	0080: 80 mm	X: Default letter	350 351
B68451: Film on reel, self-adhesive	C: 0,4 mm			
B68452: Film on reel, copper-coated (only in combination with C351!)			A: 35 µm B: 50 µm C: 75 µm	351

Material	Thickness (mm)	Extra features	Ordering code
C350	0,2		B68450-A0080-X350
C351	0,2		B68450-A0080-X351
C350 C350	0,2 0,2	self-adhesive	B68451-A0080-X350 B68451-A0080-X350
C351 C351	0,3 0,3	self-adhesive	B68451-B0080-X351 B68451-B0080-X351
C351 C351	0,2 0,2	copper-coated	B68452-A0080-X351 B68452-A0080-X351

FPC film is supplied in units of 50 m length.

1) Copper coating only in combination with C351.

Physical properties (material values defined on 0,2 mm thick film)

Material	Symbol	Unit	C350	C351[3]
Initial permeability[1] f = 1 MHz	μ_i		9 ± 20 %	9 ± 20 %
Flux density (near saturation)[1] H = 25 kA/m f = 10 kHz	B_S	mT	255	255
Remanent flux density[1] H = 25 kA/m f = 10 kHz	B_r	mT	9	9
Coercive field strength[1] H = 25 kA/m f = 10 kHz	H_C	A/m	600	600
Relative loss factor[1] f = 10 MHz f = 1 GHz	$\tan\delta/\mu_i$		 < 0,005 < 0,400	 < 0,005 < 0,400
Hysteresis material constant	η_B	10^{-3}/mT	< 2	< 2
Temperature coefficient[1]	$\alpha = \Delta\mu/\mu\Delta T$	1/K	$< 5 \cdot 10^{-5}$	$< 5 \cdot 10^{-5}$
Density		kg/m^3	2930	2930
Resistivity[1] f = 1 kHz f = 10 MHz	ρ	Ωm	 500 100	 500 100
Dielectric constant[1] f = 1 kHz f = 10 MHz	ε_r		 700 21	 700 21
Dielectric strength		kV/mm	1	0,8
Max. operating temperature	T_{max}	°C	120	200
Tensile strength[2]	σ_Z	N/mm^2	1,5	2,5
Tearing resistance[2]		%	25	25
Compressibility[2]	κ	N/mm^2	70	70

1) T = 25 °C in accordance with IEC 51 (CO) 282
2) T = 23 °C and 50 % r.h.
3) UL 94, flame class V0 (listed E 140 693)

Symbol	Meaning	Unit
A	Cross section of coil	mm^2
A_e	Effective magnetic cross section	mm^2
A_L	Inductance factor; $A_L = L/N^2$	nH
A_{L1}	Minimum inductance at defined high saturation ($\triangleq \mu_a$)	nH
A_{min}	Minimum core cross section	mm^2
A_N	Winding cross section	mm^2
A_R	Resistance factor; $A_R = R_{Cu}/N^2$	$\mu\Omega = 10^{-6}\ \Omega$
B	RMS value of magnetic flux density	Vs/m^2, mT
ΔB	Flux density deviation	Vs/m^2, mT
$\hat{B}$	Peak value of magnetic flux density	Vs/m^2, mT
$\Delta\hat{B}$	Peak value of flux density deviation	Vs/m^2, mT
$B_{\_}$	DC magnetic flux density	Vs/m^2, mT
B_R	Remanent flux density	Vs/m^2, mT
B_S	Saturation magnetization	Vs/m^2, mT
C_0	Winding capacitance	F = As/V
CDF	Core distortion factor	$mm^{-4,5}$
DF	Relative disaccommodation coefficient $DF = d/\mu_i$	
d	Disaccommodation coefficient	
E_a	Activation energy	J
f	Frequency	s^{-1}, Hz
f_{cutoff}	Cut-off frequency	s^{-1}, Hz
f_{max}	Upper frequency limit	s^{-1}, Hz
f_{min}	Lower frequency limit	s^{-1}, Hz
f_r	Resonance frequency	s^{-1}, Hz
f_{Cu}	Copper filling factor	
g	Air gap	mm
H	RMS value of magnetic field strength	A/m
$\hat{H}$	Peak value of magnetic field strength	A/m
$H_{\_}$	DC field strength	A/m
H_c	Coercive field strength	A/m
h	Hysteresis coefficient of material	10^{-6} cm/A
$h/\mu_i{}^2$	Relative hysteresis coefficient	10^{-6} cm/A
I	RMS value of current	A
$I_{\_}$	Direct current	A
$\hat{I}$	Peak value of current	A
J	Polarization	Vs/m^2
k	Boltzmann constant	J/K
k_3	Third harmonic distortion	
k_{3c}	Circuit third harmonic distortion	
L	Inductance	H = Vs/A

Symbol	Meaning	Unit
$\Delta L/L$	Relative inductance change	H
L_0	Inductance of coil without core	H
L_H	Main inductance	H
L_p	Parallel inductance	H
L_{rev}	Reversible inductance	H
L_s	Series inductance	H
l_e	Effective magnetic path length	mm
l_N	Average length of turn	mm
N	Number of turns	
P_{Cu}	Copper (winding) losses	W
P_{trans}	Transferrable power	W
P_V	Relative core losses	mW/g
PF	Performance factor	
Q	Quality factor ($Q = \omega L/R_s = 1/\tan \delta_L$)	
R	Resistance	Ω
R_{Cu}	Copper (winding) resistance ($f = 0$)	Ω
R_h	Hysteresis loss resistance of a core	Ω
ΔR_h	R_h change	Ω
R_i	Internal resistance	Ω
R_p	Parallel loss resistance of a core	Ω
R_s	Series loss resistance of a core	Ω
R_{th}	Thermal resistance	K/W
R_V	Effective loss resistance of a core	Ω
s	Total air gap	mm
T	Temperature	°C
ΔT	Temperature difference	K
T_C	Curie temperature	°C
t	Time	s
t_v	Pulse duty factor	
$\tan \delta$	Loss factor	
$\tan \delta_L$	Loss factor of coil	
$\tan \delta_r$	(Residual) loss factor at $H \rightarrow 0$	
$\tan \delta_e$	Relative loss factor	
$\tan \delta_h$	Hysteresis loss factor	
$\tan \delta/\mu_i$	Relative loss factor of material at $H \rightarrow 0$	
U	RMS value of voltage	V
$\hat{U}$	Peak value of voltage	V
V_e	Effective magnetic volume	mm^3
Z	Complex impedance	Ω
Z_n	Normalized impedance $\lvert Z\rvert_n = \lvert Z\rvert /N^2 \times \varepsilon\ (l_e/A_e)$	Ω/mm

Symbols and Terms

Symbol	Meaning		Unit
α	Temperature coefficient (*TK*)		1/K
α_F	Relative temperature coefficient of material		1/K
α_e	Temperature coefficient of effective permeability		1/K
ε_r	Relative dielectric constant		
Φ	Magnetic flux		Vs
η	Efficiency of a transformer		
η_B	Hysteresis material constant		mT^{-1}
η_i	Hysteresis core constant		$A^{-1}H^{-1/2}$
λ_s	Magnetostriction at saturation magnetization		
μ	Relative complex permeability		
μ_0	Magnetic field constant		Vs/Am
μ_a	Relative amplitude permeability		
μ_{app}	Relative apparent permeability		
μ_e	Relative effective permeability	for series components	Ωm^{-1}
μ_i	Relative initial permeability		mm^{-1}
μ'_p	Relative real (inductive) component of $\overline{\mu}$		s
μ''_p	Relative imaginary (loss) component of $\overline{\mu}$		s^{-1}
μ_r	Relative permeability	for parallel components	
μ_{rev}	Relative reversible permeability		
μ'_s	Relative real (inductive) component of $\overline{\mu}$		
μ''_s	Relative imaginary (loss) component of $\overline{\mu}$		
μ_{tot}	Relative total permeability derived from the static magnetization curve		
ρ	Resistivity		
$\Sigma l/A$	Magnetic form factor		
τ_{Cu}	DC time constant $\tau_{Cu} = L/R_{Cu} = A_L/A_R$		
ω	Angular frequency; $\omega = 2\,\Pi f$		

The commas used in numerical values denote decimal points.

All dimensions are given in mm.

SMD Surface-mount device

Ordering code structure

1 RM, P, TT/PR, EP, ER9,5, ER11 cores

(Example here RM 4)

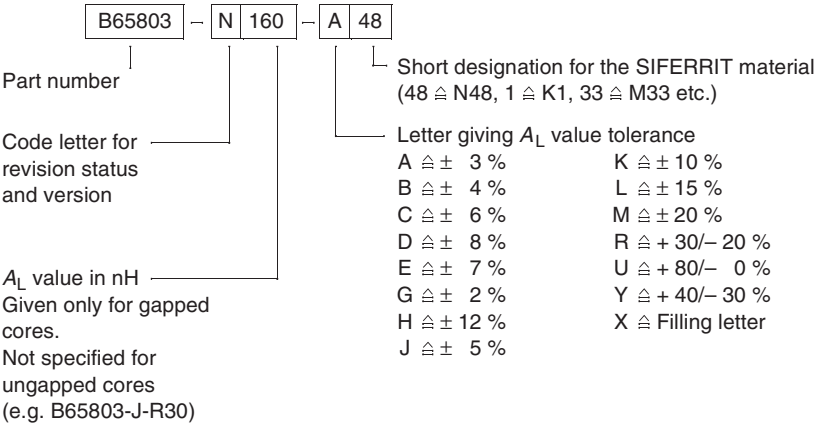

2 E, ELP, ER, ETD, EC, EFD, EV cores

These cores are supplied as single units; each packing unit contains only cores either with or without shortened center leg (gap dimension »*g*«). The typical value given in the tables for the A_L value applies to a core set consisting of one core with a shortened center leg and one core without a shortened center leg (dimension »*g*« approx. 0). E cores with a toleranced A_L value are available on request. We then prefer a symmetrical air gap distribution.

Ordering example (here ETD 29)

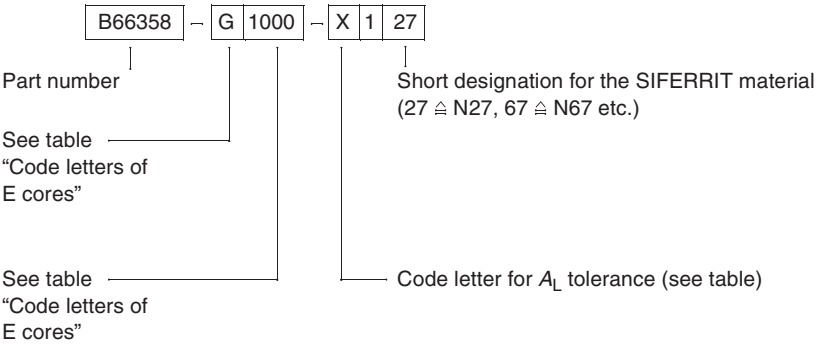

Versions (code letters) of RM cores

Type	with center hole (without threaded sleeve)	with center hole (with threaded sleeve)	without center hole	low-profile version
RM 4	A	N	J	P
RM 5	C	N	J	P
RM 6	C	N	J	P
RM 7	A	N	J	P
RM 8	D	F	J	P
RM 10	D	N	J	P
RM 12	—	—	E	P
RM 14	—	—	E	P

Versions (code letters) of P cores

Type	with center hole (without threaded sleeve)	with center hole (with threaded sleeve)	without center hole
P 3,3 × 2,6	—	—	C
P 4,6 × 4,1	B	—	—
P 5,8 × 3,3	D	—	—
P 7 × 4	A	—	—
P 9 × 5	D	T	W
P 11 × 7	D	T	W
P 14 × 8	D	T	W
P 18 × 11	D	T	W
P 22 × 13	D	T	W
P 26 × 16	D	T	W
P 30 × 19	D	T	W
P 36 × 22	D	T	W
P 41 × 25	J	—	—

Versions (code letters) of E cores

Code letter	Pairing	Code number	Tolerance
G	E - E	Air gap dimensions in µm Not specified f. ungapped cores	Air gap toleranced
U	E - E	A_L value in nH	A_L value, asymmetric air gap
A	E - E	A_L value in nH	A_L value, symmetric air gap
W	E - I (ELP cores)	A_L value in nH	A_L value
P	I core (plate f. ELP cores)	—	—
E	customized set	—	—
F	mirror polished	—	—

Herausgegeben von EPCOS AG
Marketing Kommunikation, Postfach 80 17 09, 81617 München, DEUTSCHLAND

Mit den Angaben in dieser Broschüre werden die Bauelemente spezifiziert, keine Eigenschaften zugesichert. Bestellungen unterliegen den vom ZVEI empfohlenen Allgemeinen Lieferbedingungen für Erzeugnisse und Leistungen der Elektroindustrie, soweit nichts anderes vereinbart wird.

Diese Broschüre ersetzt die vorige Ausgabe.

Fragen über Technik, Preise und Liefermöglichkeiten richten Sie bitte an den Ihnen nächstgelegenen Vertrieb der EPCOS AG oder an unsere Vertriebsgesellschaften im Ausland.

Bauelemente können aufgrund technischer Erfordernisse Gefahrstoffe enthalten. Auskünfte darüber bitten wir unter Angabe des betreffenden Typs ebenfalls über die zuständige Vertriebsgesellschaft einzuholen.

Published by EPCOS AG
Marketing Communications, P.O. Box 80 17 09, 81617 Munich, GERMANY

The information contained in this brochure describes the type of component and shall not be considered as guaranteed characteristics. Purchase orders are subject to the General Conditions for the Supply of Products and Services of the Electrical and Electronics Industry recommended by the ZVEI (German Electrical and Electronic Manufacturers' Association), unless otherwise agreed.

This brochure replaces the previous edition.

For questions on technology, prices and delivery please contact the Sales Offices of EPCOS AG or the international Representatives.

Due to technical requirements components may contain dangerous substances. For information on the type in question please also contact one of our Sales Offices.